

**GENETIC AND BEHAVIOURAL  
ADAPTATIONS OF *DROSOPHILA*  
*MELANOGASTER* TO  
CIRCADIAN AND SEASONAL  
SELECTION PRESSURES**

Thesis submitted for the degree of  
Doctor of Philosophy  
at the University of Leicester

by  
**Joseph Watkins**

Department of Genetics and Genome Biology  
University of Leicester  
August 2021

# ABSTRACT

## Genetic and Behavioural Adaptations of *Drosophila melanogaster* to Circadian and Seasonal Selection Pressures

Joseph Watkins

The changing of the seasons results in predictable environmental changes that exert strong seasonal selection pressures on all organisms. The most predictable is the daily oscillation of light (photoperiod) and temperature (thermoperiod). To survive the oncoming winter, *Drosophila melanogaster* enters a type of dormancy called diapause, characterized by an arrest in ovary development. In the long hot summer months, *D. melanogaster* alter their activity so that it is more diurnal with the emergence of the Afternoon (A) component.

This thesis further investigates *D. melanogaster*' response to the changing seasons through genetic and behavioural dissection. In doing so, two novel regulators for diapause were discovered. The first is a role for the microRNA (*miRNA*) *miR-276*, particularly the *miR-276b* parologue, which inhibits *timeless* and thus promotes diapause. This finding represents the first evidence of a *miRNA-mRNA* interaction experimentally proven to regulate diapause in *D. melanogaster*. The second is an inhibitory role of the long forgotten *0.9* gene which, unlike at higher temperatures, acts independently of *PERIOD*.

The role of temperature and light under simulated natural environmental conditions was also found to act in an unexpected way to regulate diapause. Under these conditions, the gradual changes rather than absolute or sudden changes in light and temperature must be synchronize. Only if they are in synch will the fly enter diapause. A similar relationship was also discovered in the

study of the A component. Gradual changes in temperature were found to be the overriding regulator of the A component via TrpA1, in a promoter and isoform specific manner. However, light is important in the timing of the A component through the action of the Rhodopsins Rh3 and Rh6.

## ACKNOWLEDGMENTS

I sit here now, adding the final touches to this thesis. A thesis that encapsulates a project which has dominated my life for the past 5 years. And I can honestly say that I am exhausted. It has been a hard 5 years, struggling with many problems both academic and personal. Switching from full time to part time, and at times, feeling overwhelmed. However, it has been worth it. I have had some amazing experiences and met some amazing people, and, hopefully, I have managed to do a bit of science along the way!

The first person who deserves more thanks than anyone is my supervisor Bambos Kyriacou, with whom I shared more than just ideas - especially in Krakow! I will always cherish the long hard-fought debates about the intricacies of and sometimes hard to interpret world of football! However, we (almost) always managed to squeeze in some science at the end of our meetings, and Bambos proves that you can be fun and have a sense of humour but still be a brilliant scientist. His guidance and advice were paramount to getting me through the problems with incubators, faulty fly stocks, a collapsing building, mid-project blues, and a pandemic. I am also grateful for his enormous generosity throughout my time in Leicester, particularly in the final months, ensuring that my write up went as smooth as possible.

I would also like to offer special thanks to Ezio, Flav and Rob for their intellectual input to my project and for always being happy to share ideas and their time. In addition, our technician Helen needs special mention for her tireless commitment to ensuring the laboratory does not fall apart and managing to juggle the expectations and needs of so many people!

I would also like to thank all members of laboratory 124 and the surrounding laboratories for their friendship and companionship during my time at Leicester.

Particular mention goes to Alex, Charlotte and Kate. Without you I would have done a lot more science, but I would have also not made it to the end! Special thanks also to Charlotte, Liam, Tunde and Nikola who rented my spare room at various times during the 5 years, without you I would be considerably poorer!

During my time at Leicester, I also took many opportunities to expand my PhD experience outside of the laboratory. I would like to say thank you to both Cas and Marie for introducing me to the world of outreach which remains amongst the fondest memories of my PhD. Also, to Fred, Ezio and Swidi for giving me the opportunity to teach in their undergraduate modules, and to Rob for mentoring me during my internship at the BBSRC.

Finally, but by no means least, I would like to extend a huge thank you to all my friends and family from beyond the University. You all supported me from near and afar during my journey, often going to great measure to help me when I needed it. Particularly to my partner Elena, for the many loaves of fresh bread and other snacks you allowed me to get fat on whilst slaving away on my thesis.

## LIST OF ABBREVIATIONS

<b>A</b> = afternoon bout of locomotor activity	<b>DN1(a/p)/2/3</b> = dorsal neurons
<b>aa</b> = amino acid	<b>DNA</b> = deoxyribonucleic acid
<b>AC</b> = anterior cells	<b>DopR1/2</b> = DOPAMINE RECEPTOR 1/2 protein
<b>AGO1</b> = ARGONAUT 1 protein	<b>E</b> = evening bout of locomotor activity
<b>aMe</b> = accessory medulla	<b>E-box</b> = CACGTG sequences
<b>ANOVA</b> = analysis of variance	<b>Ecd</b> = ecdysone hormone
<b>BDBT</b> = BRIDE OF DOUBLE TIME protein	<b>EDTA</b> = Ethylenediaminetetraacetic acid
<b>bp</b> = base pair	<b>EtOH</b> = Ethanol
<b>CA</b> = corpora allata	<b>EYA</b> = EYES ABSENT protein
<b>CC</b> = corpora cardiaca	<b>FAD</b> = Flavin adenine dinucleotide
<b>Cho</b> = chordotonal organs	<b>FOXO</b> = FORKHEAD BOX O transcription factor
<b>CK2</b> = CASEIN KINASE 2 protein	<b>GFP</b> = Green Fluorescent Protein
<b>CLK</b> = clock	<b>GL</b> = GLASS protein
<b>CNS</b> = central nervous system	<b>H-B eyelet</b> = Hofbauer–Buchner eyelet
<b>CRY</b> = CRYPTOCHROME protein	<b>ILS</b> = Insulin-Like Signalling
<b>CTT</b> = C-terminal tail	<b>InR</b> = Insulin Receptor
<b>CWO</b> = CLOCKWORK ORANGE protein	<b>IPC</b> = Insulin Producing Cells
<b>CYC</b> = CYCLE protein	<b>IS</b> = Insulin-like Signalling
<b>DBT</b> = DOUBLE TIME protein	<b>ITP</b> = Ion Transport Peptide
<b>DD</b> = constant darkness	<b>JET</b> = JETLAG protein
<b>DEL</b> = deletion	<b>JH</b> = Juvenile Hormone
<b>dILP</b> = drosophila Insulin-Like Peptide	<b>JHBP</b> = Juvenile Hormone Binding Protein
<b>dmp18</b> = <i>D. melanogaster</i> per intron 8	

<b>Kb</b> = kilo base	<b>PIP2</b> = Phosphatidylinositol Bisphosphate
<b>LD</b> = light-dark cycle	
<b>LL</b> = constant light	<b>PL</b> = Pars Lateralis
<b>LM</b> = light-moonlight cycle	<b>PLC-β</b> = Phospholipase C (alternative name for NORPA)
<b>LNd</b> = lateral dorsal neurons	<b>PP1</b> = Phosphatases Protein
<b>LPN</b> = lateral posterior neurons	Phosphatase 1
<b>ls/s-tim</b> = long-short/short allele versions of the <i>timeless</i> gene	<b>PP2A</b> = Protein Phosphatase 2A
<b>M</b> = morning bout of locomotor activity	<b>PYX</b> = PYREXIA protein
<b>Ma</b> = million years ago	<b>R1-6</b> = photoreceptor cells 1-6
<b>miRNA</b> = micro-RNA	<b>Rh1-7</b> = Rhodopsins 1-7
<b>miRNA</b> = micro-RNA	<b>RISC</b> = RNA-Induced Silencing Complex
<b>mRNA</b> = messenger RNA	<b>RNA</b> = ribonucleic acid
<b>NMO</b> = NEMO protein	<b>RNAi</b> = RNA interference
<b>NORPA</b> = NO RECEPTOR POTENTIAL A protein (alternative name for PLC- β)	<b>S</b> = siesta, mid-day rest in locomotor activity
<b>NPF</b> = Neuropeptide F	<b>s/l-LNv</b> = lateral ventral neurons (small and large)
<b>OAMB</b> = Octopamine receptor in Mushroom Body	<b>SEM</b> = standard error of the mean
<b>PAL</b> = Posterior Antennal Lobe	<b>SGG</b> = SHAGGY protein
<b>PBS</b> = Phosphate-Buffered Saline	<b>SNP</b> = single nucleotide polymorphism
<b>PCR</b> = polymerase chain reaction	<b>sNPF</b> = Short Neuropeptide F
<b>PDF</b> = Pigment Dispersion Factor	<b>sNPFR1</b> = sNPF Receptor 1
<b>PDFR</b> = PDF Receptor	<b>TF</b> = transcription factors
<b>PDP1</b> = PAR Domain Protein 1	<b>TIM</b> = TIMELESS protein
<b>PER</b> = PERIOD protein	<b>To</b> = TAKEOUT protein
<b>PI</b> = Pars Intercerebralis	<b>TOR</b> = Target Of Rapamycin protein
<b>Pi3K</b> = phosphatidylinositol-4,5-bisphosphate 3-kinase	

**TRP** = Transient Receptor

Potential channel

**TrpA1** = Transient Receptor

Potential Ankyrin Subtype 1

channel

**TTFL** =transcription/translation

feedback loop

**TYF** = TWENTY-FOUR protein

**UAS** = upstream activation

sequence

**UPD2** = UNPAIRED 2 protein

**UTR** = untranslated region

**VNC** = ventral nerve cord

**VRI** = VRILLE protein

**WT** = wild-type

**ZT** = Zeitgeber time

# TABLE OF CONTENTS

<b>ABSTRACT .....</b>	i
<b>ACKNOWLEDGMENTS .....</b>	iii
<b>LIST OF ABBREVIATIONS.....</b>	v
<b>1. INTRODUCTION.....</b>	1
1.1 Introduction.....	1
1.2 Circadian rhythmicity .....	1
1.2.1 <i>Drosophila melanogaster</i> as a model for circadian rhythmicity.....	2
1.2.2 The molecular architecture of the <i>Drosophila</i> circadian clock.....	3
1.2.3 The neuronal network of the <i>Drosophila</i> circadian clock ...	8
1.2.4 The circadian-linked visual system in <i>Drosophila</i> .....	11
1.2.5 Rhodopsin wavelength specificity .....	13
1.2.6 Light-mediated circadian entrainment .....	15
1.2.7 Temperature-dependent entrainment of the <i>Drosophila</i> clock.....	18
1.3 Seasonality .....	22
1.3.1 Seasonal adaptation strategies .....	23
1.3.2 Dormancy.....	24
1.3.3 Dormancy in <i>D. melanogaster</i> .....	27
1.3.4 Diapause in nature .....	30
1.3.5 Hormonal control of diapause .....	35
1.3.6 Insulin-like signalling and diapause.....	35
1.3.7 Hormonal control of diapause downstream of the IPCs ..	41
1.3.8 Neurosensory regulation upstream of the IPCs.....	43
1.3.9 The circadian clock and diapause .....	47
1.4 Motivations and aims.....	51
<b>2. MATERIALS AND METHODS.....</b>	53
2.1 Fly stock maintenance.....	53
2.2 Diapause .....	53
2.2.1 Experimental design.....	53

2.2.2 Dissection of flies prior to diapause scoring .....	54
2.2.3 Scoring diapause .....	54
2.3 Locomotor activity.....	55
2.3.1 Experimental design.....	55
2.3.2 Recording rhythmicity.....	55
2.4 Genomic DNA extraction .....	56
2.5 mRNA and miRNA extraction .....	57
2.6 DNA and RNA quantification .....	57
2.7 DNase treatment.....	57
2.8 Reverse Transcription .....	57
2.8.1 Reverse transcription of mRNA.....	58
2.8.2 Reverse transcription of miRNA.....	58
2.9 Polymerase chain reaction (PCR) .....	58
2.10 Genotyping .....	60
2.10.1 <i>per<sup>D</sup></i> genotyping .....	60
2.11 Genotyping for diapause-related alleles .....	60
2.11.1 Genotyping <i>cpo</i> SNP A356V .....	61
2.11.2 Genotyping for <i>s-tim</i> and <i>ls-tim</i> .....	61
2.12 Quantitative PCR (qPCR).....	62
2.12.1 qPCR of cDNA derived from mRNA.....	62
2.12.2 qPCR of cDNA derived from microRNA .....	63
2.13 Gel electrophoresis.....	63
2.14 Statistical Analysis.....	64
<b>3. THE ROLE of <i>miR-276b timeless</i> IN THE REGULATION DIAPAUSE</b>	
.....	65
3.1 Introduction .....	65
3.1.1 microRNAs .....	65
3.1.2 Circadian functions of miRNAs in <i>D. melanogaster</i> .....	68
3.1.3 miRNA control of diapause in <i>D. melanogaster</i> .....	71
3.1.4 Regulation of diapause by Timeless .....	72
3.1.5 miRNA control of <i>tim</i> .....	74
3.1.6 Regulation of timeless via <i>miR-276</i> .....	77
3.2 Aims .....	79
3.3 Materials and Methods .....	79

3.3.1 Fly stocks .....	79
3.3.2 Calculation of rhythmicity .....	80
3.3.3 Diapause scoring .....	80
3.3.4 qPCR analysis of <i>tim</i> mRNA .....	80
3.3.5 qPCR analysis of <i>miR-276b</i> miRNA.....	80
3.4 Results .....	81
3.4.1 The effect of knock-down of <i>miR-276a</i> and <i>miR-276b</i> expression via <i>miRNA</i> -sponges on diapause levels .....	81
3.4.2 The effect of overexpression of <i>miR-276b</i> on diapause levels.....	82
3.4.3 The effect on diapause levels of heterozygous knock-out mutants of <i>miR-276a</i> and <i>miR-276b</i> .....	83
3.4.4 The effects of genetic manipulation of <i>miR-276a</i> and <i>miR-276b</i> expression on rhythmicity.....	85
3.4.5 The effect of deletion and partial deletion of the <i>miR-276</i> seed site of <i>tim</i> on diapause levels .....	87
3.4.6 The effect of genetic manipulation of <i>miR-276</i> on <i>tim</i> mRNA levels at 11.5 °C.....	88
3.4.7 The effect of genetic manipulation of <i>miR-276</i> on <i>per</i> mRNA levels.....	90
3.4.8 Expression of <i>miR-276b</i> in the head and body at differing temperatures.....	91
3.5 Discussion .....	92
<b>4. THE ROLE OF <i>per</i> SPLICING AND THE 0.9 GENE IN DIAPAUSE REGULATION .....</b>	<b>102</b>
4.1 Introduction.....	102
4.2 Aims .....	107
4.3 Materials and Methods .....	107
4.3.1 Fly Stocks .....	107
4.3.2 Diapause scoring .....	108
4.4 Results .....	108
4.4.1 The effect on diapause of overexpressing <i>dmp18</i> splice-locked <i>UAS-per</i> lines.....	108

4.4.2 The effect on diapause of <i>RNAi</i> knock-down of the 0.9 transcript .....	109
4.4.3 The effect on diapause of 0.9 overexpression .....	111
4.4.4 The effect of <i>dmpi8</i> splicing on 0.9-dependent diapause .....	113
4.4.5 Effects of <i>dmpi8</i> splicing on diapause, independent of 0.9 .....	115
4.5 Discussion .....	117
<b>5. THE ROLE OF TEMPERATURE IN DIAPAUSE REGULATION UNDER SEMI-NATURAL ENVIRONMENTAL CONDITIONS.....</b>	<b>125</b>
5.1 Introduction.....	125
5.2 Aims .....	128
5.3 Materials and Methods .....	129
5.3.1 <i>Drosophila</i> Stocks .....	129
5.3.2 Simulation of semi-natural light and temperature profiles .....	129
5.3.3 Diapause scoring .....	130
5.4 Results .....	130
5.4.1 Generation of cyclic, natural-like thermoperiods .....	130
5.4.2 Photoperiodic effects on diapause under semi-natural light profiles .....	133
5.4.3 Semi-natural thermoperiodic effects on diapause under semi-natural light profiles .....	135
5.4.4 The effect on diapause of flies subjected to thermoperiods opposite to the subjected photoperiod .....	137
5.4.5 The effect on diapause of uncoupling the photoperiod from the thermoperiod.....	139
5.5 Discussion .....	141
<b>6. THE AFTERNOON PEAK IN SEMI-NATURAL SUMMER-LIKE CONDITIONS.....</b>	<b>151</b>
6.1 Introduction.....	151
6.1.1 The circadian clock under natural and semi-natural conditions.....	151

6.1.2 Thermo-sensation and the clock: the emerging role of TrpA1	154
6.2 Aims .....	160
6.3 Materials and Methods .....	160
6.3.1 Drosophila Stocks .....	160
6.3.2 Simulation of semi-natural light and temperature profiles	
.....	161
6.3.3 Locomotor activity .....	161
6.3.4 Calculation of $A_{onset}$ and $A_{max}$ .....	162
6.4 Results .....	163
6.4.1 Identification of the <i>TrpA1-gal4</i> driver used in the Green <i>et al.</i> (2015) study .....	163
6.4.2 Investigation of the ability of other <i>TrpA1-gal4</i> lines to target the TrpA1 <sup>+</sup> neurons responsible for regulating the A peak.....	165
6.4.3 <i>TrpA1</i> promoter and isoform specificity in regulation of the A component.....	168
6.4.4 Overexpression of TrpA1-A or TrpA1-B in a promoter-specific manner.....	171
6.4.5 Investigating a function of rhodopsins in regulating the A peak .....	172
6.4.6 The effect of rhodopsin mutants on the A peak when temperature and light are un-coupled .....	177
6.5 Discussion.....	181
<b>7. GENERAL DISCUSSION.....</b>	<b>193</b>
7.1 Evaluation of the diapause scoring methodology .....	194
7.2 The role of the circadian clock in diapause regulation .....	196
7.3 The relationship between temperature and light in diapause regulation .....	199
7.4 The Afternoon component and the startle response under semi-natural summer conditions .....	201
7.5 The relationship between temperature and light in regulating the A component.....	202
7.6 Summary .....	203
<b>8. APPENDIX .....</b>	<b>204</b>

8.1 Appendix Chapter 3.....	204
8.2 Appendix Chapter 4.....	222
8.3 Appendix Chapter 5.....	234
8.4 Appendix Chapter 6.....	246
<b>9. REFERENCES.....</b>	<b>253</b>

# 1. INTRODUCTION

## 1.1 Introduction

Two of the most predictable and consistent geophysical events that influence all life are the Earth's orbit around the Sun and its  $23.5^{\circ}$  rotation on its axis (Møller, 2010). During the summer and winter months, and away from the Equator towards the Poles there are very large fluctuations in photoperiod (hours of daylight per day) and temperature (**Figure 1-1**) (Wilczek *et al.*, 2010). These phenomena have changed very little since the Precambrian era (~620 Ma), creating the solar and seasonal cycles that govern the availability of components essential for life: light, warmth and moisture (Williams, 2000). This persistent selection pressure has led to the evolution of biological rhythms that enable organisms to suitably adapt their behaviour and biology according to the time of day or year. The importance of such rhythms is emphasised by their ubiquitous occurrence across the animal, plant and bacterial kingdoms, from cyanobacteria to mammals.

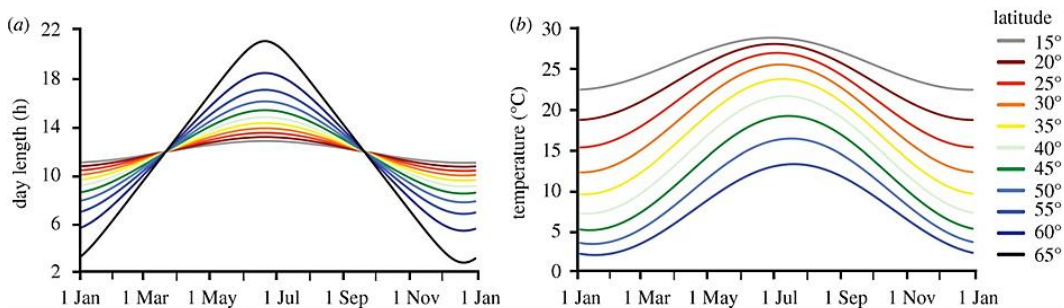


**Figure 1-1.** There is a positive correlation with the degree of change in photoperiod (a) and temperatures (b) in relation to increasing latitude (Taken from Wilczek *et al.* 2010)

## 1.2 Circadian rhythmicity

The most repetitive and predictable oscillation in the lifetime of any organism is the perpetual cycle of night and day. Therefore, it is of no surprise that almost all species, from cyanobacteria (Golden *et al.*, 1997) to humans (Reppert *et al.*, 2001), have evolved to organise aspects of their

physiology to comply with a 24-hour (circadian) schedule. This allows animals to fit into their own niche, synchronising their behaviour to that of their own species to enable successful mating, avoid predation or avoid competition. At the molecular level, the time of day can even influence the basics of cell biology, such as when a cell should divide (Farshadi *et al.*, 2020). The endogenous mechanism that controls these behaviours and physiologies is termed the “circadian clock” deriving from the Latin for near (circa) and 24-h (dies), as they usually do not run at a perfect 24-hour period (Pittendrigh, 1960). A behaviour is said to be circadian if it occurs in a predictively repetitive or rhythmic manner over the course of about a 24-hour period. Additionally, the behaviour must be entrainable to relevant cycling environmental cues or “zeitgebers”, the most common being light. However, many cues influence circadian clocks and vary from species to species. Other common zeitgebers include temperature, humidity, food availability and social interaction (Sharma and Chandrashekaran, 2005). The second characteristic of a true circadian rhythm is the ability to “free run” or continue with a circadian period in the absence of its zeitgebers, for instance under constant darkness (DD). This indicates that the behaviour is self-sustaining and is linked to an endogenous pacemaker that is not simply responsive to environmental cycles. Zeitgebers set the phase, usually through management of the correct timing of protein turnover, but are not necessary to maintain the physiological or molecular rhythm.

### **1.2.1 *Drosophila melanogaster* as a model for circadian rhythmicity**

Since Thomas Morgan’s pioneering experiments of 1910, *Drosophila melanogaster* has become the most common model to study evolution, development, behaviour and genetics. By the time of the first circadian experiments in the 1970s, *D. melanogaster* had already been accredited with two Nobel prizes for physiology and medicine. One for Morgan himself in 1933 and another to Hermann Muller in 1946. Since then, the humble fruit fly has picked up another four Nobel prizes, the most recent awarded in 2017 to Jeffrey Hall, Michael Rosbash and Michael Young for their work in

the field of Circadian Rhythmicity itself. Since the early 1970's *D. melanogaster* has remained one of the most commonly used model organisms in the field of chronobiology.

There are many physiological outputs under clock control, including eclosion, locomotor activity (Konopka and Benzer, 1971), egg-laying (Allemand and David, 1984) and the innate immune response (Shirasu-Hiza *et al.*, 2007; Stone *et al.*, 2012). Of these the most easily assayable and consequently the most well studied is locomotor activity. *Drosophila* display a rhythmic 24-hour cycle of activity and inactivity consisting of two activity peaks: a morning (M) and an evening (E) peak (**Figure 1-2**). This rhythmic pattern can be easily measured and therefore has become the standard assay for screening candidate clock genes, the first of which discovered being *period* (*per*) (Konopka and Benzer, 1971).

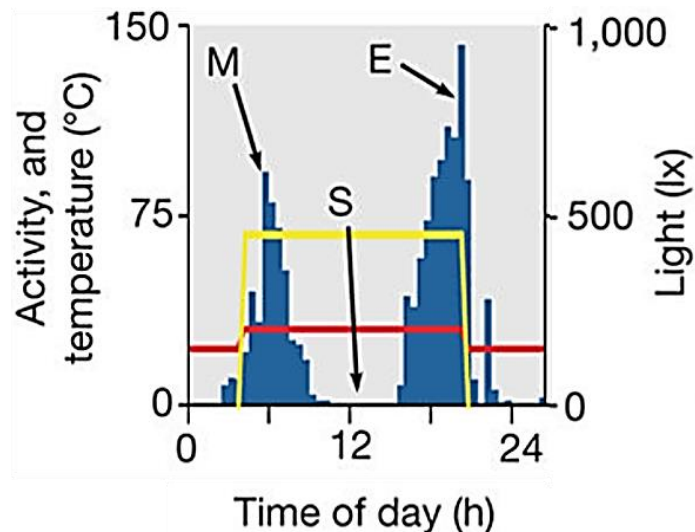


**Figure 1-2.** The typical locomotor activity profile of *Drosophila* under rectangular L:D light (yellow) and temperature (red) cycles. There are two distinct bouts of activity: a morning “M” and an evening “E” with a period of rest in between “S” (siesta). Taken from Vanin *et al.*, 2012.

### 1.2.2 The molecular architecture of the *Drosophila* circadian clock

The molecular backbone of the clock consists of cycling transcription factors (TFs) acting through two interlocked transcription/translation feedback loops (TTFL) (Hardin, 2011) (**Figure 1-3**). The genes *period* and

*timeless* are the core components of the dominant feedback loop. mRNA and protein levels display a 24-hour rhythmicity, however there is a delay between the peak of mRNA and the peak of protein expression indicative of a feedback mechanism (Hardin *et al.*, 1990). *per* and *tim* transcription begins a few hours after dawn when the bHLH transcription factors CLOCK (CLK) and CYCLE (CYC) bind as a heterodimer complex to a region of short CACGTG sequences on the *per* and *tim* promotors termed the E-box (Hao *et al.*, 1997; Allada *et al.*, 1998; Rutila *et al.*, 1998; Darlington *et al.*, 1998).

Translation of *per* and *tim* is mediated via interaction with the ATX2 complex, specifically with the translation factors TWENTY-FOUR (TYF) (Lim *et al.*, 2011; Lim and Allada, 2013) and LSM12 (Lee *et al.*, 2017). This translational regulatory step is thought to contribute to the delay between mRNA accumulation and protein accumulation, however PER and TIM protein levels are also tightly regulated at a post-translational level. The casein kinase DOUBLETIME (DBT) phosphorylates PER on the N-terminal serine (S47) (Price *et al.*, 1998; Chiu *et al.*, 2008) allowing SLIMB to bind and target PER for ubiquitin-mediated degradation via the proteasome pathway (Ko *et al.*, 2002; Grima, 2002). PER degradation is advanced via phosphorylation of DBT by BRIDE OF DOUBLETIME (BDBT) which enhances its kinase affinity (Fan *et al.*, 2013). TIM can bind to and stabilise the PER-DBT complex protecting it from degradation and in this state DBT binding to PER in fact increases its stability (Kloss *et al.*, 2001; Top *et al.*, 2018). Further stability is maintained through the action of the phosphatases Protein Phosphatase 1 (PP1) and Protein Phosphatase 2A (PP2A) which dephosphorylate TIM and PER respectively (Fang *et al.*, 2007; Sathyanarayanan *et al.*, 2004).

PER and TIM protein levels begin to accumulate in the evening, about 12 hours after lights on (ZT12), at which point they begin to re-localise to the nucleus, aided by phosphorylation of PER by Casein Kinase 2 (CK2) (Ju-Ming *et al.*, 2002) and of TIM by SHAGGY (SGG) (Martinek *et al.*, 2001; Top *et al.*, 2016). Once in the nucleus PER inhibits its own transcription via binding to the C-terminus of CLK (Chang *et al.*, 2003). PER-bound CLK is

susceptible to phosphorylation resulting in its inability to bind to the E box of the *per* or *tim* promotores and causes a halt in *per* and *tim* transcription from ZT18 until the start of a new round of the cycle at dawn (Darlington *et al.*, 1998; Lee *et al.*, 1999). In addition to displacement of CLK via the PER-repressor complex, phosphorylation events decrease CLK-dependent transcription via targeted degradation. The TIM-PER-DBT complex enables the kinase NEMO (NMO) to phosphorylate CLK and speed up CLK protein turnover (Yu *et al.*, 2011).

At dawn, light resets the clock via activation of the blue-light sensitive protein CRYPTOCHROME (CRY) (Emery *et al.*, 1998; Stanewsky *et al.*, 1998). Light activates CRY through reduction of its bound FAD cofactor, resulting in a conformational change of the CRY protein: exposing its C-terminal tail (CTT) and a groove for TIM and other factors to bind (Hoang *et al.*, 2008; Ozturk *et al.*, 2011; Czarna *et al.*, 2013; Vaidya *et al.*, 2013). TIM binds to activated CRY and the TIM-CRY complex is targeted for proteolytic degradation via the binding of the F-box containing E-3 ubiquitin ligase JETLAG (JET) and the light-activated E3 ligase RAMSHACKLE (encoded by the *BRWD3* gene) to the exposed CTT (Busza *et al.*, 2004; Koh *et al.*, 2006; Peschel *et al.*, 2009; Ozturk *et al.*, 2013). Consequently, CRY-dependent TIM degradation results in the dismantlement of the TIM-PER heterodimer, thus leaving PER susceptible to DBT mediated degradation (Busza *et al.*, 2004). PER degradation is not immediate but instead is completed several hours after dawn (ZT04). This is because DBT phosphorylates PER in a cascade of steps before finally phosphorylating serine 47 to propagate SLIMB-targeted degradation (Chiu., *et al* 2008). Once PER levels are sufficiently degraded, its inhibition of CLK-CYC binding to the E-boxes of the *per*, *tim* and other circadian controlled promoters enables transcription to restart and the cycle begins again.

The *tim-per* TTFL is the predominant regulator of circadian behaviour in *Drosophila* and is necessary for all circadian output. However, an additional feedback loop enables further control of the clock: the *C/k* loop (Glossop *et al.*, 1999). The CLK-CYC heterodimer has been found to bind not only to

the *per* and *tim* E-boxes but also to E-boxes of additional transcription factors that directly influence *Clk* transcription (Cyran *et al.*, 2003). During daylight hours, in the absence of PER inhibition, CLK-CYC activates transcription of *PAR domain protein 1* (*Pdp1*) (Cyran *et al.*, 2003) and the PAR-domain containing *vriile* (*vri*) (Glossop *et al.*, 2003). Both proteins bind to the same region of the *Clik* promoter termed the VRI/PDP1-box (ATTACATAAC) (Cyran *et al.*, 2003). VRI binding represses *Clik* transcription whereas PDP1  $\epsilon/\delta$  acts as an activator (Glossop *et al.*, 2003; Zheng *et al.*, 2009). Although both genes are under the control of CLK-CYC activation there is a considerable delay in PDP1 mRNA and protein accumulation compared to VRI. This leads to temporal repression and activation of CLK during the day and aids in the correct timing of the circadian oscillator (Cyran *et al.*, 2003). Further to the differential expression patterns of PDP1 and VRI, the actual role PDP1 has in regulating the clock has been disputed (Cyran *et al.*, 2003; Benito *et al.*, 2007). Initial follow up experiments by Benito and colleagues (2007) indicated that inhibition or overexpression of PDP1 had little effect on cycling CLK levels at neither the mRNA nor protein level. Instead, it was suggested that PDP1 has a downstream function in circadian output: assayed through locomotor experiments (Benito *et al.*, 2007). Although this does seem to be the case, later investigation indicated that the  $\epsilon$ -specific isoform of PDP1 was able to influence both CLK and CRY transcription and thus is considered a regulator of the central circadian oscillator (Zheng *et al.*, 2009).

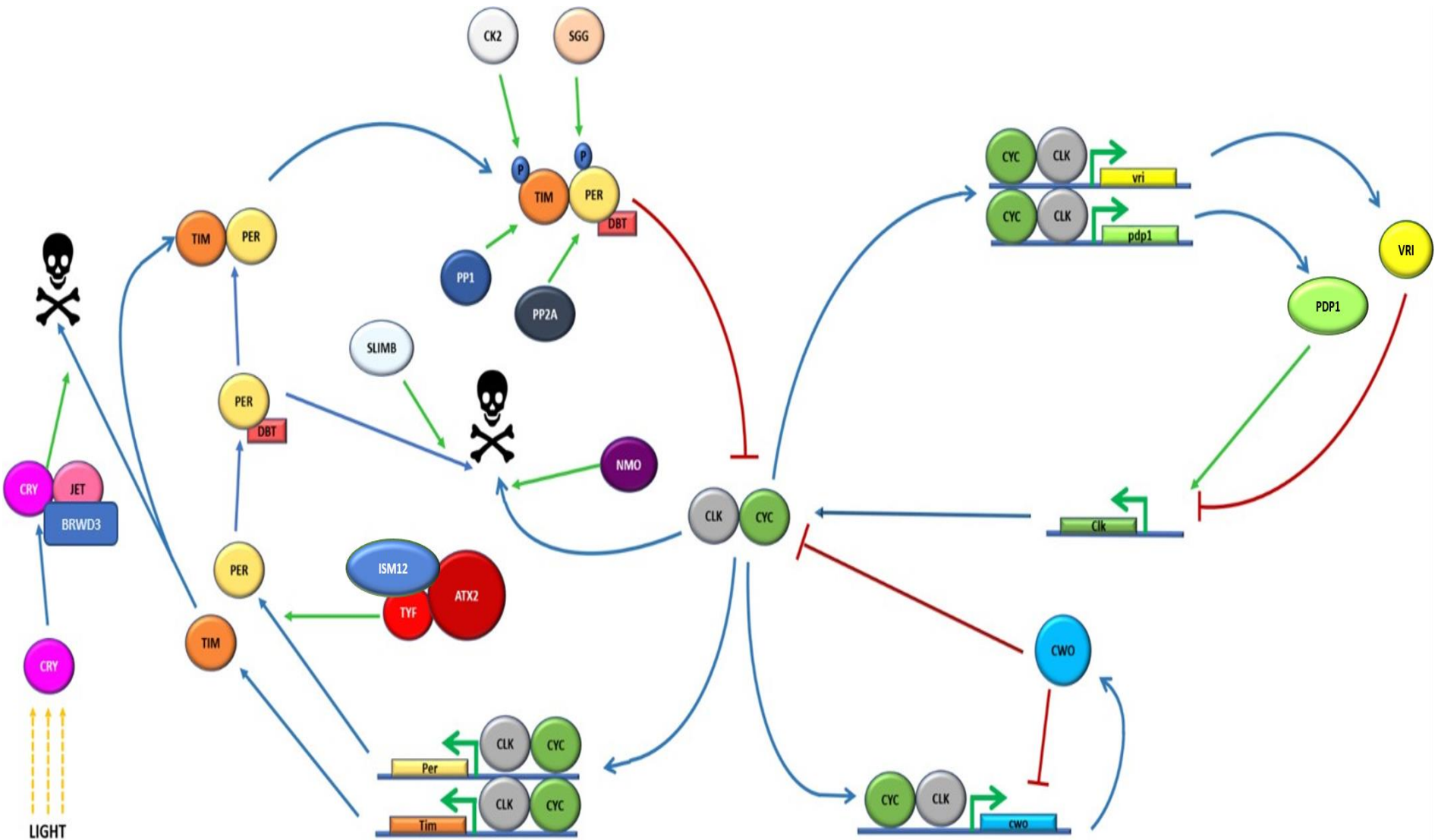


**Figure 1-3.** The key components of the Drosophila molecular clock. Cycling levels of PER, TIM and CLK control circadian synchronisation: regulated via complex transcription/translation feedback loops (TTFLs) centrally linked via CLK-CYC. Green arrows indicate positive or enhancive interaction whereas red connections indicate inhibitory interactions. The skull and crossbones symbolise protein degradation (CRY-mediated degradation of TIM, SLIMB-mediated degradation of PER, or NMO-mediated degradation of CLK).

Further to PDP1 and VRI, an additional component to the *Clk*-loop, CLOCKWORK ORANGE (CWO) was discovered which links into both the *per-tim* and *Clk*-loops (Kadener *et al.*, 2007). CWO contains both an E-box and a bHLH domain enabling it to regulate its own expression as well as that of other core clock components (*per*, *tim*, *vri*, *Pdp1*) (Richier *et al.*, 2008). However, CWO's main function is in aiding PER-dependent displacement of CLK from its E-box targets via competitive binding. CWO E-box binding affinity is lower than that of CLK-CYC but higher than that of PER-CLK-CYC and disrupted CWO expression decreases the repressive ability of PER (Zhou *et al.*, 2016). These data suggest that CWO is necessary for efficient displacement and repression of CLK-CYC by PER.

The molecular clock evolved millions of years ago in ancestors common to all animalia (Bhadra *et al.*, 2017). Therefore, the genetic and molecular architecture are conserved. However, as species have continued to evolve the individual components are modified or begin to facilitate alternative roles. For example, in mammals, PER and CRY form a heterodimer complex to inhibit CLOCK which, in complex with BMAL1, promotes PER and CRY expression. The second TTFL controls transcription of *Ror* and *Rev-Erb* which have opposing roles on *Bmal1* transcription. BMAL1 activates transcription of *Ror* and *Rev-Erb* thus closing the loop (Bhadra *et al.*, 2018).

### 1.2.3 The neuronal network of the *Drosophila* circadian clock

The presence of cycling PER levels in a 24hour rhythm is indicative of a tissue having circadian timekeeping capabilities. As such, a *period* driven-luciferase assay performed by Plautz and colleagues (1997) uncovered circadian oscillation in several fly tissues: head, antennae, eyes, proboscis, legs, wings, malpighian tubules and testes. In mammals, many of these tissues can maintain some degree of circadian rhythmicity independent of CNS connection but the central “master” oscillator is said to be in the brain. Only the master clock can control the circadian outputs of mammals in a controlled and adaptable manner. On the other hand, in flies, peripheral tissues are able to maintain molecular rhythmicity and phase shift to light independent of the brain as they contain CRY. Nonetheless, many complex behaviours require a functional clock in the fly brain to interpret peripheral inputs and elicit appropriate physiological responses (Herzog, 2007).

The neuronal component of the central clock of *D. melanogaster* consists of ~150 neurons (~75 cells per hemisphere) grouped together into distinct clusters based on their location, mainly the Lateral Neurons (LN) and the Dorsal Neurons (DN). Communication is achieved predominantly via neural peptides such as Pigment Dispersing Factor (PDF), Neuropeptide F (NPF), short Neuropeptide F (sNPF) and Ion Transport Peptide (ITP), of which PDF has the greater and most complicated relationship with the clock (Peng *et al.*, 2003; Helfrich-Förster *et al.*, 2009; Guo *et al.*, 2014; He *et al.*, 2017). As advances in the field unpick the neuronal map apart, several subgroups of clock neurons have been defined based on function, communicative abilities and spatial specificity (Sheeba *et al.*, 2008; Beckwith *et al.*, 2015) (**Figure 1-4**). The DN's are now classified into 3 subsets DN1 (~16 cells), DN2 (2 cells), DN3 (~40 cells) and the LN's have been broken down into several sub-divisions: The dorsal Lateral Neurons (LNd) made of 6 cells, the Lateral ventral Neurons (LNv) – separated into small and large subgroups (s-LNv) and (l-LNv) consisting of 4 cells each, and the Lateral Posterior Neurons (LPN) made of 3 cells. The 5<sup>th</sup> s-LNv is identified separately from the other s-LNv's since it does not express PDF but instead expresses ITP (Helfrich-Förster *et al.*, 2007). The DN1s have also been separated into anterior

(DN1a) containing 2 cells and posterior (DN1p) containing 14 cells (Shafer *et al.*, 2006).

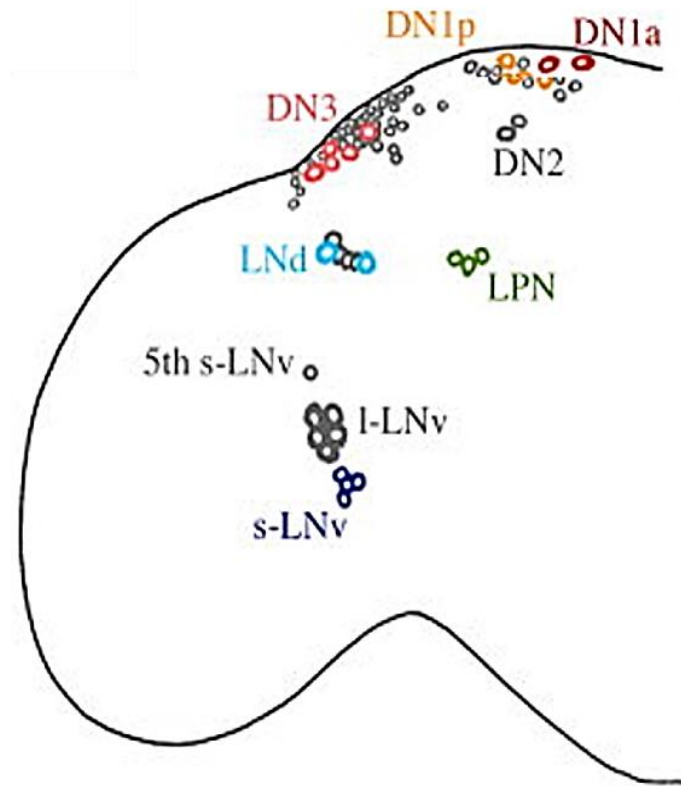


**Figure 1-4.** The neuronal map of one hemisphere of the *Drosophila* clock. The larger cells within each cluster are labelled in colour. (Taken from Shafer *et al.* 2006)

The traditional model of circadian neurobiology is that autonomous clusters control different aspects of circadian output (assayed via locomotor activity). This hypothesis was based on the findings of two simultaneously published papers that have spearheaded circadian neurobiology in the 21<sup>st</sup> century (Grima *et al.*, 2004; Stoleru *et al.*, 2004). Their findings separated several clock cell clusters into two distinct groups each with their own clock, governing either the morning locomotor activity (M) or the evening (E). The s-LNvs controlled the morning oscillator whilst the collective action of the LNd, 5<sup>th</sup> s-LNv and the DN1 cells were responsible for the evening oscillator. Furthermore, Ca<sup>2+</sup> cycles in the key morning and evening pacemaker neurons have been found to be coupled to the M and E peaks of activities respectively and are able to be phase shifted under entraining conditions (Liang *et al.*, 2016). This system was termed the “dual oscillator”,

however the relationship between each oscillator is not one of equality. The sLNvs were considered to be dominant over the evening cells, controlling the rhythms of each cell cluster to match their own via a circadian release of PDF (Grima *et al.*, 2004; Stoleru *et al.*, 2004; Fernández *et al.*, 2008; Shafer *et al.*, 2008). This creates a hierarchical model to ensure that all the individual clocks within the overall master clock are synchronised.

Although this simplistic “hierarchical dual oscillator” model paved the way for many avenues of research into the circadian neuronal map, a decade and a half of further investigation has proven the reality to be much more complex. Recent advances in genetics have allowed for targeted mutation of specific genes in specific tissues through combining the CRISPR/CAS9 system with the UAS-Gal4 system (Delventhal *et al.*, 2019; Schlichting *et al.*, 2019). Mutating out either *per* or *tim* in specific clock neurons dismantled the traditional hierarchical model. Loss of the molecular clock in both the morning and evening cell clusters was sufficient to induce arrhythmicity, but loss of the clock in only one or the other could not (Delventhal *et al.*, 2019; Schlichting *et al.*, 2019). This suggests a compensatory nature between the cell clusters rather than a dominance of the s-LNvs which had become dogma in the early years of the field. Furthermore, it has been shown through several studies that the individual cell clusters, and indeed, individual cells within clusters, have a very plastic and dynamic communication network (Shafer *et al.*, 2006; Fernandez et al., 2008; Dissel *et al.*, 2014; Gorostiza *et al.*, 2014; Yao and Shafer, 2014; Beckwith *et al.*, 2015; (Roberts *et al.*, 2015; Liang *et al.*, 2016; Schlichting *et al.*, 2016; Fernandez *et al.*, 2020). Competing endogenous clocks influence each other’s periodicity and it is the combined effect which determines the overall rhythm. This would provide a logical mechanism where changes in the environment would shift the equilibrium and thus adapt the fly’s periodicity accordingly.

#### **1.2.4 The circadian-linked visual system in *Drosophila***

Light is one of the strongest zeitgebers for circadian entrainment in *Drosophila* and is linked molecularly to the clock via CRY. CRY is expressed in neurons in several clock cell clusters: in all the s-LNvs, I-LNvs, half of the LNdS and some of the DN1s (Yoshii *et al.*, 2008). However, flies expressing a null mutant form of CRY ( $\text{CRY}^0$ ) may lose their phase-shifting abilities in response to light pulses but are still entrainable in light-dark cycles (LD) (Emery *et al.*, 1998; Stanewsky *et al.*, 1998). Light entrainment to the environmental light regime is also achieved via photoreceptor cells in the fly compound eyes. The transcription factor GLASS (GL) is required for differentiation of the photoreceptor cells during development and GL mutant flies are unable to entrain to environmental light regimes (Helfrich-Förster *et al.*, 2001).

Light input is sensed via a G-protein coupled family of 7 Rhodopsins (Rh1 – Rh7) that undergo conformational changes in response to light activating their coupled chromophore retinal. Retinal is extremely sensitive and uptake of a single photon of light triggers the transformation from a Rhodopsin to a Metarhodopsin, activating cellular signalling cascades via activation of a coupled G $\alpha$  protein (Kiselev, A. and Subramaniam, 1994). Phospholipase C (PLC- $\beta$ ) also known as ‘no receptor potential A’ (NORPA) is subsequently activated and propagates cellular signalling cascades via the PIP2 pathway (reviewed by Hardie and Juusola, 2015). This eventually leads to the depolarisation of the membrane and the release of the neural transmitter histamine.

The *Drosophila* compound eye is made up of 800 individual units called ommatidia, each containing 8 photoreceptors named R1-R8. Each photoreceptor type expresses a specific Rhodopsin different from the rest (**Figure 1-5**). R1-R6 form a ring structure and express the most abundant Rhodopsin: Rhodopsin 1 (Rh1), encoded by the gene *ninaE* (O'Tousa *et al.*, 1985). R7 and R8 situate in the centre of the ring stacked upon each other. R7 can express either Rh3 or Rh4 (Fryxell and Meyerowitz, 1987; Montell *et al.*, 1987) whereas R8 can express either Rh5 or Rh6 (Chou *et al.*, 1996; Huber *et al.*, 1997; Papatsenko *et al.*, 1997). Two types of ommatidia were

initially classified: pale and yellow, and were found to be randomly dispersed across the eye. The pale ommatidia make up ~30% of all ommatidia, expressing Rh3 in the R7 photoreceptor and Rh5 in the R8 photoreceptor. Yellow ommatidia express Rh4 in R7 and Rh 6 in R8 cells and account for ~70% of the ommatidia in the compound eye (Chou *et al.*, 1999). Two additional smaller sub-types of ommatidia have since been reported that are expressed in lower numbers. The dorsal yellow ommatidia express both Rh3 and Rh4 in the R7 photoreceptors and Rh6 in the R8s (Mazzoni *et al.*, 2008). Secondly, the dorsal rim area (DRA) ommatidia express Rh3 in both the R7 and R8 photoreceptors. The function of these unusual ommatidia is not clearly defined but initial reports indicate they may be involved in sensing polarised light to aid navigation (Wernet *et al.*, 2012).

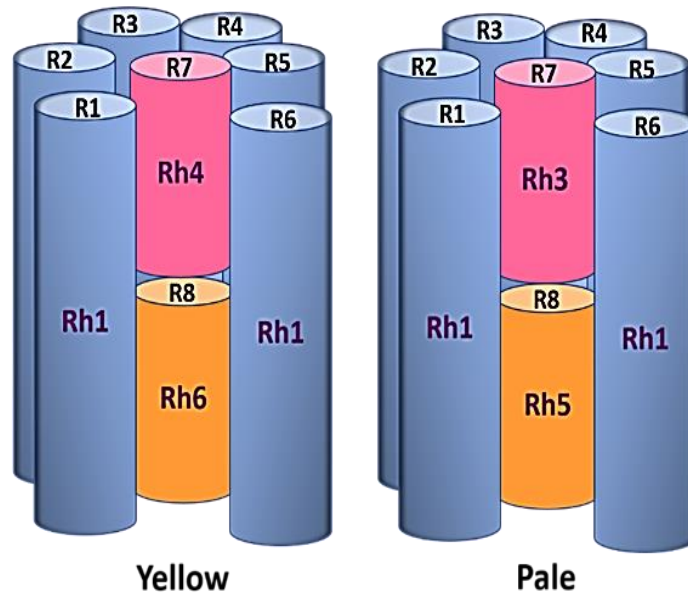


**Figure 1-5.** Schematic representation of the arrangement of photoreceptors in the fly ommatidia and their corresponding Rhodopsin expression. R1 – R6 photoreceptors form a ring structure and express Rh1. In yellow ommatidia R7 expresses Rh4 and R8 expresses Rh6. In pale ommatidia R7 expresses Rh3 and R8 expresses Rh5.

### 1.2.5 Rhodopsin wavelength specificity

*Drosophila* have six main Rhodopsins which combined can detect a wide spectral wavelength range. This is important as it allows the detection of colour as well as the ability to detect light sources within a limited spectrum. All the major Rhodopsins are expressed in the compound eye

except for Rh2 which is instead expressed in the ocelli (Pollock and Benzer, 1998) and is important for flight stabilisation (Taylor and Krapp, 2007). Rh6 is also expressed in the Hofbauer–Buchner (H–B) eyelet that has neuronal connections to the AC neurons and thus the LNvs (Helfrich-Förster *et al.*, 2002). Rh1 is the most abundant Rhodopsin and the most sensitive. It can detect blue light at a peak sensitivity of 486nm and is necessary for the detection of movement (Yamaguchi *et al.*, 2008). The R7 and R8 photoreceptor expressed Rhodopsins are responsible for colour perception: Rh3 and Rh4 are sensitive to UV light with peak sensitivities at 331nm and 355nm respectively, Rh5 is sensitive to blue light (442nm) and Rh6 is sensitive to green light (515nm) (Salcedo *et al.*, 1999) (**Figure 1-6**). Unsurprisingly, mutational studies have shown that Rh5 and Rh6 are necessary for entrainment to green and yellow light respectively (Hanai and Ishida, 2009) and that Rh1 and Rh6 entrain to red light (Hanai *et al.*, 2008). Interestingly, the R7 and R8 photoreceptors also express CRY providing a dual mechanism for photosensation (Yoshii *et al.*, 2008).

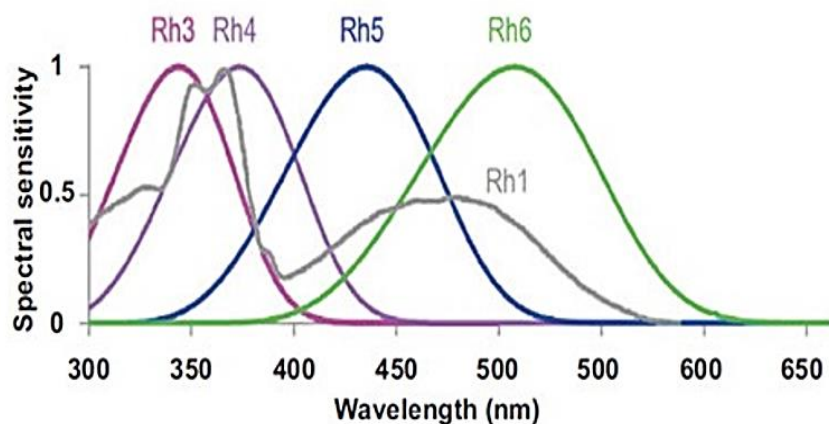


**Figure 6.** Wavelength sensitivity amongst the six *Drosophila* Rhodopsins (Taken from Behnia and Desplan 2015).

A 7<sup>th</sup> Rhodopsin (Rh7) sensitive to violet light has recently been discovered with expression in the PDF positive LNv cells and is thought to be important for photo-entrainment under low-light conditions or in response to short light pulses (Ni *et al.*, 2017). This provides the possibility of a direct link between

light and the molecular clock in addition to CRY. The precise mechanism of the Rh7-mediated response to light is still unknown, further complicating the possible entrainment routes the clock can take in response to light.

### 1.2.6 Light-mediated circadian entrainment

Light entrainment to LD cycles has been shown to be achieved via two distinct pathways: a CRY-dependent, photoreceptor independent pathway, and a photoreceptor-dependent, CRY-independent pathway (Stanewsky *et al.*, 1998; Helfrich-Förster *et al.*, 2001). NORPA-dependent entrainment has been found to have stronger reactions to advances in photoperiod whereas CRY dependent entrainment seems to be better at reacting to delayed photoperiods (Saint-Charles *et al.*, 2016). The CRY-dependent entrainment pathway has also been indicated to act in two distinct mechanisms as CRY-dependent entrainment reacts differently to light pulses than it does to changing LD cycles (Saunders *et al.*, 1998; Stanewsky *et al.*, 1998; Kistenpfennig *et al.*, 2012).

An interesting study by Alejevski *et al.* (2019) has indicated a role of signal integration of all the photoreceptors to the Rh6-expressing R8 cells. The histamine receptor HisCL1 located on the Rh6<sup>+</sup> R8 neurons receives histaminergic signalling from the other photoreceptors of the eye to synchronise the light response in LD (Alejevski *et al.*, 2019). This would place the Rh6<sup>+</sup> R8s as the focal point of light entrainment from which light information would be dissipated out to the clock.

The traditional view was that the morning cells (s-LNvs) were the major centre for visual input into the clock. However, input into many clock cells in both the morning and evening cell clusters have been identified (Li *et al.*, 2018; Guo *et al.*, 2018). In particular, the I-LNvs transmit signals from the eyes via PDF signalling into the accessory medulla to the s-LNvs and LNds to synchronise light-dependent circadian responses. Furthermore, the I-LNvs use light-induced signals from the eyes to regulate clock-dependent sleep/arousal at dawn and dusk (Shang *et al.*, 2008).

As mentioned earlier, the original hierarchical model of the central clock had been challenged via dissection of clock cell communication (Yao and Shafer, 2014; Dissel *et al.*, 2014; Liang *et al.*, 2017; Delventhal *et al.*, 2019; Schlichting *et al.*, 2019). Methodological dissection of the visual input system by Li *et al.* (2018) through optogenetic stimulation of the compound eye, ablation of neuronal connections, and electrophysiological recording further challenged this concept. Li found that neurons from all clock cell clusters responded to some extent when the visual system was stimulated with a laser (**Figure 1-7A**). The dendrites of these clock neurons all merge on the accessory medulla (aMe) area of the brain. Furthermore, light input from the HB and compound eye are channelled through the aMe before being transmitted to the clock. Ablation of the aMe renders all visual system-clock connections null (Li *et al.*, 2018). Therefore, rather than the s-LN<sub>v</sub>s receiving all light input and then synchronising the rest of the clock in a hierarchical model, light is received by the aMe which then transmits the information to several different clock neurons in parallel (**Figure 1-7B**). It was also found that the CRY<sup>+</sup> sNPF<sup>+</sup> LN<sub>d</sub>s are light-responsive but not directly via the aMe. Instead, the ITP<sup>+</sup> LN<sub>d</sub>s and the 5<sup>th</sup> s-LN<sub>v</sub> (through parallel circuits) activate the sNPF<sup>+</sup> LN<sub>d</sub>s in response to light (Li *et al.*, 2018).

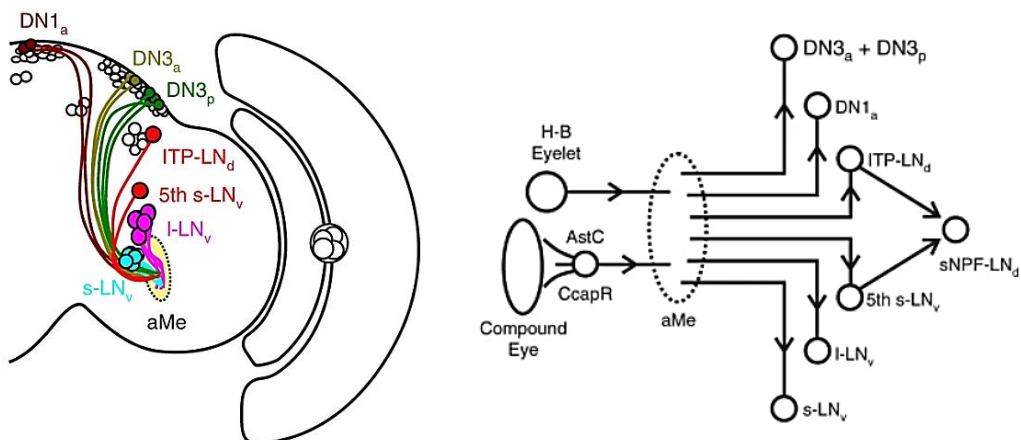


**Figure 1-7.** **A)** Diagram representing the arborization of clock neuron dendrites to the aMe. Clock cells that are light-sensitive via the aMe are coloured according to their cluster of origin. **B)** Schematic showing the parallel circuits for light entrainment. Light input from the compound eye and H-B eyelet are transmitted into the aMe. The signal is then transmitted via parallel circuits to clock cells in several circuits. The signal is propagated to the sNPF-LNds in an additional step, via the IPT-LNds and the 5<sup>th</sup> s-LNv. (Taken from Li *et al.*, 2018)

A third pathway, independent of both CRY and NORPA has also been proposed but the underlying mechanisms for which are less understood. The first evidence came from the discovery that Rh5 and Rh6 can entrain the clock in a *norpA<sup>P41</sup>* (loss of function) background (Szular *et al.*, 2012). Furthermore, Saint Charles and colleagues (2016) could separate the Rhodopsins, and thus photoreceptor classes, into two distinct groups. Rh1, 3, 4 and 6 could entrain via the NORPA-dependent pathway (in a CRY mutant background) under low light conditions but Rh2 and Rh5 could not (Saint-Charles *et al.*, 2016). A more recent study by the Stanewsky lab (Ogueta *et al.*, 2018) delved into this further. They found that using light sources that gradually (albeit, via short-spaced steps) increase/decrease light to simulate dawn/dusk, *norpA<sup>P41</sup>* and *cry<sup>b</sup>* double mutant flies still maintain entrainability but at a slower rate. Thus, implying the presence of a NORPA-CRY-independent light entrainment pathway, consistent with Saint-Charles's findings (2016) (**Figure 1-8**). However, knocking out the eye-specific Rhodopsins Rh1,5,6 alongside the *norpA<sup>P41</sup>*, *cry<sup>b</sup>* double mutants prevents light entrainability definitively. This implies that Rh1, Rh5 and Rh6 are capable of entraining the clock independently of NORPA or CRY. Instead of utilising PLC-β, this pathway signals via PLC21C and is specific to the s-LNvs (Ogueta *et al.*, 2018).

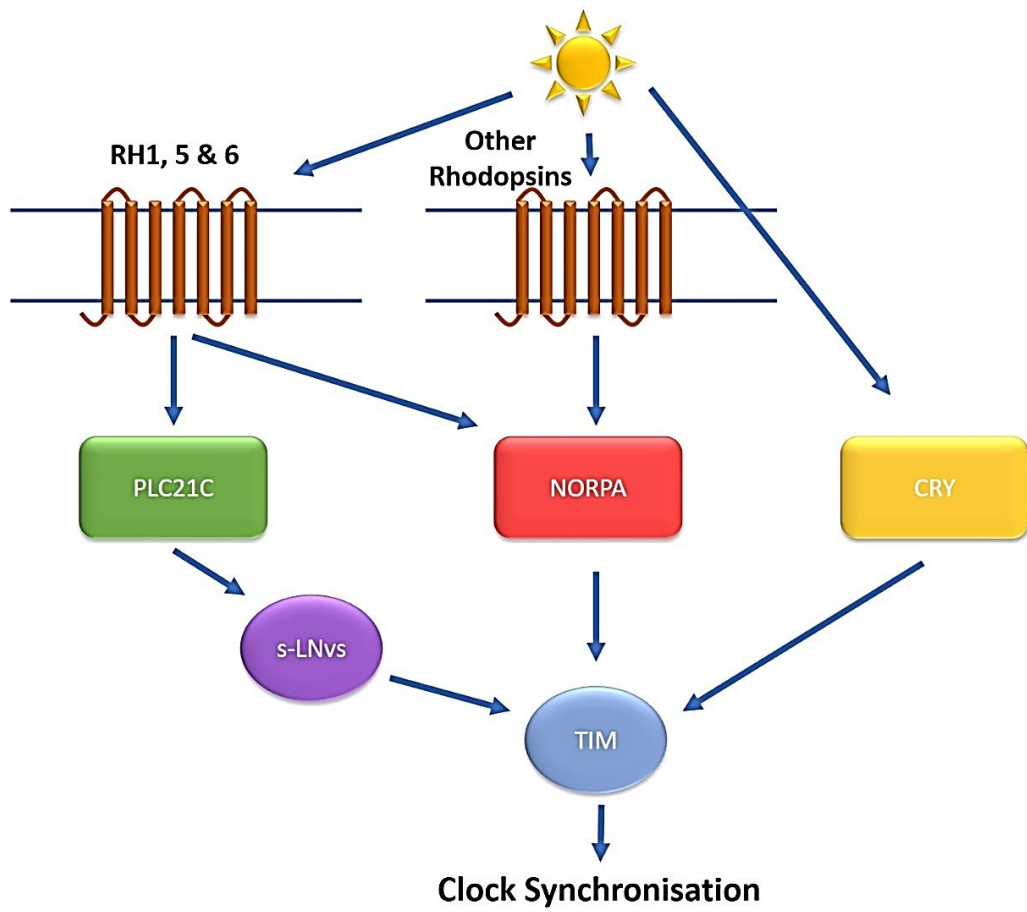


**Figure 1-8.** A schematic representing the 3 alternative pathways the clock can utilise to entrain to light (as proposed by (Ogueta *et al.*, 2018)). Light can activate CRY directly in the clock cells to enable entrainment. Alternatively, entrainment can be achieved via the Rhodopsins. Either via NORPA or specifically for Rhodopsins Rh1, Rh5 and Rh6 via PLC21C which signals to the s-LNvs.

### 1.2.7 Temperature-dependent entrainment of the *Drosophila* clock

Although much is known about how the molecular clock interacts and responds to light, less is known about the involvement of temperature. *Drosophila* kept under DD as well as constant light (LL) conditions can entrain to rectangular temperature cycles and can influence TIM and PER protein cycling. (Wheeler *et al.*, 1993; Tomioka *et al.*, 1998; Glaser and Stanewsky, 2005). This data provided evidence that temperature has a key role in regulating the clock.

For the clock to entrain to its thermal environment it must be able to sense temperature fluctuations. This is achieved (mostly) by the membrane-bound temperature-gated ion channels TrpA1 and Pyrexia (Pyx) which are a part of the thermal transient receptor potential (TRP) protein family. Pyrexia is necessary for temperature entrainment in low thermal cycles and is expressed in the chordotonal organs (Cho) (Wolfgang *et al.*, 2013), whereas TrpA1 has a more influential role in higher temperature cycles and is expressed in the AC cells and unlabelled neurons in the brain as well as several other peripheral locations (Lee and Montell, 2013). TrpA1 is also expressed in almost all the clock neuron clusters: LPN, LNv, LNd, DN1, DN2 and DN3, however expression is only limited to a few cells in each cluster (Lee and Montell, 2013).

Temperature cycles either in DD or in low-light LD can entrain several core neuronal clock clusters, generally with a greater effect in DNs over LNs (Picot *et al.*, 2009; Yoshii *et al.*, 2009). The relative phase shift in response to changing temperature however varies greatly between the clock cells. The DNs and LPNs could be entrained by temperature but the LNvs could not (Miyasako *et al.*, 2007). This suggests that different clock clusters are preferentially entrained to either temperature or light. The Emery lab (Busza *et al.*, 2007) found that cells in both the evening and the morning oscillators are entrainable to temperature in the absence of light, but the morning oscillator cells inhibit the evening cells, resulting in a slower entrainability to temperature than to light, thus ensuring that light is the dominant zeitgeber. This work however was done using very broadly expressing promoters and when dissecting the clock cells more precisely, the story may be more complex as discussed previously (Yao and Shafer, 2014; Dissel *et al.*, 2014; Liang *et al.*, 2017; Li *et al.*, 2018; Delventhal *et al.*, 2019; Schlichting *et al.*, 2019).

At the molecular level, CRY has been found to have a role in temperature entrainment (Picot *et al.*, 2009; Yoshii *et al.*, 2010). It was found that in the CRY<sup>+</sup> s-LNv; 5th s-LNv; LNd; DN<sub>1a</sub>; DN<sub>1p</sub>; and DN<sub>3</sub>, PER and TIM cycling was entrained to LD cycles as opposed to temperature whereas in the CRY<sup>-</sup>

$\text{DN}_{1p}$ ;  $\text{DN}_2$ ; and LPN cells, cycling was entrained to temperature. This differentiation however was lost in CRY mutant flies in which the ordinarily CRY<sup>+</sup> cells also preferentially synchronise to temperature over light suggestive of an inhibitory role of CRY in temperature entrainment. Moreover, under constant light (LL), temperature cycles are able to rescue arrhythmicity by overriding the CRY-mediated degradation of TIM and therefore PER (Glaser and Stanewsky, 2005). Chen *et al.* (2020) found that this was via NORPA, which, under constant light, inhibits CRY expression.

A recent study from our lab (Azevedo *et al.*, 2020) indicates that the DN1s inhibit the s-LNvs through glutamate signalling to prevent pacemaker function in constant light (and under constant temperature). Moreover, Fernandez *et al.* (2020) implicate dendritic plasticity of the s-LNvs as important for temperature entrainment. Impairing dendritic remodelling of these cells, which occurs in a cyclic manner and peaks during the early morning, resulted in locomotor defects. Interestingly, this was only observed when using temperature cycles but not when temperature was kept constant (Under DD) (Fernandez *et al.*, 2020). This was via an inhibition of glutamate signalling from the DN1p cells to the s-LNvs, suggesting a mechanism for circadian-timed synchronisation of s-LNvs to temperature cycles via the DN1ps. The DN1a cells have also been implicated in relaying temperature input to the s-LNvs via the neuropeptide CCHamide1 (CCHa1) to control morning and siesta activity (Fujiwara *et al.*, 2018).

The DN2s too have been identified as strong temperature entrainers in several studies (Picot *et al.*, 2009; Yoshii *et al.*, 2010; Kaneko *et al.*, 2012; Gentile *et al.*, 2013; Tang *et al.*, 2017). It was found that inhibition of the molecular clock in the DN2s was sufficient to impede temperature entrainment as well as the rhythmic temperature preference behaviour (Kaneko *et al.*, 2012) suggesting a role for the DN2s in temperature-dependent circadian output. It has also been shown in larval brains that the DN2s are capable of entraining PDF positive LNvs to temperature under DD or daylight-moonlight (LM) conditions. Contrarily, the LNvs under standard LD conditions can entrain the DN2s via PDF signalling (Picot *et al.*, 2009).

The same results have been replicated in the adult brain and have indicated that the anterior cells (AC) provide the thermal-sensory input required for DN2 temperature entrainment (Tang *et al.*, 2017).

Outside of the central clock, the mechanosensory system in the peripheral organs of the fly also have an important role in temperature entrainment. In fact, entrainment in LL through the above-described CRY-independent signalling pathway was significantly inhibited in *nocte* mutants (Azevedo *et al.*, 2020). The chordotonal organs (Cho) in the fly limbs express *nocte* and feedback to the central brain to synchronise the clock to temperature cycles (Sehadova *et al.*, 2009). Thermocycles are sensed by these organs, which contain their own circadian rhythmicity, and transmitted to the DN1s and LNds via NOCTE as well as the Ionotropic Receptor 25a (IR25a) (Chen *et al.*, 2015; Chen *et al.*, 2018).

Another temperature sensitive receptor expressed in the Cho is PYREXIA (PYX). *pyx* is expressed in a specialised stretch-activated Cho called the Johnston's organ which is located in the fly antennae (Tang *et al.*, 2013). PYX<sup>+</sup> neurons in the antennae send temperature-induced signals to TRPA1 expressing neurons (AC) in the brain that transmit the signals to the posterior antennal lobe (PAL). This acts as a centre to collate temperature and humidity input from the periphery and propagate the information to other centres of the brain, including the DN1s (Tang *et al.*, 2013; Frank *et al.*, 2015). Inhibition of *pyr* in the antennae results in a dyssynchronisation of the clock in the DN1s and s-LNvs in either DD or LL. This leads to unstable locomotor rhythms but only at lower temperatures (16°- 20°C) (Wolfgang *et al.*, 2013; Roessingh *et al.* 2019). Another circuit has been mapped from the sacculus of the antennae through the PAL and finally contacting the DN1a cells. This specific neural pathway has been implicated in sensing temperatures below 25°C to control the timing of sleep and arousal (Alpert *et al.*, 2020). The arista, another structure in the fly antennae, has also been shown to transmit temperature signals to the DN1p cells and also contributes to sleep/wake cycles (Yadlapalli *et al.*, 2018).

One of the most prominent and multifunctional thermoreceptors in *D. melanogaster* is TrpA1. It is expressed in a range of neurons including a population of AC neurons that contact the s-LNvs (Hamada *et al.*, 2008). However, to date, studies to try to link TrpA1 to entrainment of the clock have failed (Roessingh *et al.*, 2015; Tang *et al.*, 2017). TrpA1 has however been shown to be needed for correct phasing of the morning and evening peaks of activity in response to high temperatures and in suppressing the siesta (Roessingh *et al.*, 2015; Das *et al.*, 2016). The variability in expression patterns of the available *TrpA1-Gal4* lines, the experimental set up between experiments, and the discovery of several promoters and isoforms of TrpA1 may mean that its circadian role needs more probing (Zhong *et al.*, 2012; Roessingh and Stanewsky, 2017). Furthermore, its recent role in controlling behaviour in more natural-like conditions is still in its infancy (Green *et al.*, 2015; Das *et al.*, 2015; see also **chapter 6**)

The emerging model is that the clock neuronal clusters differ in preference to light or temperature entrainment. Even within cell clusters there may be several different input pathways providing zeitgeber information. Cell-cell signalling via a complex network enables the different oscillators to combine to decide the overall entrainment preference. This enables the fly to adapt the most appropriate response to an ever changing and dynamic environment.

## 1.3 Seasonality

Adaptability to the daily oscillations in an organism's environment clearly offers an evolutionary advantage, but organisms are also subject to annual cycles. The tilt of the earth's axis and its relative distance from the sun throughout its orbit, produces seasonality. Unlike the circadian cycle of 24 hours, seasonal cycles have a period of 12 months. In polar regions, organisms experience dramatic changes in photoperiod over the course of the year, oscillating from almost complete darkness to constant light

(Wilczek *et al.*, 2010), and in the tropics, changes in the environment occur due to the cycling of the wet and dry seasons. In temperate regions, organisms experience a milder but still significant combination of tropic and polar-like seasonal oscillations.

Food and water availability, predator presence and avoidance, shelter suitability, cold and heat tolerance can all be affected by the environmental shift in weather and climate throughout the year. This can have consequences for an organism or species ability to survive and/or produce offspring that can make it to adulthood. Therefore, organisms do not just have to evolve to survive the day-to-day fluctuations in their environment but the dramatic changes associated with each rotation around the sun.

### **1.3.1 Seasonal adaptation strategies**

If seasonality is a strong enough driving force to drive a species' evolution, there are only two strategies that species can take to improve its survival credentials. Either they escape the change through migration, or they stay and change their behaviour and physiology according to the current and upcoming season. Regardless of the strategy, organisms must be able to predict the change in season before it happens. A squirrel can't suddenly find itself in the middle of winter without any fat reserves, and no acorns buried. A blue whale cannot suddenly realise that its food supply of krill is 1000km away.

As hinted at above, one common strategy applied across the animal kingdom to escape either cold inhospitable winters, or dry noxious summers is to migrate to more favourable lands. Many species undergo such seasonal migrations each year, sometimes covering vast distances such as the arctic tern (*Sterna paradisaea*) which travels up to 40,000km from breeding to feeding grounds (Egevang *et al.*, 2010), or the caribou (*Rangifer tarandus*) that travels over 5000km over land (Fancy *et al.*, 1989). Even some insect species migrate, such as the monarch butterfly (*Danaus*

*plexippus*) which spends the majority of its lifespan in migration and navigates via the earth's magnetic field (Guerra *et al.*, 2014). Interestingly, migratory populations of *D. plexippus* genetically differ compared to non-migratory populations, with an emphasis on genes associated with the vitamin A synthesis pathway (Merlin *et al.*, 2020). Even more dramatic is the migration of the globe skimmer dragonfly (*Plantala flavescens*) which can be up to 18,000 km taking 4 generations to complete, and even requires crossing over the Himalayas (Hobson *et al.*, 2012).

The strategy of migration is a suitable choice for large animals with long lifespans. However, many species have evolved not to escape seasonal challenges "in space" but "in time". A commonly known strategy utilised by many mammals and some large cold-blooded animals is to hibernate. This adaptation is characterised by a state of inactivation, where the metabolism, activity and body temperature are lowered to preserve energy to outlive the undesired season. If this occurs in the winter it is termed hibernation, but if it occurs in the summer, it is termed aestivation. Examples of hibernators are hamsters (Tamura *et al.*, 2005) and bears (Evans *et al.*, 2016), and of aestivators are tortoises (Geffen and Mendelssohn, 1989) and dormice (Bieber and Ruf, 2009).

### 1.3.2 Dormancy

Although some insects migrate, such as the monarch butterfly (Guerra *et al.*, 2014) the majority have evolved to enter a state of dormancy, much akin to hibernation and aestivation in mammals, but with a key difference. Dormancy is an adaptive response to changes in the environment that triggers not only the slowdown of metabolism and a decrease or even cessation of activity, but also a slowdown or arrest in development and/or reproduction (Koštál, 2006). The nature in which the organism interprets and reacts to environmental changes determines if its dormancy is further classified as "Diapause" or "Quiescence" (**Table 1-1**).

**Table 1-1.** The main differences of the quiescence and diapause phenotypes.

	<b>Quiescence</b>	<b>Diapause</b>
<b>Stimulus</b>	Adverse environmental stresses	Anticipatory environmental stresses
<b>Response</b>	Immediate, reactionary, exogenous	Pre-programmed, anticipatory, endogenous
<b>Effect</b>	Direct (via slowed or paused growth) halt in development/reproduction, altered metabolism, altered behaviour	Indirect (via altered neuroendocrine pathways) halt in development/reproduction, altered metabolism, altered behaviour
<b>Timing (onset)</b>	Direct response to adverse stress	Prior to adverse stress
<b>Timing (offset)</b>	Upon removal of adverse stress	When pre-programmed conditions are met and may last longer than the adverse stress

Quiescence is a reactionary version of dormancy in which an organism responds directly to stress stimuli caused by a change in its environment. It is triggered once the limiting environmental factor falls below a given threshold, for example, if the temperature drops to a certain level. Once this change has passed and the environmental conditions are more favourable, for example, the temperature rises back above the physiological threshold, the organism leaves its dormant state and development is resumed. This cessation of dormancy and resumption of development will occur regardless of how long the organism has been dormant for, and regardless of other environmental factors (Danks, 1987; Koštál, 2006).

Diapause is a more sophisticated pre-programmed endogenous response to a predictive change in the environment. These environmental changes

are often specific and independent of other environmental stresses. It is characterised by an actively induced neuroendocrinological response which causes a pause in development, increased resistance to stress, altered metabolism, and altered behavioural activity. (Koštál, 2006). This enables diapause phenotypes to be predictive in nature and, although diapause-inducing triggers are anticipatory of upcoming unfavourable conditions, they may not be adverse themselves. Furthermore, unlike quiescence, the organism may have limited capability to respond to changing environmental stimulus and stresses whilst in a diapausing state. Only when the precise pre-programmed conditions are met will the organism exit diapause. This prevents a premature escape, for instance, during an unusual warm patch in the middle of winter (Danks, 1987; Koštál, 2006).

In some species, diapause may be followed by a period of quiescence. The pre-programmed conditions to exit diapause may be met, however, if the other environmental stresses persist, continuation of reproduction would not be favourable. Under these conditions, some species enter a post-diapause quiescence (Koštál, 2006). For example, the photoperiod may govern the endogenous diapause response of an organism to ensure that development is paused over the winter. However, if when winter ends, the environmental temperature is still too low, the endogenous diapause phenotype may be replaced by an exogenous quiescent phenotype (post-diapause quiescence). Only once the temperature rises will the organism exit dormancy fully and resume reproduction/development (Koštál, 2006).

The diapause phenotype can also be separated into facultative and obligatory diapause. Facultative species will only enter diapause if the environmental cues are just right – or, more appropriately, “just wrong” - this may mean that during some years an organism will not diapause at all, or even in some cases, never in its lifetime. An example of a facultative diapausing species is the parasitic wasp *Nasonia vitripennis* (Saunders *et al.*, 1970; Wolschin and Gadau, 2009). Obligatory species will always enter diapause regardless of environmental cues. Species hardwired to enter obligatory diapause often have a yearly lifecycle. An example of an

obligatory diapausing species is the gypsy moth *Lymantria dispar* (Leonard, 1968).

In addition to the classification of dormancy based on its onset/offset, it can also be classified according to the life stage which is affected. Dormancy can occur at any stage of an insect's development. The silkworm *Bombyx mori* diapauses during the embryonic stage (Yamashita, 1996), the corn borer *Ostrinia nubilalis* as a larva (Goto *et al.*, 2001), the grape moth *Lobesia botrana* as a pupa (Roditakis and Karandinos, 2001), and the Colorado potato beetle *Leptinotarsa decemlineata* as an adult (De Wilde *et al.*, 1959).

### 1.3.3 Dormancy in *D. melanogaster*

*D. melanogaster* evolved as a species in sub-Saharan Africa and migrated to colonise Asia, Europe and eventually, through the help of human migration and maritime travel, the Americas and Australia (David and Capy, 1988; Lachaise *et al.*, 1988; Li and Stephan, 2006; Keller, 2007; Laurent *et al.*, 2011; Duchen *et al.* 2013; Sprengelmeyer *et al.*, 2020) (**Figure 1-9**) . This migration period also marked a shift from a woodland insect into a more cosmopolitan species through their commensalism with humans (Mansourian *et al.*, 2018; Sprengelmeyer *et al.*, 2020). Interestingly however, latest data suggest that although migration across Africa and into the Middle East may have occurred around 13,000 years ago, migration into Europe may be as recent as just 1,800 years (Sprengelmeyer *et al.*, 2020). Furthermore, colonisation of Australia and America by *D. melanogaster* only occurred alongside human recolonisation of these continents 300-400 years ago (Keller, 2007). This commensalism with humans also provides another level of complexity as the gene pool differs across the Americas based on the origin of the pioneering individuals. More northernly latitudes were colonised by Northern Europeans (and thus northern latitude flies), whereas the central and southern latitudes were mostly colonised by Southern Europeans (and thus southern latitude flies). Additionally, due to the transatlantic slave trade, admixture from African *Drosophila* populations is

also much more prevalent in central and southern latitudes compared to the north (Kao *et al.*, 2015).

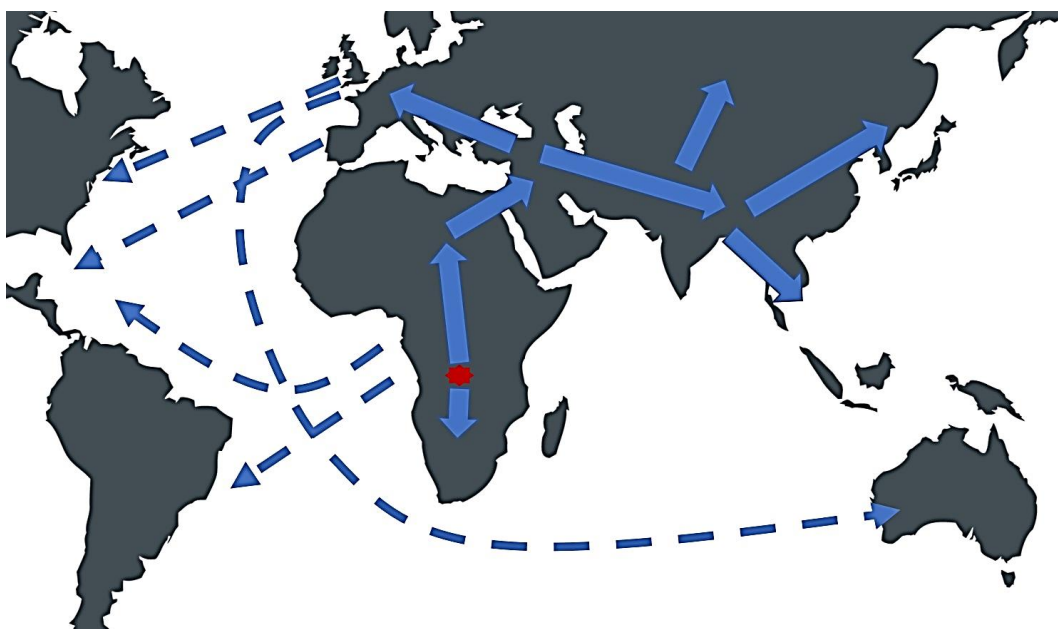


**Figure 1-9.** The estimated migratory routes of *Drosophila melanogaster* since its evolution as a species. The red star indicates the approximate origin of the species (possibly somewhere between Zambia and Zimbabwe). The dashed arrows represent human-aided migration across the sea. (Image created on Microsoft PowerPoint from the following literature: David and Capy, 1998; Li and Stephan, 2006; Keller, 2007; Laurent *et al.*, 2011; Duchen *et al.*, 2013; Sprengelmeyer *et al.*, 2022).

Consequently, *D. melanogaster* with its already well established and comprehensive genetic toolbox offers a superb model to study evolution and adaptation of a species to different climates (Flatt, 2020). With the relatively recent and ongoing colonisation and recolonisation of the species to certain regions it also offers the opportunity to study evolution in real-time.

There are several consistent latitudinal clines in natural *Drosophila* populations studied across several continents. In general, as latitude increases, body size increases (David and Bocquet, 1975; Fabian *et al.*, 2015; Kapun *et al.*, 2016b), life span increases (Durmaz *et al.*, 2018), and the ability to cope to various stress responses increases (Da Lage *et al.*, 1990; Frydenberg *et al.*, 2003; Hoffmann *et al.*, 2005; Rajpurohit *et al.*, 2018) at the expense of decreased fecundity associated with reproductive

dormancy (Mitrovski and Hoffmann, 2001; Schmidt *et al.*, 2005; Schmidt and Paaby 2008; Zonato *et al.*, 2018; Durmaz *et al.*, 2019).

Under optimum laboratory conditions *D. melanogaster* females are capable of laying up to 100 eggs per day and may produce up to 3000 eggs in their life time (Shapiro, 1932; McMillan *et al.*, 1970; Klepsatel *et al.*, 2013). In the wild however, where food availability, temperature, humidity, predation and many other factors will not be optimum, the rate of egg production is expected to be considerably less. Nevertheless, the metabolic cost is considerable, and, as pre-adult life stages of *D. melanogaster* are unable to survive winter at high latitudes (Izquierdo, 1991; Hoffmann, 2010), it would be wasteful to continue to expand energy on such a costly production line. Therefore, *D. melanogaster* has evolved an adult facultative, winter, reproductive dormancy to ensure genetic survival beyond the winter months (Saunders *et al.*, 1989, Saunders and Gilbert, 1990).

The mortality rate of *D. melanogaster* usually increases with age, similar to most species. However, flies that are in dormancy maintain similar survival levels as newly eclosed flies, even after 9 weeks. They are also more resistant to heat or cold shock and to oxidative stress than non-diapausing flies (Tata *et al.*, 2001; Ayrinhac *et al.*, 2004; Pegoraro *et al.*, 2014; Anduaga *et al.*, 2018). *Drosophila* during dormancy have altered metabolism compared to non-dormant flies, exhibited by a breakdown of glycogen into trehalose and glucose (Kubrak *et al.*, 2014; Anduaga *et al.*, 2018).

Dormancy in *Drosophila* is triggered by a shortening photoperiod and a decreasing temperature (decreasing below 14°C) consistent with the onset of winter within temperate regions (Saunders and Gilbert, 1990, Emerson *et al.*, 2009a). Saunders and colleagues initially characterised *Drosophila* dormancy as “diapause”, however there has been debate as to the appropriateness of this terminology within the field (Tatar *et al.*, 2001; Emerson *et al.*, 2009a; Zhao *et al.*, 2016; Zonato *et al.*, 2017; Lirakis *et al.*, 2018). This is because of the nature of its dormancy. After several weeks under constant low temperatures, or as a response to an increase in

temperature, *Drosophila* readily exit diapause (Tatar *et al.*, 2001; Emerson *et al.* 2009b). This led to the suggestion that *Drosophila* dormancy is more like a “quiescence” than a “diapause” phenotype. However, using more “natural-like” experimental parameters in which temperature and photoperiod were decreased in incremental steps each week for several weeks, dormancy levels were maintained (Zonato *et al.*, 2017). The transcriptional profile also differs between diapausing and non-diapausing flies and between tissues, with differing expression patterns in ovaries compared to heads (Zhao *et al.*, 2016). Diapausing flies placed into sub-zero temperatures are also more “cold-hardened” and able to withstand these low temperatures than non-diapausing flies. This correlation is independent of the temperature to which flies are reared prior to exposure to sub-zero temperatures and suggests a more dynamic “diapause-like” phenotype (Anduaga *et al.*, 2018). For consistency with the majority of the literature, dormancy in *Drosophila* for the remainder of this report will be referred to as “diapause”. The exact scoring criteria for determining if a fly is in diapause or not will be discussed in **chapters 2.2.3 and 7.1**.

### 1.3.4 Diapause in nature

As well as debate over the classification of diapause in *D. melanogaster*, there has also been debate in the literature as to when or how this diapause evolved. Initial diapause experiments were performed on laboratory strains nearly a century old originating from North America (Saunders and Gilbert, 1990). However, studies using more recently caught “natural” lines from varied continents and latitudes often provided contradictory data (Schmidt *et al.*, 2005; Tauber *et al.*, 2007; Emerson *et al.*, 2009b; Schmidt, 2011; Fabian *et al.*, 2015; Zonato *et al.*, 2017).

Both Schmidt (2011) and Fabian *et al.* (2015) did not find any incidence of diapause amongst African populations, suggesting that diapause is a relatively young phenotype specific to European and European-derived populations. However, Schmidt only tested a limited number of populations

from a very low latitude where diapause levels would be expected to be low. Schmidt did still find some levels of diapause that were very shallow. Fabian and colleagues had a much more varied and larger number of populations but used an unconventional diapause scoring method. In this study, diapause was scored as either a ‘yes’ or a ‘no’ for an entire population if more than half the individuals were diapausing after 4 weeks at 11°C. This means that a population that may have 49% of individuals in diapause would be ignored from their results and classed as “non-diapausing”. This of course omits a lot of data.

Diapause is prevalent amongst American populations which show a clear latitudinal cline when subjected to the same experimental parameters, with greater levels of diapause in northernly populations compared to the south (Schmidt *et al.*, 2005). However, Emerson and colleagues (2009b) did not find any photoperiodic effect in North American populations in relation to diapause inducibility. This implies that amongst these populations, temperature not photoperiod may be responsible for differing diapause levels. This is contradictory to studies of European populations that have a very shallow latitudinal cline yet show a clear photoperiodic response (Tauber *et al.*, 2007; Pegoraro *et al.*, 2017).

A possible explanation for the discrepancies between studies could be attributed to the differing experimental parameters, both in the photoperiod lengths tested (8:16 vs 10:14 hours of light) and in the length of time flies were kept in these conditions before diapause scoring (12 days vs 28 days). Therefore, Zonato and colleagues (2017) decided to conduct a comprehensive study of all these populations after both 12 and 28 days, and under the more diapause-inducing photoperiod of LD8:16. They found that both American and European populations showed photoperiodism at 12 days (consistent with the European studies (Tauber *et al.*, 2007; Pegoraro *et al.*, 2017)) but both populations lost their photoperiodic effect at 28 days (consistent with the American study (Emerson *et al.*, 2009b)). It appears that the results between the two studies are not contradictory at all and were actually due to differing experimental set up. Furthermore, Zonato

*et al* (2017) extended their study to African populations. It was found that using more conventional scoring methods that were less omitting than in Fabian (2015), 70% of populations studied expressed diapause levels above 40% after 12 days. Consistent with the European and American lines, the diapause levels were reduced dramatically after 28 days, concurrent with both Fabian (2015) and Schmidt (2011). Photoperiodism however was very weak in most populations tested consistent with Schmidt (2011).

It is interesting that the diapausing phenotype in flies from all three continents is not sustained when scored after 28 days. This is counterintuitive as, in the wild, to survive the seasons flies would need to diapause for several months, much longer than 4 weeks. Zonato and her colleagues looked to explore this further by creating a more natural-like experimental set up which subjected flies over several months to temperature and photoperiods that gradually decrease each week to mimic the onset of winter, and then gradually increase again to mimic the ending of winter. Under these conditions, flies were able to maintain high levels of diapause for much longer (10/12 weeks compared to 4 weeks of flies kept in constant conditions) (Zonato *et al.*, 2017).

The weak cline in diapause levels observed in European populations is also counterintuitive (Pegoraro *et al.*, 2017). If diapause is an adaptive trait, then a strong cline would be expected with greater diapause occurrence in northern populations compared to southern populations as seen in America (Schmidt *et al.*, 2005). However, directional selection of a newly emerged pro-diapause allele was found to be masking an underlying cline (Zonato *et al.*, 2018). An allele of the gene *timeless* (*ls-tim*) is known to be diapause-inducing, probably due to its decreased sensitivity to light, providing an adaptive response to long photoperiods (Tauber *et al.*, 2007; Sandrelli *et al.*, 2007; Peschel *et al.*, 2009). It was found that this allele originated in southern Italy between 300 and 3000 years ago (Zonato *et al.*, 2018). However, as migration into Europe has recently been more accurately mapped, a better estimate may be 300 – 1800 years (Sprengelmeyer *et al.*, 2020). This is relatively recent in evolution and the allele has not yet reached

equilibrium. Therefore, there is more of the pro-diapausing allele in southern populations than in northern populations, thus masking any underlying cline (Zonato *et al.*, 2018). Indeed, in North America, there is a strong latitudinal cline in the occurrence of the *Is-tim* allele which matches with the strong cline in diapause observed (Pegoraro *et al.*, 2017). This is likely due to a founder effect whereby a small subpopulation colonised the “new world” through human commensalism ~300-400 years ago.

Upon standardising the data from the field and filling in the gaps, it is now most probable to conclude that diapause in *D. melanogaster* is an ancestral adaptation evolved in Africa and strengthened in European and European-derived populations (Zonato *et al.*, 2017). The reason why diapause would have evolved in populations living in the tropics where photoperiod is relatively stable compared to temperate regions, and the temperature does not drop too low, is intriguing in itself. It has long been suggested that diapause coevolved from a generic stress-coping response to the wet-dry season experienced in sub-tropical Africa to avoid food shortage and desiccation (Denlinger, 1986; Pullin 1996; Zhao *et al.*, 2016). Mansourian and colleagues (2018) offer a tempting alteration to this theory, revolving around the availability of a particular fruit in the region (see below), and once again, helped along by human commensalism.

European and American populations are known to prefer to feed, mate, and lay eggs on citrus fruit, and in particular, oranges (Dweck *et al.*, 2013). In the forests of Zimbabwe, near to the ancestral home of *D. melanogaster*, grows the marula fruit. Both wild African and American laboratory strains of *D. melanogaster* (but not other Drosophilid species) have a very strong preference for the marula fruit compared to other fruit, including their preferred European citrus fruit orange (Mansourian *et al.*, 2018). This was, in part, due to a citrus-like odorant (Ethyl Isovalerate) produced by marula which activates the Or22a olfactory neuronal circuit, similar to the species *D. erecta* that uses the same mechanism to ensure seasonal-specialism to the *Pandanus* cones (Rio, 1983; Linz *et al.*, 2013). *D. melanogaster* may

have adapted a seasonal dormancy-like response to entrain their life-cycle to the availability of the preferred marula fruit.

Early human tribes in these forests collected and stored the fruit thus prolonging the marula season (Walker, 1995). *D. melanogaster* has a high alcohol tolerance, and is more comfortable in dark spaces compared to closely related *Drosophilae* species (McKenzie and Parsons, 1972; David *et al.*, 2004). This may have allowed it to fulfil this niche. It is thus likely that it evolved alongside this seasonal selection pressure not in line with changing photo/thermo periods but with the availability of the marula fruit. Indeed, *D. melanogaster*'s most closely related cousin, *D. simulans*, was found to have a steady population throughout the year in Zimbabwe, whereas *D. melanogaster* showed clear population booms during the "marula season" (Mansourian *et al.*, 2018). *D. simulans* do not show geographic clines and struggle to survive high latitudes during the winter. In Europe, it is thought that *simulans* populations either die during the winter and re-populate these areas each summer or undergo a type of small-scale migration (Sedghifar *et al.*, 2016). It is then possible, that the shallow seasonal dormancy of *D. melanogaster* evolved in sub-tropical Africa, and was then adapted by later European and American populations that evolved and are continuing to evolve to survive the cold, short winter days of temperate and sub-arctic latitudes.

The fact that colonisation of these climates may be as recent as 1,800 years, it is no wonder that the dormancy/diapause phenotype of these flies is less robust than in other insect species: It is still in its early stages of evolution. Indeed, we can see this evolution in real-time by the spread of the pro-diapausing *Is-tim* allele across Europe (Tauber *et al.*, 2007; Pegoraro *et al.*, 2017; Zonato *et al.*, 2018). Diapause in *D. melanogaster* not only acts as a model for understanding the phenotype itself, but also as an interesting study at how organisms are able to adapt their survival mechanisms to new selection pressures and vastly different environments than they evolved in. This will become increasingly interesting as global warming persists and *D.*

*melanogaster* colonise evermore northern latitudes where the environment presents even more dramatic seasonality.

### 1.3.5 Hormonal control of diapause

Diapause induction in insects, including *D. melanogaster*, is highly hormone-dependent. The main endocrine centres in the adult female fly are the protocerebrum (specifically the *pars intercerebralis* (PI) and *pars lateralis* (PL)), the *corpora allata* (CA) and *corpora cardiaca* (CC) located in the abdomen, the fat bodies, and the ovaries (specifically the ovarian follicle and nurse cells) (Toivonen and Partridge, 2009). From these centres, hormones are released in a regulated and systemic manner in response to either diapause-inducing or non-diapause inducing stimulus to regulate egg-chamber development (**Figure 1-10**). This is achieved either through direct release to the target tissue via extended axons, or indirectly through secretion into the haemolymph system (Géminard *et al.*, 2009; Schiesari *et al.*, 2016).

### 1.3.6 Insulin-like signalling and diapause

Insulin-like signalling (ILS) is the most well-studied molecular and genetic regulator of diapause and appears to be the limiting step that decides if egg-chamber development will halt or continue. This was most elegantly demonstrated by Schiesari *et al.* (2016) through the use of various genetic manipulations of the ILS pathway to force flies to enter diapause in non-diapausing conditions, or to maintain total fecundity in ordinarily diapausing conditions. Many other studies have also helped to map out and understand the mechanism of ILS control of diapause (LaFever *et al.*, 2005; Williams *et al.*, 2006; Grönke *et al.*, 2010; Bai *et al.*, 2012; Kubrak *et al.*, 2014; Schiesari *et al.*, 2016; Liu *et al.*, 2016; Rauschenbach *et al.*, 2017; Durmaz *et al.*; 2019).

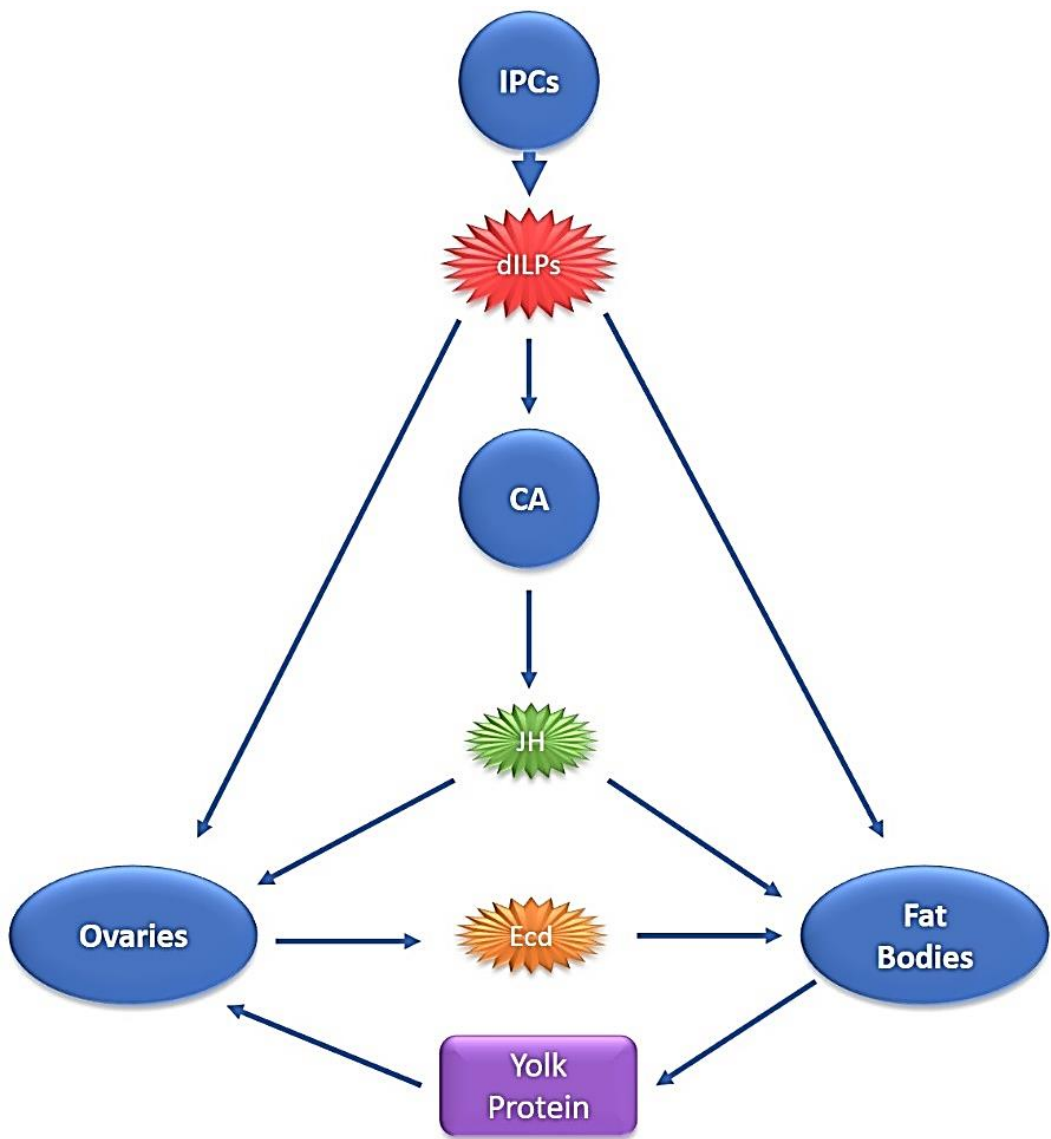


**Figure 1-10.** A simplified schematic of the endocrine signalling system governing vitellogenesis. The insulin producing cells (IPCs) produce drosophila insulin-like peptides (dILPs) which are secreted and bind to receptors in the *corpora allata* (CA), Ovaries and Fat bodies. The CA produces Juvenile Hormone (JH) which is secreted to the fat bodies and ovaries. The Ovaries produce Ecdysone (Ecd) which is secreted to the fat bodies. The fat bodies then produce the Yolk proteins needed for vitellogenesis and these are taken up by the ovaries.

Downregulation of *phosphatidylinositol-4,5-bisphosphate 3-kinase* (*Pi3K*), a key component of ILS pathway, results in an increase in diapause (Williams *et al.*, 2006). Furthermore, there is a clear latitudinal cline in genetically differing alleles of *Pi3K*. Its importance in diapause may be sufficient to drive this cline providing an advantage for certain alleles in higher latitudes (Williams *et al.*, 2006). Several other SNPs/alleles present in components

of the ILS pathway have also been shown to have latitudinal clines in studies conducted from natural populations across several continents: *dilp3*, *dilp5*, *InR*, *forkhead (FKH) box O transcription factor (foxo)*, target of rapamycin (*TOR*), *tuberous sclerosis complex 1 (tsc1)*, *target of brain insulin (Tobi)*, *14-3-3 $\epsilon$* , and *phosphatidylinositol-4,5-bisphosphate 3-kinase (Pi3K)* (Fabian *et al.*, 2012; Kapun *et al.*, 2012a; Paaby *et al.*, 2014; Durmaz *et al.*, 2019). The majority of these studies did not investigate diapause levels directly, thus, their precise effects on this phenotype is speculative. Nonetheless, clines in ILS correlate with diapause associated traits, such as resistance to starvation, altered metabolisms, decreased fecundity and increased longevity.

The ILS pathway begins with the insulin-like ligands themselves. There are 8 *drosophila*-Insulin-Like-Peptides (dILPs) identified in *D. melanogaster*, dILP1-7 all bind to the same receptor, Insulin Receptor (*InR*) (Grönke *et al.*, 2010) whereas dILP8 binds to the Lgr3 receptor and is the most unique dILP in terms of its amino acid sequence (Colombani *et al.*, 2012; Garelli *et al.*, 2015; Okamoto and Yamanaka, 2015). Although the dILPs all share homology, and indeed some share redundancy and compensation (Grönke *et al.*, 2010), distinct functionality is achieved through differing expression patterns, both temporally and spatially (**Table 1-2**).

**Table 1-2.** The expression of each *D. melanogaster* Insulin Like Peptide (dILPs) in the adult female fly, including expression, location and its role in diapause. References for each expression pattern and evidence in diapause induction for each dILP is given.

dILP	Expression in Adult Females	Known role in diapause?	References
dILP1	IPCs (only in diapausing flies)	Increased expression when diapausing, role unknown.	Liu <i>et al.</i> , 2016
dILP2	IPCs	Antagonistic	Brogiolo <i>et al.</i> , 2001; Rulifson <i>et al.</i> , 2002
dILP3	IPCs	Antagonistic	Brogiolo <i>et al.</i> , 2001; Rulifson <i>et al.</i> , 2002
dILP4	NO	NO	
dILP5	IPCs, Follicle cells in the ovaries	Antagonistic	Brogiolo <i>et al.</i> , 2001; Rulifson <i>et al.</i> , 2002
dILP6	Adipose cells in fat bodies	Agonistic	Okamoto <i>et al.</i> , 2009; Bai <i>et al.</i> , 2012
dILP7	Abdominal neurons in VNC	NO	Yang <i>et al.</i> , 2008a
dILP8	Ovaries	Unknown	Colombani <i>et al.</i> , 2012

dILP2, dILP3 and dILP5 are all expressed in the median neurosecretory cells (MNCs) located in the *Pars intercerebralis* (PI) of both the larval and adult brain (Broughton *et al.*, 2005), specifically, in a population of 14 cells that are commonly referred to as the Insulin Producing Cells (IPCs). Of these three dILPs, dILP2 accounts for 80% of the expression from the IPCs (Buch *et al.*, 2008), although this may not be the case when in diapause-

inducing conditions. Ablation of the IPCs prevents egg formation and forces females to enter diapause. Furthermore, mutants for these three dILPs (dILP2,3,5) displayed a 100% diapause phenotype in flies kept at 12°C for 28 days. Strikingly, this diapause state was still maintained when these mutant flies were switched to temperatures as high as 19°C, much higher than normal diapause-inducing temperatures (Schiesari *et al.*, 2016). dILP5 is also expressed at high levels in the follicle cells of the ovaries (Brogiole *et al.*, 2001).

Expression of dILP1 is unusual in the adult fly and it is absent in males and in non-diapausing females after only a few hours post-eclosion (Rulifson *et al.*, 2002; Broughton *et al.*, 2005). However, in diapausing females, dILP1 expression is maintained in the IPCs for up to 9 weeks. Expression is lost once flies exit diapause-inducing conditions and cannot be re-induced (Liu *et al.*, 2016). dILP1 expression in the IPCs is upregulated by dILP6 released from the fat bodies, as well as the neurotransmitter sNPF released from the *pars lateralis* (PL), but is negatively regulated by dILP2,3 and 5. Interestingly, *dilp1* mutants show no change in diapause levels, suggesting either a compensatory redundancy with the other IPC dILPs or perhaps that dILP1 signalling is downstream of diapause induction (Liu *et al.*, 2016).

dILP6 is expressed predominantly in adipose cells in the fat bodies located in the head and abdomen (Okamoto *et al.*, 2009; Bai *et al.*, 2012). Overexpression of *dilp6* increases diapause incidence and induces metabolic change across the entire body of the fly as well as increased resistance to oxidative stress (Bai *et al.*, 2012). dILP6 is also involved in a negative feedback loop with the anti-diapausing hormone Juvenile Hormone (JH) in the fat bodies, and in negative regulation of the IPCs via inhibition of DILP2,3,5 expression (Bai *et al.*, 2012; Rauschenbach *et al.*, 2017).

dILP7 is expressed in abdominal neurons located in the ventral nerve cord (VNC) that connect to the female reproductive tract (Yang *et al.*, 2008a), however, surprisingly, dILP7 does not seem to be important for reproduction

or fecundity (Grönke *et al.*, 2010). Likewise, dILP4 too plays no part in diapause regulation. It is a non-adult dILP and mostly expressed at the embryonic stage of development in the midgut and mesoderm (Brogiole *et al.*, 2001).

The relatively recently discovered dILP8 has been predominantly studied in the pre-adult stages of *Drosophila* development, particularly the larval stage, but not in the context of adult diapause (Colombani *et al.*, 2012; Sanchez *et al.*, 2019; Boulan *et al.*, 2019). Expression is however found in the ovaries (Colombani *et al.*, 2012) and dILP8 is known to block ecdysone synthesis in developing larvae (Boulan *et al.*, 2019), a vital hormone in egg-chamber development, suggesting a possible role in diapause regulation in adult flies.

Binding of the dILPs to InR at their target tissue (ovary, corpora allata, fat body, IPCs) activates an intracellular signalling cascade (**Figure 1-11**) (reviewed in Stocker and Hafen, 2000; Semaniuk *et al.*, 2021). dILP-bound InR self-phosphorylates, activating itself (Yenush *et al.* 1996) and resulting in the recruitment and phosphorylation of its intracellular substrate CHICO (Clancy *et al.*, 2001). *Drosophila*, with even weak hypomorphic mutants of *chico*, show elevated diapause levels across a range of temperatures compared to wild type flies (Schiesari *et al.*, 2016). The CHICO-InR complex then allows activation of PI3K which in turn phosphorylates the membrane-bound phosphatidylinositol (4,5)-diphosphate (PIP2) into phosphatidylinositol (3,4,5)-trisphosphate (PIP3) (Leevers *et al.*, 1996). The role of PI3K in diapause induction has also been documented, and unsurprisingly, mimics the phenotype of *chico* mutants (Williams *et al.*, 2006). PIP3 phosphorylates Akt, a *Drosophila* protein kinase B (Sarbassov *et al.*, 2005) which, as well as indirectly activating the Target of Rapamycin (TOR) signalling pathway (Reviewed by Ersahin *et al.*, 2015), phosphorylates and thus deactivates *Drosophila* forkhead transcription factor (dFO XO) (Jünger *et al.*, 2003; Puig *et al.*, 2003). The deactivated form of dFO XO is prevented from entering the nucleus where it would otherwise bind to the promoters of many stress and growth-related genes (Jünger *et*

*al.*, 2003; Kramer *et al.*, 2003), including many related to diapause (Bai *et al.*, 2012; Mirth *et al.*, 2014; Koyama *et al.*, 2014; Schiesari *et al.*, 2016). One interesting target of FOXO is the promoter of InR which ensures that ILS in the cell is ready for further signalling events, providing a positive feedback mechanism (Puig *et al.*, 2005).

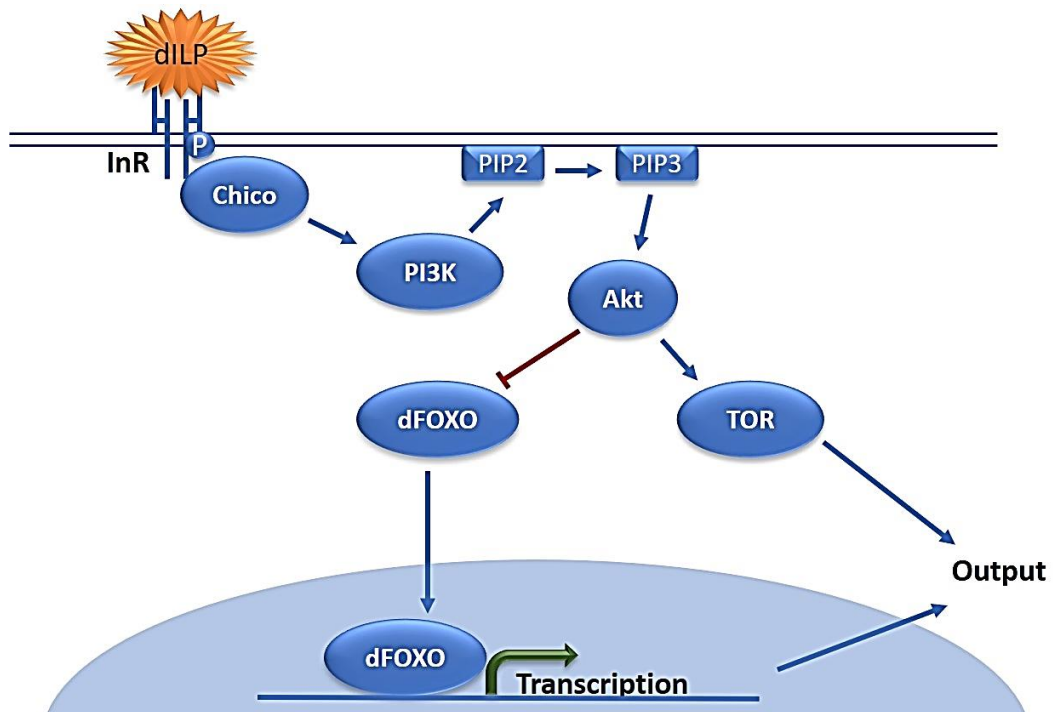


**Figure 1-11.** dILP signalling cascade. The dILPs bind to the insulin receptor (InR) activating it via self-phosphorylation. Chico is recruited which activates PI3K, which in turn converts PIP2 into PIP3. PIP3 activates Akt which indirectly activates the TOR signalling pathway and also inhibits dFO XO. This inhibition of dFO XO prevents it from entering the nucleus where it would otherwise act as a transcription factor.

### 1.3.7. Hormonal control of diapause downstream of the IPCs

From the IPC's, dILP<sub>2,5</sub> and probably dILP<sub>3</sub> are secreted into the haemolymph and bind to InR in the CA resulting in the synthesis of Juvenile Hormone (JH) (Richard *et al.*, 2005; Tu *et al.*, 2005; Schiesari *et al.*, 2016; Rauschenbach *et al.* 2017; Andreatta *et al.*, 2018). JH has been shown to be essential in diapause regulation, and Inhibition of JH synthesis or JH secretion has been demonstrated to prevent vitellogenesis (Bownes, 1982;

Saunders *et al.*, 1990; Flatt *et al.*, 2005; Tu *et al.*, 2005; Flatt and Kawecki, 2007).

JH secreted from the CA targets both the ovaries and the fat bodies. In the fat bodies it induces the synthesis of yolk proteins used in the early stages of egg-chamber development (Saunders *et al.*, 1990; Socha *et al.*, 1991) as well as activating dILP6 expression (Rauschenbach *et al.*, 2017). In the ovaries, JH further activates yolk protein production by the follicle nurse cells, as well as activating synthesis and secretion into the haemolymph of the hormone ecdysone (Richard *et al.*, 1998; Richard *et al.*, 2001). Ecdysone is then taken up by the fat body and converted into its active form 20-hydroxyecdysone (20-OH Ecd) which binds to the transcription factor Ecd-Receptor (Carney and Bender, 2000; Petryk *et al.*, 2003; Okamoto and Yamanaka, 2020).

20-OH Ecd promotes the expression of mid-late-stage yolk protein production in the fat body (Richard *et al.*, 1998; Buszczak *et al.*, 1999; Carney and Bender, 2000; Richard *et al.*, 2001). Ecdysone production is essential for late-stage egg-chamber development and topical application of the hormone is able to reverse diapause (Richard *et al.*, 1998; Richard *et al.*, 2001; Tatar *et al.*, 2001). Although 20-OH Ecd is essential for vitellogenesis, too high levels of the active hormone during early stages of vitellogenesis (pre-stage 9) results in apoptosis of the follicle nurse cells and thus hindered egg-chamber development. JH levels at this stage counteracts the pro-apoptotic nature of 20-OH Ecd demonstrating that a controlled balance of the two hormones is needed (Soller *et al.*, 1999). 20-OH Ecd in the fat body also regulates dILP6 expression which in turn acts as a negative feedback loop to negatively regulate JH expression in the fat body and CA, and dILP2,3,5 expression in the IPCs (Bai *et al.*, 2012; Rauschenbach *et al.*, 2017). Once post-stage 9 of vitellogenesis, both JH and 20-OH Ecd work in synergy to complete vitellogenesis and complete egg-chamber development (Soller *et al.*, 1999; He *et al.*, 2011).

Under diapause-inducing conditions, dILP production in the IPCs is dramatically reduced (Schiesari *et al.*, 2016), which in turn leads to a decrease in JH and 20-OH Ecd production (Saunders *et al.*, 1990; Richard *et al.*, 2001). This inevitably results in a lack of yolk protein produced and thus vitellogenesis is blocked (Saunders *et al.*, 1990; Soller *et al.*, 1999; Flatt *et al.*, 2005; Tu *et al.*, 2005; Flatt and Kawecki, 2007) (**Figure 1-12**).

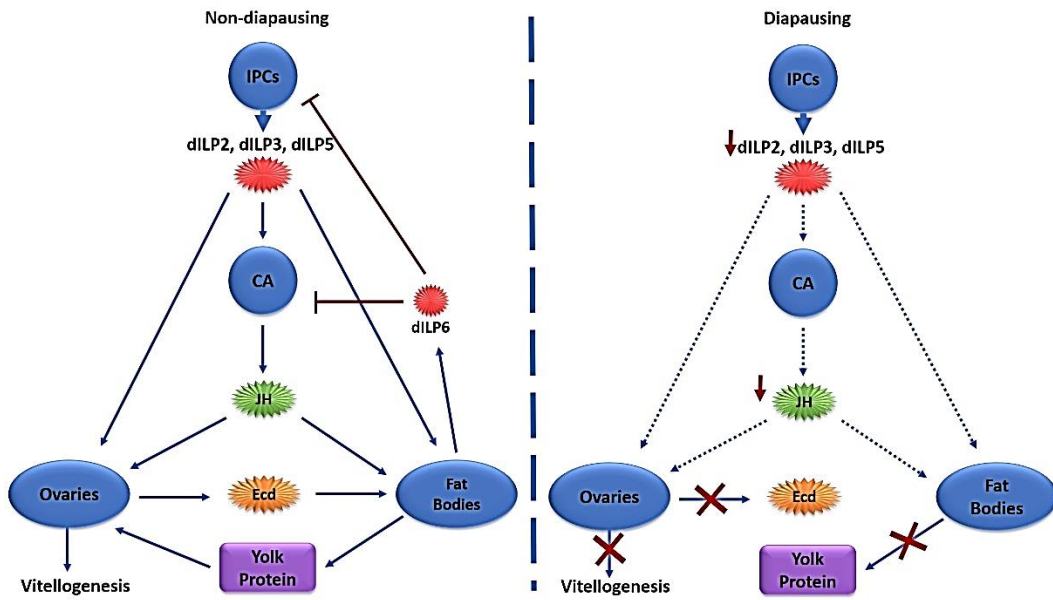


**Figure 1-12.** A simplified schematic of the endocrine signalling system governing vitellogenesis under non-diapausing (A) and diapausing (B) conditions. A) Under non-diapausing conditions, the insulin producing cells (IPCs) produce drosophila insulin-like peptides (dILPs), specifically dILP2, dILP3 and dILP5, which are secreted and bind to receptors in the *corpora allata* (CA), Ovaries and Fat bodies. The CA produces Juvenile Hormone (JH) which is secreted to the fat bodies and ovaries. The Ovaries produce Ecdysone (Ecd) which is secreted to the fat bodies. The fat bodies then produce the Yolk proteins needed for vitellogenesis and these are taken up by the ovaries. The fat body also produces dILP6 which has an inhibitory feedback role in repressing JH synthesis in the CA and dILP synthesis in the IPCs to prevent excessive signalling. B) Under diapausing conditions, dILP production from the IPCs is inhibited, resulting in less JH produced in the CA. This effects all downstream signalling and therefore yolk protein production in the fat bodies is arrested. This results in a halt in vitellogenesis and therefore the diapausing phenotype.

### 1.3.8 Neurosensory regulation upstream of the IPCs

Control of the insulin pathway and downstream endocrine systems are clearly fundamental in the regulation of vitellogenesis and diapause.

However, the fly requires the ability to sense and interpret environmental changes in order to make the decision to enter diapause or not. The components involved and the mechanisms used to achieve this have remained the most poorly understood area of the field. It is only recent advancements that have started to shine light on the elements upstream of ILS (Andreatta *et al.*, 2018; Nagy *et al.*, 2019; Abrieux *et al.*, 2020).

A recent study by Abrieux and colleagues (2020) has attempted to understand the link between environmental stimulus and endocrine output through their investigation of the developmental gene Eyes Absent (EYA). EYA is a co-transcription factor important for the development of the *Drosophila* compound eye as well as other developmental processes (Bonini *et al.*, 1993; Bai and Montell, 2002), and until recently had not been thought to have much of a role in the adult fly. However, Abrieux *et al.* (2020) demonstrated EYA expression in both the optic lobe and in the IPCs of adult flies. When EYA expression was knocked down in either tissue there was a reduction in diapause levels, whereas overexpression in either tissue had the opposite effect suggesting an agonistic role of EYA in diapause regulation. Furthermore, both mRNA and protein levels of EYA are higher, and continue to increase over time, in diapause-inducing conditions compared to non-diapause-inducing conditions (Abrieux *et al.*, 2020). An interesting observation in the study was that both mRNA and protein levels show circadian oscillation, suggesting a possible circadian influence. Additionally, the time at which EYA protein levels peak changes in line with changes in photoperiod. However, due to a limitation in experimental design, it is unclear if the effects were due to photoperiod or to subtle temperature changes. The group also found that EYA protein stability is directly linked to that of the circadian protein TIM (for a more detailed account see **chapter 3**). However, mutation of the essential circadian gene *Clk* showed no change in diapause levels, suggesting that EYA sensing of photoperiod (or temperature) is independent of a working clock. Although this work provides one input of environmental signal to the IPCs *eya* mutants were not able to knock down diapause incidence completely, and EYA overexpression was not capable to force a 100% diapause incidence

(unlike manipulation of ILS (Schiesari *et al.*, 2016)). Therefore, there are likely other pathways and input mechanisms upstream of ILS.

The IPCs express several receptors for aminergic neurotransmitters which allow reception of signals from adjacent neurons. These include the serotonin receptor 5-hydroxytryptamine receptor 1A (5-HT1A) which has been shown to regulate dILP2 and dILP5 expression in the IPCs (Luo *et al.*, 2012; Andreatta *et al.*, 2018). Knock down of 5-HT1A causes an increase in *dilp2* and *dilp5* mRNA and results in a decrease of diapause. On the other hand, constitutive activation of 5-HT1A cells via the sodium channel NaCHBac has the opposite effect, suggesting a diapause-inducing role of serotonin in the brain. Furthermore, 5-HT1A knock down in the IPCs led to a reduction in downstream ILS in the abdomen and thorax adding support to its role at inhibiting diapause via insulin signalling (Andreatta *et al.*, 2018).

Octopamine too may have a regulatory role of ILS from the IPCs, but in an antagonistic manor. The Octopamine Receptor in Mushroom Body (OAMB) is expressed in the IPCs and known to regulate dILP production (Luo *et al.*, 2014). Unlike serotonin, knock down of OAMB in the IPCs did not have any effect on diapause levels. However, activation of OAMB<sup>+</sup> neurons with NaCHBac did decrease diapause, suggesting that octopamine acts in an antagonistic way to inhibit diapause under non-diapausing conditions (Andreatta *et al.*, 2018). In other studies, flies mutant for dILP2,3,5 have decreased levels of Octopamine, however diapause levels are increased (Metaxakis *et al.*, 2014; Schiesari *et al.*, 2016). The role of octopamine in diapause regulation therefore remains unclear.

Diapausing females show very high levels of another aminergic neurotransmitter, dopamine. Compared to flies kept at non-diapause-inducing conditions, diapausing flies can express up to twice as much dopamine (Andreatta *et al.*, 2018). The dopamine receptor (DopR1) is expressed in the IPCs, CA and fat body, all major endocrine signalling

centres involved in diapause (Gruntenko *et al.*, 2012; Rauschenbach *et al.*, 2017; Andreatta *et al.*, 2018). Mutants in genes required for dopamine synthesis (*pale* and *Ddc*) or for *DopR1* cause a decrease in diapause levels in flies kept in diapause-inducing conditions (Andreatta *et al.*, 2018). Localised knock-down of the receptor in either the IPC, CA or fat body also caused a reduced diapause phenotype suggesting a key role for dopamine signalling in all diapause-linked endocrine centres. Knock-down of the other dopamine receptor *DopR2* however had no effect on diapause. Andreatta and colleagues (2018) also found that inhibition of Protein Kinase A in these tissues had the same effect and disrupted both ILS and JH synthesis further linking dopamine to ILS-dependent diapause (Andreatta *et al.*, 2018).

GABAergic signalling and insulin signalling is also strongly linked, especially in response to feeding, with feedback from the fat body negatively influencing expression of dILP2,3 and 5 from the IPCs. This is achieved through the release of Dilp6 and UNPAIRED 2 (UPD2) from the fat body which activate GABAergic neurons adjacent to the IPCs which communicate directly to the IPCs (Enell *et al.*, 2010; Rajan and Perrimon, 2012; Sheldon *et al.*, 2011). However, the involvement of GABA signalling in the IPCs seems to be limited to control of metabolism either in a non-diapausing manor, or perhaps downstream of diapause-induction (Andreatta *et al.*, 2018).

Although Serotonin and Dopamine promote (and Octopamine possibly inhibits) diapause induction through contact with the IPCs, and in the case of dopamine also the CA and fat bodies, which neurons these neurotransmitters are released from still remains unclear. Identification of these neurons will help fill in the missing piece of the puzzle of diapause induction: how are environmental cues interpreted and transmitted to the IPCs (and other endocrine centres) to promote/inhibit diapause induction?

### 1.3.9 The circadian clock and diapause

For diapause to be an effective seasonal phenotype the organism must be able to tell which time of year it is in. This could evolve as an independent mechanism, or it could co-evolve with the circadian clock. The latter is the more logical option as the circadian machinery of the organism is already capable of determining day length, and it is decreasing day length and daily temperatures that signals the approach of winter.

The strongest zeitgeber for circadian rhythmicity in *D. melanogaster*, and indeed most organisms is light. However, the diapause phenotype only appears to be permissive to changes in photoperiod in the temperature ranges of 10-13°C (Saunders *et al.*, 1989). This is not uncommon, as temperature-specific photoperiodism is found to regulate diapause in many insect species (Bradshaw and Holzapfel, 2010). However, in *D melanogaster*, there is much debate to the relevance of photoperiod even in the permissive range (Tatar *et al.*, 2001; Emerson *et al.*, 2009b; Zhao *et al.*, 2016; Zonato *et al.*, 2017; Anduaga *et al.*, 2018; Lirakis *et al.*, 2018; Nagy *et al.*, 2018) (See also **chapter 5**). The fact that the same experiments conducted by different groups often present opposite results further adds confusion to the link between seasonality and the clock (Helfrich and Englemann, 1987; Saunders *et al.*, 1989; Saunders, 1990; Nunes and Saunders, 1999; Tauber *et al.*, 2007; Emerson *et al.*, 2009b; Bradshaw and Hozapfel, 2010; Andreatta *et al.*, 2018).

A mechanism linking circadian and seasonal clocks together was first proposed by Bunning in 1936, termed the “Bunning hypothesis” (Saunders, 2005). The model states that the photoperiodic diapause response utilises a light-sensitive aspect of the circadian clock at a very specific period of the day. During long summer days, light would activate this “sensitive” component and inhibit diapause, however in short winter days this sensitive period would fall during the night and thus inhibition is lifted and diapause induced. This model was further modernised and updated by Pittendrigh who theorised two alternate versions, the external and the internal

coincidence models (Pittendrigh, 1972). An alternative model is one that does not involve the circadian clock and was termed the hourglass model by Lees (1973) which too has been elaborated on over the years to produce variations on the theme (Nunes and Saunders, 1999; Bradshaw and Hozapfel, 2010). The basis for the hourglass model is that the organism “counts” the number of hours in darkness/ in light, possibly through the accumulation of a protein, compound or signalling event, and this informs the decision to diapause or not.

For photoperiodic diapause to be truly dependent on a working circadian clock, a detrimental change in the clock should have detrimental effects on diapause too. This is however difficult to investigate, as it would require separating photoperiodic diapause components from non-photoperiodic diapause components. The two may be interlinked and components interchangeable. The fact that the clock neurons are responsive to temperature as well as light makes this increasingly difficult (Zhang *et al.*, 2010a; Zhang *et al.*, 2010b). Nevertheless, using genetic manipulation of core components of the well-studied circadian clock (see **chapter 1.2**) its link to diapause control can be assessed.

The DN1 clock neurons in adult flies have been shown to have synaptic connection to the IPCs and have been shown to promote circadian-timed secretion of dILPs to control metabolism in the fat bodies (Barber *et al.*, 2016). Although this study did not look at diapause itself, metabolism from the fat bodies is a key component of diapause. Furthermore, the DN1s are important clock cells for coordination of light and temperature input into the clock (Miyasako *et al.*, 2007; Zhang *et al.*, 2010a; Zhang *et al.*, 2010b). It is possible that environmental temperature or light input into the central clock via the DN1s is relayed to the IPCs to regulate ILS in a diapause context.

The IPC cells also contain receptors for the circadian neurotransmitter peptides sNPF and PDF, sNPDR1 and PDFR respectively (Lear *et al.*, 2005; Shafer *et al.*, 2008; Kapan *et al.*, 2012; Carlsson *et al.*, 2013). Nagy and colleagues (2019) found that secretion of both neuropeptides from the

s-LNv clock cells activated IPC cells via an increase of cAMP and this resulted in a reduction of diapause, possibly due to an inhibition of ILS (Nagy *et al.*, 2019).

The IPCs seem to have an anatomical and probable functional link to clock cells: But this does not implement the circadian clock itself in diapause regulation. To do so, mutational studies of core clock genes is needed. Indeed, unpublished data from previous laboratory members have found that mutants for the core clock genes *per*, *tim*, *clk* and *cyc* all effect diapause levels: Martin Anduaga (2018) found that *Clk<sup>Jrk</sup>*, *cyc<sup>0</sup>* and *per<sup>01</sup>* mutant flies all showed reduced diapause whereas *cry<sup>b</sup>* flies had elevated diapause levels. Furthermore, the rearing temperature of flies in these mutants showed a significant and dramatic difference in diapause incidence (Martin Anduaga, 2018). Gesto (2011) found that *per<sup>01</sup>* and *Clk<sup>Jrk</sup>* mutants had lower diapause incidence. He also found that *tim<sup>01</sup>* flies had increased diapause levels (consistent with Tauber *et al.*, (2007) but contradictory to Andreatta *et al.* (2018)). From these observations it would favour the theory of a circadian clock working as a single module to regulate diapause induction because any mutation of a core component of the clock has an effect on diapause. Unfortunately, data from the published field is less straightforward.

The circadian gene with the strongest link to diapause so far is *timeless*. The *tim* gene has two distinct alleles *s-tim* and *ls-tim*. The *ls-tim* allele enhances diapause levels across photoperiods (Tauber *et al.*, 2007) thought to be due to inhibited binding of CRY to the LS-TIM isoform and therefore a reduced sensitivity to light (Sandrelli *et al.*, 2007). Interestingly, comparison between the two alleles does not affect the photoperiodic response in *D. melanogaster* as the rate of change in diapause as photoperiod changes is identical in both alleles. Instead, the *ls-tim* allele enhances diapause levels across all photoperiods (Tauber *et al.*, 2007). The effects of null mutations of TIM however have been contradictory between studies. Tauber *et al.* (2007) found an increased diapause incidence in *tim<sup>01</sup>* flies and a loss of photoperiodism, whereas Andreatta *et al.* (2018) found the opposite. Likewise, Gesto (2011) found an increase in diapause in *tim<sup>01</sup>*

mutants whereas Martin Anduaga (2018) found no difference in diapause levels, although the rearing conditions between the two studies were different.

Unlike *tim*<sup>01</sup>, *per*<sup>0</sup> mutant flies appear to maintain photoperiodicity in relation to diapause incidence. Original studies on circadian genes and diapause by Saunders showed that *per*<sup>0</sup> mutants were still able to sense changes in photoperiod similar to that of wild type flies. However, the levels of diapause compared to wild type flies did differ (Saunders *et al.*, 1989). This would indicate that the photoperiodic element of diapause control is not reliant on a functional clock. On the other hand, there is evidence that the arrhythmicity of the *per*<sup>0</sup> mutation is weak, and that in combination with the *cry*<sup>b</sup> mutation a PER-independent rhythmicity via TIM takes over, possibly via the I-LNvs (Dowse *et al.*, 1987; Helfrich and Engelmann, 1987; Collins *et al.*, 2005).

What is clear is that, components of the clock are important in regulating diapause. However, if this is due to pleiotropy of individual genes, mainly *timeless*, or due to regulation via the circadian module as a whole, is yet to be convincingly decoded.

## 1.4 Motivations and aims

The study of circadian rhythmicity in *D. melanogaster* has already proven fruitful for humanity, evident both anecdotally via the multiple contributions to medicine but also objectively via accreditation of the 2017 Nobel prize. Exercise (Wolff and Esser, 2019), metabolism (Dyar *et al.*, 2017), sleep disorders (Haspel *et al.*, 2020), renal function (Johnston *et al.*, 2018), cardiovascular diseases (Kaper *et al.*, 2018), pharmacology (Stéphanou *et al.*, 2018), and cancer (Sulli *et al.*, 2019) are just a selection of fields that have benefitted.

Humanity, as a species, has evolutionarily recently altered the zeitgebers we experience due to technological advancement such as artificial light and heat. This not only has consequence for our own health but that of other species subjected to urban living whose circadian clocks evolved outside of these artificial parameters. Therefore, studying the clock in a more natural setting is the important next step to better understand societal impact on chronobiology. This is what forms the basis of **chapter 6**.

The remainder of this thesis concentrates on diapause (**Chapters 3, 4 & 5**). On the surface, the purpose of studying diapause may at first seem as a means to satisfy arbitrary curiosity. This alone is a noble pursuit, and humanity and science benefits from a greater understanding of the natural world. However, the study of diapause also has significance in relation to biodiversity as well as direct and indirect consequences to humanity. Study into diapause led to the discovery of JH, and this subsequently led to the creation of Methoprene, an insecticide that blocks mosquitos developing into adults and thus vectors for disease (Staal, 1975; Bai *et al.*, 2010). Furthermore, the conserved nature of the insulin signalling pathway, and diapause-related metabolism between humans and *Drosophila* has implications in human-related disease management, particularly in relation to aging, diabetes and obesity (Claeys *et al.*, 2002; Denlinger *et al.*, 2008).

Aside from human benefit, diapause in *D. melanogaster* is relatively young and still evolving (Zonato *et al.*, 2017; Mansourian *et al.*, 2018; Sprengelmeyer *et al.*, 2020). Coupled with the increasing threat of global warming to ecosystem survival, the chance to study evolution in real time within a model organism with such an extensive genetic toolbox may aid in the management/control of the ongoing climate crisis (Bradshaw and Holzapfel, 2001; Umina *et al.*, 2005; Pierrehumbert, 2019).

This thesis aims to further investigate the genetic underpinnings of the diapause phenotype and in doing so better understand the relationship between the circadian clock and the diapause phenotype (**Chapters 3 & 4**). This thesis also will investigate the role that temperature has in controlling diapause in a more natural-like environment through the creation of semi-natural temperature profiles that enable smooth cyclic oscillations of temperature throughout the day (**Chapter 5**).

## 2. MATERIALS AND METHODS

### 2.1 Fly stock maintenance

Flies were kept in plastic tube vials in a standardised maize-based fly-food (**Table 1-1**). Stocks prior to experimentation were raised in a communal stock room kept at 25°C in L:D 12:12. For long-term storage, stocks were kept in a communal stock room at 18°C, L:D 12:12.

**Table 2-1.** Fly food recipe for maintenance of stocks and experimental flies

Component	Quantity
Water	7.5L
Maize	504g
Brewer's yeast	350g
Agar	59.5g
Glucose	555g
20% Nipagin in ethanol (added after boiling)	94.5ml
Propionic acid (added after boiling)	21ml

### 2.2 Diapause

#### 2.2.1 Experimental design

Flies were expanded in the 25°C stockroom prior to experimentation. Parental flies were pushed regularly to ensure no cross contamination with F1 progeny. On day 10 post-embryo, newly emerged flies were culled at the beginning of the day (ZT0-1). Newly emerged flies after this point were then collected at ZT4, ZT8, and ZT12 in fresh food vials and placed into incubator systems set at diapause-inducing conditions (expanded upon in each relevant chapter) for 14 days. Each “sample” placed into its incubator

contained between ~60 – 80 flies. Unless otherwise stated, diapause inducing conditions refers to 11.5°C at L:D 8:16. Unless otherwise stated, the incubator system used is an LMSTM 201 cooled incubator (11853410, ThermoFisher Scientific).

### **2.2.2 Dissection of flies prior to diapause scoring**

After 14 days in diapause-inducing conditions, flies were removed from their incubator at ZT6, immediately anesthetised by CO<sub>2</sub> and drowned in 70% industrial methylated spirit (IMS). After ~10 seconds in IMS, flies were washed 3 x 15 minutes in deionised water, and finally placed in 1x Phosphate-Buffered Saline (PBS) diluted from the following prepared 10x PBS recipe (**Table 2-2**):

**Table 2-2.** Recipe for 1L of 10x PBS

Compound	Quantity
NaCL	200g
KCL	5g
KH <sub>2</sub> PO <sub>4</sub>	5g
Na <sub>2</sub> HPO <sub>4</sub> ·2H <sub>2</sub> O	27.8g

Female flies were then dissected as described by Saunders *et al.* (1989), and scored for diapause incidence.

### **2.2.3 Scoring diapause**

Diapause in *Drosophila* has traditionally been scored as females whose egg chambers are previtellogenic (stages 0-7 according to King's classification (King, 1970)). However, some groups have observed that *Drosophila* actually blocks its oogenesis pre-stage 10 (Tatar *et al.*, 2001; Lee *et al.*, 2011). As such, in this study there are two methods of scoring diapause: a) scoring diapause using the traditional method (Saunders *et al.*, 1989) which was applied to experiments conducted at earlier stages of this project. b) scoring diapause from both stage <8 and <10, thus providing twice as much information for very little extra effort/time (**Figure 2-1**).

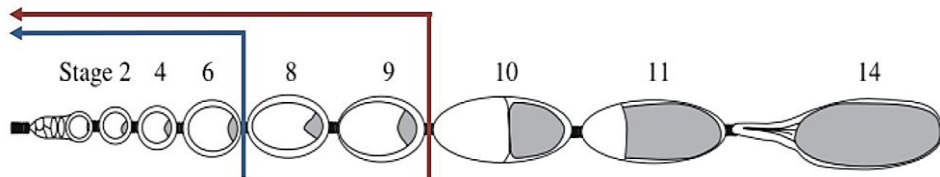


**Figure 2-1.** Schematic representation of the diapause scoring criteria used in this study. Each egg stage is represented as defined by King (1970). The yolk protein is represented in grey, whereby at each stage the relative amount of yolk protein increases. The traditional way of scoring diapause is from egg stage <8 (blue arrow), however it has been argued that scoring from egg stage <10 is more accurate (red arrow). Adapted from Ogienko *et al.*, 2007.

## 2.3 Locomotor activity

### 2.1 Experimental design

Individual flies were anaesthetised by CO<sub>2</sub> 3 days after eclosion and placed into glass vials with fly food at one end with a plastic cap to act as a lid, and a cotton plug at the other end. These were then placed into Trikinetiks *Drosophila* Activity Monitors (DAM) (Trikinetiks Inc, Waltham, USA) which contain an infra-red laser beam connected to Trikinetiks DAM computer software as described in Rosato and Kyriacou (2006). Each time the fly crosses the infra-red beam its activity is recorded and tallied in 30-minute intervals. These monitors were placed into incubator systems under environmental conditions as described in each relevant chapter.

#### 2.3.1 Recording rhythmicity

Flies in DAM activity monitors were placed into incubator systems set to environmental parameters described in each relevant chapter for five days. After the fifth day, flies are subjected to free-running conditions of constant darkness (D:D). The in-house spectral analysis and autocorrelation plug in for Microsoft Excel® 2016 “BeFly!” (Allebrandt *et al.*, 2013) was used to analyse the data. BeFly! separates the activity data into sine and cosine waves displayed as a spectrogram. Monte Carlo simulations then generate 100 randomisations to the data to calculate 95% and 99% confidence limits. Peaks that breach the 99% confidence limit and confirmed in the auto correlation graph were considered to be significant.

Peaks that occurred between 18hours and 30hours were considered to be circadian in nature and these flies were considered to be “rhythmic”.

## 2.4 Genomic DNA extraction

Individual flies were anesthetised by CO<sub>2</sub> and placed in 0.5ml PCR tubes and squashed with a miniature pestle in 50µl of squishing buffer (**Table 2-3**) for 10-15 seconds.

**Table 2-3.** Squishing buffer recipe

Compound	Quantity
EDTA (0.5M)	80 µl
Tris HCL pH8.2 (1M)	200 µl
NaCL (4.5M)	110 µl
Molecular grade ddH <sub>2</sub> O	19.61 ml

Proteinase K was added fresh to the squishing buffer prior to each new experiment to avoid enzyme degradation. 5µl of 40µg/ml of proteinase K was added per 1ml of squishing buffer. The squashed fly in solution was then placed into a cyclic water bath for the following program (**Table 2-4**).

**Table 2-4.** DNA extraction thermal cycler program

Temperature	Time
37°C	45 minutes
95°C	3 minutes
10°C	Infinite

## 2.5 mRNA and miRNA extraction

50 $\mu$ l of either *mRNA* or *miRNA* was extracted from 25-30 fly heads or 25-30 fly bodies via the Maxwell® 16 LEV simplyRNA Cells Kit (Promega, AS1270) using the Maxwell® 16 Instrument (Promega, AS2000) supplied by NUCLEUS Genomics facility (University of Leicester). Flies placed in Eppendorf tubes were homogenised for 30 seconds via a miniature pestle on ice in 1-Thioglycerol/Homogenization Solution supplied by the manufacturer. Subsequent steps were then followed as per the manufacturer's instructions.

## 2.6 DNA and RNA quantification

DNA and RNA was quantified and quality checked via the NanoDrop 8000 Spectrophotometer supplied by the NUCLEUS Genomics facility (University of Leicester).

## 2.7 DNase treatment

Any residual genomic DNA was removed from RNA extracted from the Maxwell® 16 instrument via the TURBO DNase kit (AM1907, ThermoFisher Scientific). The following protocol was followed:

1. 0.1 $\mu$ l of 10x TURBO DNase Buffer was mixed with 1 $\mu$ l of RNA and made up to a final volume of 10 $\mu$ l.
2. The mixed sample was incubated for 30 minutes at 37°C
3. 0.1 $\mu$ l of DNase inactivation reagent was added to the sample and placed in a shaker at room temperature for 5 minutes
4. Samples are centrifuged for 1.5 minutes at 10.000xg and the supernatant transferred to a new RNase-free PCR tube.

## 2.8 Reverse transcription

### 2.8.1 Reverse transcription of *mRNA*

10 $\mu$ l of mRNA per sample was added to 10 $\mu$ l of 2X RT master mix made via the High-Capacity cDNA Reverse Transcription Kit (Cat# 4368813 Thermo Fisher Scientific). The samples were run in a thermal cycler with the following program (**Table 2-5**):

**Table 2-5.** Thermocycle program for RT of mRNA.

Temperature	Time
25°C	10 minutes
37°C	120 minutes
85°C	5 minutes
10°C	infinite

### 2.8.2 Reverse transcription of miRNA

5 $\mu$ l of miRNA was mixed with 7 $\mu$ l RT Reaction Mix made via the TaqMan™ MicroRNA Reverse Transcription Kit (Cat# 4440886). 3 $\mu$ l of 5X RT primer was added and the mixed samples were run in a thermal cycler with the following program (**Table 2-6**):

**Table 2-6.** Thermocycle program for RT of microRNA.

Temperature	Time
16°C	30 minutes
42°C	30 minutes
85°C	5 minutes
10°C	Infinite

## 2.9 Polymerase Chain Reaction (PCR)

Primers were designed via Primer3web, version 4.1.0 (Koressaar and Remm, 2007). A general PCR mix was used (**Table 2-7**) however it was optimised for individual experiments. The 11.1x PCR buffer used was created with the following recipe (**Table 2-8**):

**Table 7.** PCR reaction mix used as a general template. \* The 11.1x buffer recipe is presented in Table 8.

Component	Quantity
11.1x Buffer*	2µl
Forward Primer	0.25µl
Reverse Primer	0.25µl
Taq Polymerase	0.2µl
Molecular-grade water	6.3µl

**Table 2-8.** PCR 11.1x buffer recipe

Component	Quantity
Tris HCL pH 8.8 (2M)	167 µl
Ammonium Sulphate (1M)	83 µl
MgCl <sub>2</sub> (1M)	33.5 µl
2-mercaptoethanol	3.6 µl
EDTA pH 8	3.4 µl
dATP (100mM)	75 µl
dCTP (100mM)	75 µl
dGTP (100mM)	75 µl
dTTP (100mM)	75 µl
BSA Albion (50mg/ml)	17 µl
Molecular-grade water	68 µl

The PCR mix was then run in a GS4 Multi Block Thermal Cycler (G-Storm) under a generic PCR amplification program (**Table 2-9**); however, the optimum annealing temperature will vary depending on the primer pair used per experiment, and the elongation time will vary depending on the length of fragment amplified.

**Table 2-9.** General PCR amplification program used. \* Program will vary depending on primers used and length of fragment amplified.

Cycles	Temperature	Time
1	98°C	2 minutes

30	92°C	45 seconds
	50 - 65°C*	30 seconds
	72°C	0.75 – 2 minutes*
1	72°C	10 minutes
1	10°C	Infinite

## 2.10 Genotyping

Genotyping of flies was achieved via specific PCR amplification techniques.

### 2.10.1 *per<sup>0</sup>* genotyping

To genotype flies for the *per<sup>0</sup>* mutation the following primers were used: per0F – ACGGTAATGAAGAAGGGTCAGA & per0R – GGGCCTGGAAGGTGAAATG. The PCR program used had an annealing temperature of 56°C and an elongation time of 30 seconds. The PCR product was then digested via the restriction enzyme XbaI (**Table 2-10**) in a thermocycle for 1 hour at 37°C, followed by 5 minutes at 92°C.

**Table 2-10.** *XbaI* restriction reaction mix for *per<sup>0</sup>* genotyping

Component	Quantity
10X cut smart buffer	5 µl
XbaI enzyme	1 µl
PCR product	10 µl
Water	34 µl

The restricted solution was then ran on a 1.5% agarose gel and analysed for the presence of DNA bands. A single band at 407bp indicates a wild-type *per* whereas two bands at 168bp and 238bp indicates the *per<sup>0</sup>* mutant

## 2.11 Genotyping for diapause-related alleles

The *tim-s/ls* and the *cpo* SNP A356V alleles have a strong influence on diapause induction. Therefore, prior to use in diapause assays all flies with unknown backgrounds were genotyped for both alleles.

### 2.11.1 Genotyping *cpo* SNP A356V

To genotype flies for the *cpo* A356V mutation the following primers were used: cpo-F - AACATCCGTTGCTGCTGTC & cpo-R - CCCCAAGCTGTCACCTTTGT. The annealing temperature was 55°C and the elongation time 30 seconds. The PCR product was then digested by the restriction enzyme *BsiEI* (**Table 2-11**) in a thermocycle for 1 hour at 37°C, followed by 5 minutes at 92°C.

**Table 11.** *BsiEI* restriction reaction mix for *cpo* A356V genotyping.

Component	Quantity
10X cut smart buffer	5 µl
<i>BsiEI</i> enzyme	1 µl
PCR product	10 µl
Water	34 µl

The restricted DNA was then ran on a 1.5% agarose gel. The *cpo356<sup>Val</sup>* allele will result in two DNA fragment bands of 222bp and 281bp, whereas the *cpo356<sup>Ala</sup>* allele will result in three bands of 90bp, 132bp and 281bp.

### 2.11.2 Genotyping for *s-tim* and *ls-tim*

Genotyping for the *s-tim* and *ls-tim* genotype was done so according to the methods set out in Tauber et al. (2007). Two individual PCR reactions were performed using a Forward primer either specific to *s-tim* (s-timF - TGGAATAATCAGAACTTTAT) or specific to *ls-tim* (ls-timF - TGGAATAATCAGAACTTTGA). A common reverse primer was used for both reactions (timR - AGATTCCACAAGATCGTGTT). A control primer pair was used to account for false-negative reactions (timCF -

CATTCATTCCAAGCAGTATC & *timCR* – TATTCACTGAACTTGTGAATC). The annealing temperature used was 55°C and the elongation time was 1 minute. The resultant PCR product was then run on a 1.5% agarose gel. The *s-tim* amplicon fragment is 692bp, the *ls-tim* fragment is 693bp and the control fragment is 487bp.

## 2.12 Quantitative PCR (qPCR)

### 2.12.1 qPCR of cDNA derived from mRNA

Analysis of mRNA levels via qPCR was achieved using the SYBR™ Green PCR Master Mix (ThermoFisher, #4309155). Primers were designed to amplify short ~100bp sequences using Primer3 software (Koressaar and Remm, 2007). 1 µl of cDNA was added to 2.5 µl of the SYBR-Green 2x Buffer along with 1 µl of the Forward and Reverse primer mix, and made up to 5 µl with molecular grade, RNase free water. The samples were run on a LightCycler 480 system (Roche) supplied by the Nucleus Genomics facility (University of Leicester) using the following qPCR and melting curve program (**Table 2-12**).

**Table 2-12.** The qPCR amplification program followed by the melting curve program used for qPCR analysis of cDNA.

Cycles	Temperature	Time
1	95°C	5 minutes
45	95°C	15 seconds
	62°C	30 seconds
	72°C	30 seconds
<b>Melting Curve</b>	65-97°C	30 seconds

The accompanying LightCycler 480 Software (Roche) was used to calculate the crossing points (Cp). Three technical replicates and a no-RT control were used for each sample. Data for replicas in which the Cp values are within 0.75 of each

accepted and the mean value used. Data was then normalised and compared to their respective controls.

### 2.12.2 qPCR of cDNA derived from microRNA

Preparation of *miRNA* derived cDNA for qPCR analysis was done using TaqMan™ MicroRNA Assay (ThermoFisher, # 4427975). 0.5 µl of the 20X assay mix was added to 5 µl of TaqMan™ Universal Master Mix II, with UNG (ThermoFisher, # 4440038) and 3.84 µl of molecular-grade water. This mixture was then transferred to 96-well plates and 0.67 µl of cDNA template or molecular-grade water control was added to each sample. Samples were then run in a LightCycler 480 system (Roche) supplied by the Nucleus Genomics facility (University of Leicester) using the following qPCR and program (**Table 2-13**).

**Table 2-13.** qPCR program used to quantify miRNA levels post reverse transcription.

Cycles	Temperature	Time
1	50°C	2 minutes
1	95°C	10 minutes
40	95°C	15 seconds
	60°C	1 minute

The accompanying LightCycler 480 Software (Roche) was used to calculate the crossing points (Cp). Three technical replicates and a no-RT control were used for each sample. Data for replicas in which the Cp values are within 0.75 of each accepted and the mean value used. Data was then normalised and compared to their respective controls.

### 2.13 Gel electrophoresis

Amplified DNA from PCR reactions were ran on agarose gels with concentrations ranging from 0.5%-2% depending on the fragment size. The gel contained ethidium bromide in a concentration of 0.5µg/ml. DNA was mixed with loading dye (**Table 2-14**) in a ratio of 1 µl of dye per 5 µl of DNA. Samples were

then loaded into the agarose gel and ran at a voltage of 80-120V in a gel tank containing 1X TBE buffer (**Table 2-15**). The Hyperladder I (Bioline) DNA marker was loaded in the lane prior to the first loaded sample to enable verification of fragment length and molecular weight. Gels were analysed via the GeneGenius bio-imaging system (Syngene) using the GeneSnap 6 software (Synoptics).

**Table 2-14.** recipe for 6x gel electrophoresis loading dye

Component	Quantity
Bromophenol blue	0.25g
Ficoll	31.25g
5x TBE	250ml

**Table 2-15.** recipe for TBE.

Component	Quantity
Trisma base	1090g
Boric Acid	550g
EDTA	93g
Distilled and filtered water	To 10L

## 2.14 Statistical Analysis

All graphs were created and statistical tests carried out via the GraphPad Prism 7 software unless otherwise stated.

### **3. THE ROLE of *miR-276b* AND *timeless* IN THE REGULATION DIAPAUSE**

#### **3.1 Introduction**

##### **3.1.1 microRNAs**

microRNAs (*miRNAs*), are non-coding *mRNA* transcribed in the range of ~100 to ~1000 nucleotides long, but after processing, are typically only ~22 nucleotides in length. A functional role for *miRNAs* was first discovered in *C. elegans*, serendipitously in 1993 (Lee *et al.*, 1993) and, in 2000, *miRNAs* were found to be functional in several other species, including humans and *D. melanogaster* (Pasquinelli *et al.*, 2000). Research in the 21<sup>st</sup> century has since proven that *miRNAs* are essential in regulating a vast array of biological processes in a plethora of organisms (Gebert and MacRae, 2019) with significant implications for human health (Mingardi *et al.*, 2018).

*miRNAs* can be found anywhere within the genome, either in intergenic regions or within coding genes. They are either transcribed individually or as “clusters” of closely spaced *miRNAs*, such as the *miR-317* cluster. This cluster is made up of three *miRNAs*: *miR-317*, *miR-34* and *miR-277* and is under the control of 20-OH Ecd to regulate the immune response (Xiong *et al.*, 2016). Most *miRNAs* are transcribed by RNA polymerase II, much in the same way as *mRNA* transcription, to produce primary *miRNAs* (pri-*miRNAs*) which fold into double-stranded hairpin structures (Lee *et al.*, 2002) (**Figure 3-1**). The double-stranded-RNA binding protein Pasha, in complex with the RNase-III enzyme Drosha binds to the pri-*miRNA*. This activates Drosha-dependent cleavage of the 5'cap and poly-A tail to create a pre-*miRNA* (Lee *et al.*, 2003). The pre-*miRNA* is then directed to the cytoplasm where another RNase-III cleavage protein Dicer-1 completes the cleavage to create a double stranded mature *miRNA* (Lee *et al.*, 2003; Jaubert *et al.*,

2007; Siomi *et al.*, 2008). Due to the cleaving nature of Drosher and Dicer, the resulting *miRNA* has imperfect complementation due to an exposed 5' phosphate and a ~2-nucleotide overhang on the 3' end (Lee *et al.*, 2003). The *miRNA* then binds to the RNA-induced silencing complex (RISC) via AGO-1 which activates degradation of the “passenger” strand of the *miRNA* by RISC to create a single stranded “guide” *miRNA*. AGO-1 bound *miRNA* then binds to its target *mRNA*, usually at the 3'-UTR (Schwarz *et al.*, 2003; Li and Liu, 2011; Wilson and Doudna, 2013). The entirety of the *miRNA* guide strand does not bind to its target *mRNA*. Instead, only a small number of nucleotides at the 5' end termed the “seed site” bind. The length of the seed site is usually 5-6 nucleotides long and is located between nucleotides 2-9 (counting from the 5' end) (Lewis *et al.*, 2005; Nahvi *et al.*, 2009). *miRNA-mRNA* binding in the RISC complex promotes *mRNA* degradation via GW182, thus altering the rate of translation of the target *mRNA*, and consequently, its protein levels (Behm-Ansmant *et al.*, 2006).

The expression of *miRNAs* is varied, and like coding genes they have their own promoters that allow spatial and temporal expression. They can bind to several targets, sometimes even hundreds, and single *mRNAs* can be targeted by several different *miRNAs*. This provides the organism with a greater scope for controlling protein expression than just via transcription factors and post-transcriptional/translational modification alone. It has also led to the evolution of and conservation of 3'UTRs of certain genes. This is particularly true for genes involved in development which have very specific expression patterns in time and space and as such their 3'UTRs can be unusually long, with several *miRNA* seed-site binding sequences (Stark *et al.*, 2005).

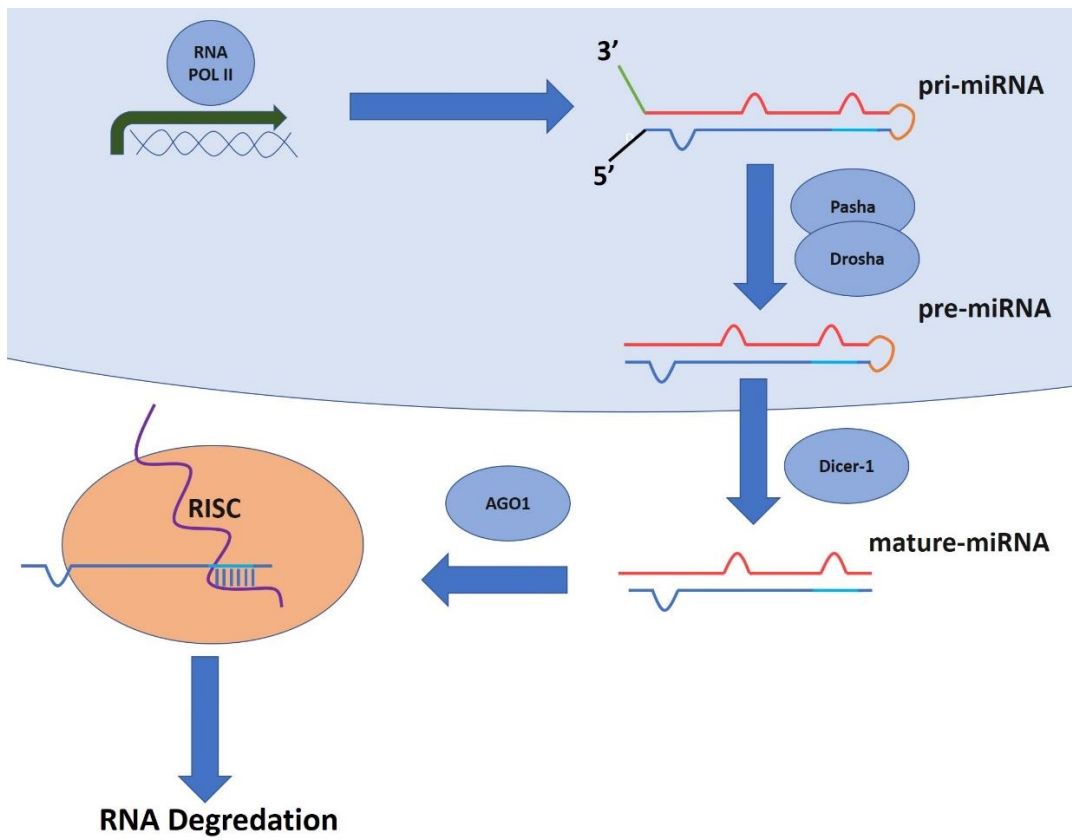


**Figure 3-1.** The biogenesis of miRNA. RNA Polymerase II (RNA POL II) transcribes from the genome to produce primary miRNA (pri-miRNA) made up of a “passenger” strand (red) and a guide strand (blue) which contains the seed site (turquoise). The pri-miRNA forms a hairpin structure linked via a loop (orange) with an exposed 5’ cap (black) and 3’ Poly-A tail (green). Pasha and Drosha bind to pri-miRNA and cleave the 5’cap and Poly-A tail to form pre-miRNA. pre-miRNA exits the nucleus and is cleaved by Dicer-1 to form mature miRNA. The mature miRNA enters the RNA-induced silencing complex (RISC) via AGO1 which mediates degradation of the passenger strand. The single-stranded miRNA guides RISC to its target mRNA (purple) and binds to it via the seed site. This targets the mRNA for degradation.

In *Drosophila*, novel roles of *miRNA* regulation are constantly being uncovered. Notch signalling, an essential pathway in *Drosophila* development, is highly regulated by *miRNAs*: for example, by *miR-1* and *miR-7* (Da Ros *et al.*, 2013; Zhu *et al.*, 2017). Other *miRNAs* with important function in *D. melanogaster* include: *miR-124*, *miR-137*, and *miR-184* which have been implicated in neurodegeneration and associated diseases (Kong *et al.*, 2015a; Kong *et al.*, 2015b; Peng *et al.*, 2015), and *miR-14*, *mir-278*, and *mir-305* which have been implemented in regulation of metabolism and

energy homeostasis (Xu *et al.*, 2003; Teleman *et al.*, 2006; Foronda *et al.*, 2014).

### 3.1.2 Circadian functions of *miRNAs* in *D. melanogaster*

*miRNAs* have also been heavily implicated in the control of the circadian clock and its outputs (Table 3.1). Mutation of GW182, a key protein that binds to AGO-1 to enable effective binding of *miRNAs*, renders flies arrhythmic (Zhang *et al.*, 2013). It was found that GW182-dependent *miRNA* signalling is downregulated in response to light, which, in turn, prevents its degradation of DNC, the enzyme responsible for converting cAMP into AMP. This ultimately results in a decrease in PDFR signalling, which is essential in the circadian response to light (Zhang *et al.*, 2013).

**Table 3-1.** The circadian-linked control of *miRNAs* in *D. melanogaster*, including the mRNA target for each *miRNA*, the circadian role that the *miRNA* expresses, and the relevant references. For a more detailed explanation of the circadian role of each *miRNA*, refer to the remainder of 3.1.2.

<b><i>miRNA</i></b>	<b>Binds to</b>	<b>Circadian role</b>	<b>Reference</b>
<i>bantam</i>	<i>clk</i>	Controls period length	Kadener <i>et al.</i> , 2009
<i>let-7</i>	<i>cwo</i>	Controls period length, anticipates “lights on”, promotes PDF expression	Chen <i>et al.</i> , 2014b
<i>miR-276a</i>	<i>tim</i>	Control’s rhythmicity	Chen and Rosbash, 2016
<i>miR-276b</i>	<i>tim</i>	Control’s rhythmicity	Zhang <i>et al.</i> , 2021
<i>miR-375</i>	<i>tim</i>	Control’s rhythmicity and sleep	Xia <i>et al.</i> , 2020
<i>miR-279</i>	<i>Upd</i>	Control’s rhythmicity	Luo <i>et al.</i> , 2012
<i>miR-996</i>	<i>Upd</i>	Control’s rhythmicity	Sun <i>et al.</i> , 2015
<i>miR-124</i>	?	Control’s the phasing of Evening and Morning activity	Garaulet <i>et al.</i> , 2016; Zhang <i>et al.</i> , 2016

<i>miR-210</i>	<i>Fas2</i>	Control's the phasing of Evening activity and phasing of s-LNvs axonal plasticity	Niu <i>et al.</i> , 2019
<i>miR-263b</i>	<i>Bx</i>	Control's rhythmicity	Nian <i>et al.</i> , 2019
<i>miR-263a</i>	<i>slo</i> and <i>homer</i>	Control's period length	Nian <i>et al.</i> , 2020
<i>miR-959-964</i>		Control's circadian-timed feeding and immune responses	Vodala <i>et al.</i> , 2012

The *miRNA bantam* was the first *miRNA* to be linked directly to the clock. *bantam* was found to interact with *clk* via 3 seed target sites on the *clk* 3'UTR and overexpression of *bantam* in clock cells results in a lengthened period (Kadener *et al.*, 2009). Another *miRNA* has also been linked to control of the circadian period, *let-7*. *let-7* is expressed in the LNvs and overexpression of *let-7* lengthens the period via its binding to *cwo*. The anticipation of the clock to “lights on” is also affected when *let-7* is mutated, and so is PDF expression, suggesting a complex circadian role for *let-7* (Chen *et al.*, 2014b).

To date, no *miRNA*-mediated control has been linked to *per* at any temperature, nor to *cyc* (Martin Anduaga, 2018; Pegoraro and Tauber, 2018; Anduaga *et al.*, 2019; Zhang *et al.*, 2021). However, *vri* has been found to be associated to AGO-1 at low temperatures (Pegoraro and Tauber, 2018) and *tim* has been convincingly identified as a target for *miRNAs* (Chen and Rosbash, 2016; Xia *et al.*, 2020; Zhang *et al.*, 2020). Both *miR-276a* and *miR-26b* bind to the 3'UTR of *tim* in an interaction that is important for maintaining rhythmicity (Chen and Rosbash, 2016; Zhang *et al.*, 2021). Furthermore, Xia and colleagues (2020) identified an interesting feedback mechanism of the clock via *miR-375*. They found that *miR-375* expression is rhythmically controlled as an output of the clock,

probably downstream of *Clk*, and binds to *tim* in the I-LNvs to control circadian rhythmicity and sleep (Xia *et al.*, 2020).

Other *miRNAs* affect the output of the clock rather than the core molecular architecture itself. A *miRNA* with a profound connection to clock output is *miR-279*. Overexpression of this *miRNA* causes the activity of flies to become arrhythmic and it is thought to target the JAK/STAT signalling component *unpaired (upd)* in the dorsal neurons and the I-LNvs (Luo *et al.*, 2012). *miR-279* is also thought to share redundancy with *miR-996* which too targets *upd*. However, due to the much higher abundance of *miR-279*, the contribution of *miR-996* is thought to be small (Sun *et al.*, 2015). Another, *miR-124*, is expressed in clock cells and displays an oscillating expression pattern (Yang *et al.*, 2008b). However, it acts downstream of the molecular clock as mutation of *miR-124* does not alter the oscillation of the core clock components PER or TIM (Zhang *et al.*, 2016). Instead, *miR-124* regulates the fly activity as an output of the clock, and is found to control the phasing of the E and M peaks (Garaulet *et al.*, 2016; Zhang *et al.*, 2016).

*miR-210* has a multi-functional role in the clock. It targets the *mRNA* which encodes the cell-adhesion protein Fasciclin 2 (Fas2) in the optic lobe to control the correct phasing of the evening peak of activity, and in the s-LNvs to control the correct phasing of axonal branch plasticity (which contact the Dorsal neurons). Both pathways were found to be independent of the other suggesting a diverse role *miR-210*-regulated *Fas2* plays in the clock (Niu *et al.*, 2019). Another *miRNA* has also been implicated in circadian-phased plasticity of the s-LNv axonal projections. Nian and colleagues (2019) found that *miR-263b* binds to the *mRNA* of the LIM-only transcription factor Beadex (Bx). *miR-263b* mediated control of *Bx* was found to be essential to maintain correct phasing of s-LNv structural plasticity, and inhibition of binding or mutation of either partner resulted in high levels of arrhythmia (Nian *et al.*, 2019). The sister *miRNA* of *miR-263b*, *miR-263a*, also has clock-related functions in the LNvs but via a different mechanism. *miR-263a* binds to both *slo* and *homer* to control the circadian period and overexpression leads to an unusually long period length (Nian *et al.*, 2020).

Other circadian *miRNAs* are expressed outside of the central clock, such as the *miR-959-964* cluster which regulates the circadian-timed feeding and immune responses via the peri-cerebral fat body (Vodala *et al.*, 2012).

### **3.1.3 *miRNA* control of diapause in *D. melanogaster***

*miRNA* control of diapause has been identified in several insect species, including the flesh fly *Sarcophaga bullata* (Reynolds *et al.*, 2017), the mosquito *Culex pipiens* (Meuti *et al.*, 2018), the ear worm *Helicoverpa zea* (Reynolds *et al.*, 2019), and in the nematode *C. elegans* (Zhang *et al.*, 2011; Gabaldón *et al.*, 2020). However, very little study has been conducted on the relevance of *miRNAs* on diapause in *D. melanogaster*. A pioneering study by Pegeraro and Tauber (2018) used AGO-1 pull downs, micro array analysis and overexpression experiments to screen for *miRNAs* that could be important for photoperiodism at low temperatures. It was found that more *miRNAs* were overexpressed and 10x more genes enriched in AGO-1 immunoprecipitation pull down assays in long photoperiods than short. Moreover, genes showing photoperiodic enrichment differences included those involved in the ecdysone signalling pathway, insulin signalling pathway, and fat body development and metabolism (Pegeraro and Tauber, 2018), all processes essential in diapause regulation and output. The authors then looked at the diapause phenotypes of the *miRNAs* identified to show strong photoperiodic expression patterns. These were *miR-2b*, *miR-11*, *miR-34*, *miR-274*, *miR-184* and *miR-285*. It was found that *miR-2b* and *miR-274* have higher expression in long photoperiods than short, and overexpression led to a reduction of diapause in short days. Whereas *miR-184* has higher expression in short days and overexpression led to a reversed diapause phenotype, with more diapause in long photoperiods than in short (Pegeraro and Tauber, 2018). The mechanism by which these *miRNAs* work to elicit these phenotypes is still unknown, and their targets not experimentally identified. Also, whether the other *miRNAs* identified by Pegeraro (*miR-11*, *miR-34*, and *miR-285*) are involved in photoperiodic diapause is even less clear, and any effects are likely to be downstream of diapause induction.

The Pegoraro and Tauber study (2018), although a first in its field and yielding interesting results, is not exhaustive in its identification of diapause-linked *miRNAs*. There may be other *miRNAs* that the study was unable to detect. Firstly, the AGO-1 pull down assay and *miRNA* micro array experiments were only performed using whole fly heads. This will of course capture *miRNAs* working in the brain or surrounding head tissue, but excludes any *miRNAs* regulating diapause in the body, for example in the ovaries, fat bodies, or CA. Secondly, the screen was aimed at identifying only photoperiodic *miRNAs*. However, the photoperiodic nature of diapause in *Drosophila* is minimal, and there may be *miRNAs* acting in response to other cues in the head, or indeed in the body. As temperature is the overriding regulator of diapause there are likely temperature-dependent diapause-regulating *miRNAs* that remain undiscovered. Thirdly, there may be *miRNAs* that are involved in photoperiodic diapause but for which expression is not itself photoperiodic and these too would have been missed in the screen. This chapter uncovers two additional *miRNAs* that were not identified in the Pegoraro and Tauber study (2018) and assesses their link between the circadian and diapause phenotypes.

### 3.1.4 Regulation of diapause by Timeless

An obvious target which may have been missed by Pegoraro and Tauber (2018) is *timeless* and its previously associated *miRNA*, *miR-276*. TIM had previously been suggested to be present at low, almost undetectable levels at cold temperatures (Majercak *et al.*, 1999). However, recent advances have revealed that *tim* undergoes alternative-splicing that differs according to temperature. The colder isoforms (*tim-cold*, and *tim-short&cold*) have differing C-terminus tails than the warmer isoforms (*tim-medium* and the canonical *tim-long*) (Montelli *et al.*, 2015; Anduaga *et al.*, 2019). Older studies used antibodies that bound to the C-terminus of warmer isoforms and therefore expression of the colder isoform versions of the protein were missed (Majercak *et al.*, 1999). Using an antibody for the N-terminal tail rather than the C-terminus, Abrieux and colleagues (2020)

found high levels of TIM expression at 10°C. This helped solve the mystery of the link between TIM and diapause that had been shown to be strong in several studies (Tauber *et al.*, 2007; Sandrelli et al 2007; Gesto, 2011; Zonato *et al.*, 2017; Andreatta *et al.*, 2018; Abrieux *et al.*, 2020).

Whether TIM regulates diapause via the clock, via an independent photoperiodic sensing mechanism, or via a different route entirely is still unclear. Mutation studies show that loss of TIM results in a change in diapause levels, the direction of which differs between studies (Tauber *et al.*, 2007; Gesto, 2011; Abrieux *et al.*, 2020). The strong diapause phenotype between different alleles of TIM (*s-tim* vs *ls-tim*) was found to be independent of photoperiod (Tauber *et al.*, 2007) even though they show strong light-dependent circadian phenotypes in warmer conditions (Sandrelli *et al.*, 2007). This would suggest that TIM regulates diapause independently from the clock in a non-photoperiodic mechanism.

On the other hand, Abrieux and colleagues (2020) more recently offer another explanation. They found that TIM protein levels are directly linked to that of the co-transcription factor Eyes Absent (EYA). It was found that EYA is expressed in both the IPCs and within the visual system, particularly within the optic lobes, and when knocked out in either tissue resulted in a reduction in diapause. However, overexpression of EYA via *gmr-gal4* resulted in an increase in diapause, but not when overexpressed in the IPCs. Both *eya* mRNA and protein levels oscillate throughout the day in a circadian manner. Interestingly, although mRNA levels do not change in differing photoperiods, protein levels do. A change in photoperiod of 8 hours from LD16:8 to 8:16 resulted in an 8-hour phase shift in the peak of protein expression. This also meant that in the long photoperiod, the peak occurred in the middle of the light phase, whereas in the short photoperiod protein peaked in the middle of the dark phase. This was interpreted as a photoperiodic effect, however, the incubators used in this study were unable to maintain a constant temperature when lights were on, creating a 0.25°C “step up” in temperature. This may sound small, but a previous study from our laboratory observed that temperature cycles of 0.3°C were created as

artifacts of photoperiod changes within incubators. This caused a significant decrease in diapause levels under long “photoperiods” because this small difference in daily temperature (between LD8:16 and LD16:8 for example) will impact on the ability of flies to maintain diapause when compounded across multiple days (most studies maintain females for 12 to 28 days before ovary dissection). When this artificial temperature cycle was removed, diapause levels of wild type flies kept in long photoperiods dropped significantly (Anduaga *et al.*, 2018). Therefore, the diapause phenotype observed in Abrieux’s study is more likely temperature-dependent rather than photoperiodic. Additionally, *eya* mRNA and protein levels increase over time when kept in colder, diapause-inducing temperatures (10°C) compared to non-diapausing temperatures (25°C) independent of photoperiod (Abrieux *et al.*, 2020). In nature, solar radiation (temperature) is directly proportional to solar light and thus the photoperiod, therefore, whether the EYE-TIM relationship is light or heat dependent will not effect its phenotype. However, to understand the true link between the environment, the circadian clock, and diapause, understanding the distinction between light-dependent and temperature-dependent phenotypes is important.

It was found that EYA expression correlates with TIM expression, and knock down of TIM reduces EYA and vice-versa (Abrieux *et al.*, 2020). The opposite is true when either protein is overexpressed. This is due to protein-protein interactions which stabilises each other, offering protection from degradation. Furthermore, the more cold-specific isoform versions of TIM stabilise EYA better than warm-specific isoforms (Abrieux *et al.*, 2020). Expression of the *tim-cold* (*tim-c*) and *tim-short&cold* (*tim-sc*) isoforms were much higher in flies kept at 10°C compared to flies kept at 25°C, whereas the *tim-medium* (*tim-m*) and *tim-long* (*tim-l*) isoforms were dramatically reduced (Abrieux *et al.*, 2020). This was consistent with Anduaga and colleagues’ (2019) comparison of splicing levels at 18°C, 25°C and 29°C. All of these evidences point more towards a temperature-dependent mechanism controlling the EYA-TIM interaction rather than photoperiod.

### 3.1.5 miRNA control of *tim*

The temperature-dependent alternative splicing of *tim* was found to be linked to *miRNA*-mediated control which determines final TIM protein expression (Anduaga *et al.*, 2019). AGO1 pull down and subsequent sequencing of mRNAs indicated that *miRNA* regulation of *tim* increases as temperature decreases. *tim-sc* is not associated with *miRNA* control, but the other three isoforms are, and their association with *miRNA* regulation increases as temperature decreases (Anduaga *et al.*, 2019). The relevance of these findings can be summarised in the following model (see also **Figure 3-2**).

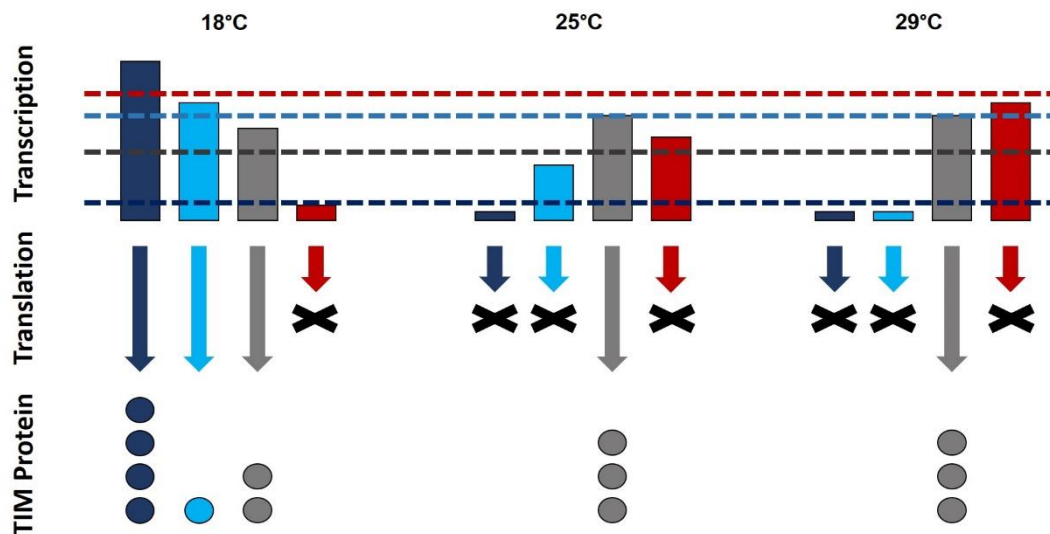


**Figure 3-2.** Model of temperature-dependant *tim* splicing and its relationship to miRNA control. Each *tim* isoform is represented in a different colour: *tim-sc* (dark blue), *tim-c* (light blue), *tim-m* (red), and *tim-l* (grey). Transcription of each isoform is temperature-dependent (represented by the height of the relevant bars). miRNAs determine the threshold of transcription each isoform requires in order to be translated (dashed lines), only if transcription is above this threshold will translation occur. This alters the relative expression of each protein isoform (represented by the relative quantity of circles). (Redrawn and adapted from Anduaga *et al.*, 2019).

At cold temperatures, more *tim-sc* and *tim-c* is transcribed than at warmer temperatures. On the other hand, *tim-m* is transcribed more at warmer temperatures. *tim-l* transcription is not temperature-dependent and is fairly consistent across temperature ranges, albeit with slightly reduced

expression at 18°C (Anduaga *et al.*, 2019). *miRNAs* control the level of translation for each isoform so that only when transcription is higher than a given threshold, translation is achieved. *tim-m* has very high levels of *miRNA* control at all temperatures whereas *tim-sc* is not under *miRNA* control at all. As a result, *tim-m* is never translated and possibly plays a regulatory role (Shakhmantir *et al.*, 2018). At low temperatures, *tim-c* and *tim-sc*, transcription is above the “threshold” set by *miRNA* control, and are therefore translated, expressing high protein levels. *tim-l*, although transcribed relatively abundantly, has lower translation than *tim-c* and *tim-sc* due to a high *miRNA* determined threshold, it therefore has a low TIM ratio in comparison. At higher temperatures, *tim-c* and *tim-sc* are transcribed at low levels, below their respective thresholds, resulting in very low levels of translation and protein expression. On the other hand, *tim-l* is transcribed above its threshold and therefore dominates the TIM expression ratio. (Anduaga *et al.*, 2019). At diapause-inducing temperatures, the ratio probably shifts further, with less *tim-l* transcribed and translated. This would explain the abundance of TIM via N-terminal binding antibodies, but not C-terminal binding antibodies (Majercak *et al.*, 1999; Abrieux *et al.*, 2020). However, this has not been experimentally determined and is therefore speculative. This was planned to be conducted during the work presented in this thesis, however, due to technical difficulties, time and resource constraints, the experiment was unable to be successfully completed.

This mechanism is conserved across several tested *Drosophila* species. Interestingly, the abundance of particular isoforms and the magnitude of difference in expression between isoforms correlates with the importance of adaptability to temperature for a particular species (Anduaga *et al.*, 2019). For example, the African species *D. yakuba* has much more *tim-m* than other species at all temperatures, and its expression levels are the same for high temperature ranges (25°C vs 29°C) but differ when temperature falls (18°C).

Several *miRNAs* with temperature-dependent expression patterns were predicted to bind to the *tim* isoforms. Some were unique to a specific isoform

and some were shared. (Anduaga *et al.*, 2019). However, amongst them was *miR*-210, (discussed earlier in this chapter) which has been implicated in circadian control in the s-LNvs (Neu *et al.*, 2019). *miR*-375 (also discussed earlier), has since been shown to bind to *tim* in the I-LNvs to control sleep and circadian rhythmicity (Xia *et al.*, 2020). Unfortunately, the Anduaga study (2019) did not investigate these predicted *miRNAs* further so the role of the other *miRNAs* in *tim* regulation remains speculative. Moreover, there may be other *miRNAs* that do not have temperature-dependent expression patterns that were missed. Amongst these may be *miR*-276.

### 3.1.6 Regulation of *timeless* via *miR*-276

*miR*-276 is not found in mammals but is highly conserved in insects and is linked to several biological functions, including reproduction and metabolism in *Anopheles* mosquitos (Lampe *et al.*, 2019), insecticide resistance in the aphid *Aphis gossypii* (Wei *et al.*, 2016), egg hatching in locusts (He *et al.*, 2016) and neuronal function in the honey bee *Aphis mellifera* (Hori *et al.*, 2011). In most studies, across species, the target genes of *miR*-276 differ, highlighting the multi-target nature and complex evolutionary history of *miRNAs*. In *D. melanogaster*, *miR*-276 exists as two *miRNA* paralogs, *miR*-276a and *miR*-276b (**Figure 3-3**) and each paralog has been shown to bind to the 3'UTR of *tim* in two independent studies (Chen and Rosbash, 2016; Zhang *et al.*, 2021). *miR*-276a and *miR*-276b are separated by 45kb and therefore their expression is controlled by distinct promoters. This results in differing expression patterns as *miR*-276a is expressed at 10x greater abundance than *miR*-276b in brains of flies kept at 25°C (Czech *et al.*, 2008). The passenger strand of each *miRNA* is identical but the guide strand differs by a single nucleotide. Although this affects the secondary structure of the *miRNA* (prior to processing), the seed sites are identical. Therefore, hypothetically, both *miRNAs* can target the same *mRNAs* (provided they are expressed in the same cells).

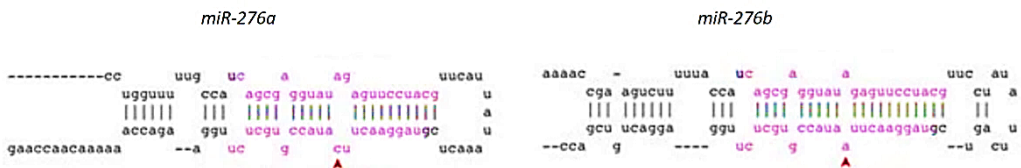


**Figure 3-3.** The genetic sequences and structure of *miR-276a* and *miR-276b*. The mature *miRNA* sequences are represented in **purple** and the differing nucleotide is indicated with a **red arrow**. (Adapted from Li et al., 2013).

At temperatures physiologically favoured by *D. melanogaster* (25°C) and under standard LD 12:12 light cycles, *miR-276a* displays a light-dependent cyclic expression pattern (Chen and Rosbash, 2016). In the absence of light, expression is lost immediately, suggesting that the oscillation is a direct response to light itself and not under circadian control. The expression of *miR-276a* is regulated by the transcription factor CF2 which also displays a cyclic expression pattern and binds to the genomic region upstream of *miR-276a* (Chen and Rosbash, 2016). Knockdown or overexpression of either *cf2* or *miR-276a* results in a loss of circadian rhythmicity and synchronisation suggesting that *miR-276a* targets an essential component of the circadian clock. Indeed, it was found that *miR-276a* binds to the 3'UTR of *tim* and is essential for controlling the correct expression levels of TIM in PDF<sup>+</sup> clock cells (Chen and Rosbash, 2016).

Recently, the other *miR-276* parologue, *miR-276b*, was also linked to the clock via *tim* binding (Zhang et al., 2021). Interestingly, it was found that the *miR-276b* promoter contains an E box. This allows CLK to bind and directly regulate *miR-276b* transcription. *miR-276b* then feeds into the negative feedback loop via binding to *tim* mRNA, regulating TIM levels and therefore circadian rhythmicity. (Zhang et al., 2021). *tim* and *miR-276b* are co-expressed in the LNds, LNvs, DNs and the pars intercerebralis (PI) neurons which are the likely sites of interaction (Zhang et al., 2021). *miR-276b* is also expressed in the fan body, mushroom body, and ellipsoid body (Li et al., 2013; Zhang et al., 2021). In these tissues, *miR-276b* is thought to control sleep independently from the circadian phenotype via binding to *tim*, *npfr1* and *DopR1* (Zhang et al., 2021). Interestingly, *DopR1* has also been shown

to be under control of *miR*-276a in the mushroom bodies to regulate olfactory memory formation, and in the ellipsoid body to regulate behavioural responses to odorants (Li *et al.*, 2013).

## 3.2 Aims

Timeless has already been strongly linked to diapause induction in *D. melanogaster* (Tauber *et al.*, 2007; Gesto, 2011; Zonato *et al.*, 2017; Andreatta *et al.*, 2018; Abrieux *et al.*, 2020), and *tim* translation is highly dependent on *miRNA* control (Chen and Rosbash, 2016; Anduaga *et al.*, 2019; Xia *et al.*, 2020; Zhang *et al.*, 2021). Therefore, this chapter aims to investigate the role of *miRNAs* in regulating *tim*-dependent diapause control. As *miR*-276 has previously been identified as a regulator of *tim* in a range of tissues, including most of the clock cells, this chapter focuses on the *miR*-276-*tim* interaction. Both paralogues of *miR*-276 were investigated for their relevance in diapause, and their binding to *tim* under diapause-inducing conditions investigated. This uncovers the first known *miRNA*-*mRNA* interaction experimentally confirmed to control diapause in *D. melanogaster*.

## 3.3 Materials and Methods

### 3.3.1 Fly stocks

In this chapter the following pre-existing laboratory stocks were used: w<sup>1118</sup>, w<sup>1118</sup>;tim-gal4/CyO, w<sup>1118</sup>;UAS-scramble-sponge;UAS-scramble-sponge, w<sup>1118</sup>;UAS-miR-276a-sponge;UAS-miR-276a-sponge, w<sup>1118</sup>;UAS-miR-276b-sponge;UAS-miR-276b-sponge. The *tim*\*6, *tim*\*24 and *tim*\*3 mutants were donated by Michael Rosbash (Chen and Rosbash, 2016). The *miR*-276a<sup>ko</sup> and *miR*-276b<sup>ko</sup> mutant lines and the UAS-*miR*-276b overexpression line were ordered from the Bloomington stock centre

(58906, 58907 and 59899 respectively) and *miR-276b-gal4* was ordered from the Kyoto stock centre (103994).

### **3.3.2 Calculation of rhythmicity**

Flies were reared at 25°C LD 12:12 and 3-day old males or 3-day old virgin females were used to study rhythmicity as described in Material and Methods 2.3. Flies were entrained for 5 days in LD 12:12 at either 16°C or 25°C and then subjected to 7 days of D:D. Only the last three days of L:D were used in analysis of rhythmicity to avoid previous entrainment in their rearing conditions confusing analysis.

### **3.3.3 Diapause scoring**

Flies were scored for diapause as described in Material and Methods 2.2.

### **3.3.4 qPCR analysis of *tim* and *per* mRNA**

Flies pre-eclosion were reared at 25°C. <4hrs post-eclosion flies were placed in diapause-inducing conditions (11.5°C LD 8:16) for 14 days. At ZT12 on day 14, flies were snap-frozen in liquid nitrogen and RNA extraction, reverse transcription and qPCR analysis performed as described in Material and Methods 2.5, 2.8.1 and 2.12.1. The following primers were used:

<i>perAB_F</i>	(AGGAGGGACCAGACACAGCAC),	<i>perA_R</i>
(AGGCAATTGCTCACTCGTT),		<i>perB-R</i>
(CGAAGAACATCGTTCCAGGAC),		<i>qPCR_tim_F</i>
(ACTCCGCAGGGTCAGTTAA),		<i>qPCR_tim_R</i>
(CACTTCCGCAACAACAGAGT),		<i>GAPDH2_F</i>
(ACCGATTTCCTCAGCGACA),	and	<i>GAPDH2_R</i>
(GGTGGGTAGTGTTCTGGTGTCC)		

### **3.3.5 qPCR analysis of *miR-276b* miRNA**

Flies pre-eclosion were reared at 25°C. <4hrs post-eclosion flies were either placed in diapause-inducing conditions (11.5°C LD 8:16) or non-diapausing conditions (25°C LD 12:12) for 14 days. At ZT12 on day 14, flies were snap-frozen in liquid nitrogen and RNA extraction, reverse transcription and qPCR analysis performed as described in Material and Methods 2.5, 2.8.2 and 2.12.2. The *miRNA* probes used were: TaqMan™ MicroRNA Assay dme-miR-276b and TaqMan™ MicroRNA Assay 2S rRNA (Thermofisher # 4440886 & 4427975 respectively).

## **3.4 Results**

### **3.4.1 The effect of knock-down of *miR-276a* and *miR-276b* expression via *miRNA-sponges* on diapause levels**

To test if *miR-276* has a role in diapause regulation, *miRNA* sponge lines were used to knock down expression of either parologue (**Figure 3-4**). These lines, created by the *miRNA* sponge library (Fulga *et al.*, 2015), utilise an *mCherry* marker fused to several copies of either *miR-276a* or *miR-276b*, or to a scrambled control with no predicted binding in *Drosophila*. These lines work in an identical way as RNA interference lines do, but instead of binding to *mRNA* they bind to mature *miRNA*. This sequesters the *miRNA* reducing its abundance and thus reducing its effectiveness at regulating target *mRNA* levels. Each sponge is fused to a *UAS* sequence and was expressed via *tim-gal4*. Both sponges for *miR-276a* (blue) and *miR-276b* (green) reduced diapause levels compared to the scramble control (red) (P=0.0063 and P=0.0002 respectively)

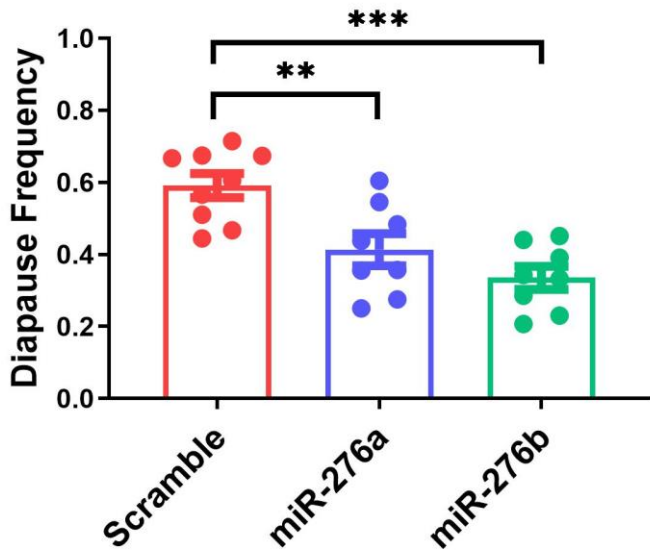


**Figure 3-4.** Diapause levels due to knockdown of miR-276a and miR-276b expression via miRNA-sponges. Transgenic flies expressed either the *UAS-scramble* control (red), *UAS-miR-276a-sponge* (blue), or *uas-miR-276b-sponge* (green) under the control of *tim-gal4*. The genotype of each fly line was *CpO356<sup>Val</sup>*, *Is-tim*. Diapause was scored from stage < 8. Dots represent repeats, bars represent Mean ± SEM. Significance was calculated via one way ANOVA followed by Tukey's multiple comparison test (See appendix 8-3-2, \* = P<0.05, \*\*=P<0.001, \*\*\* = P<0.0001. In total, 1050 flies were dissected.

### 3.4.2 The effect of overexpression of *miR-276b* on diapause levels

Reducing the expression of *miR-276a* or *miR-276a* reduces diapause levels (**Figure 3-4**), presumably because of a reduced interaction with its target mRNA. To test if the reverse is true when *miR-276* is overexpressed, a similar approach was taken (**Figure 3-5**). Transgenic *tim-gal4* flies were crossed to either wild-type flies in a *w<sup>1118</sup>* background (red), or to *UAS-miR-276b* flies (blue). As expected, diapause levels increased in flies overexpressing *miR-276b* compared to non-overexpression flies when diapause was scored from either stage < 8 (**Figure 3-5A**, P=0.0004) or < 10 (**Figure 3-5B**, P=0.0028).

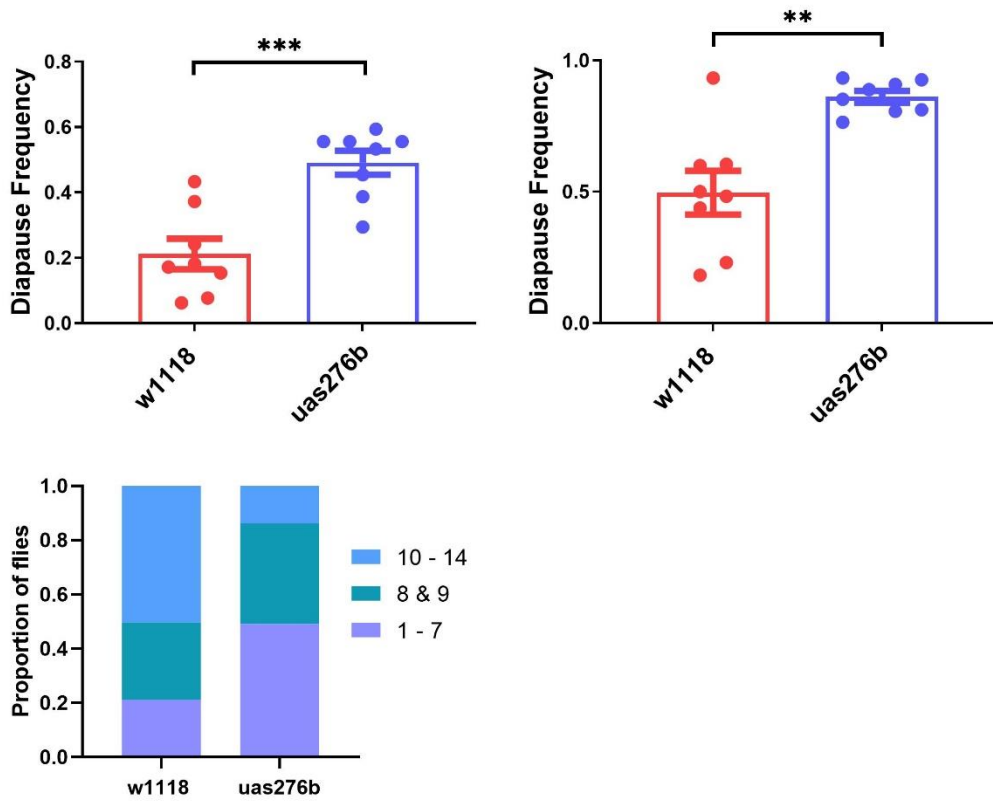


**Figure 3-5.** Diapause levels due to miR-276b overexpression. **A&B).** Transgenic flies containing *tim-gal4* were crossed to either *w<sup>1118</sup>* flies (red), or to *UAS-miR-276b* flies in a *w1118* background (blue). The genotype of each fly line was *CpO356<sup>Val</sup>, s-tim*. Diapause was scored from stage < 8 (**A**) and stage < 10 (**B**). Dots represent repeats, bars represent Mean ± SEM. Significance was calculated via one way ANOVA followed by Tukey's multiple comparison test (See Appendix 8-3-5), \* = P<0.05, \*\*=P<0.001, \*\*\* = P<0.0001. **C).** Stacked % of flies for each genotype that displayed each egg-stage grouping as their most advanced egg stage upon dissection. In total, 419 flies were dissected.

### 3.4.3 The effect on diapause levels of heterozygous knock-out mutants of *miR-276a* and *miR-276b*

*miR-276* has a clear function in diapause regulation (**Figures 3-4** and **3-5**), however, from these experiments alone, it is impossible to determine which parologue is responsible as knock down via sponges or overexpression experiments effects both *miR-276a* and *miR-276b*. To address this issue, mutants were used in which only the *miR-276a* paralog or only the *miR-276b* are knocked-out (**Figure 3-6**). Unfortunately, homozygous mutants for *miR-276a* are unhealthy and therefore not suitable

for experimental analysis. However, heterozygous mutants are viable and have been successfully used in previous studies (Chen and Rosbash, 2016). Therefore, to allow for direct comparison between paralogues, only heterozygous mutants were used. Knock-out mutant flies were crossed to either wild-type flies (blue and green) or to each other to generate double heterozygous mutant flies (orange) and their diapause levels compared to that of wild-type flies (red) scored from egg stage <8 (**Figure 3-6A**) or <10 (**Figure 3-6B**).

Diapause levels decreased slightly in *miR-276a*<sup>KO</sup> (blue) compared to wild-type flies (red), however this was not statistically significant (**Figure 3-6A**, P=0.3085; **B**, P=0.3217). On the other hand, *miR-276b*<sup>KO</sup> flies (green) had significantly decreased diapause levels compared to wild type flies (**Figures 3-6A**, P=0.0090; **B**, P=0.0069). In *miR-276a*<sup>KO</sup>/*miR-276b*<sup>KO</sup> heterozygous double mutant flies (orange) diapause levels also decreased compared to wild-type flies (**Figures 3-6A**, P=0.0002; **B**, P=0.0003). Furthermore, there was a significant decrease in diapause in these flies compared to that of the *miR-276a*<sup>KO</sup> flies (**Figures 3-6A**, P=0.0053; **B**, P=0.0105), but not compared to *miR-276b*<sup>KO</sup>. This suggests that *miR-276b*<sup>KO</sup> is the most important paralog in diapause regulation, but that *miR-276a*<sup>KO</sup> still has a small additive effect.

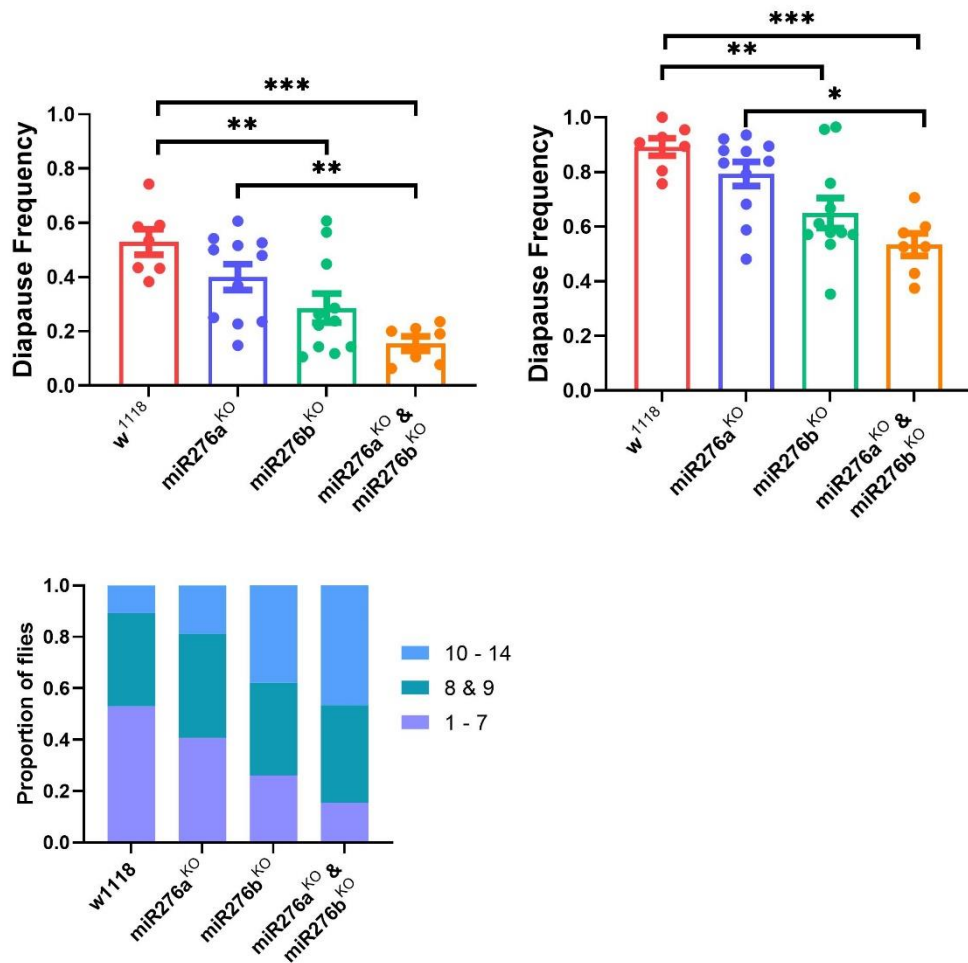


**Figure 3-6.** Diapause levels due to heterozygous mutation of the *miR-276* paralogues. **A&B).** *miR-276a<sup>KO</sup>* flies (blue) or *miR-276b<sup>KO</sup>* flies (green) were crossed to *w<sup>1118</sup>* flies or crossed together (orange) to generate trans-heterozygotes. The genotype of each fly line was *CpO356<sup>Ala</sup>*, *Is-tim*. Diapause was scored from stage < 8 (**A**) and stage < 10 (**B**). Dots represent repeats, bars represent Mean ± SEM. Significance was calculated via one way ANOVA followed by Tukey's multiple comparison test (See Appendix 8-3-6), \* = P<0.05, \*\* = P<0.001, \*\*\* = P<0.0001. **C).** Stacked % of flies for each genotype that displayed each egg-stage grouping as their most advanced egg stage upon dissection. In total, 934 flies were dissected.

### 3.4.4 The effects of genetic manipulation of *miR-276a* and *miR-276b* expression on rhythmicity

Although both homologues have identical seed-sites, and therefore can target the same mRNAs, data from this chapter show that their regulation of diapause levels differs significantly (**Figure 3-6**). Previous studies had shown that *miR-276a* (Chen and Rosbash, 2016) and *miR-276b*

(Zhang *et al.*, 2021) are important for maintaining rhythmicity in flies. However, both studies only investigated one paralog or the other and neither study looked at females, nor at temperatures lower than 25°C. Therefore, circadian locomotor experiments were conducted to compare the rhythmicity of either paralog, in both males and females, and at both 16°C and 25°C. Rhythmicity was calculated for wild type flies, flies heterozygous mutant for either *miR-276a* or *miR-276b*, flies heterozygous mutant for both *miR-276a* and *miR-276b*, and flies overexpressing *miR-276b* via *tim-gal4* (**Figure 3-7**).

Wild-type flies showed no significant difference in rhythmicity levels between sexes (**Figure 8-3-7, Appendix 8-3-7**). At 16°C, there was no significant difference in rhythmicity between male or female flies in any genotype. However, at 25°C there was a significantly lower level of rhythmicity levels in males than females in trans-heterozygotes and flies overexpressing *miR-276b* via *tim-gal4*. At 16°C, *miR-276a* heterozygotes showed significantly lower levels of rhythmicity compared to wild type flies, and this was more pronounced in females than males ( $P=0.009$  and  $P=0.0028$  respectively). This was not true at 25°C as neither sex showed a significant change compared to wild-type flies. *miR-276b* heterozygotes also had decreased level of rhythmicity at 16°C (females  $P=0.0213$  and marginally in males  $P=0.06$ ). At 25°C there was no change in rhythmicity levels for *miR-276b* heterozygotes compared to wild-type flies. Trans-heterozygotes for *miR-276a* and *miR-276b* had significantly lower rhythmicity at both temperatures when compared to wild-type flies. At 25°C, males showed a stronger decrease in rhythmicity than females ( $P=0.0002$  and  $P=0.0116$  respectively), however at 16°C the decrease in rhythmicity is similar between sexes ( $P<0.0001$  for both sexes). Overexpression of *miR-276b* via *tim-gal4* had the greatest effect on rhythmicity at both temperatures and both sexes ( $P<0.0001$ ). At 25°C, there is a greater decrease in rhythmicity in males than in females for this genotype, but due to the limitations of the statistical test it is not possible to quantify (**Appendix 8-3-7**).

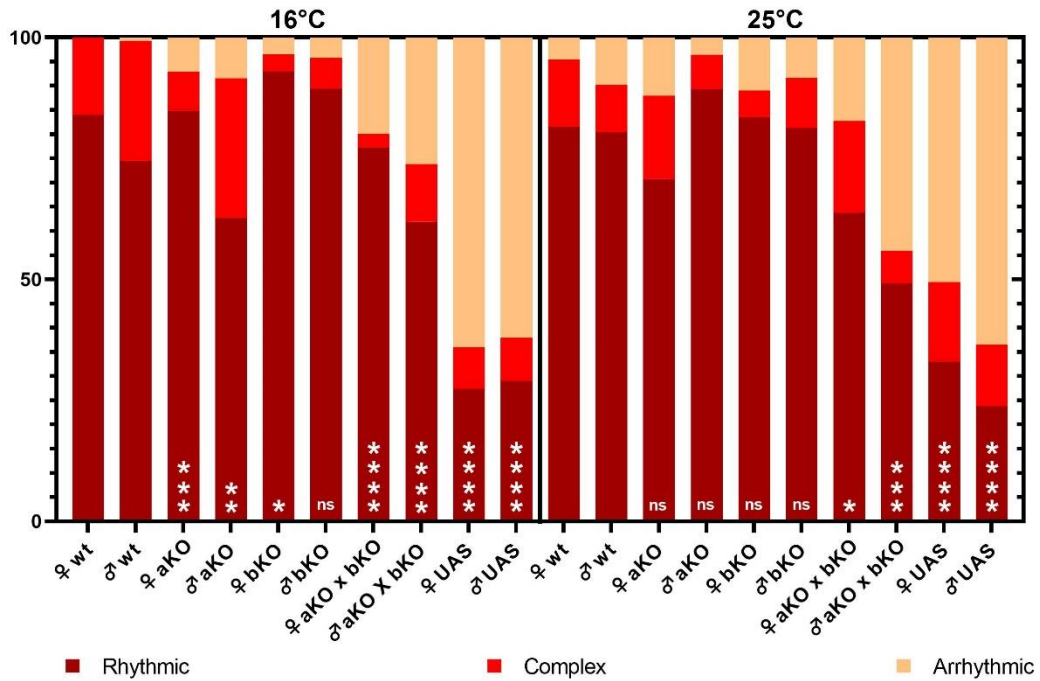


**Figure 3-7.** Rhythmicity levels of flies under different *miR-276* genetic manipulation. Each column represents the proportion of flies that were either rhythmic (**burgundy**), arrhythmic (**red**), or displayed complex rhythms (**orange**). Both males and females were tested at two temperatures: (16°C (**left**) and 25°C (**right**)). All flies were in a *w<sup>1118</sup>* background and each *miRNA* knock-out (KO) line was heterozygous for its respective *miRNA* (either *miR-276a*, *miR-276b*, or both). The *miR-276b* overexpression line (*UAS*) was crossed to *tim-gal4*. Statistical significance was calculated via Chi-square test (See appendix 8-3-7). Statistical significance shown on the figure is that of each genotype compared to its corresponding wt line with the same sex and same experimental temperature. ns = no significance, \* = P<0.05, \*\* = P<0.01, \*\*\* = P<0.001. In total, 1758 flies were analysed.

### 3.4.5 The effect of deletion and partial deletion of the *miR-276* seed site of *tim* on diapause levels

Altering expression levels of the *miR-276* paralogs show that *miR-276b*, and possibly to a lesser extent *miR-276a*, have a regulatory role in diapause induction, but does not reveal their mRNA targets. *In vitro*, and at warmer temperatures *in vivo*, *miR-276* has been shown to bind to *tim* (Chen and Rosbash, 2016; Zhang *et al.*, 2021). To test if this interaction is responsible for the diapause phenotype previously identified (**Figures 3-4, 3-5 & 3-6**), flies that contained deletions of varying sizes within the *miR-276* seed target site of *tim* were used (**Figure 3-8**). These flies are as follows: *tim*\*24 (**orange**) which contains a single nucleotide deletion, *tim*\*6 (**green**)

which contains a 3 bp deletion, and *tim*\*3 (**blue**) which contains a 10bp deletion covering the entire seed site. Partial deletion of the seed-site showed no change in diapause levels when compared to flies with wild-type *tim* (**red**). However, full deletion of the seed site with the *tim*\*3 mutant (**blue**) resulted in a large reduction in diapause levels ( $P<0.0001$ ), genocopying the effects of knock down or heterozygous mutation of *miR-276b* (**Figures 3-4 and 3-6**).

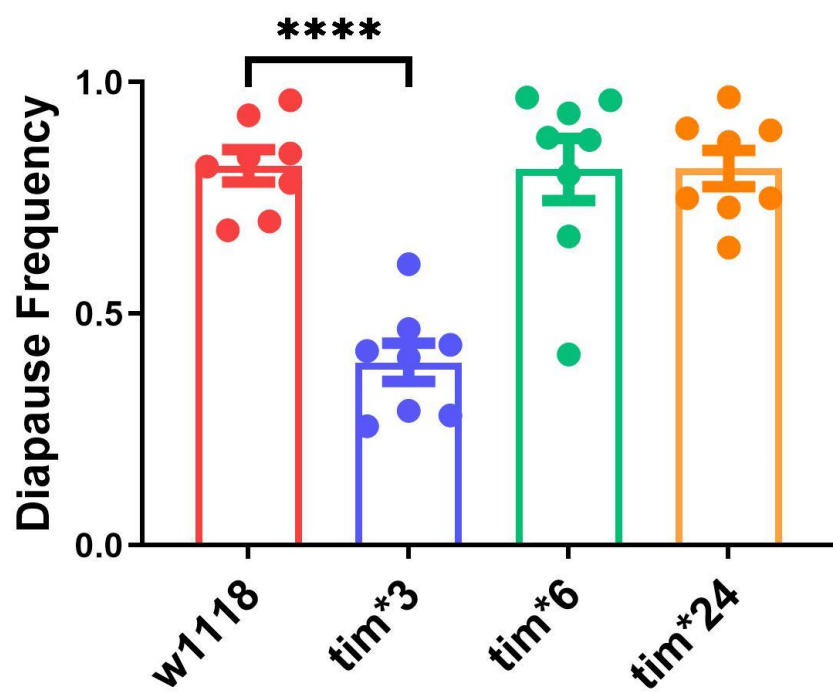


**Figure 3-8.** Diapause levels of flies containing various mutations in the *miR-276* seed site of *tim*. Flies were in a *w<sup>1118</sup>* background and either contained wild-type *tim* (**red**), a 10bp deletion covering the entire seed site (**blue**), a 3bp partial deletion of the seed-site (**green**), or a single nucleotide deletion in the seed site (**orange**). The genotype of each fly line was *CpO356<sup>VAL</sup>*, *ls-tim*. Diapause was scored from stage < 8. Dots represent repeats, bars represent Mean  $\pm$  SEM. Significance was calculated via one way ANOVA followed by Tukey's multiple comparison test (See Appendix 8-3-9), \* =  $P<0.05$ , \*\* =  $P<0.01$ , \*\*\* =  $P<0.0001$ . In total, 912 flies were dissected.

### 3.4.6 The effect of genetic manipulation of *miR-276* on *tim* mRNA levels at 11.5 °C

To further validate *tim* as a target for *miR-276*-mediated diapause regulation, the mRNA levels of *tim* were calculated via quantitative PCR in flies with various genetic manipulations of *miR-276a* or *miR-276b* kept at 11.5°C for 14 days. (**Figure 3-9**). As diapause is under control of several endocrine organs throughout the body as well as the head, both the fly whole head (**red**) and the fly body (**blue**) were assessed individually. ANOVA reveals a Genotype x Tissue interaction ( $F_{df} = 03.165$ ,  $P=0.023$ ), and strong Genotype ( $F_{df} = 8.717$ ,  $P<0.0001$ ) and Tissue ( $F_{df} = 20.11$ ,  $P<0.0001$ ) effects. In the head, there was no difference in *tim* expression levels regardless of genotype. Although, heterozygous mutants of *miR-276b* have slightly elevated *tim* levels, but this is not statistically significant. In the body, *tim* levels increase by over 2-fold in *miR-276a* or *miR-276b* heterozygous mutants ( $P<0.0001$  for both). In heterozygous double mutants there is also an increase in *tim* levels, but to a lesser extent ( $P<0.029$ ). Flies overexpressing *miR-276b* via *miR-276b-Gal4* gave interesting results in the body. Unexpectedly, *tim* levels were not significantly reduced in the head or body compared to the wild-type flies. ( $P=0.1726$ ). The mean *tim* levels in these flies were actually higher than the wild-type flies, although this is not statistically significant

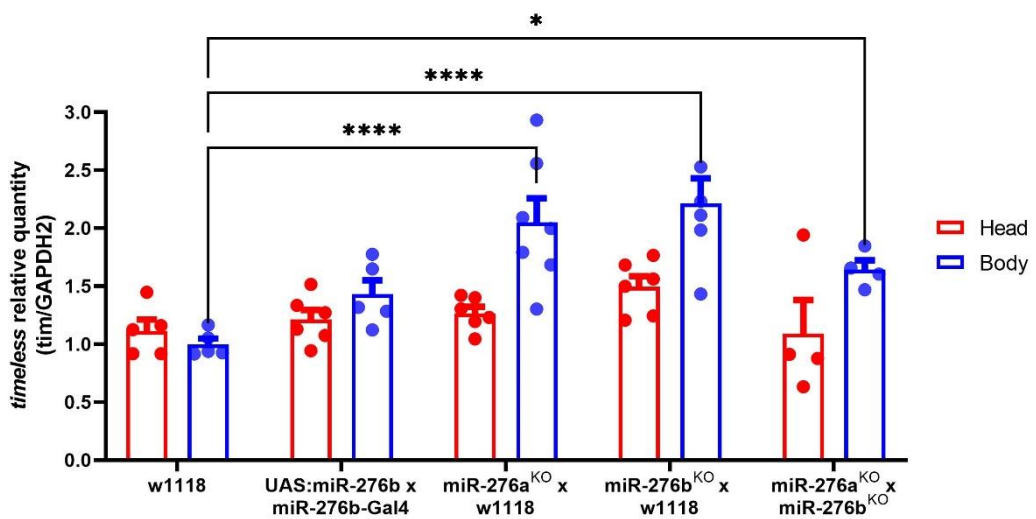


**Figure 3-9.** Relative *tim* mRNA levels in flies with varying genetic manipulations of *miR-276a* and *miR-276b* expression kept at 11.5°C for 14 days. Fly heads (**red**) and bodies (**blue**) were separated and RT-qPCR performed individually. Data was normalised against expression levels of *GAPDH2* for each sample and presented as a ratio to the mean of *w<sup>1118</sup>* flies in the body, with this being set as “1”. Dots represent repeats, bars represent Mean ± SEM. Significance was calculated via two-way ANOVA followed by Dunnett’s multiple comparison test (See appendix 8-3-11), \* = P<0.05, \*\* = P<0.01, \*\*\* = P<0.001, \*\*\*\* = P<0.0001. Each sample contained 25 heads or 25 bodies.

### 3.4.7 The effect of genetic manipulation of *miR-276* on *per* mRNA levels

The alternatively spliced *dmp18* intron in the 3’UTR of *per* has been predicted as a target site for *miR-276b* (Martin Anduaga, 2018). Although no previous studies have found any evidence for *miRNA* control of *per* (Martin Anduaga, 2018; Pegoraro and Tauber, 2018; Anduaga *et al.*, 2019; Zhang *et al.*, 2021) it was of interest to reconfirm these findings (**Figure 3-10**). Furthermore, if *miR-276* is regulating *tim* expression in clock cells then a loss of TIM will also affect the stability of PER, and consequently the negative feedback mechanism of the molecular clock, influencing *per* levels also. As mentioned, the predicted seed site of *miR-276* on *per* is located in the alternatively spliced *dmp18* intron (See also **chapter 4**). Therefore, only the non-spliced *perA* isoform of *per* should permit *miR-276* binding. If binding of either *miR-276a* or *miR-276b* occurs then manipulation of *miR-276* expression should affect the ratio of *perA* to *perB*. However, concurrent with previous studies, the ratio between *perA* and *perB* was consistent across all genotypes both in the head and the body, with no significant tissue effect ( $F_{df} = 1.368$ ,  $P=0.2482$ ), genotype effect ( $F_{df} = 1.247$ ,  $P=0.3044$ ), or interaction effect ( $F_{df} = 0.8118$ ,  $P=0.5242$ ) (**Figure 3-10**).

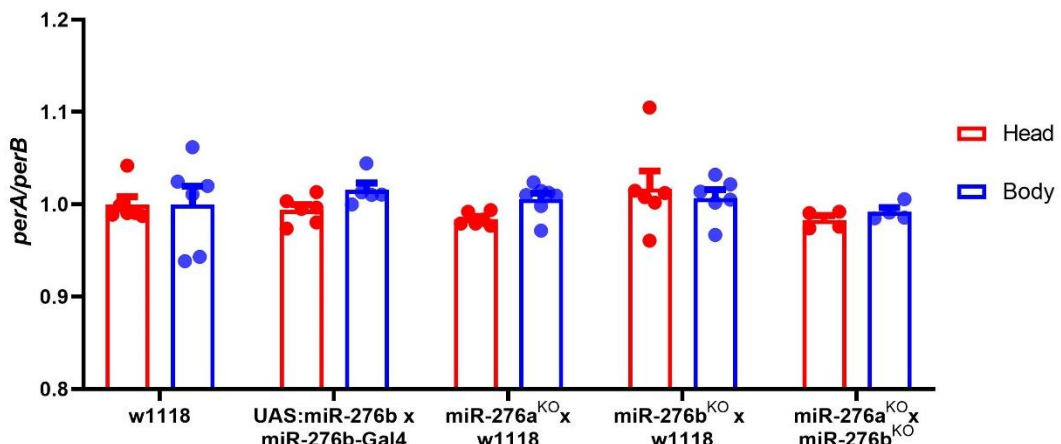


**Figure 3-10.** Relative *perA*/*perB* mRNA ratio in flies with varying genetic manipulations of *miR-276a* and *miR-276b* expression kept at 11.5°C for 14 days. Fly heads (red) and bodies (blue) were separated and RT-qPCR performed individually. Data was normalised against the mean ratio of *w<sup>1118</sup>* flies in the body, with this being set as “1”. Dots represent repeats, bars represent Mean ± SEM. Significance was calculated via two-way ANOVA followed by Dunnett’s multiple comparison test, \* = P<0.05, \*\* = P<0.01, \*\*\* = P<0.001, \*\*\*\* = P<0.0001. Each sample contained 25 heads or 25 bodies.

### 3.4.8 Expression of *miR-276b* in the head and body at differing temperatures

The effects of manipulating the expression of *miR-276b* appear to differ depending on the tissue that is assayed (**Figure 3-9**), or the temperature the experiment is conducted in (**Figure 3-7**). This could be because the expression pattern of *miR-276b* is temperature or tissue-specific. *miRNA*-specific reverse transcription followed by *miRNA*-specific qPCR was conducted on whole heads and on bodies of wild type flies reared at either 11.5°C or 25°C (**Figure 3-11**). ANOVA results show no significant Tissue x Temperature ( $F_{df} = 1.451$ ,  $P=0.2424$ ), no Temperature ( $F_{df} = 0.5859$ ,  $P=0.4533$ ) but a significant Tissue effect with relatively higher levels in the body at both temperatures ( $F_{df}= 6.536$ ,  $P=0.018$ ). However, *post hoc* tests revealed no significant differences between any individual Tissue/temperature groups.

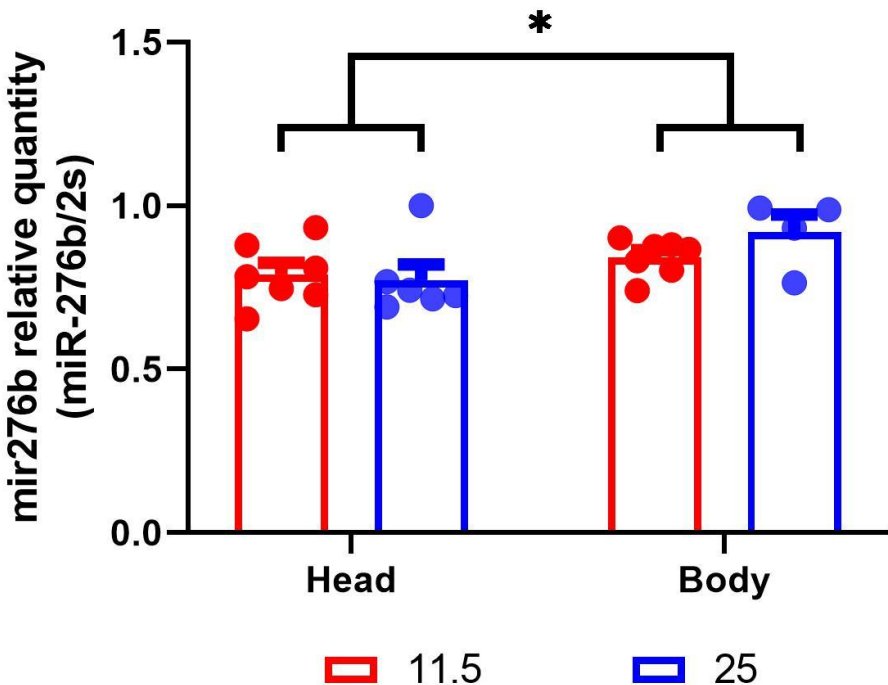


**Figure 3-11.** Relative *miR-276b* levels of wild-type flies reared at either 11.5°C (red) or 25°C (blue) in either the head (left) or body (right). Dots represent repeats, bars represent Mean  $\pm$  SEM. Significance was calculated via two-way ANOVA followed by Dunnett's multiple comparison test (See appendix 8-3-15), \* = P<0.05, \*\* = P<0.01, \*\*\* = P<0.001, \*\*\*\* = P<0.0001. Each sample contained 25 heads or 25 bodies.

### 3.5 Discussion

Although *tim* has been shown to be heavily involved in diapause regulation (Tauber *et al.*, 2007; Gesto, 2011; Zonato *et al.*, 2017; Andreatta *et al.*, 2018; Abrieux *et al.*, 2020) and regulation of *tim* by *miRNAs* has been well documented (Chen and Rosbash, 2016; Anduaga *et al.*, 2019; Neu *et al.*, 2019; Xia *et al.*, 2020; Zhang *et al.*, 2021), until now, no link between the two has been documented. This chapter identifies *miR-276* as a regulator of diapause, particularly the parologue *miR-276b*, albeit with some redundancy with *miR-276a*. Overexpression of *miR-276b* results in an increase in diapause levels (**Figure 3-5**), whereas knock-down of expression via *miRNA* sponges reduces diapause (**Figure 3-4**) indicating that *miR-276b* regulates diapause agonistically. Furthermore, heterozygous

mutation of *miR-276b* not *miR-276a* showed a significant decrease in diapause levels (**Figure 3-6**) which was enhanced further when both mutations were combined in trans-heterozygotes. Indicating that *miR-276a* can also have an additive effect on diapause (**Figure 3-6**).

*miR-276b* has multiple confirmed and predicted target genes and several with relevance to the circadian clock and/or diapause-related signalling pathways. These include *tim* (Chen and Rosbash, 2016; Zhang *et al.*, 2021), *per* (Collins, 2014; Martin Anduaga, 2018; Zhang *et al.*, 2021), *DopR1* & *npf1* (Zhang *et al.*, 2021), and CK2 (Yang *et al.*, 2008b). This chapter identifies *tim* as a target of *miR-276b* at low temperatures, and that this interaction is important for the regulation of diapause. The *miRNA* sponges for *miR-276b* (**Figure 3-4**) were expressed via *tim-gal4*, thus, the decrease in diapause observed must occur in cells co-expressing *tim* and *miR-276b*. Furthermore, manipulation of *miR-276b* expression resulted in changes in *tim* expression (**Figure 3-9**), as heterozygous mutants for either *miR-276a*, *miR-276b* or a combined double mutant increased *tim* levels. Finally, deletion of the *miR-276b* seed site of *tim* phenocopied the decrease in diapause observed in heterozygous mutant flies or flies expressing *miRNA* sponges for *miR-276b* (**Figure 3-8**). Taken together, these results imply that the diapause phenotype observed is at least in part due to a direct interaction between *miR-276b* and *tim*.

However, the results of the qPCR experiment investigating *tim* levels in response to manipulated *miR-276a/b* expression are not straightforward (**Figure 3-9**). The *miR-276a* and *miR-276b* heterozygous mutant flies showed an increase in *tim* expression. The heterozygous double mutant for both *miR-276a* and *miR-276b* also showed an increase in *tim* levels, but to a lesser extent than the individual mutants. This is unexpected because when both paralogues are mutated it creates an additive effect on diapause levels (**Figure 3-6**). It would therefore be expected that an additive increase in *tim* expression would also be seen.

The other unexpected result in the qPCR data is that overall *tim* levels remain unchanged when *miR-276b* is overexpressed (**Figure 3-9**). If knock-down of *miR-276b* increases *tim* levels, then it would be expected that an overexpression would decrease them. Overexpression of *miR-276b* in the RT-qPCR experiment was via *miR-276b-gal4* not the *tim-gal4* promoter used in the diapause experiments (**Figures 3-4 and 3-5**). This was so that only cells with intrinsically overlapping *tim* and *miR-276* expression were targeted. If this subset of cells is small, then subtle differences in overall *tim* expression could be masked. However, the heterozygous mutant flies would also have only had an effect on *tim* in the same cells but were still capable of altering *tim* levels enough to see a significant difference (**Figure 3-9**). Therefore, this reasoning is unlikely. Another explanation could be due to the fact that experiments were carried out at a low diapause-inducing temperature (11.5°C) and that expression of *miR-276B-gal4* was too low to create a noticeable effect. However, this is unlikely as *tim-gal4* driving the miRNA-sponges was able to elicit an effect. Nonetheless, it would be worthwhile assaying the effectiveness of each *gal4* driver at low temperatures. Indeed, these experiments were planned but due to time constraints were not completed. Furthermore, experiments in this chapter used either one or the other promoter but did not compare both together. It would be interesting to look at diapause levels when *miR-276b* is overexpressed via *miR-276b-gal4* or *tim* mRNA levels when *miR-276b* is overexpressed via *tim-gal4*.

Furthermore, Chen and Rosbash (2016) overexpressed *miR-276a* via *tim-gal4* and *Pdf-gal4* and found a decrease in rhythmicity compared to wild-type flies, which was also significantly greater than the effect observed with heterozygous *miR-276a<sup>KO</sup>* mutants. However, Zhang *et al.* (2021) instead used the *miR-276b-gal4* promoter to drive overexpression of *miR-276b* and found no change in rhythmicity, but did find a significant difference in *miR-276b* homozygous knock out flies. Clearly the strength of the two promoters or their tissue specificity may be quite different, leading to complications in interpreting different experimental strategies, in a range of temperatures. Nevertheless, a possible explanation for discrepancies between promoters

may be due to the complex nature of *miR-276b* control of the clock and the clocks control of *miR-276b*.

There are at least 4 different mechanisms for control of *tim* via *miR-276b* either directly, or indirectly via the clock (**Figure 3-12**). In addition to *tim*, Zhang *et al.* (2021) found that *miR-276b* also targets *Pdp1*, *npf1*, and *DopR1*. *Pdp1* is a key component of the molecular clock that promotes transcription of CLK. CLK binds to the E-box of the *tim* promoter to activate *tim* transcription (Cyran *et al.*, 2003). CLK expression is also linked to *tim* expression via another *miRNA*. CLK promotes *miR-375* transcription, either directly or downstream of other CLK-activated transcription factors, which then binds to the 3'UTR of *tim* (Xia *et al.*, 2020). Furthermore, flies with the *cyc* mutation *cyo<sup>01</sup>* have elevated *miR-276b* levels compared to wild type flies (Yang *et al.*, 2008b), possibly due to inhibition of the CLK/CYC-*miR-375* feedback loop. Another predicted target of *miR-276b* is CK2 (Yang *et al.*, 2008b). CK2 phosphorylates PER to enable entry of the PER-TIM heterodimer into the nucleus where it inhibits *tim* expression (Lin *et al.*, 2002; Akten *et al.*, 2003). If *miR-276b* does indeed bind to CK2 then it would prevent the self-inhibition of *tim* transcription by TIM. *miR-276b* is also predicted to target *per* via binding to the alternatively spliced *dmp18* intron (Martin Anduaga, 2018). No change in the *perA:perB* spliceoform ratio was observed when *miR-276b* expression was either up or down regulated (**Figure 3-10**) indicating that *miR-276b* does not bind to *per*, consistent with previous studies (Martin Anduaga, 2018; Pegoraro and Tauber, 2018; Anduaga *et al.*, 2019; Zhang *et al.*, 2021). However, both absolute *perA* and absolute *perB* levels proportionally decrease if *miR-276b* is overexpressed in the head, and proportionally increased if both *miR-276a* and *miR-276b* are knocked-out in the body (**Appendix 8-3-16** and **8-3-17**). It is therefore clear that although *period* splicing is not affected by *miR-276b* expression, overall *period* levels are, most probably via inhibition of one the many aforementioned circadian targets of *miR-276b*, including *timeless*.

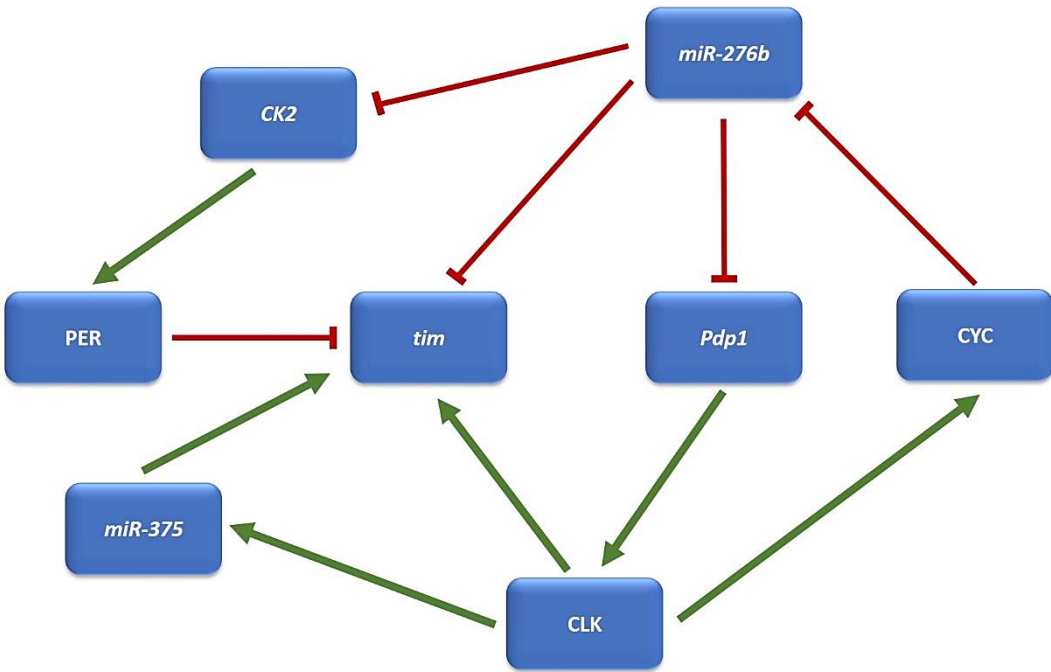


**Figure 3-12.** The web of direct and indirect interactions between *tim* and *miR-276b*. Green arrows indicate agonistic interactions, whereas red indicates antagonistic interactions.

The different regulatory mechanisms of *miR-276b* might therefore induce different effects on *tim*, some increasing and some decreasing *tim* levels, either directly or indirectly. As *tim* is also involved in its own negative feedback loop, and *miR-276b* expression is also controlled by several components of the clock, the relationship between *tim* and *miR-276b* is clearly very complicated. Therefore, it is possible that *miR-276b* overexpression has differing effects on overall *tim* levels depending on the tissue in which it is overexpressed. In each cell, the target genes will each have their own threshold which transcription must reach before it is able to be translated to a physiological level. *miR-276b* expression will partially set this threshold for each gene. This has already been interpreted experimentally for *tim* expression at differing temperatures between 18°C and 29°C (Anduaga *et al.*, 2019). It is possible that in cells where *miR-276b* and *tim* expression overlap, the threshold for a phenotypic change in *tim* levels, either through direct binding to *tim* or indirectly through other targets, differs between tissues.

*miR-276b* has already been linked to several independent biological functions in a range of tissues (Yang *et al.*, 2008b; Li *et al.*, 2013; Chen and

Rosbash, 2016; Zhang *et al.*, 2021). Therefore, although *tim* levels may decrease when *miR-276b* is overexpressed in tissue relevant for diapause control, in other tissues *tim* levels may increase. This may be particularly true if *tim* acts in a pleiotropic manner in its regulation of diapause, independently from the clock. The clock is functional in peripheral tissue even at temperatures as low as 10°C (Ralf Stanewsky, pers comm). In these clock cells, control of *tim* expression may differ from diapause-relevant non-clock cells. These differing levels of *tim* expression may “cancel out” each other when assaying for changes in *tim* expression in whole fly head or whole fly bodies (**Figure 3-9**).

Another explanation for the inability of *miR-276b* overexpression to change *tim* levels may be that endogenous expression levels of *miR-276b* are already enough to fully saturate *tim*. Therefore, no matter how much *miR-276b* is overexpressed it cannot reduce *tim* levels any further. Knockdown of *miR-276b* expression via heterozygous mutants reduces saturation and allows for some *tim* to escape in these cells and an increase in *tim* levels is observed (**Figure 3-9**). However, overexpression of *miR-276b* (via *tim-gal4*) causes an increase in diapause levels (**Figure 3-5**). If the above model is correct then it would imply that the diapause phenotype observed would be due to non-*tim* targets of *miR-276b* (because *tim* is already saturated in wild-type flies). This is plausible given the many targets of *miR-276b*. This may also be an artifact of using the *tim-gal4* driver to drive expression of *miR-276b* where it would not ordinarily be expressed, thus targeting non-*tim* mRNAs that have diapausing phenotypes.

Which model is correct remains unknown, but repeating each experiment using both *gal4* drivers would eliminate some speculation. Moreover, narrowing down the location of the diapause-relevant *miR-276b*<sup>+</sup> cells via neurogenetic dissection using various tools in the *Drosophila* armoury, and then conducting tissue-specific qPCR or single-cell qPCR may present more interpretable results. Additionally, conducting *miR-276b* overexpression and knock-out experiments in a *tim*<sup>0</sup> and in a *tim*<sup>\*6</sup> mutant

background to distinguish between *tim*-related and unrelated effects on diapause could prove helpful.

Data from this chapter also examined rhythmicity of flies with various genetic manipulations of both *miR-276a* and *miR-276b*, thus combining the experiments of both Chen and Rosbash (2016), and Zhang *et al.* (2021) (**Figure 3-7**). In this experiment, both *miR-276a* and *miR-276b* were studied in parallel as heterozygous mutants. It was found that heterozygous *miR-276a*<sup>KO</sup> flies have a decreased rhythmicity (consistent with Chen and Rosbash (2016)), but only at lower temperatures (16°C as opposed to 25°C). On the other hand, *miR-276b* heterozygous mutant flies showed no significant change in rhythmicity, contradicting Zhang *et al.* (2021) who observed a significant decrease in rhythmicity of up to 60% in *miR-276b*<sup>KO</sup> compared to wild type flies. However, they used a homozygous mutant, whereas in this chapter heterozygotes were used. The reasoning for this, as explained earlier, is that *miR-276a* homozygous mutant flies are unhealthy. Using heterozygous mutants for *miR-276b* as well as for *miR-276a* enabled a direct comparison between paralogues. Examining the data for trans-heterozygous double mutants of *miR-276a* and *miR-276b* (**Figure 3-7**) there is a large significant decrease in rhythmicity compared to both the wild type flies and to the individual single mutant flies. Therefore, it is likely that the levels of expression of the heterozygous single mutant of *miR-276b* is not sufficiently reduced enough to effect rhythmicity and does not necessarily contradict the findings of Zhang *et al.* Analogous to the diapause experiment (**Figure 3-6**), one paralog dominates the phenotype but both have an additive effect. In circadian rhythmicity the *miR-276a* paralog dominates, whereas in seasonal diapause induction the *miR-276b* paralog dominates.

Results from overexpression of *miR-276b* via *tim-gal4* showed the largest effect on rhythmicity (**Figure 3-7**), consistent with Chen and Rosbash (2016) but contradictory to Zhang *et al.* (2021), who instead used the *miR-276b-gal4* promoter. It is interesting why results differ so much across experiments depending on the *gal4* promoter of choice. Even more curious

is the fact that although overexpression did not create a phenotypic effect on rhythmicity in the Zhang *et al* study, overall *tim* levels in the fly head did decrease significantly (Zhang *et al.*, 2021). An explanation was not suggested in the paper, but it could be explained by some of the same logic applied to the *tim* mRNA results of this chapter (**Figure 3-9**) discussed previously.

The precise tissue and location of the *tim*<sup>+</sup>, *miR*-276b<sup>+</sup> cells responsible for regulating diapause have not been identified in this study. However, through comparison of *tim* mRNA levels, the location of these cells is more likely to be in the body than the head. *miR*-276b expression levels were found to be equally abundant in the head and the body. Expression levels were also identical comparing expression levels at 11.5°C or 25°C (**Figure 3-11**). Although this is not very informative, it does explain why *miR*-276b was not identified as a regulator of *tim* expression in the Anduaga *et al.* study (2019) because *miRNAs* were screened based on their temperature-dependent expression pattern. Comparison of *tim* expression between the head and the body under various *miR*-276b genetic manipulations is more informative in locating the tissue-specificity of diapause control (**Figure 3-9**). In this experiment, altering *miR*-276b expression had significant impact on *tim* levels in the body (discussed extensively earlier in this chapter) but in the head *tim* levels remained constant regardless of *miR*-276b manipulation (**Figure 3-9**). This does not necessarily prove a correlation between the *tim* expression levels in the body and the diapause phenotype. Diapause-related expression may be limited to a small set of cells that are masked by expression changes in other larger cell clusters. Nonetheless, this result suggests that the body is the more likely location and offers a good place to start narrowing the search. A tissue and cell-specific screen had been planned as part of this chapter to identify the spatial location of *miR*-276b-*tim*-dependent diapause control. Unfortunately, due to time constraints, this screen was not carried out. If, indeed, the screen found that the *miR*-276b-*tim*-dependent diapause phenotype is body tissue-specific, it would uncover an intriguing dual-functionality of the *tim*-*miR*-276 interaction in *D. melanogaster*. It would imply that at warmer temperatures, the *miR*-276a

paralog dominates to control *tim* expression in the head, whereas at colder temperatures the *miR-276b* paralog dominates control of *tim* expression in the body, the former to control circadian rhythmicity and sleep, and the latter to control seasonal diapause. However, as stated, this is only speculative until the spatial location of the diapause-related *tim<sup>+</sup>*, *miR-276b<sup>+</sup>* cells are investigated.

In addition to further investigation of the spatial nature of the *tim-miR-276b* diapausing phenotype, it would also be advantageous to study the other targets of *miR-276b* in relation to diapause. *npf1*, *CK2* and *DopR1* all have links to the circadian clock, and *npf1* and *DopR1* have implications in the control of sleep (Han *et al.*, 1996; Kume *et al.*, 2005; He *et al.*, 2013a; He *et al.*, 2013b). Therefore, not only would study of these genes dissect out the *tim*-dependent effects from *tim*-independent effects of *miR-276b* regulation of diapause, it would also investigate further the role of the clock as a whole. *DopR1* is of particular interest as it is expressed in a range of diapause-related tissues: IPCs, CA and fat body (Gruntenko *et al.*, 2012; Rauschenbach *et al.*, 2017; Andreatta *et al.*, 2018). Knock down of *DopR1* in either of these tissues reduces diapause levels compared to wild type flies and correlated with decreased ILS and JH synthesis (Andreatta *et al.*, 2018). Furthermore, the seed site for *miR-276b* located in the 3'UTR of *DopR1* is highly conserved across 12 different *Drosophila* species (Li *et al.*, 2013).

In conclusion, this chapter uncovers a novel *miRNA* as a regulator of diapause, *miR-276b*, which binds to and regulates *tim* expression. This is the first time a *miRNA-mRNA* interaction has been confirmed to control diapause in *D. melanogaster*. The nature of this interaction in diapause control, as well as its relevance in rhythmicity was investigated and can be summarised as follows:

- Both *miR-276a* and *miR-276b* expression regulates diapause in an agonistic manner, but *miR-276b* is the dominant regulator.

- *miR-276b* binds to the 3'UTR of *tim* and this interaction promotes diapause.
- This interaction most likely occurs in the fly body not the fly head.
- Knock down of *miR-276b* expression results in an overall increase in *tim* expression, but the effect of overexpressing *miR-276b* on *tim* expression are unclear.
- Both *miR-276a* and *miR-276b* expression regulates rhythmicity at non-diapausing conditions (16°C - 25°C), but *miR-276a* is the dominant paralog.
- Manipulation of *miR-276a/b* has a greater effect on rhythmicity at 16°C than at 25°C.
- Total *miR-276b* expression is not temperature-specific, and is equally abundant in the head as in the body.
- The contribution of other targets of *miR-276b* to diapause regulation remains unexplored.

## 4. THE ROLE OF *per* SPLICING AND THE 0.9 GENE IN DIAPAUSE REGULATION

### 4.1 Introduction

The canonical *period* gene contains seven protein-coding exons followed by a further two non-coding exons which make up the 3'UTR (Citri *et al.*, 1987) (**Figure 4-1**). The 89bp 8<sup>th</sup> intron, termed *dmpi8*, separates the two 3'UTR exons and undergoes alternative splicing to create two isoforms of *per*. The *perA* isoform retains *dmpi8* whereas with *perB* the intron is spliced out. This alternative splicing event in *D. melanogaster* has been found to be temperature-dependent and has been associated with seasonal adaptation (Majercak *et al.*, 1999; Collins *et al.*, 2004; Majercak *et al.*, 2004; Low *et al.*, 2008; Low *et al.*, 2012; Yang and Edery, 2019; Breda *et al.*, 2020). As temperature decreases, *dmpi8* splicing increases. This leads to a phase advance in *per* and therefore in PER, which consequently results in earlier morning and evening peaks of activity (Majercak *et al.*, 1999). The sleep and arousal rhythms of flies is also affected by the *per* slicing phenomenon, with flies sleeping more during the siesta in warmer days compared to cold (Cao and Edery, 2015). The ability to control the timing and amplitude of the siesta allows flies the maximum amount of foraging time during warmer daylight hours in the winter, and prevents flies from foraging when temperatures are too hot in the summer and desiccation is a risk.

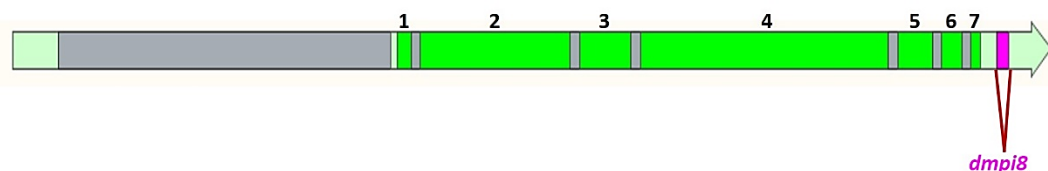


**Figure 4-1.** Genomic map of the *per* gene. Exons (bright green) are numbered from 1-7, introns are represented in grey. The untranslated regions are shaded in light green. The alternatively spliced 8<sup>th</sup> intron (*dmp18*) is coloured in pink. (Created in the program SnapGene).

Splicing is dependent on the binding of components of the multiprotein complex “spliceosome” to recognition sequences that surround the spliced intron. These elements are called the 3' splice site (3'SS), the 5' splice site (5'SS) and the branch point (BS) (Chasin, 2008). Alternative splicing of *dmp18* is controlled via low-affinity binding of the spliceosome complex. At high temperatures, the spliceosome complex binds inefficiently and therefore splicing is reduced, whereas, at lower temperatures the reverse is true (Low *et al.*, 2008). Splicing is enhanced in *norpA<sup>P41</sup>* mutant flies implicating an inhibitory role of signalling via the visual system (Collins *et al.*, 2004; Majercak *et al.*, 2004). It was found that NORPA-dependent *per* splicing is regulated via Rh2, Rh3, and Rh4 in the compound eyes at high temperatures, whereas *per* splicing at low temperatures is mediated by the CRY+ LNdS (Breda *et al.*, 2020). The mechanism by which NORPA inhibits *dmp18* splicing is still unknown.

Sequencing of wild-caught flies across America identified two haplotypes of the 3' UTR of *per* in relation to *dmp18*, termed VT1.1 and VT1.2 (Low *et al.*, 2012). These two haplotypes have identical 3'SS and 5'SS that allow imperfect binding of splicing elements permitting thermo-sensitive alternative splicing. However, VT1.1 has a general non-thermal-regulated tendency to splice more easily compared to VT1.2 across temperature ranges. The haplotypes differ by four SNPs, termed SNP1-4, and two deletions termed DEL1 and DEL2 (Low *et al.*, 2012) (**Figure 4-2**).

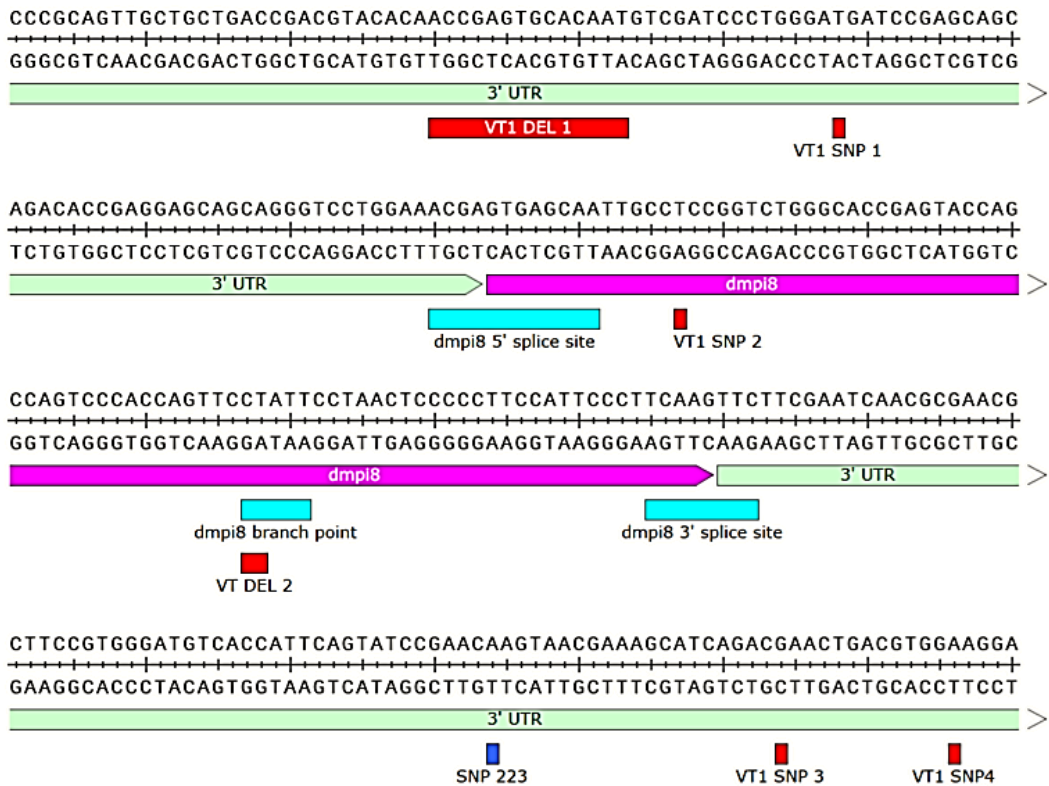


**Figure 4-2.** Genomic sequence of the *per dmp18* intron (pink) and surrounding 3' UTR (light green). The 3' splice-site, 5' splice-site, and the branch point are indicated in light blue. The VT1.1 SNPs and deletions are indicated in red whereas SNP223 is indicated in dark blue. (Created in SnapGene).

Recently, a mechanism by which these SNPs alter splicing has been suggested. The serine/arginine (SR) protein B52 was found to bind to *per* mRNA, probably downstream of the 3'SS, to enhance splicing efficiency in clock neurons and regulate the siesta. The VT1.1 haplotype has stronger B52 binding than VT1.2 (Zhang *et al.*, 2018). This may be due to the two SNPs, SNP3 and SNP4, which are located near to the predicted B52 binding site (Low *et al.*, 2012). However, unexpectedly, there was no latitudinal cline found for these SNPs in either American (Low *et al.*, 2012), or European (Collins, 2014) populations. Collins did find a strong latitudinal cline in another SNP, SNP223, located in close proximity to SNP3 and SNP4. It may be that this SNP has significance in B52 binding and therefore offers a seasonal advantage for temperate flies (Collins 2014). Furthermore, temperature-induced splicing of *dmp18* also seems to be specific to temperate *Drosophila* species, i.e., *D. melanogaster* and *D. simulans*. The Afro-equatorial species *D. yakuba* and *D. santomea* do not show thermal-

sensitive splicing of *dmp18*. This is logical as their environmental temperature does not fluctuate significantly throughout the year and therefore thermosensitive splicing would not offer a seasonal advantage (Low *et al.*, 2008).

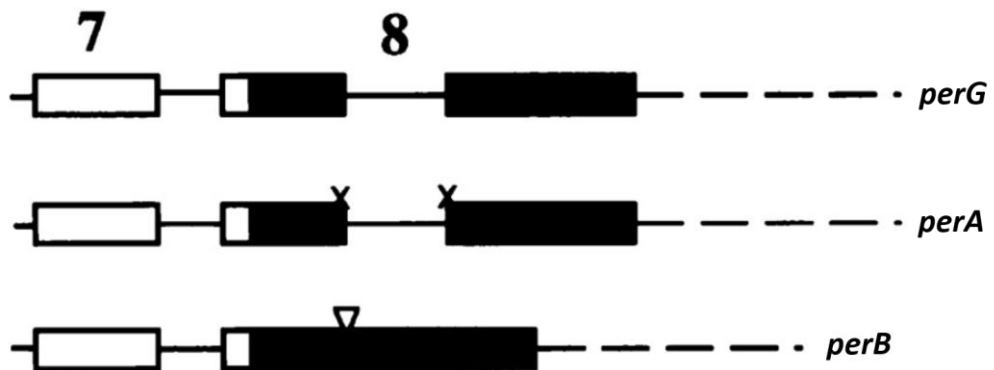


**Figure 4-3.** Genomic map showing the differences between the *per<sup>A</sup>*, *per<sup>B</sup>*, and the *per<sup>G</sup>* transgenes in the 3'UTR surrounding intron *dmp18*. White boxes represent coding sequences, black boxes represent noncoding sequences, solid lines represent introns, and broken lines represent 3'UTR flanking sequences. The X's in *per<sup>A</sup>* represent mutagenized 3' and 5' splice junctions and the inverted triangle in *pe<sup>A</sup>* indicates the deleted *dmp18* intron. Adapted from (Cheng *et al.*, 1998).

Splicing of *dmp18* has recently been implicated in diapause control from members of our laboratory. Collins (2014) first found that splice-locked flies (**Figure 4-3**) which only express the non-spliced *perA* variant showed a decrease in diapause levels compared to flies expressing only *perB*. This was also true using natural fly lines that possessed the VT1.1 haplotype compared to flies possessing VT1.2 (Collins, 2014) (**Appendix 8-4-1**). This result was then genocopied in flies that overexpressed either splice-locked *perA* or splice-locked *perB* via the *UAS-Gal4* system in *tim<sup>+</sup>* cells (Martin Anduaga, 2018) (**Appendix 8-4-3**). Taken together, along with previous data showing increased splicing at low temperatures (Low *et al.*, 2008), these data imply the following model: That in diapause-inducing conditions, *dmp18* splicing increases and the ratio of *perA*:*perB* shifts towards *perB* resulting in an increased tendency to enter diapause. The actual PER protein produced is identical between the two isoforms as *dmp18* is located in the 3'UTR (**Figure 4-1**). Therefore, any diapause regulation must be

occurring post-transcriptionally but pre-translation. Martin Anduaga (2018) and Collins (2014) proposed that *miRNAs* could be responsible, however, no evidence for *miRNA* control of *per* has been found from multiple studies (Martin-Anduaga, 2018; Pegoraro and Tauber, 2018; Anduaga *et al.*, 2019; Zhang *et al.*, 2021). Here we also observe no change in *per* levels when genetically manipulating the *miRNA* identified by Martin-Anduaga to be most likely associated to the *dmp18* intron (see **chapter 3, Figure 3.10**).

In a recent study, the splicing event of *dmp18* itself and not the transcribed product has been shown to have physiological consequences for the regulation of sleep (Yang and Edery, 2019). In early studies of the *per* gene, before the genetics revolution of the 21<sup>st</sup> century, an adjacent gene was thought to encode one of five *mRNA* products transcribed from the vicinity of the *per* locus (Reddy *et al.*, 1984). This was later found to be a different gene entirely, encoding a member of the Takeout (To) family with a Juvenile Hormone Binding Protein (JHBP) domain. Its initial mistaken identity was due to an overlapping 3'UTR with the *per* 3'UTR (Hamblen *et al.*, 1986). Due to its length, it was named the “0.9 kb” transcript. The 0.9 kb expression was initially thought to oscillate throughout the day which led the Brandeis group to suggest that it encoded the PER product (Zehring *et al* 1984). However, a later study observed that the cycling was an artefact of high levels of 0.9 kb expression prior to eclosion which is itself a rhythmic phenotype (Lorenz *et al* 1989) and the role of the 0.9 kb transcript was largely forgotten.

Recently however, the Edery laboratory have reinvestigated 0.9 and found it to have a direct interaction with *dmp18* splicing. Unexpectedly, the function of *per* splicing to control activity and sleep in response to temperature changes was not due to the *per* product itself but due to an indirect control of 0.9 expression (Yang and Edery, 2019). Flies in a *per*<sup>0</sup> background in which splicing of *dmp18* was enhanced had a decreased siesta compared to flies with wild-type levels of splicing. When the 0.9 gene is mutated with a premature STOP codon within its open reading frame, the decreased siesta phenotype seen in splice-enhanced flies is lost (Yang and Edery,

2019). This implies that 0.9 transcription is enhanced when *dmp18* splicing is upregulated and that the increase in 0.9, not PER-B is responsible for the seasonal adaptation to temperature changes, i.e., less siesta in colder days. Indeed, flies with enhanced *dmp18* splicing had higher 0.9 mRNA expression compared to wild type flies, irrespective of PER protein function (Yang and Edery, 2019). The mechanism by which this phenomenon occurs is unknown. Yang and Edery propose that due to the close proximity of the 0.9 to *dmp18* and the relatively small size of 0.9, binding of the spliceosome to *dmp18* may stimulate transcription of 0.9, perhaps by opening up the chromatin structure to enable transcription factors to bind.

## 4.2 Aims

The splicing event of *dmp18* is highly temperature dependent and has already been linked to diapause (Collins, 2014, Martin Anduaga, 2018). The mechanism by which this occurs is curious as there is no known link to miRNA interactions, and the final protein product is identical in each isoform. The work by the Edery laboratory offers a possible explanation through the interaction between *per* splicing and 0.9 transcription, but any effect this phenomenon has on diapause is yet to be explored. Therefore, this chapter aims to discover the mechanism by which *dmp18* splicing regulates diapause. Results from previous work is confirmed (Martin Anduaga, 2018), a novel diapause-regulating gene identified, and a direct link between *dmp18* and 0.9 explored.

## 4.3 Materials and Methods

### 4.3.1 Fly Stocks

In this chapter the following pre-existing laboratory stocks were used: *per<sup>0</sup>;UAS-perA*, *per<sup>0</sup>;UAS-perB*, *per<sup>0</sup>;UAS-perG*, *per<sup>0</sup>;UAS-attB*, *w<sup>1118</sup>;tim-gal4*. UAS-RNAi-0.9 (2<sup>nd</sup> chromosome) was ordered from the Bloomington stock centre (105930). The transgenic lines containing various genetic

manipulations of *dmp18*, *per* and *0.9* were donated by Isaac Edery and were originally made by his laboratory (Yang and Edery, 2019) from transgenic lines created previously (Low *et al.*, 2008). The genetic manipulations were via the addition of premature STOP codons either in *0.9* or *per*, and the cloning in of splice-enhanced sequences at the 3' and 5' splice sites of *dmp18*.

### 4.3.2 Diapause scoring

Flies were scored for diapause as described in Material and Methods 2.2.

## 4.4 Results

### 4.4.1 The effect on diapause of overexpressing *dmp18* splice-locked *UAS-per* lines

Before investigating the mechanism by which *dmp18* splicing regulates diapause, the positive correlation between splicing and diapause levels had to be confirmed. The *UAS-Gal4* system was utilised to drive expression of *dmp18* splice-locked variants of the *per* transgene using a *tim-gal4* driver in a *per<sup>0</sup>* background (**Figure 4-4**). These transgenic flies included an empty vector control (*uas-attb*) which is in essence a *per<sup>0</sup>* fly line, a copy of the untampered *per* transgene (*perG*) which should splice with the same regulation as intrinsic *per*, a splice-locked version of *per* in which *dmp18* is never spliced out (*perA*), and a splice-locked version in which *dmp18* is not present (*perB*). Overexpression of *perG* led to an increase in diapause compared to the *attb* empty vector (*per0*) control (P=0.0026). Overexpression of *perA* resulted in *per<sup>0</sup>*-like levels of diapause (compared to *perG*, P=0.0157, to *attb*, P=0.91), whereas overexpression of *perB* resulted in diapause levels almost identical to *perG* (compared to *perG*, P=0.9809, to *attb*, P=0.0058, to *perA*, P=0.0336). Consequently, blocking splicing results in a decrease in diapause levels.

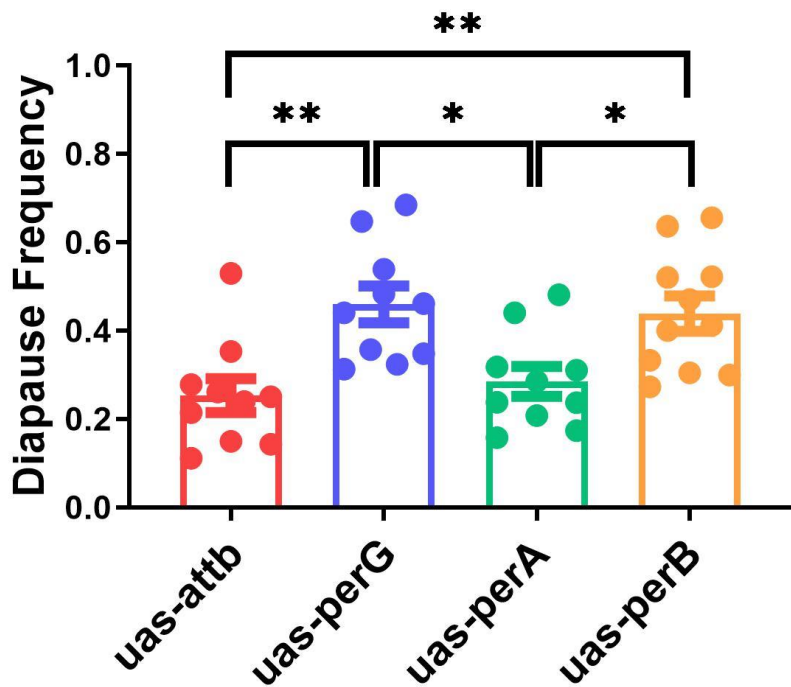


**Figure 4-4.** Diapause levels in splice-locked *per* transgenic flies. *UAS-perA* (green) – full expression of *dmp18*; *UAS-perB* (orange) – no expression of *dmp18*; *UAS-perG* (blue) – *dmp18* under intrinsic control; *UAS-attB* – empty vector control with no *per* expressed. All flies were crossed into a *per*<sup>0</sup>, *CpO356<sup>VAL</sup>*, *s-tim* background. Diapause was scored from stage < 8. Dots represent repeats, bars represent Mean ± SEM. Data was arcsine transformed before statistical analysis. Significance was calculated via one way ANOVA followed by Tukey's multiple comparison test (See Appendix 8-4-5), \* =P<0.05, \*\*=P<0.001, \*\*\* = P<0.0001. In total, 1069 flies were dissected

#### 4.4.2 The effect on diapause of *RNAi* knock-down of the 0.9 transcript

Edery and Yang (2019) found that the *To-like* gene, 0.9, has a temperature-regulated function in controlling the sleep/activity of flies dependent on *dmp18* splicing. Therefore, based on the results obtained from over-expression of *dmp18* splice variants (Figure 4-4) and previous data showing that 0.9 expression increases as temperature decreases (Low *et al.*, 2012; Collins, 2014; Martin-Anduaga, 2018) it is possible that the same mechanism has relevance to diapause. Consequently, 0.9 expression was knocked-down via *tim-gal4* driven *RNAi*, and diapause levels assessed (Figure 4-5).

Diapause was scored based on the traditional scoring method, from stage <8 (**Figure 4-5A**) as well as scoring from stage <10 (**Figure 4-5B**). Diapause levels increased when *0.9* expression was knocked down (green) compared to control flies expressing either *UAS-RNAi* crossed to *w<sup>1118</sup>* (red) (**Figure 4-5A**, P<0.0001, **Figure 4-5B**, P<0.0001) or *tim-gal4* crossed to *w<sup>1118</sup>* (blue) (**Figure 4-5A**, P=0.0006, **Figure 4-5B**, P<0.0001) constructs. This was true when using either scoring method but with slightly greater significance levels if diapause was scored from stage <10 (**Figure 4-5B**).

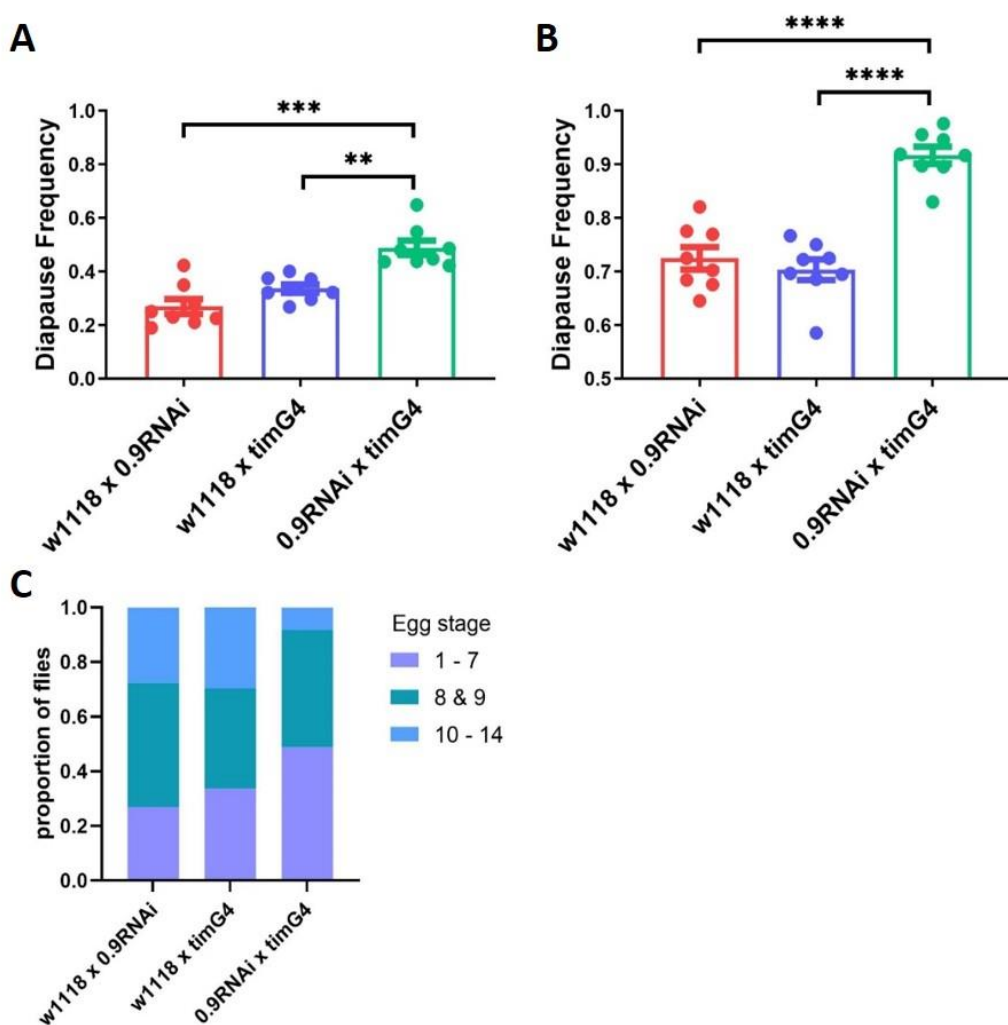


**Figure 4-5.** Diapause levels in *0.9-RNAi* flies. **A&B)**. *RNAi* of *0.9* was driven by *tim-gal4* (green) and diapause levels compared to its driver control (blue) and *RNAi* construct control (red).. The genotype of each fly line was *CpO356<sup>Ala</sup>, s-tim*. Diapause was scored from stage < 8 (**A**) and stage < 10 (**B**). Dots represent repeats, bars represent Mean ± SEM. Significance was calculated via one way ANOVA followed by Tukey's multiple comparison

test (See Appendix 8-4-7), \* = $P<0.05$ , \*\*= $P<0.001$ , \*\*\* =  $P<0.0001$ . **C**). Stacked % of flies for each genotype that displayed each egg-stage grouping as their most advanced egg stage upon dissection. In total, 992 flies were dissected.

#### 4.4.3 The effect on diapause of 0.9 overexpression

Yang and Edery (2019) created several transgenic lines in their investigation of 0.9 and *dmp18* splicing (**Figure 4-6**). The basis of these lines was an insertion of a construct containing *per* with its promotor and 3'UTR region, and 0.9 with its associated promoter and 3'UTR region (which overlaps with that of *per*) via P-element insertion. The difference between transgenic lines was as follows: Each line either contained a wild-type *per* coding region, or one with a premature STOP codon creating a non-functional protein. Each line either contained a wild-type *dmp18* intron that undergoes intrinsic splicing control, or one that had enhanced splicing whereby splicing efficiency is almost at 100%. Each line either contained a wild-type 0.9 gene, or one with a premature STOP codon creating a non-functional protein. Through different combinations of these genetic differences, the relationship between *dmp18* splicing and 0.9 in diapause control can be explored.

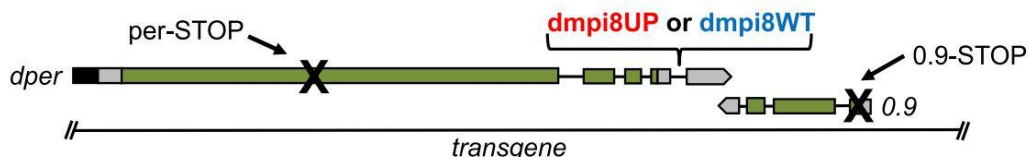


**Figure 4-6.** The *per*-0.9 transgenes created by Yang and Edery, 2019. The foundation of the transgene includes both *per* and 0.9 genomic sequences (green), their untranslated regions (grey), and their promoters. Each transgene either has the canonical versions of *per* and/or 0.9 or a premature STOP codon in *per* and/or 0.9. Each transgene also has either the canonical wild-type *dmp18* (blue) or the splicing-enhanced *dmp18* (red). (Taken from Yang and Edery, 2019).

The first two of these transgenes to be used in this study had the following *per-dmp18-0.9* composition: Both had the wild-type version of PER and wild-type version of *dmp18*, and they either contained the wild-type version of 0.9 (**Figure 4-7A & 4-7B**, red) or the 0.9-STOP version (**Figure 4-7A & 4-7B**, blue). The 0.9-WT transgenic flies are essentially an overexpression line as

the intrinsic 0.9 is still present in the genome, whereas the 0.9-STOP flies lose this overexpression. Overexpression of 0.9 (red) showed a significant decrease in diapause levels compared to non-overexpressing flies (blue). This was true when diapause was scored at either stage <8 (**Figure 4-7A**, P=0.0055) or at stage <10 (**Figure 4-7B**, P=0.0041). Consequently, an extra copy of the 0.9 reduces diapause, consistent with the RNAi results from **Figure 4-5**.

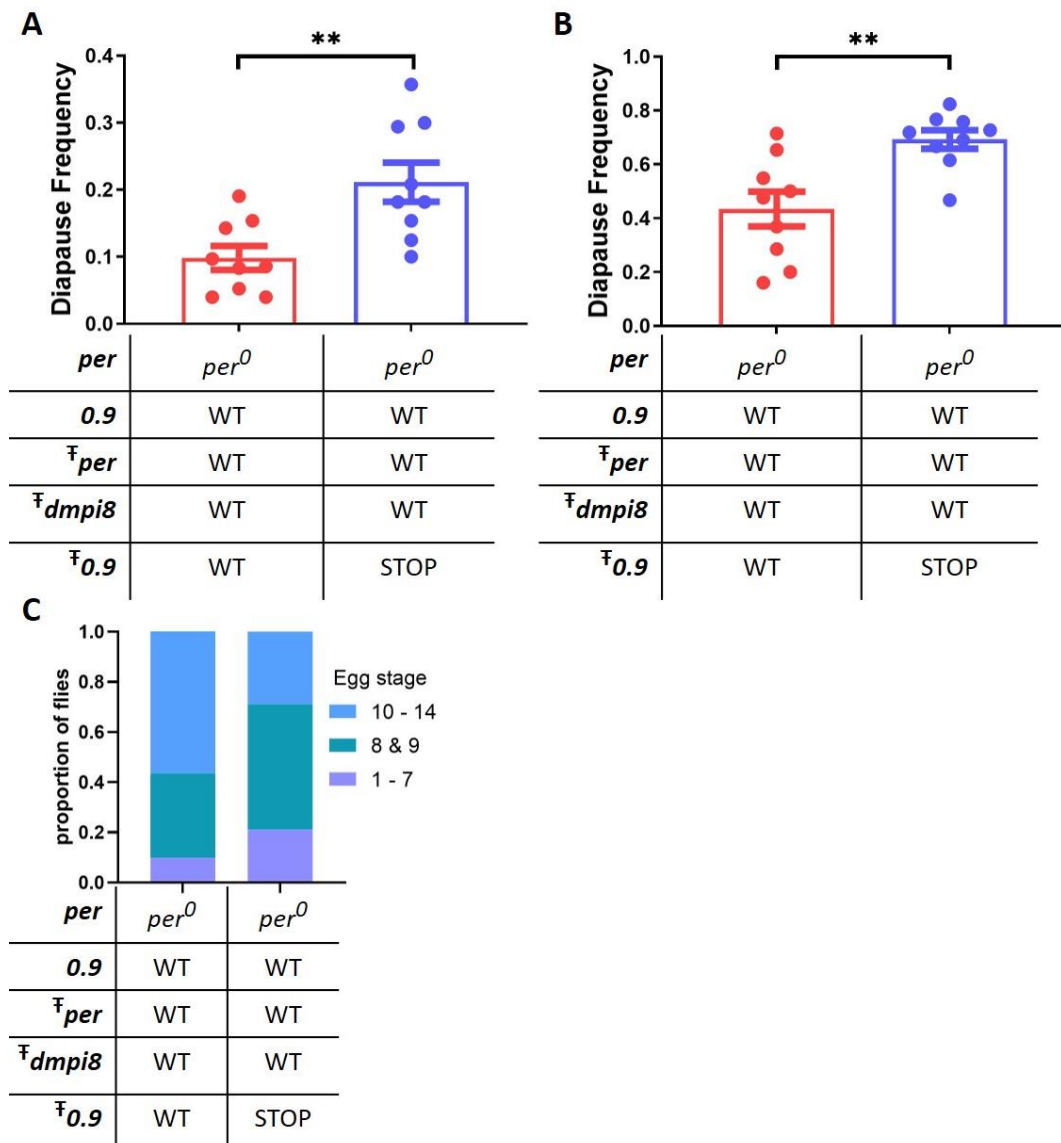


**Figure 4-7.** Diapause levels due to 0.9 overexpression.  $\ddagger$  refers to DNA within the transgene, other DNA represents endogenous gene expression. **A&B)**. Transgenic flies expressing either an extra copy of wild-type 0.9 (red), or an extra copy of 0.9-STOP (blue) i.e., 0.9 wild-type expression. Flies were crossed into a  $per^0$ ,  $CpO356^{Ala}$ ,  $s\text{-}tim$  background but contained a wild-type *per* rescue within the transgenic construct. Diapause was scored

from stage < 8 (**A**) and stage < 10 (**B**). Dots represent repeats, bars represent Mean ± SEM. Significance was calculated via Welch's t test (See Appendix 8-4-9), \* = $P<0.05$ , \*\*= $P<0.001$ , \*\*\* =  $P<0.0001$ . **C**). Stacked % of flies for each genotype that displayed each egg-stage grouping as their most advanced egg stage upon dissection. In total, 547 flies were dissected.

#### 4.4.4 The effect of *dmp18* splicing on 0.9-dependent diapause

Both *per* splicing and 0.9 expression levels effect diapause levels (**Figures 4-4, 4-5 & 4-7**), but this does not indicate a direct link between the two. To investigate any link, three transgenic fly lines were used with the following *per-dmp18-0.9* composition: All three transgenes contained the *per*-STOP version of *per* to eliminate any PER-dependent effects from *dmp18* splicing, two transgenes contained wild-type *dmp18* but either the wild-type 0.9 or 0.9-STOP, and the third transgene contained wild-type 0.9 but enhanced *dmp18* splicing (*dmp18UP*). All three lines were in an intrinsic *per<sup>0</sup>* background with intrinsic wild-type *dmp18* splicing and wild-type 0.9 (**Figure 4-8**).

There was a decrease in diapause levels between flies expressing the wild-type 0.9 within the transgene compared to transgenic flies expressing the premature STOP codon for 0.9 (**Figure 4-8**, red vs blue, **4-8A**  $P=0.0003$  & **4-8B**  $P<0.0001$ ) consistent with **Figure 4-7**. Comparison of diapause levels of the transgenic line containing enhanced splicing (green) gives interesting results. Comparing it to the *per*-STOP-*dmp18*-WT-0.9-STOP line (red) a more dramatic decrease in diapause is seen than with the *per*-STOP-*dmp18*-WT-0.9-WT line and with a greater statistical significance ( $P<0.0001$ ). However, this is only true when scoring diapause at stage <8 (**Figure 4-8A**) and not for scoring at <10 (**Figure 4-8B**). Moreover, comparing the enhanced splicing line (green) to the wild-type splicing line (blue) there is no significant difference ( $P=0.0841$ ) between their levels of diapause, albeit, there is a visible decrease in diapause. Consequently, splicing of *dmp18* has minimal effect on diapause in the absence of PER.

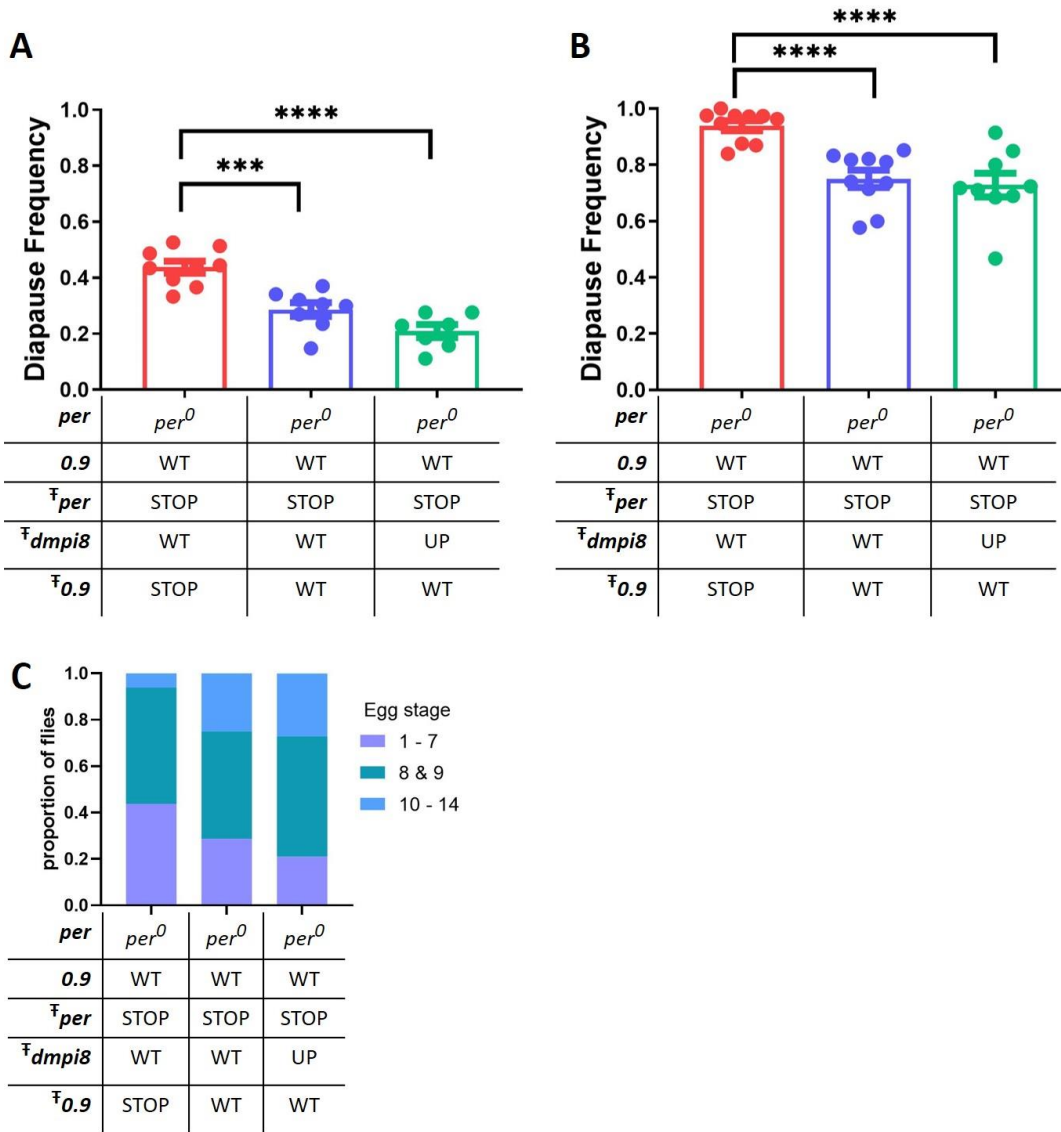


**Figure 4-8.** The role of *dmp18* splicing and 0.9 in a *per*-STOP background.  $\ddagger$  refers to DNA within the transgene, other DNA represents endogenous gene expression. **A&B).** Flies contained the following transgenic insertions: *per*-STOP, *dmp18*-WT, 0.9-STOP (red); *per*-STOP, *dmp18*-WT, 0.9-WT (blue); *per*-STOP, *dmp18*-UP, 0.9-WT (green). Flies were crossed into a *per*<sup>0</sup>, *CpO356<sup>Ala</sup>*, *s-tim* background. Diapause was scored from stage < 8 (**A**) and stage < 10 (**B**). Dots represent repeats, bars represent Mean  $\pm$  SEM. Significance was calculated via one-way ANOVA followed by Tukey's multiple comparison (See Appendix 8-4-11), \* =  $P < 0.05$ , \*\* =  $P < 0.001$ , \*\*\* =  $P < 0.0001$ . **C)** Stacked % of flies for each genotype that displayed each egg-stage grouping as their most advanced egg stage upon dissection. In total, 994 flies were dissected.

#### **4.4.5 Effects of *dmpi8* splicing on diapause, independent of 0.9**

Results presented earlier in this chapter show that 0.9 has a regulatory role in diapause and that this may be enhanced by splicing of *dmpi8*, albeit minimally. It is also shown that this phenotype is independent of PER. However, this does not rule out a role for PER-dependent *dmpi8* splicing on diapause, independent of 0.9. Therefore, to test this hypothesis, the following two transgenic lines were used: The first transgene (**Figures 4-9A & 4-9B**, red) contained the wild-type *dmpi8* whereas the second (**Figures 4-9A & 4-9B**, blue) contained the enhanced splicing version of *dmpi8*. Both transgenes contained wild-type PER and 0.9-STOP to ensure any effect of enhanced *dmpi8* splicing on diapause are PER-dependent and not 0.9-dependent. All three lines were in an intrinsic *per<sup>0</sup>* background with intrinsic wild-type *dmpi8* splicing and wild-type 0.9. Comparing these two lines either when scoring diapause at stage <8 or at stage <10 revealed no significant effects (P= 0.3037, P= 0.099 respectively). This suggests, at least with these transgenic lines and these experimental parameters, that *dmpi8* splicing does not have a 0.9-independent effect on diapause.

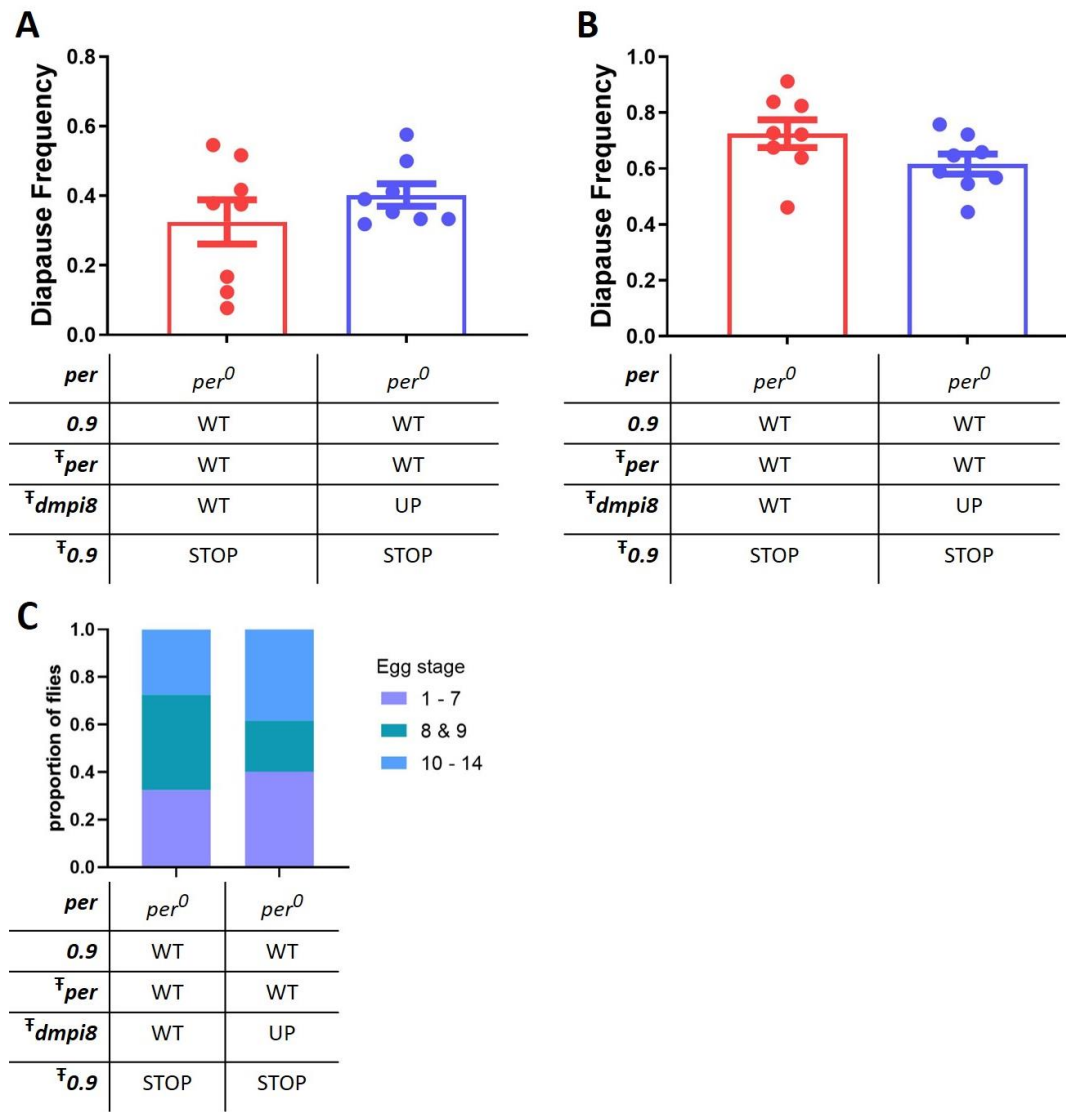


**Figure 4-9.** The role of *dmp18* splicing and PER in a 0.9-STOP background. † refers to DNA within the transgene, other DNA represents endogenous gene expression. **A&B).** Flies contained the following transgenic insertions: *per*-WT, *dmp18*-WT, 0.9-STOP (red); *per*-WT, *dmp18*-UP, 0.9-STOP (blue). Flies were crossed into a *per*<sup>0</sup>, *CpO356<sup>Ala</sup>*, *s-tim* background. Diapause was scored from stage < 8 (**A**) and stage < 10 (**B**). Dots represent repeats, bars represent Mean ± SEM. Significance was calculated via Welch's t test (See Appendix 8-4-13), \* = P<0.05, \*\*=P<0.001, \*\*\* = P<0.0001. **C).** Stacked % of flies for each genotype that displayed each egg-stage grouping as their most advanced egg stage upon dissection. In total, 459 flies were dissected.

## 4.5 Discussion

The most confident conclusion that can be drawn from the results of this chapter is that 0.9 has an important regulatory role in diapause. Yang and Edery (2019) had already found a link of 0.9 expression in the control of sleep, and diapause is, after all, “the big sleep” in insects. They found that more *dmp18* splicing results in higher 0.9 expression. This leads to less sleep during the day and a smaller siesta. This is consistent with data from this chapter in which higher levels of 0.9 results in lower levels of diapause, as seen through either knocking down 0.9 (**Figure 4-5**) or overexpressing 0.9 (**Figure 4-7**). This would imply that 0.9 acts as an antagonist of both circadian sleep and seasonal diapause. It is also clear that the function of 0.9 is independent of PER function. Diapause levels decreased in flies overexpressing the transgenic 0.9 gene compared to flies overexpressing the non-functional 0.9-STOP transgene in both a wild-type *per* (**Figure 4-7**) or *per*-STOP (**Figure 4-8**) transgenic background.

Although the role of 0.9 in diapause induction appears to be independent of PER expression, the relationship of *dmp18* splicing on 0.9 expression seems less straightforward. At non-diapause inducing temperatures, as temperature decreases, 0.9 expression increases due to an enhancement in *dmp18* splicing, resulting in reduced diurnal sleep (Yang and Edery, 2019). This is logical, as a decreased siesta allows flies to forage in the warmer, lighter times of day during the autumn months (Majercak *et al.*, 1999). The same trend of increasing *dmp18* splicing with decreasing temperature also continues at diapause-inducing conditions, as low as 10°C, and possibly lower (Montelli *et al.*, 2015). However, this leads to a paradox. If *dmp18* splicing at these temperatures still enhances 0.9 expression then 0.9 inhibition of diapause would increase as temperature decreases (**Figures 4-5, 4-8 & 4-9**). This of course is counter-intuitive as diapause is highly temperature-dependent and should increase as temperature falls.

Data from this chapter (**Figure 4-8A**) shows that diapause levels in 0.9-WT flies with enhanced *dmpi8* splicing are lower than flies with wild-type *dmpi8*, with greater significance when compared to 0.9-STOP flies. However, there is no statistical significance between *dmpi8*-WT and *dmpi8*-UP flies. This means that the effects of *dmpi8* splicing on diapause is minimal in these flies. Furthermore, the decrease in diapause levels is only seen when scored from stage <8 (**Figure 4-8A**) and not for flies scored from stage <10 (**Figure 4-8B**). This means that although there is a small difference in the proportion of flies with pre-vitellogenic arrested egg-development, the overall number of flies that go on to produce mature eggs is the same.

Another important consideration of the data is that although splicing increases as temperature decreases, in non-transgenic flies, the change is from ~80:20 unspliced:spliced at 25°C to ~45:55 at 10°C (Montelli *et al.*, 2015). This is consistent with qPCR data from **chapter 3** where the mean ratio of *PerA*:*PerB* in wildtype flies at 11.5°C was 0.999 in the head, and 1.051 in the body. Experiments with the *dmpi8*-UP transgenic flies from this current chapter express a 0:100 splicing ratio (Yang and Edery, 2019). There is still endogenous *dmpi8* splicing happening in these flies so the ratio will not be entirely one sided. Nonetheless, the subtle dependency of *dmpi8* splicing on 0.9-dependent diapause observed in this chapter (**Figure 4-8**) is likely to be negligible or absent if splicing efficiency was closer to the expected ~50:50 ratio. Therefore, it is unlikely that splicing of *dmpi8* contributes to the phenotype outside of artefactual experimental design. The 0.9 promoter itself, not the trans action of *dmpi8*, is what regulates 0.9-dependent diapause.

Although *dmpi8* splicing does not appear to have much influence on 0.9-dependent diapause, this does not rule out a role of *dmpi8* splicing independent of 0.9. Data from previous laboratory members indicated a diapause-inhibitory role of *perA* (Collins, 2014; Martin Anduaga, 2018). This chapter confirmed this observation when either *perA*, *perB*, *perG* or the empty vector *attB* was overexpressed using the *tim-Gal4* promoter (**Figure 4-4**). However, no significant difference in diapause was observed when

comparing diapause levels between *dmp18-UP* and *dmp18-WT* flies, using the *per-dmp18-0.9* transgenic lines (**Figures 4-8 & 4-9**). There are several possible explanations as to why this was the case.

Firstly, although the splicing of *dmp18* is manipulated in both the *UAS-perA/B/G/attB* and the *per-dmp18-0.9* experiments (**Figures 4-4** and **4-9** respectively), they cannot be directly compared. The *dmp18-WT* transgenic flies (**Figure 4-9**) express *per* as if they were *perG* (**Figure 4-4**) whereas the *dmp18-UP* transgenic flies (**Figures 4-9**) express *per* as if they were *perB* (**Figures 4-4**) (albeit, with differing promoters between the two sets of experiments). However, there is no comparative transgenic line within the *per<sup>0</sup>, per-dmp18-0.9* fly lines (**Figure 4-9**) to the *per<sup>0</sup>, tim-gal4, UAS-perA* line (**Figure 4-4**). This is unfortunate, as it was the *UAS-perA* line that exhibited a phenotype when compared to WT *per* expression (*UAS-perG*) not *UAS-perB*. Therefore, the lack of a phenotype from the *per-dmp18-0.9* fly lines (**Figures 4-8 & 4-9**) does not contradict the results of the *UAS-perA/B/G/attB* phenotype (**Figure 4-4**). It is possible that at diapause-inducing temperatures, the splicing ratio is already skewed enough to elicit its maximum influence on diapause, and skewing the ratio further is redundant. This would explain why no phenotype is observed when comparing either the *UAS-perB* or *dmp18-UP* transgenic flies to *UAS-perG* and *dmp18-WT* transgenic flies (**Figures 4-4 and 4-9 respectively**).

To directly assay the effects of *dmp18* splicing on diapause control independent of 0.9 expression, a *per-dmp18-0.9* transgenic line will need to be created in which *dmp18* splicing is suppressed, mimicking the *UAS-perA* transgenic line. This line would need to be in a 0.9-STOP, *per*-STOP double mutant background and compared to the *dmp18-WT* and *dmp18-UP* transgenic lines under the same background. If there is indeed a phenotype similar to the *UAS-perA/B/G/attB* from this experiment, then it can be concluded that the *dmp18*-splicing event itself has a diapause effect independent of both 0.9 and PER function. Moreover, to more conclusively separate 0.9 dependent diapause effects from *dmp18*-splicing diapause effects, 0.9 overexpression and RNAi knockdown of 0.9 should be

conducted within a *per*<sup>0</sup>, *tim-Gal4*, *UAS-perB* genetic background in which no splicing is taking place. These experiments were planned, however, due to time constraints were not carried out.

Secondly, the genetic backgrounds as well as the transgenes expressed from each set of experiments (**Figures 4-4, and 4-8 & 4-9**) differ. The flies from each experiment were crossed into flies of different origin, and the *CpO* genotype differed: *UAS-perA/B/G/attB* transgenic flies contained the *CpO356<sup>VA</sup>* variant (**Figures 4-4**), whereas the *per-dmp18-0.9* transgenic flies contained the *CpO356<sup>ALA</sup>* variant (**Figures 4-8 & 4-9**). The *CpO* genotype directly affects diapause levels and could therefore alter the experimental parameters needed to elicit a *dmp18* splicing-dependent phenotype (Schmidt *et al.*, 2008). Moreover, the *per-dmp18-0.9* transgenic lines contained an extra copy of 0.9 and therefore an “overexpression” of 0.9 (**Figure 4-8**) (unless the 0.9-STOP version was used (**Figure 4-9**)), whereas the *UAS-perA/B/G/attB* flies do not contain 0.9 in their transgene. Although the influence of *dmp18* splicing on the expression of 0.9 is not reciprocal at warmer temperatures (>18°C) (Yang and Edery, 2019), it is unknown if this is true at colder temperatures. If this is indeed the case, the presence of the 0.9 promoter in the *per-dmp18-0.9* lines (**Figures 4-8 & 4-9**) may mask the *dmp18* splicing-dependent diapause phenotype observed in transgenic flies in which the 0.9 promoter is absent (**Figure 4-4**). To better understand the relationship between 0.9 expression and *dmp18* splicing at diapause-inducing temperatures, RT-qPCR assays of *perA* and *perB* flies with and without a 0.9 promoter present in their transgenes, and RT-qPCR of 0.9 under a *dmp18-WT* and a *dmp18-UP* genetic background will need to be conducted.

Thirdly, experimental conditions between the two sets of experiments (**Figures 4-4, and 4-8 & 4-9**) may have had a masking effect on an observable phenotype. Martin Anduaga (2018) found that the splice-locked *perA/B/G/attB* flies only displayed a significant difference in diapause levels if the experiment was conducted within a narrow temperature range. She found that 11°C was optimum, but at 10°C all significance was lost, and at

12°C only *perA* vs *perB* flies showed significance, with no significance if compared to the *perG* or *attB* controls (Martin Anduaga, 2018) (**Appendix 8-4-3**). Indeed, observing the results of **Figure 4-9A** of this chapter, there is a slight increase in the mean diapause levels of *dmp18-UP* flies compared to *dmp18-WT* flies when scored at stage <8 (the same stage at which Martin Anduaga (2018) scored diapause), but it is very subtle and non-significant. Therefore, it is possible that the experimental conditions were not optimum for a significant diapause phenotype between the *dmp18-UP* and *dmp18-WT* transgenic flies to be observed. Repeating the experiment but at different temperatures may resolve this.

Another possible limitation in experimental design in this thesis and in diapause studies in general is the use of *tim-gal4* to overexpress *per*. Traditionally, the *tim-gal4* promoter rather than *per-gal4* has been used to drive *per* expression. This is because the overlapping expression of *per* and *tim* in relation to the clock is sufficient for circadian studies, and the *per-gal4* promoter is much weaker than *tim-gal4* (Kaneko *et al.*, 1997; Stanewsky *et al.*, 1998; Kaneko *et al.*, 2000; Kaneko and Hall, 2000). Therefore, it has become standard experimental practice to use the *tim-gal4* as a replacement for *per-gal4*. However, expression of *tim* and *per* outside of the clock, and especially at low, diapause-inducing temperatures, is less well understood and it may therefore, in hindsight, be inappropriate to interchange promoters. The experiments with the *UAS-perA/B/G/attB* lines utilised the *tim-Gal4* promoter (**Figure 4-4**) whereas the experiments using the *per-dmp18-0.9* transgenes relied on the *per* promoter (**Figure 4-9**). This may have led to the differences seen between experiments. However, Collins (2014) used natural lines expressing VT1.1 and VT1.2, or splice-locked transgenic flies to assess *dmp18* splicing on diapause. He found a strong increase in diapause levels with increased *dmp18* splicing in both experiments (**Appendix 8-4-1 & 8-4-2**). These experiments did not use *tim-gal4* but relied on intrinsic or transgenic *per* promoters. Therefore, it is unlikely that the differences seen between **Figure 4-4** and **Figure 4-9** of this chapter are due to differences in the promoter.

The molecular mechanism by which 0.9 inhibits diapause is still unknown. 0.9 is a member of the Takeout (To) superfamily which in *D. melanogaster* comprises 23 homologous genes. The genes within the To family show low sequence homology and except for a select few such as *takeout* itself, have not been studied in much detail. Most To proteins contain binding domains, particularly JHBP domains and are predicted to function as carrier proteins (Vanaphan *et al.*, 2012). Unlike the majority of To genes, 0.9 does not display male biased expression patterns and is equally expressed in both males and females (Vanaphan *et al.*, 2012). However, since 0.9 was ruled out as an mRNA transcript of *per*, it has had almost no experimental study until the Yang and Edery paper (2019). 0.9 does however contain a JHBP domain and may inhibit diapause through interaction with JH.

JHBPs are common in many insect species and are secreted into the haemolymph where they bind to JHs to guide them to their target tissue (Hidayat *et al.*, 1994; Lazareva *et al.*, 2007). In *D. melanogaster*, JHBPs do not exist, however To proteins have been hypothesised to carry out similar roles. For example, Takeout expression in the fat bodies reduces JH levels and causes a reduction in male fertility and courtship as a trade-off to prolong life during stressful conditions (Chamseddin *et al.*, 2012). JHBP transgenes from other insect species (*B. mori* and *A. aegypti*) are able to partially rescue male courtship in *to* mutant *D. melanogaster* males (Saurabh *et al.*, 2018) suggesting that this phenotype is due to direct To-JH binding.

In *D. melanogaster* *To* is under circadian control via Pdp1 $\epsilon$  to regulate feeding behaviour and its expression in the fat bodies allows for circadian entrainment to predictable daily feeding schedules (Sarov-Blat *et al.*, 2000; Benito *et al.*, 2010). Furthermore, *To* is upregulated in the fat bodies of *chico* mutant flies, and extends the life-span of these flies in response to dietary restriction (Bauer *et al.*, 2010). As *chico* is an important component of ILS, this may imply a link between To proteins and diapause. Indeed, in the mosquito *C. pipiens* *to* is upregulated in diapausing females to aid in metabolism and lipid storage (Sim *et al.*, 2015; Chang and Meuti, 2020). It

was also found that both *to* and *Pdp1* mRNA oscillate in long photoperiods and show a similar upregulation of expression in diapause inducing conditions (Chang and Meuti, 2020). However, unfortunately, a direct interaction between the two proteins was not explored.

0.9 may be acting as a JHBP in *D. melanogaster* to bind to JH, possibly in the haemolymph. If this binding is present, it could be acting in one of two ways. 1) it binds to JH to aid JH signalling, possibly by guiding it to its target tissue or protecting it from JH esterases. 2) it binds to JH to inhibit its function, possibly by preventing it from finding its target tissue, or inhibiting the binding of JH to its targets. JH levels decrease in diapause-inducing conditions, which leads to an inhibition of vitellogenesis (Saunders *et al.*, 1990; Soller *et al.*, 1999; Flatt *et al.*, 2005; Tu *et al.*, 2005; Flatt and Kawecki, 2007). It can be concluded, from data in this chapter, that increased 0.9 levels results in decreased diapause. Therefore, it is most likely that 0.9-binding to JH would lead to an increase in JH signalling supporting hypothesis “1”, in a similar way in which JHBPs function in other insects (Hidayat and Goodman, 1994; Lazareva *et al.*, 2007). There is also a third hypothesis, namely that 0.9 is acting independently of JH. In the mosquito *Aedes aegypti* JHBP regulates the innate immune response to stress independently of JH signalling (Kim *et al.*, 2020). This may also be true in the aphid *R. padi*. To expression is upregulated when *R. padi* is exposed to insecticides and is essential in the insecticide sensitivity and resistance response (Peng *et al.*, 2021).

Whether 0.9 acts via mechanism 1 or 3 to inhibit diapause is not clear. Manipulating 0.9 expression in diapause inducing conditions to assay JH expression and components downstream of JH signalling would be useful. Also, JH-0.9 binding assays should be conducted. This would determine whether 0.9 effects JH expression/function and if this is through direct interaction or not. The tissue in which this interaction takes place could also be dissected through RNAi of 0.9 in different tissues via the *UAS-Gal4* system. Is 0.9 expressed in the brain and secreted into the haemolymph? Or is it expressed in diapause-relevant tissues such as the fat bodies?

Overall, the results of this chapter uncover a novel regulator of diapause, 0.9. Furthermore, this chapter investigates the relationship between 0.9 expression, *per* splicing, and PER expression. The results of the chapter can be summarised as follows:

- 0.9 expression has an antagonistic role on diapause induction.
- 0.9-dependent regulation of diapause is independent of PER.
- 0.9-dependent regulation of diapause is (probably) independent of *dmp18*-splicing.
- The role of *per* splicing in regulating diapause independent of 0.9 is still unclear. Although, overexpression of *perA* has an inhibitory effect on diapause levels.

# **5. THE ROLE OF TEMPERATURE IN DIAPAUSE REGULATION UNDER SEMI- NATURAL ENVIRONMENTAL CONDITIONS.**

## **5.1 Introduction**

In insects, true diapause is a robust phenotype that is highly photoperiodic, as discussed previously (**Chapter 1.3.2**). However, in *D. melanogaster*, the photoperiodic response has been considered weak (Saunders *et al.*, 1989; Saunders, 1990; Emerson *et al.*, 2009b). Temperature has a much greater impact on diapause induction and flies readily exit diapause in response to a rise in temperature even if the photoperiod (and thus time of year) is still winter-like. Furthermore, when temperature is kept constant and the photoperiod does not change, flies begin to exit diapause after several weeks, even if neither environmental factor has changed (Zonato *et al.*, 2017). This has caused a long-standing debate concerning the correct terminology when describing ‘diapause’ in *D. melanogaster* (See **Chapter 1.3.3**).

The diapause adaptation evolved to respond to changing daily cues that indicate the changing of season and the approach of winter. However, studies of diapause have been conducted almost exclusively in unchanging laboratory conditions. Under these conditions, temperature is kept constant throughout the course of the experiment neither changing during the day or from day-to-day. Likewise, photoperiod remains constant across the course of experiments. Therefore, although a sudden change from being reared at 25°C in a 12:12 LD photoperiod to being placed in diapause-inducing temperatures at more winter-like photoperiods may shock flies into a diapause phenotype, it is not enough to maintain it for more than four weeks (Emmerson *et al.*, 2009; Schmidt, 2011; Zonato *et al.*, 2017). There may be

diapause-regulating mechanisms that are sensitive to gradual changes in temperature and light that are unable to contribute to the phenotype under such conditions.

Several studies have started to uncover the effects that more natural-like conditions have on regulating the circadian clock and its outputs in both mammals and in *Drosophila* (Gattermann *et al.*, 2008; Daan *et al.*, 2011; Menegazzi *et al.*, 2012; Vanin *et al.*, 2012; Menegazzi *et al.*, 2013; Montelli *et al.*, 2015; Green *et al.*, 2015; Das *et al.*, 2015) (See also **Chapter 6**). However, in relation to diapause, very few studies have attempted to create more realistic environmental parameters (Zonato *et al.*, 2017; Nagy *et al.*, 2018).

Zonato and colleagues (2017) studied the diapause phenotype over a longer duration of 12 weeks, much longer than the standard 2 – 4 weeks. To do this they created more realistic experimental parameters whereby both a flat temperature and rectangular photoperiod changed from week-to-week in a step-wise manner. At the start of each week the temperature would either increase or decrease by 1°C and the photoperiod would change by 1h. This roughly simulated an approaching winter followed by an upcoming spring, condensed into a 12-week period. It was observed that under these conditions diapause levels were greater than flies kept at a constant temperature and photoperiod. The diapause phenotype was also maintained for the duration of the experiment. Even when temperature and photoperiod began to increase (after week 8), diapause levels still remained high, albeit with a weekly decrease (Zonato *et al.*, 2017).

Although the experimental setup used by Zonato *et al* (2017) was an improvement from previous studies, it still relied on rectangular light and flat temperature profiles, and conditions only changed from week-to-week. This meant that flies were kept at a constant temperature and photoperiod for entire weeks at a time. Nonetheless, their results clearly showed that even under these crudely “realistic” conditions, the diapause phenotype is more robust than previously believed (Saunders *et al.*, 1989; Saunders, 1990;

Tata *et al.*, 2001; Tauber *et al.*, 2007; Emerson *et al.*, 2009b; Schmidt, 2011; Fabian *et al.*, 2015). Nagy and colleagues (2018) also studied photoperiodic diapause using semi-natural simulated light profiles. Under their experimental parameters, several distinct LED lights covering a wide wavelength spectrum were used and could be programmed to generate gradual daily cyclic light patterns. This enabled light to be studied in an incubator setup that mimicked the solar light flies are subjected to in nature, including different wavelength compositions between dawn-midday-dusk. Flies were subjected to semi-natural light profiles to mimic either a short day (9:16) or a long day (15:9) at a constant 12°C. Simultaneously, flies were also kept in the same conditions but using rectangular single-source white LED light profiles. It was observed that flies kept in the semi-natural short photoperiod had enhanced diapause levels compared to their rectangular L:D controls, whereas for the longer photoperiod the opposite was true. This result clearly showed that under more natural-like conditions, flies display a stronger photoperiodic diapause than in standard laboratory conditions. Indeed, the flies kept in either 9:15 or 15:9 rectangular photoperiods showed no photoperiodic effects on diapause levels (Nagy *et al.*, 2018).

The identification of a strong photoperiodic effect when using natural-like light profiles is even more significant for the field than may be obvious. Traditional light sources from incubators or lightboxes used to study diapause (and also study the circadian clock) use either fluorescent tubes or more-energy efficient LEDs. The former has been found to create artificial temperature cycles as 60%-80% of the electrical input is dissipated as heat (Pegoraro *et al.*, 2014). The latter still gives off a small amount of heat and has also been suggested to create a greenhouse effect within the tubes that flies are kept, also creating an artificial temperature cycle (Tauber *et al.*, 2007; Pegoraro *et al.*, 2014). Indeed, Anduaga and colleagues (2018) found that even an artificial thermocycle of 0.3°C is enough to generate a perceived “photoperiodic” diapause effect. Therefore, the shallow photoperiodic nature of *D. melanogaster* observed under rectangular laboratory conditions in previous studies may actually not be due to photoperiod at all. This phenomenon is highlighted in a recent publication

(Abrieux *et al.*, 2020) in which a photoperiodic diapause effect was claimed between TIM and EYA but an artificial thermoperiod of 0.25°C was present (See **chapter 3**). However, the incubator system used in the Nagy *et al.* (2018) study was more sophisticated than those most commonly used in the literature and contain built-in feedback mechanisms that account for artificial heat created from the light source. This keeps the temperature true and constant between photoperiods. Consequently, the findings of Nagy and colleagues (2018) can be viewed as a “re-discovery” of photoperiodism as a regulator of diapause, which is only present using natural-like light profiles.

Although this study (Nagy *et al.*, 2018) is the most “natural-like” study of diapause to date, it still only goes half-way. Temperature was kept flat and constant regardless of whether light was rectangular or cyclic. Therefore, the effects of temperature on diapause under natural-like conditions were not assessed. In a circadian context, temperature has been found to be even more prominent in natural thermal cycles than laboratory conditions, and in the warmest summer months is more dominant than light (Green *et al.*, 2015). As temperature is already by far the more dominant component at regulating *Drosophila* diapause in the laboratory (Emerson *et al.*, 2009a; Anduaga *et al.*, 2018), its importance in nature is worth re-investigating.

## 5.2 Aims

A precedent has recently been set by several studies (Zonato *et al.*, 2017; Anduaga *et al.*, 2018; Nagy *et al.*, 2018) in which the experimental parameters of diapause experiments must be carefully considered. The relevance of photoperiodism in regulating diapause has been downplayed in laboratory conditions (Anduaga *et al.*, 2018; Nagy *et al.*, 2018) but reinforced in natural-like conditions (Nagy *et al.*, 2018). This chapter aims to investigate the role of temperature in diapause regulation under more natural-like temperature cycles in which temperature gradually changes over the course of a day to mimic the environment flies are subjected to in

nature. This is the first of such study conducted and, when compared to Nagy and colleague's study of natural-like light, will help assess the relationship of photoperiod and temperature on diapause control in nature.

## 5.3 Materials and Methods

### 5.3.1 *Drosophila* Stocks

Two populations of flies were used in this study. Both populations had originally been wild-caught in 2008 and kept as isofemale lines until 2016. At this point they were combined into a population which were subsequently donated from a previous laboratory member. They were then kept as a population stock prior to experimentation. The first natural-caught population was from Rende in southern Italy ( $39^{\circ}19'53''N$ ). The second were caught from Houten in central Holland ( $52^{\circ}01'41.99''N$ ). Both populations were genotyped as  $CpO^{Val}$  and  $ls-tim$ .

### 5.3.2 Simulation of semi-natural light and temperature profiles

The simulated light profiles were created via a bespoke custom-built light simulator created by Stefano Bastianello, Euritmi, Venetian Institute of Molecular Medicine, Padova, Italy, referenced in Green *et al.* 2015 and Nagy *et al.* 2018. This light simulator consists of 6 LED light sources, each with a different light spectra peak: ANSI White (4000K), Royal-blue (448nm), Blue (470nm), Cyan (505nm), Green (530nm), and Amber (590nm). This enables coverage of the whole solar light spectra that *D. melanogaster* are able to detect via their 7 Rhodopsins. An individual LED of each of the 6 light sources were placed in 4 separate clusters housed in light-proof casing containing holes of varying size. Through the custom programmed software accompanying the light simulator, precise light intensities can be achieved through altering the current supplying each LED light in each cluster. This enables the creation of accurate cyclic natural-like light profiles that differ in light composition and light intensity throughout the

day and night. Two “photoperiods” were used in this chapter: 9:15 and 15:9 as used by Nagy *et al.* 2018.

Temperature profiles were created via the Memmert IPP500 peltier incubator systems Celsius software, explained in detail in. These machines are highly sophisticated and flexible with built-in feedback mechanisms. This ensures that temperature fluctuations are not influenced by radiation emitted by light sources. They also calculate the rate of temperature change needed to reach the next “plotted point”. This enables a gradual smooth cycle in temperature without any “steps” that oscillates over a 24-hour period. Two thermoperiods of 9:15 and 15:9 was used in this chapter and are explained in more detail in the results section.

### **5.3.3 Diapause scoring**

Flies were scored for diapause as described in Material and Methods 2.2.

## **5.4 Results**

### **5.4.1 Generation of cyclic, natural-like thermoperiods**

The Memmert IPP500 peltier incubator system is highly sophisticated and flexible. It is capable of calculating the rate of temperature change needed over time from one “plotted point” to the next to ensure a smooth curve. This allows the creation of natural-like temperature profiles that cycle gradually without any sharp “step ups” in temperature. Two thermoperiods, and two photoperiods created via bespoke programmable light simulators (described in Methods and also in Vanin *et al.*, 2012; Green *et al.*, 2015; Nagy *et al.*, 2018) were used to create several combinations of semi-natural environmental profiles (**Figure 5-1**). This enabled investigation into the relationship between photoperiod and temperature in controlling the diapause phenotype.

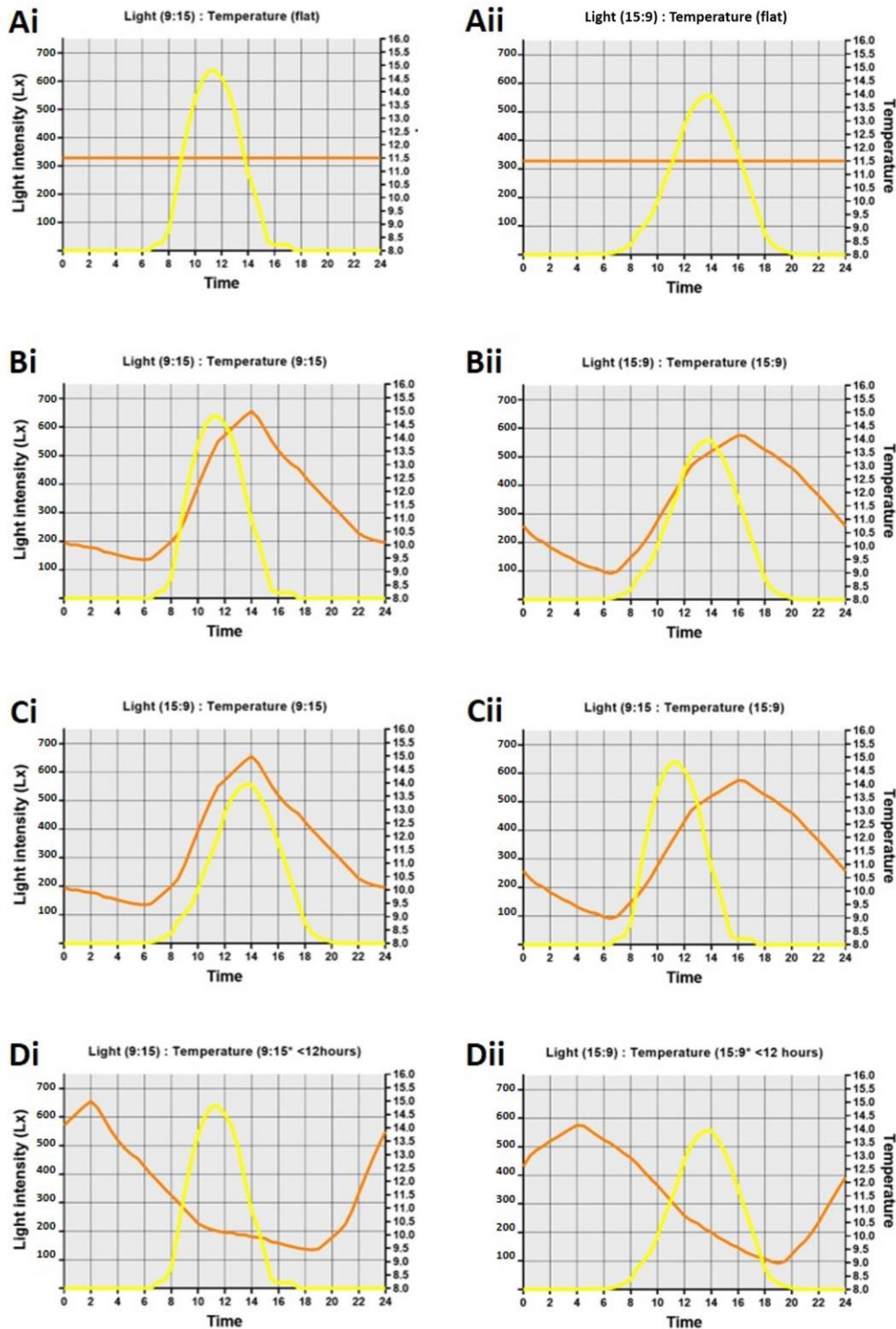


**Figure 5-1.** Thermoperiod (red) and photoperiod (yellow) cycles created and used during this chapter. **A**) Temperature was kept flat at a constant 11.5°C whereas the light cycled as either a short photoperiod of 9:15 (**Ai**) or as a long photoperiod of 15:9 (**Aii**). **B**) Both light and temperature cycle to mimic either a short day with a photoperiod of 9:15 (**Bi**) or a long day with a photoperiod of 15:9 (**Bii**). The average temperature was kept at 11.5°C. **C**) The thermoperiod and photoperiod were uncoupled so that the thermoperiod mimicked that of a short day (9:15) whereas the photoperiod mimicked that of a long day (15:9) (**Ci**), or vice versa (**Cii**). **D**) The thermocycle was out of sequence with the photocycle by 12 hours, so that when the photoperiod is mimicking the day, the thermocycle is mimicking the night. The length of the photoperiod and thermoperiod were identical, either 9:15 (**Ci**) or 15:9 (**Dii**).

The same two photoperiods used in Nagy *et al.* (2018) were used in this chapter (LD9:15 & 15:9). These photoperiods cover a light spectrum between 380 nm and 778 nm and can be programmed to vary the light intensity from 0.005 lx to 1,500 lx. However, the maximum light intensity of the short photoperiod (LD9:15) was set to 620 lx and the long photoperiod (LD15:9) was modified so that the area under the curve was identical to that of the short photoperiod. This was to ensure that the cumulative light the flies were subjected to was kept constant. Both temperature programs were created so that the average temperature across 24 h is 11.5°C. The long-day temperature cycle (LD15:9) was modified from data collected in the original environmental recordings in Treviso, Italy (45°65'N), and the shape of the curve based on the temperature profile created for long-summer days (Vanin *et al.*, 2012; Green *et al.*, 2015) (**Figure 5-1 Bi, Ci & Di**). This was a suitable method as temperature cycles during long days manifest in a symmetrical sinusoidal manner. However, in short-days (LD9:15), the shape of the temperature curve is not symmetrical. Instead, temperature increases rapidly during the morning, then decreases at a slowing rate during the afternoon and evening until it almost reaches a low plateau (Wilczek *et al.*, 2010; Vanin *et al.*, 2012). Consequently, the short-day temperature cycle was created based on the average hourly temperature in Leicester, U.K (latitude 52°38'N) on the 10<sup>th</sup> of November (when the photoperiod is ~LD9:15). The profile was then adjusted to ensure an average temperature of 11.5°C. (**Figure 5-1 Bii, Cii & Dii**).

## 5.4.2 Photoperiodic effects on diapause under semi-natural light profiles

In nature, in relation to the life cycle of *D. melanogaster*, light and temperature are coupled and where one exists so does the other. To investigate the effects of natural temperature profiles on diapause induction it therefore is logical to do so under simulated natural light profiles, as, after all, it is radiation from the sun that causes the daily temperature cycles. This too will help to understand the relationship between light and temperature, and thermoperiod and photoperiod. However, before investigating the effects of temperature on diapause it was necessary to assay for photoperiodic effects. This would allow for a comparison to subsequent experiments that aim to assay for thermoperiodic effects in which photoperiodicity may also be a contributing factor. Consequently, natural caught flies from both Rende (Italy) or Houten (Holland) were subjected to a flat constant temperature of 11.5°C with either a short autumnal photoperiod of LD9:15, or a long summer photoperiod of LD15:9 (**Figure 5-1A**). After 14 days females were then scored for reproductive diapause.

ANOVA results show a photoperiodic effect ( $F_{df}=26.05$ ,  $P<0.0001$ ) but no population effect ( $F_{df} =0.3955$ ,  $P=0.5334$ ) or photoperiod x population interaction ( $F_{df}=0.0569$ ,  $P=0.0.8128$ ) when diapause was scored from egg stage <8 (**Figure 5-2A**). Moreover, *post hoc* tests show a significant difference in diapause levels between photoperiods in both Houten and Rende flies ( $P=0.0077$  &  $P=0.0031$  respectively). There was also a photoperiodic effect when diapause was scored at egg stage <10 (**Figure 5-2B**) ( $F_{df}=12.03$ ,  $P<0.0014$ ) and no population ( $F_{df}=1.961$ ,  $P=0.1700$ ) or interaction ( $F_{df}=0.2107$ ,  $P=0.0.6490$ ) effects. However, when scored from egg stage <10, only in Houten flies was there a marginal *post hoc* significant difference in diapause between photoperiods ( $P=0.0412$ ).

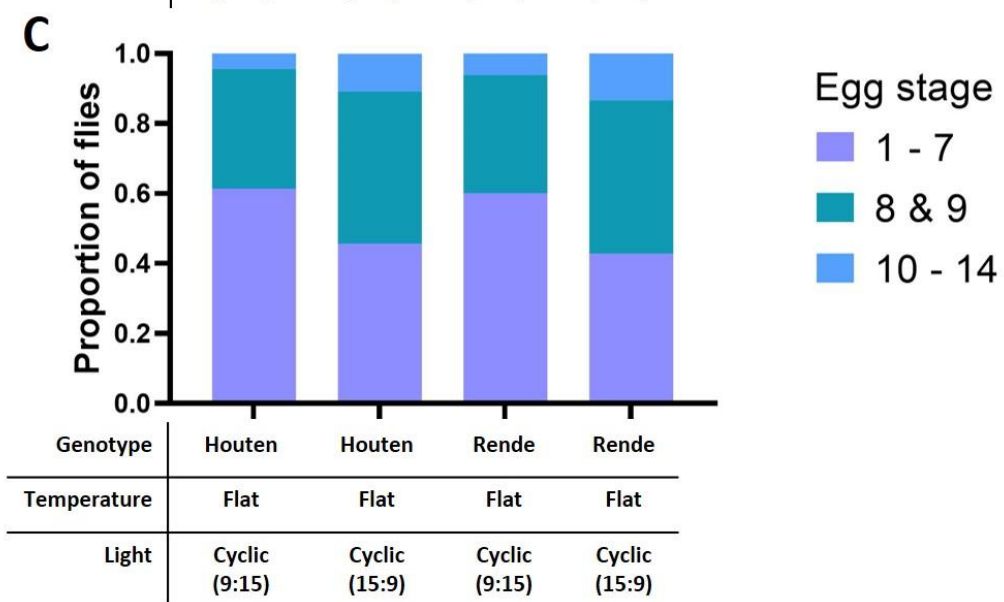
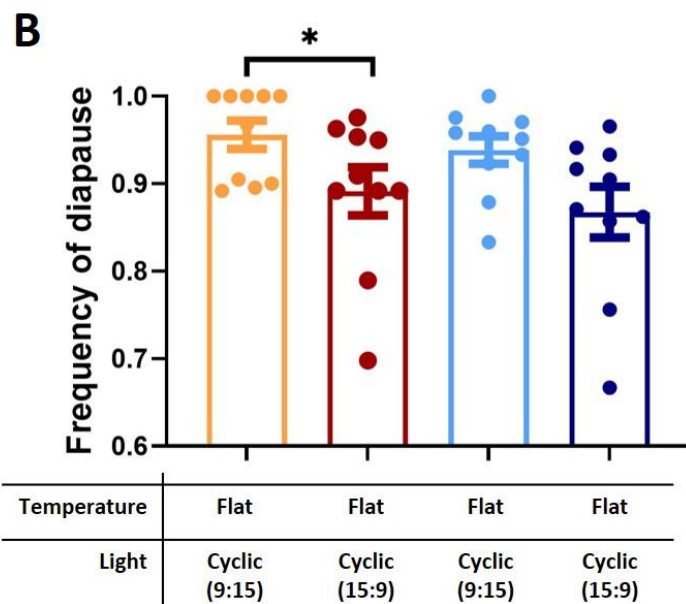
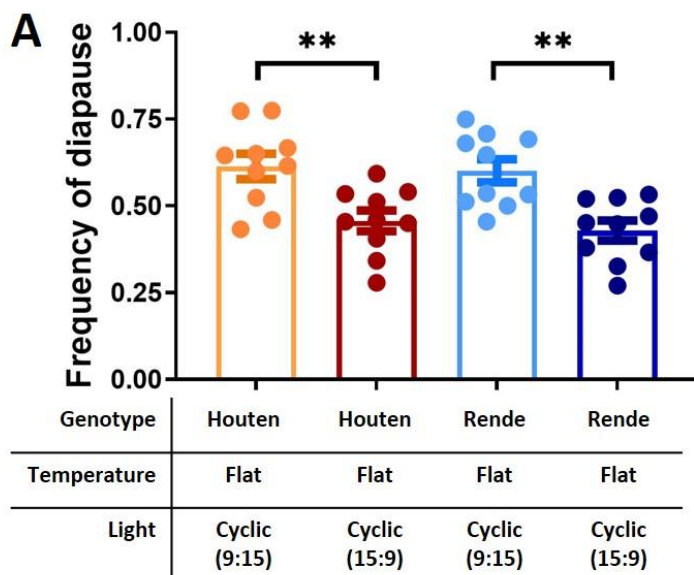


**Figure 5-2.** Diapause levels in Houten and Rende flies under differing photoperiods. Flies were kept at a flat 11.5°C temperature profile but a cyclic semi-natural light profile with a photoperiod of either LD 9:15 or 15:9. Diapause was scored from stage <8 (**A**) and stage <10 (**B**). Dots represent trials, bars represent Mean ± SEM. Significance was calculated via two-way ANOVA followed by Tukey's multiple comparison test (Appendix 8-5-2), \* = P<0.05, \*\* = P<0.01, \*\*\* = P<0.001, \*\*\*\* = P<0.0001. For **B**, data failed Anderson-Darling and D'Agostino & Pearson normality testing and were therefore arcsine transformed prior to statistical analysis. **C**) stacked % of flies for each genotype that displayed each egg-stage grouping as their most advanced egg stage upon dissection. In total, 1355 flies were dissected.

#### 5.4.3 Semi-natural thermoperiodic effects on diapause under semi-natural light profiles

Temperature has been found to be the most dominant contributor to the diapause phenotype in laboratory studies (Saunders, 1990; Emerson et al., 2009a; Anduaga *et al.*, 2018). However, it is yet to be studied under more realistic natural-like parameters. Therefore, flies were subjected to simulated natural temperature and light profiles that either mimicked a short autumnal day in which the photoperiod was 9:15, or a long summer-like day with a photoperiod of 15:9. The thermoperiods were created to mimic how they manifest under such photoperiodic conditions in nature (**Figure 5-1B**). ANOVA analysis of diapause levels indicate no population, environmental, or interaction effects when diapause was scored from either egg stage <8 (**Figure 5-3A**) ( $F_{df} = 2.244$ ,  $P=0.1428$ ;  $F_{df} = 1.870$ ,  $P=0.18$ ;  $F_{df} = 0.01214$ ,  $P=0.9129$  respectively) or egg stage <10 (**Figure 5-3B**) ( $F_{df} = 0.01947$ ,  $P=0.8898$ ;  $F_{df} = 0.7519$ ,  $P= 0.3916$ ;  $F_{df} = 0.3658$ ,  $P= 0.5491$  respectively). Tukey's multiple comparison also did not show any significant difference between any of the means (**Appendix 8-5-4**).

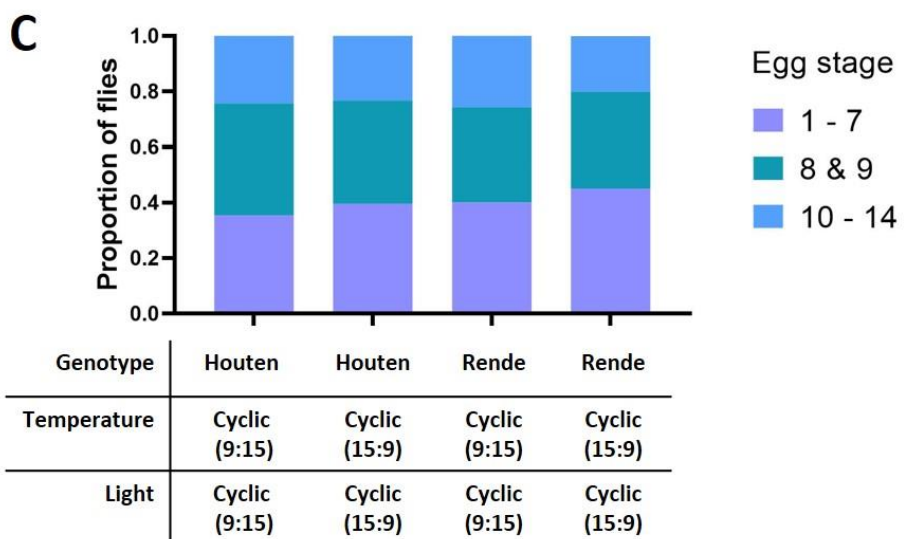
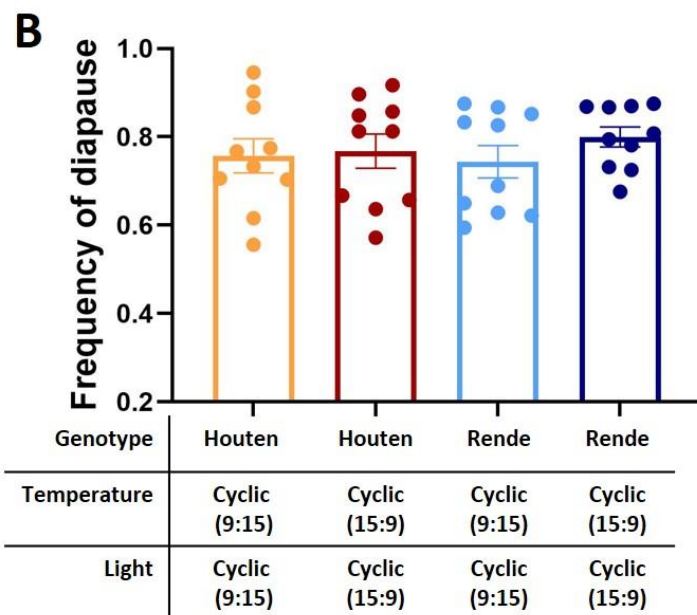
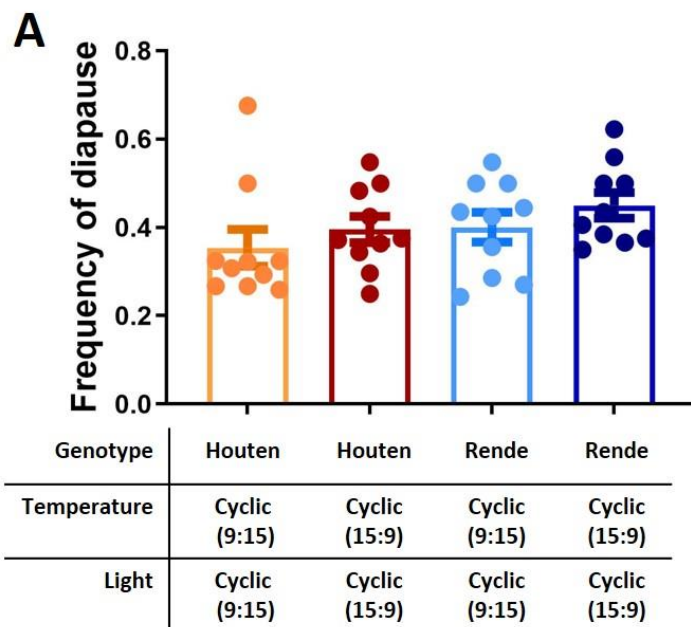


**Figure 5-3.** Diapause levels in Houten and Rende naturally caught flies under differing photoperiod and thermoperiod environmental parameters. Flies were subjected to either a coupled cyclic thermoperiod and cyclic photoperiod mimicking that of a short day (9:15) or that of a long day (15:9). Diapause was scored from stage <8 (**A**) and stage <10 (**B**). Dots represent repeats, bars represent Mean  $\pm$  SEM. Significance was calculated via two-way ANOVA followed by Tukey's multiple comparison test (Appendix 8-5-4), \* = P<0.05, \*\* = P<0.01, \*\*\* = P<0.001, \*\*\*\* = P<0.0001. Data for both **A** and **B** failed Anderson-Darling and D'Agostino & Pearson normality testing and were therefore arcsine transformed prior to statistical analysis. **C**) stacked % of flies for each genotype that displayed each egg-stage grouping as their most advanced egg stage upon dissection. In total, 1349 flies were dissected.

#### 5.4.4 The effect on diapause of flies subjected to thermoperiods opposite to the subjected photoperiod

The lack of a diapause effect when comparing flies subjected to long-day or to short-day photoperiods & thermoperiods was surprising (**Figure 5-3**). It may be that the thermoperiods used create opposing diapause-inducing/inhibiting cues than their corresponding photoperiods, and therefore cancel each other out. To test this theory, opposing thermoperiods and photoperiods were used. Flies were subjected to either a thermoperiod mimicking that of a short (9:15) day but a photoperiod mimicking a long (LD15:9) day, or to a thermoperiod mimicking that of a long (15:9) day but a photoperiod mimicking a short day (LD9:15) (**Figure 5-1C**). ANOVA analysis of diapause levels reveal no environmental ( $F_{df}=0.7152$ ,  $P=0.4090$ ;  $F_{df}=0.4657$ ,  $P=0.5006$ ) or interaction ( $F_{df}=0.01975$ ,  $P=0.8892$ ;  $F_{df}=0.7070$ ,  $P=0.4070$ ) effects, but there is a significant population effect ( $F_{df}=8.699$ ,  $P=0.0064$ ;  $F_{df}=20.72$ ,  $P<0.0001$ ) when scoring from either egg stage <8 (**Figure 5-4A**) or <10 (**Figure 5-4B**) respectively. However, Tukey's multiple comparison only reveals a significance when diapause is scored from stage <10 (**Appendix 8-5-6**).

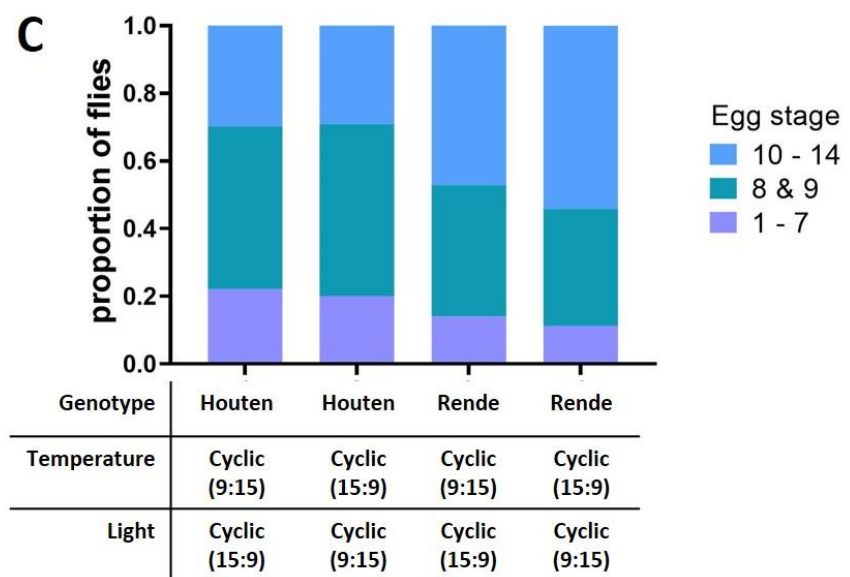
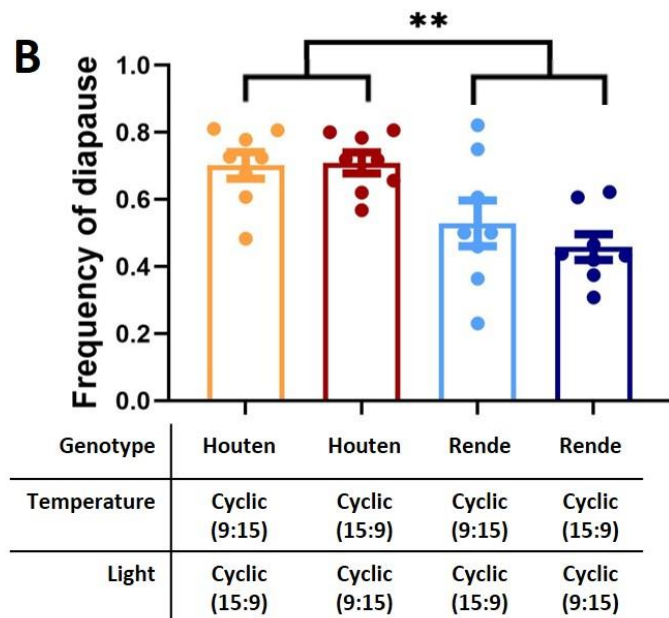
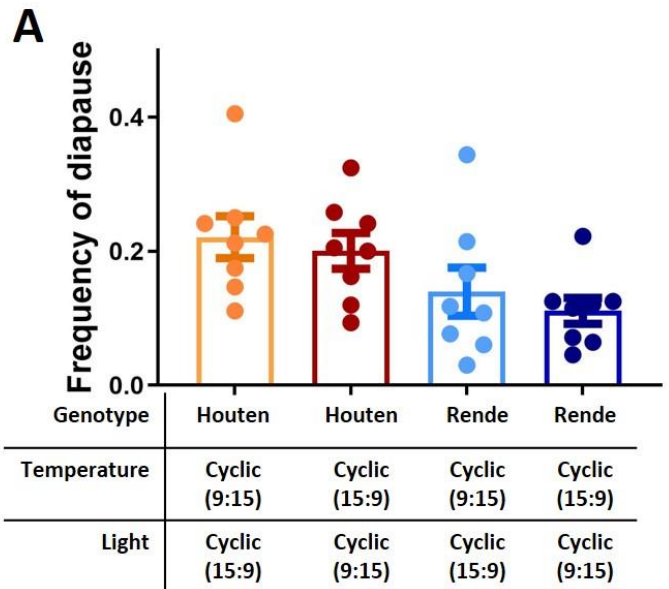


**Figure 5-4.** Diapause levels in Houten and Rende flies under opposing photoperiods and thermoperiods. Flies were subjected to either a thermoperiod mimicking that of a short (9:15) day but a photoperiod mimicking a long (15:9) day, or to a thermoperiod mimicking that of a long (15:9) day but a photoperiod mimicking a day short (9:15). Diapause was scored from stage <8 (**A**) and stage <10 (**B**). Dots represent repeats, bars represent Mean ± SEM. Significance was calculated via two-way ANOVA followed by Tukey's multiple comparison test (Appendix 8-5-6), \* = P<0.05, \*\* = P<0.01, \*\*\* = P<0.001, \*\*\*\* = P<0.0001. **C)** stacked % of flies for each genotype that displayed each egg-stage grouping as their most advanced egg stage upon dissection. In total, 1059 flies were dissected.

#### 5.4.5 The effect on diapause of uncoupling the photoperiod from the thermoperiod

When the thermoperiod and photoperiod are coupled, i.e., as light intensity begins to increase so does temperature, there is no difference in diapause levels between long-day photo/thermoperiods and short-day photo/thermoperiods if both are cycling in a natural-like manner (**Figure 5-3**). Reversing the thermocycle in relation to the photoperiodic cycle also did not have any effect on diapause levels (**Figure 5-4**). To understand if thermoperiod in relation to photoperiod has any effect on diapause, the thermoperiod was advanced in relation to the photoperiod by 12 h. This meant that when the fly perceives it to be daytime (via the photoperiod) the thermoperiod would perceive it as “night”, whereas, when the photoperiod perceives it is night-time, the thermoperiod will perceive it is the day. These conditions were tested using either short-day mimicking photoperiod and thermoperiods, or long-day mimicking photoperiod and thermoperiods (**Figure 5-1D**). ANOVA analysis of diapause levels shows no environmental ( $F_{df} = 2.888$ ,  $P=0.0990$ ;  $F_{df} = 1.326$ ,  $P=0.2581$ ) or interaction ( $F_{df} = 0.530$ ,  $P=0.4682$ ;  $F_{df}=0.01287$ ,  $P=0.9104$ ) effects but strong population effects ( $F_{df} = 374.3$ ,  $P<0.0001$ ;  $F_{df}=146.8$ ,  $P<0.0001$ ) when diapause is scored at either egg stage <8 (**Figure 5-5A**) or egg stage <10 (**Figure 5-5B**) respectively. This is confirmed by Tukey's multiple comparison test ( $P<0.0001$ ,  $P<0.0001$ ).

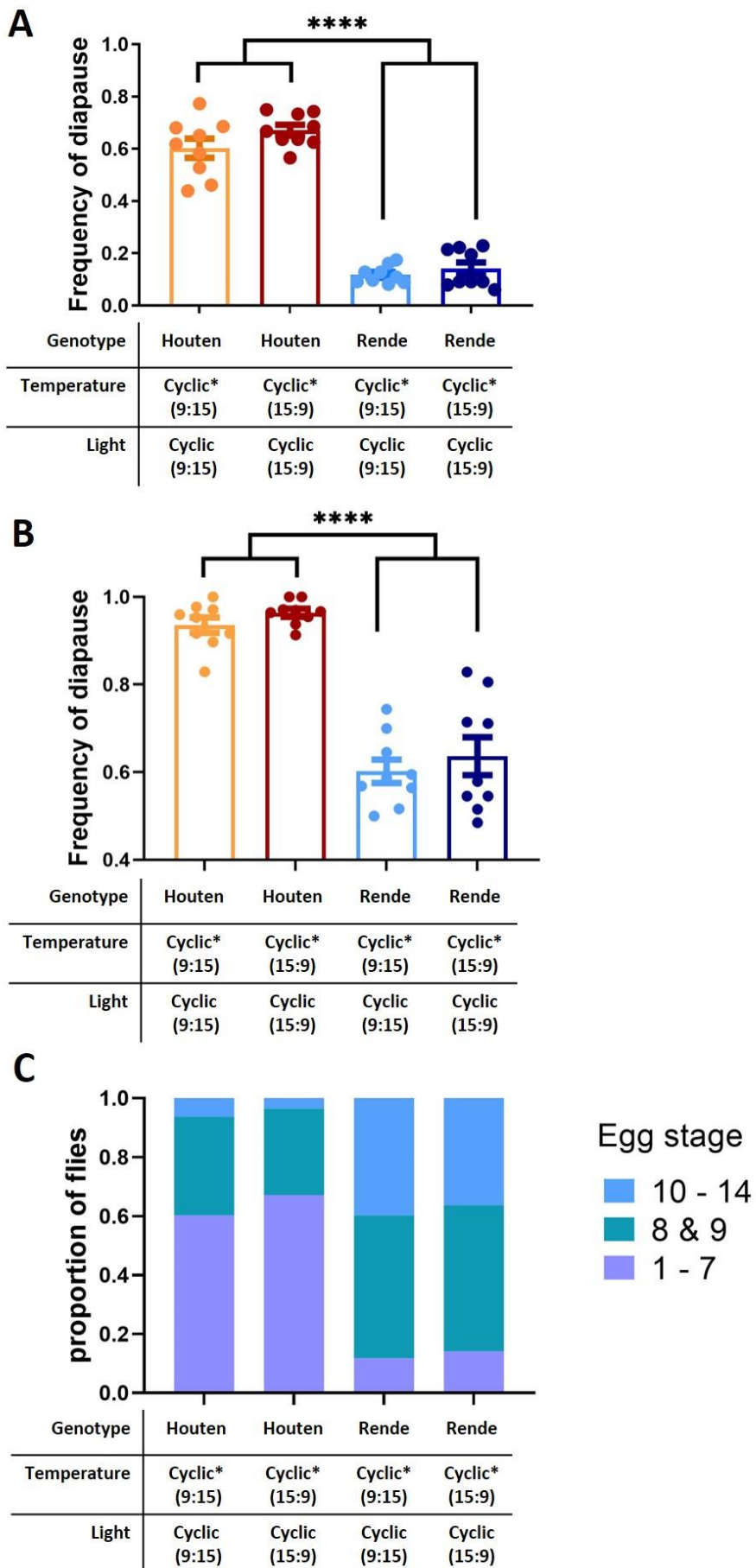


**Figure 5-5.** Diapause levels in Houten and Rende flies under opposing photoperiods and thermoperiods. Flies were subjected to either a thermoperiod and photoperiod mimicking that of a short day (9:15) or that of a long day (15:9). The thermoperiod for either day-length was advanced by 12 hours from that of its relative photoperiod. Diapause was scored from stage <8 (**A**) and stage <10 (**B**). Dots represent repeats, bars represent Mean ± SEM. Significance was calculated via two-way ANOVA followed by Tukey's multiple comparison test (See appendix 8-5-8), \* = P<0.05, \*\* = P<0.01, \*\*\* = P<0.001, \*\*\*\* = P<0.0001. Data for **A** failed Anderson-Darling and D'Agostino & Pearson normality testing and was therefore arcsine transformed prior to statistical analysis. **C**) stacked % of flies for each genotype that displayed each egg-stage grouping as their most advanced egg stage upon dissection. In total, 1253 flies were dissected.

## 5.5 Discussion

The findings of this chapter are perplexing and not simple to dissect. However, the first finding of this chapter offers a logical foothold. Flies that were kept at a constant temperature of 11.5°C but subjected to either a short photoperiod (LD 9:15) or a long photoperiod (LD 15:9) under simulated natural light profiles displayed a photoperiodic diapause phenotype (**Figure 5-2**). This is consistent with the findings of Nagy and colleagues (2018). However, the light profiles used in this study and in that of Nagy *et al.* differ. The photoperiodic profile used in both studies were identical except for the light intensity of the long-day (LD 15:9). In the Nagy study, they examined photoperiodic effects on diapause wherein the light profiles more closely mimicked those observed in the wild (Nagy *et al.*, 2018). This meant that in the long photoperiod, not only is the photoperiod itself longer, but the light intensity greater. This means that it is not clear whether the fly, under semi-natural light profiles, interprets the photoperiod itself or the overall light exposure as being diapause-inducing/inhibiting.

In this current study, the light intensity of the long (LD15:9) photoperiod was damped so that the accumulated light intensity recorded throughout the day is identical to that of the short photoperiod. This has significant implications when comparing both sets of findings. Both studies found a

photoperiodic diapause effect, so it can be concluded that this was not due to a difference in the accumulation of light experienced by the flies. Furthermore, as a consequence of normalising the overall cumulative light exposure, the maximum light intensity reached at L-max in the short photoperiod (LD 9:15) is actually higher than that of the long photoperiod (LD 15:9) (**Figure 5-1**). In the Nagy study (2018), the opposite is true. This implies that the diapause phenotype is also not due to a difference in maximum light exposure. Therefore, the photoperiodic diapause phenotype is most likely a consequence of a change in photoperiod itself and not due to a difference in light exposure, neither cumulative nor absolute.

Photoperiodic diapause effects are small or absent from many laboratory studies (Tatar *et al.*, 2001; Emerson *et al.*, 2009b; Anduaga *et al.*, 2018; Lirakis *et al.*, 2018) but using semi-natural light profiles these effects become more robust (Nagy *et al.*, 2018; **Figure 5-2**). Therefore, the length of the photoperiod itself (i.e., time lights are turned on/off) is unlikely to be the regulatory mechanism to control diapause. The difference between rectangular and semi-natural light conditions is that in the latter the fly is subjected to gradual changes in light over time. It is therefore likely that this gradual change in light intensity is what regulates diapause. It would be expected that the same is true for temperature. There is already evidence that the fly has the ability to recognise gradual temperature changes as well as absolute temperature and that these thermosensory pathways act via different mechanisms (Luo *et al.*, 2017). However, when cyclic thermoperiods were added to the semi-natural photoperiods, all photoperiodic diapause effects were lost (**Figure 5-3**). This result is indeed surprising and would suggest that either cyclic thermoperiods have an opposite effect on diapause than their corresponding photoperiod; that any exposure to high temperatures will inhibit diapause regardless of the thermoperiod and/or photoperiod; or that a photoperiodic effect on diapause is only observed in the absence of temperature input, and the diapause levels observed in nature are set by the average/absolute temperature. To test if the former theory is correct, the thermo and photo periods were uncoupled so that flies perceived a short day via temperature but a long day

via light, or *vice-versa*. Interestingly, this resulted in identical diapause levels between flies in either condition and in either population (**Figure 5-4**). If the thermoperiods have opposing roles to their corresponding photoperiods which were previously cancelling each other out (**Figure 5-3**), then an even greater difference in diapause levels than observed with just an active photoperiod (**Figure 5-2**) would be expected. As this was not the case, this theory can be ruled out. This also rules out any effects that differing maximum temperature (T-max) or minimum temperature (T-min) may have had on “cancelling out” the photoperiodic diapause effects.

This leaves two possible explanations for the loss of a photoperiodic, and the absence of a thermoperiodic diapause phenotype in these experiments. Either absolute/average daily temperature determines diapause and the photoperiod and thermoperiod are largely irrelevant in semi-natural conditions, or that there is a complex relationship between light and temperature that remains to be understood. When the thermoperiod and photoperiod were uncoupled by 12 hrs. (**Figure 5-5**), as with the previous experiments (**Figure 5-3 & 5-4**), there was no difference in diapause levels in flies under short-day photo/thermoperiods compared to long-day photo/thermoperiods. There was however a very significant difference between fly populations, with the southern European Rende flies exhibiting much lower diapause levels than the northern Houten flies in both environmental conditions.

Inspecting each experiment of this chapter in isolation does not reveal much insight into the relationship between temperature and light in regulating diapause in nature. However, compiling all the data together and comparing it as a whole offers another perspective. Data was compiled and replotted so that both photoperiods are aligned under each thermoperiod profile, and each population separated for easier comparison (**Figure 5-6**).

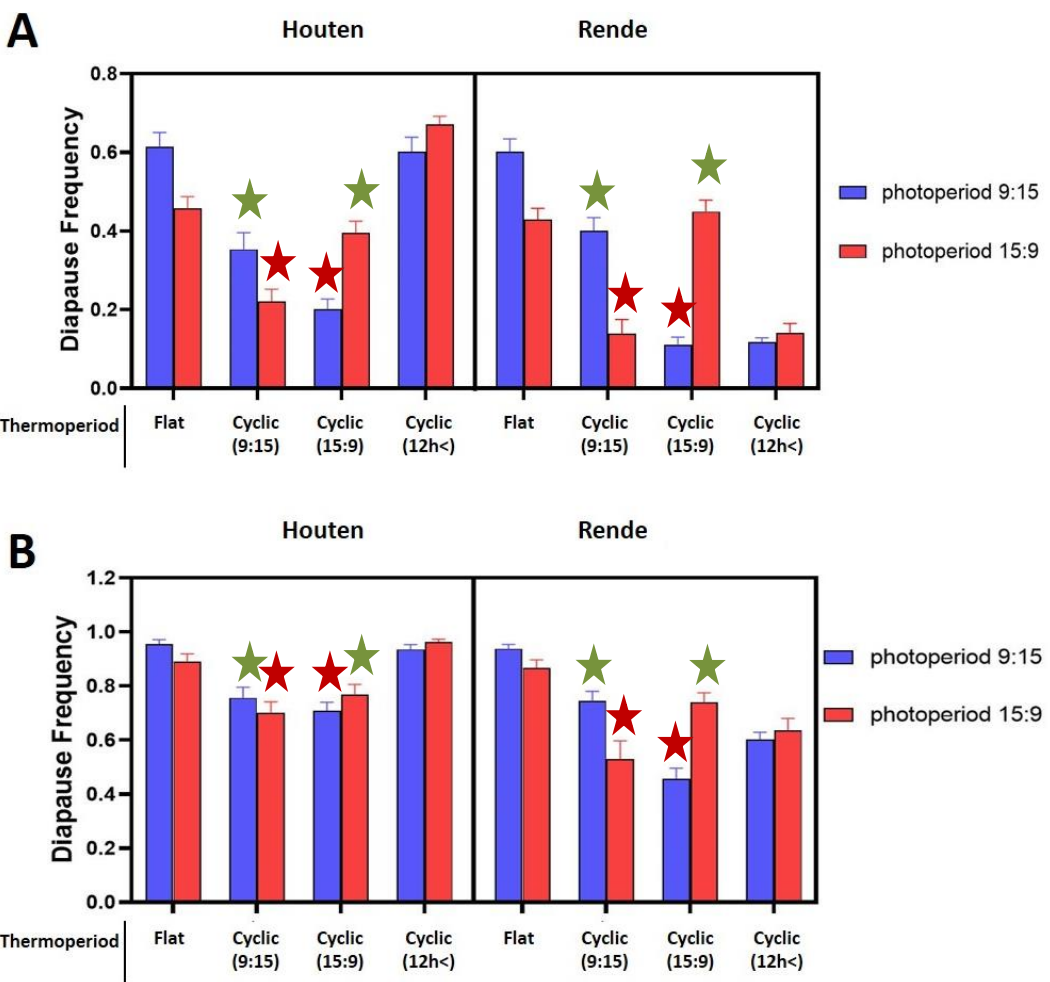


**Figure 5-6.** An alternative presentation of the data analysed in this chapter. The data is collated from several independent experiments (**Figures 2, 3, 4 & 5**). Diapause levels were calculated from either egg stage <8 (A) or egg stage <10 (B). The red and green are referenced to in the text. The "2h<" thermoperiod refers to an advanced thermoperiod compared to photoperiod, whereby temperature begins to increase 12 hours prior to light. Statistics were calculated by three-way ANOVA followed by Tukey's multiple comparison test (presented in Appendix 8-5-9 & 8-5-10).

ANOVA reveals that there are strong thermoperiodic ( $F_{df}=57.14$ ,  $P<0.0001$ ;  $F_{df}=46.13$ ,  $P<0.0001$ ) and population ( $F_{df}=83.01$ ,  $P<0.0001$ ;  $F_{df}=73.90$ ,  $P<0.0001$ ) effects across the data when diapause is scored from either <8 (**Figure 5-6A**) or <10 (**Figure 5-6B**) respectively. There are also strong thermoperiod x population ( $F_{df}=61.99$ ,  $P<0.0001$ ;  $F_{df}=15.38$ ,  $P<0.0001$ ) and thermoperiod x photoperiod ( $F_{df}=47.97$ ,  $P<0.0001$ ;  $F_{df}=14.89$ ,  $P<0.0001$ ) interactions in either scoring method. To a lesser extent there is also a

thermoperiod x population x photoperiod interaction when diapause is scored from either <8 or <10 ( $F_{df} = 3.289$ ,  $P=0.023$ ;  $F_{df} = 5.193$ ,  $P=0.002$  respectively). There was no photoperiod effect ( $F_{df} = 0.6166$ ,  $P=0.4337$ ;  $F_{df} = 0.0005$ ,  $P=0.9824$ ) and no population x photoperiod effect ( $F_{df} = 0.1346$ ,  $P=0.7143$ ;  $F_{df} = 0.2146$ ,  $P=0.6440$ ) under either scoring method. For the ANOVA table and subsequent *post hoc* tests see (**Appendix 8-5-9 & 8-5-10**)

As previously discussed, diapause levels are high when temperature is kept at a flat 11.5°C and a significant photoperiodic effect is observed, with higher diapause levels in short photoperiods. However, when the thermoperiod is cyclic there is a clear fall in diapause levels. When under a short thermocycle, there is more diapause in flies subjected to a short photoperiod than flies subjected to a long photoperiod. However, when under a long thermocycle, the opposite is true (**Figure 5-6**). Therefore, when the thermocycle and photocycle are coupled and cycle in tandem, regardless of whether they are coupled as a “long day” or a “short day”, diapause levels remain high (albeit not as high as when under a constant temperature). However, when the thermocycle and photocycle do not match diapause levels are significantly lower (**Figure 5-6**). Clearly, a mismatch between photo and thermocycle disrupts any photoperiodic effect on diapause.

Interestingly, at least in the case of the Houten flies, diapause levels are as high in flies subjected to the 12-hour out-of-phase environmental conditions (**Figure 5-5**) as to flies subjected to a flat temperature and short photoperiod (**Figure 5-2**). This discredits the possibility that the decreased diapause levels from flies subjected to cyclic thermoperiods (**Figures 5-3 & 5-4**) are due to high maximum temperatures as the maximum temperatures are equally high in the out-of-phase experiment (**Figure 5-5**).

Although diapause levels are high amongst northern European Houten flies when subjected to 12-hour out-of-phase experimental conditions, diapause levels are low in southern Rende flies (**Figure 5-5**). This phenomenon is

difficult to explain without further investigation. However, it may be due to a complex mechanism involving input from both photoperiod and thermoperiod.

It is possible that the actual thermoperiod and photoperiod themselves do not matter, but the relationship between them does. As discussed previously, photoperiodic influence under constant temperature is likely due to a sensation of a change in light intensity over time (**Figure 5-2**). This is also the likely case with temperature because differences in T-max or length of the thermoperiod do not affect diapause levels (**Figure 5-3 & 5-4**), and the average temperature is identical across experiments. Therefore, the last variable between the photoperiod and thermoperiods used in this study is the rate of change in light or temperature respectively (**Figure 5-1**). The actual temperature will fluctuate from day-to-day and week-to-week. This is also true for light intensity which varies depending on cloud cover. However, the rate of change in light intensity and temperature during the day is very predictable depending on the time of year it is. The ability of the fly to compare the rate of temperature change to the rate of photoperiod change to determine diapause inducibility is therefore a logical strategy to dictate diapause induction.

In shorter days (both in nature and simulated in this study), The sun rises quickly, resulting in a rapid change in light intensity coupled with a rapid rise in temperature. However, in longer days, sunrise occurs more slowly and results in a shallower increase in both light and temperature over a longer duration of time. It is possible that signals propagating from the rate of temperature change and the rate of light intensity change eventually arborize at one neural centre within the fly (**Figure 5-7**). If the two signals “match” then this is interpreted as an environment that is “logical”. This signal may then arborize (in the same location or elsewhere) with other diapause-inducing cues, such as humidity, absolute/average temperature and food availability (Da Lage *et al.*, 1990; Saunders and Gilbert, 1990; Tata *et al.*, 2001; Frydenberg *et al.*, 2003; Ayrinhac *et al.*, 2004; Hoffmann *et al.*, 2005; Lirakis *et al.*, 2018; Rajpurohit *et al.*, 2018). Only if the fly is in a “safe”

and “logical” environment is it able to interpret its other environmental cues to decide whether to enter diapause or not. This makes evolutionary sense, as diapause does not just result in reduced fecundity, but is also characterised by inactivity (Mitrovski and Hoffmann, 2001; Schmidt, 2011). If the local environment is unpredictable, it would not make sense for the fly to diapause but if it stays active, relocates, and if the conditions are permissive, it then can make a safe “decision” to diapause or not.

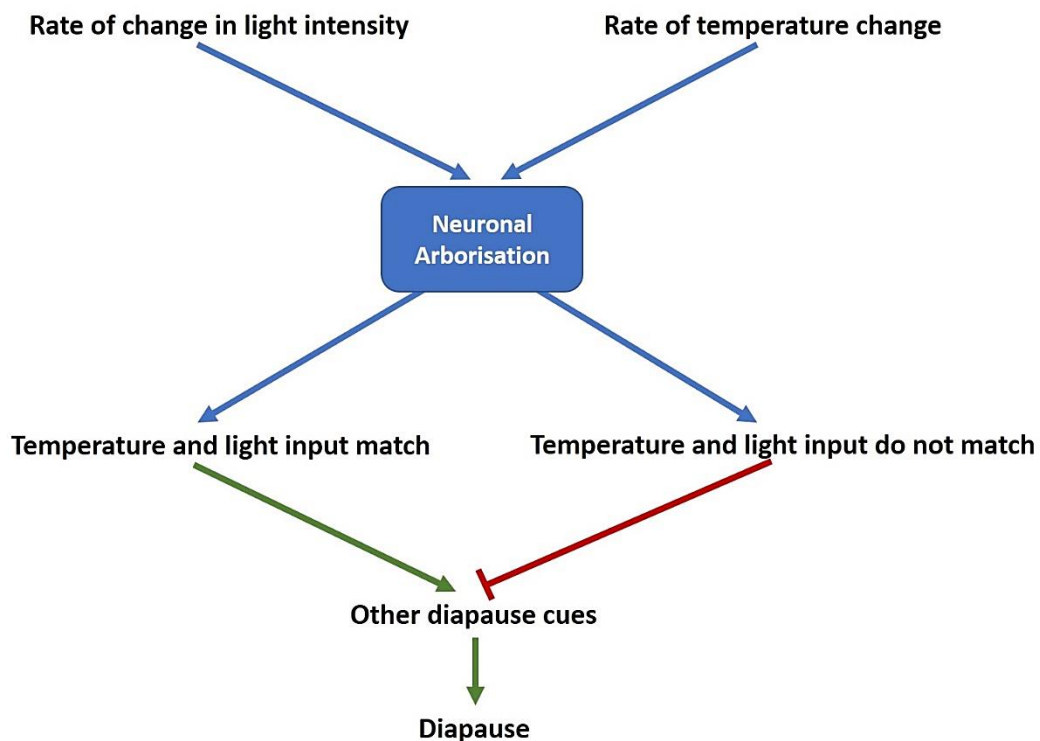


**Figure 5-7.** A schematic model of how the rate of change of natural light and temperature during the day (morning) may be interpreted by the fly to determine diapause-inducibility. Green arrows represent agonistic properties, whereas red represents repressive properties.

This model fits with the data presented from this chapter. When the thermocycle and photoperiodic cycle match (**Figure 5-6**: green stars), the fly interprets that the environment is predictable. As the average temperature is 11.5°C, a relatively large proportion of the population enter diapause. However, when the thermocycle and photoperiodic cycles do not match (**Figure 5-6**: red stars), the environment is unpredictable and diapause is denied and other diapause-inducing/inhibiting cues are

overridden. Therefore, the majority of the flies do not enter diapause. When temperature is constant (**Figure 5-2**), there is no thermoperiod and the environment becomes predictable and is permissible for diapause. Photoperiod is able to work independently, possibly outside of the proposed model, and creates a perceived artificial photoperiodic effect on diapause.

There are differing diapausing properties between the two populations investigated in this chapter when the thermocycle is advanced in relation to the photoperiodic cycle by 12 hrs. (**Figure 5-5**). Houten flies display relatively high levels of diapause under these conditions. Inspection of the thermocycle in relation to the photoperiodic cycle under these parameters (**Figure 5-1**) reveal the following: During the diurnal hours (as determined by photoperiod) the thermocycle is approaching its trough as temperature is decreasing, and in the short-day thermoperiod it is almost flat. The diapause-related mechanism that measures the rate of temperature change may only measure the rate of increase, but not rate of decrease. This makes sense as in nature the temperature does not decrease during the morning, and it is the morning in which the rate of temperature change is most obvious between thermoperiods. Therefore, under these conditions there is no sensation of rate change in temperature, thus, temperature and light signals mimic that of the flat temperature experiment (**Figure 5-2**). Indeed, diapause levels are as high, or even higher under these parameters than under the flat temperature parameters (**Figure 5-5 & 5-6**).

For Rende however the opposite is true. Diapause levels remain low when the thermocycle is advanced from the photoperiod by 12 hrs. (**Figure 5-5 & 5-6**). This may be due to the latitudinal location that these lines were caught. Rende flies are from southern Italy ( $39^{\circ}19'53''N$ ) whereas the Houten flies are from central Holland ( $52^{\circ}01'41.99''N$ ). These flies have evolved in differing environments whereby the northern Houten flies are subject to conditions in which diapause is much more advantageous than in Rende. Therefore, their relative diapause regulatory mechanisms may differ in sensitivity and indeed in timing of cues. How this relates to the observed difference when the thermocycle is advanced from the photoperiodic cycle

is hard to explain and needs further investigation. Only two populations of flies were used in these experiments. To get a better representation of population/ latitudinal differences, comparison to other populations from a range of latitudinal locations and from continents other than Europe are needed. As there is a strong latitudinal cline in diapause amongst American populations (Schmidt *et al.*, 2005) it would be especially interesting to test populations from there. Furthermore, a thermoperiodic effect on diapause independent of any light input (i.e., flies kept in DD or LL) has not been conducted. This would create a constant and predictable light-input in which thermoperiod can be assessed independent of light. This is worth doing and may uncover more unexpected results that can further elucidate the mechanism by which light and temperature input is translated to diapause induction.

Finally, if the proposed model is indeed correct, the neuronal regions to which these temperature and light inputs are processed need to be identified. These may arborize on one point, or several. The several light and temperature input pathways in relation to the circadian clock have been thoroughly researched (Glaser and Stanewsky, 2005; Picot *et al.*, 2009; Yoshii *et al.*, 2010; Kaneko *et al.*, 2012; Szular *et al.*, 2012; Lee and Montell, 2013; Wolfgang *et al.*, 2013; Saint-Charles *et al.*, 2016; Tang *et al.*, 2017; Lamaze *et al.*, 2017; Li *et al.*, 2018; Ogueta *et al.*, 2018; Azevedo *et al.*, 2020; Chen *et al.*, 2020; Fernandez *et al.*, 2020) and discussed extensively in **Chapter 1.2**.

In relation to diapause, the neuronal properties of light and temperature input has been studied to a much lesser extent (Andreatta *et al.*, 2018; Nagy *et al.*, 2019; Abrieux *et al.*, 2020) (See also **Chapter 1.3**). EYA has been identified in the optic lobe and in the IPCs where it regulates diapause in a thermo/photoperiodic manner (Abrieux *et al.*, 2020). The Stanewsky laboratory have also found that the compound eye, specifically the dendritic projections from Rh1, Rh5 and Rh6 expressing photoreceptors, interpret gradual changes in temperature within adult flies (albeit via stepped temperature profiles) via PLC21C. The same mechanism may be

responsible for sensing gradual temperature change in a diapause-related manner. Moreover, the DN1 cells which are important for integration of temperature input into the clock have direct contact with the IPCs to regulate ILS (Barber *et al.*, 2016). Furthermore, the s-LNvs also contact the IPCs to regulate diapause (Nagy *et al.*, 2019) and these neurons in circuit with the TrpA1<sup>+</sup> AC and DN2 cells are important for temperature sensation. Both the DN1s and s-LNvs also receive signals from the Johnston organ of the antennae via Pyr (Tang *et al.*, 2013). This circuit has been implicated in entrainment of the clock to low temperature thermocycles and therefore may have a role in diapause-related temperatures (Wolfgang *et al.*, 2013; Roessingh *et al* 2019). Whether the compound eye, circadian neurons, the antennae, other neuronal centres, or a combination of centres are responsible for the sensation of the rate of temperature/light change remains to be investigated. Experiments from the literature attempting to unpick the neuronal circuits responsible for light and temperature dependent diapause control should be repeated under more natural conditions to better understand the true nature of diapause control.

This chapter not only is the first of its kind to study diapause under simulated natural thermocycles, but also the first to investigate the relationship between light and temperature in diapause regulation under semi-natural conditions in parallel. As such, more questions were unearthed than answered, and further study is needed to truly elucidate the environmental control of *D. melanogaster* diapause in nature. Nevertheless, the findings of this chapter can be summarised as follows:

- In the absence of changing temperature cues (flat temperature), photoperiodic effects on diapause are due to the photoperiod length itself, not accumulated light uptake or maximum light intensity.
- Thermoperiod and photoperiod interact to control diapause under simulated semi-natural conditions.
- The regulation of diapause under simulated semi-natural conditions via thermoperiod and photoperiod is likely via the sensation of a rate

of change, not the maximum or the average temperature and light sensed across the day.

- The sensation of the rate of change of temperature and light likely occurs during the morning hours to regulate diapause.
- A new model for thermoperiod/photoperiod regulation of diapause is proposed wherein the perceived rate of change of temperature and light combine to determine if the environment is “safe”. Other cues then combine to determine diapause induction.

## 6. THE AFTERNOON PEAK IN SEMI-NATURAL SUMMER-LIKE CONDITIONS.

### 6.1 Introduction

#### 6.1.1 The circadian clock under natural and semi-natural conditions

The *Drosophila* circadian clock has been well studied and has been implicated in human health-related problems such as neurodegenerative diseases (Chen *et al.*, 2014a; Musiek *et al.*, 2015), neurological disorders (Bellivier *et al.*, 2015), metabolism (Eckel-Mahan and Sassone-Corsi., 2013), cell division and cell death (Hunt and Sassone-Corsi, 2007; Means *et al.*, 2015), as well as many others. However, until recently, study of the clock in *D. melanogaster* has always been conducted under artificial laboratory conditions.

In the laboratory, using standard incubator systems, the clock has been almost exclusively studied under rectangular light and temperature cycles. In a typical LD 12:12 cycle lights will switch on in the morning (ZT0) and then switch off again in the evening (ZT12) with absolute darkness in between. Once switched on, the light will often be at a constant intensity with only ‘white light’ LEDs or incandescent lights as the source.

Temperature is also kept in a similarly rectangular manner: usually kept at either a constant flat state or with a sudden step up in line with “dawn”, and step down in line with “dusk”. Such conditions are clearly not what *Drosophila* or any organism is subjected to in the wild.

In nature, both light and temperature follow a gradual and smooth cyclic regime consisting of various wavelengths of light that differ in intensity at different points of the day. For example, red light can penetrate the Earth’s atmosphere at times closer to astronomical twilight than blue light due to the wavelength of the light and angle the light reaches the Earth (United States Naval Observatory, 2017). In addition, the peak in temperature lags that of light by several hours, a phenomenon rarely mimicked in laboratory studies.

In the past decade, it has become apparent that many circadian-linked behaviours and indeed the circadian clock, act differently in natural conditions in relation to previously reported laboratory conditions (Vanin *et al.*, 2012; Menegazzi *et al.*, 2012; Menegazzi *et al.*, 2013; De *et al.*, 2013; Green *et al.*, 2015; Das *et al.*, 2015; Anduaga *et al.*, 2018; Nagy *et al.*, 2018; Nagy *et al.*, 2019). The first breakthrough came through the work of Vanin and colleagues (2012) who performed locomotor behavioural assays outdoors where the flies were subjected to natural temperature and light cycles. A surprising result of this study was the ability of multiple previously considered arrhythmic clock mutants to maintain behavioural rhythmicity indistinguishable from that of wild-type. This suggests that under natural conditions, temperature and light have very strong entraining capabilities and the circadian clock is much more plastic at the molecular level than traditionally believed (Grima *et al.*, 2004; Stoleru *et al.*, 2004). Indeed, a later study using (almost) cyclic temperature cycles, albeit via short-spaced “steps”, found that a functional eye is able to maintain circadian rhythmicity in relation to locomotor activity in flies lacking a functional molecular clock. (Schlichting *et al.*, 2015). Furthermore, Vanin found that the anticipatory nature of the clock to ‘lights on’ and ‘lights off’ that has been dogma for over a decade was largely an artifact. Under natural conditions the morning

anticipatory component of activity was found to have strong dependence on temperature rather than the light-anticipating clock (Vanin *et al.*, 2012).

The general activity profile of the flies was also overridden under natural conditions. Flies display crepuscular activity profiles under laboratory LD conditions and nocturnal profiles in light:moonlight (LM) conditions (Rieger *et al.*, 2007; Bachleitner *et al* 2007). However, In the natural environment flies are mostly diurnal, even when subjected to various levels of moonlight (Vanin *et al.*, 2012). The most striking difference discovered was during the afternoon. Traditionally, flies were believed to exhibit two peaks of activity during the day: a morning (M) peak and an evening (E) peak, separated by a period of rest in the afternoon termed the siesta (S). Under natural conditions the profile is drastically different. The siesta disappears completely and is instead replaced by a large peak of activity termed the afternoon (A) peak (**Figure 6-1**). The A peak is often the largest bout of activity and is highly temperature dependent, being prominent only during summer-like days (Vanin *et al.*, 2012). Remarkably, the findings of Vanin and colleagues in the wild was replicable in the laboratory using bespoke light simulators and incubators with powerful oscillating functions, thus stimulating future study into the clock under simulated natural conditions.

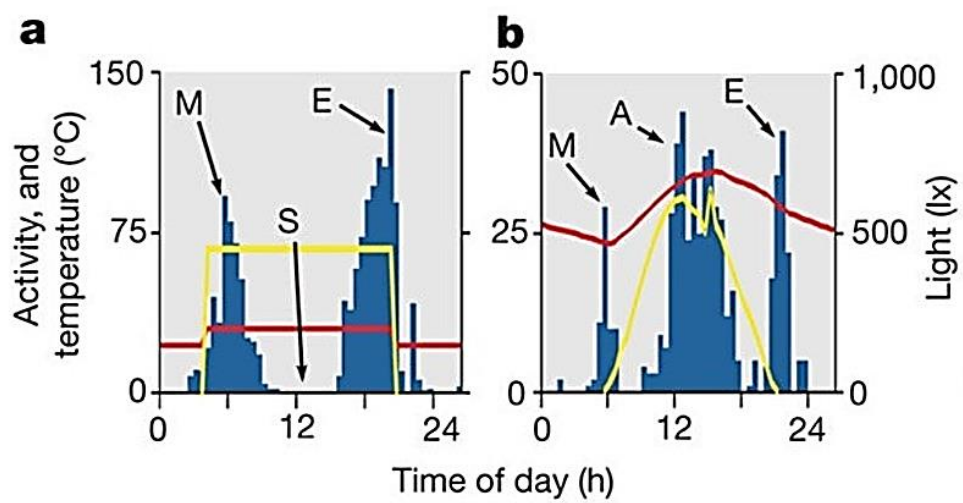


**Figure 6-1.** Comparison between laboratory locomotor profiles (**a**) and natural locomotor profiles (**b**) of *D. melanogaster*. In the laboratory there are two peaks of activity: morning (**M**) and evening (**E**) with a period of rest termed the siesta (**S**). Under natural conditions the **S** component disappears and is replaced by a period of activity in the afternoon (**A**). (Taken from Vanin *et al.*, 2012)

Since this initial ground-breaking paper, other publications have confirmed the findings of Vanin and colleagues (Menegazzi *et al.*, 2013; De *et al.*, 2013; Prabhakaran and Sheeba, 2014; Green *et al.*, 2015; Das *et al.*, 2015). Furthermore, similar findings have been reported in other *Drosophila* species (Prabhakaran and Sheeba, 2014) and in rodent models (Gattermann *et al.*, 2008; Daan *et al.*, 2011). Moreover, it has since been found that under these natural-like conditions the DNs display differential PER and TIM cycling in comparison to the LNs which have a delayed rhythm (Menegazzi *et al.*, 2013), concurrent with previously discussed laboratory-based findings (Yao and Shafer, 2014; Dissel *et al.*, 2014).

### 6.1.2 Thermo-sensation and the clock: the emerging role of TrpA1

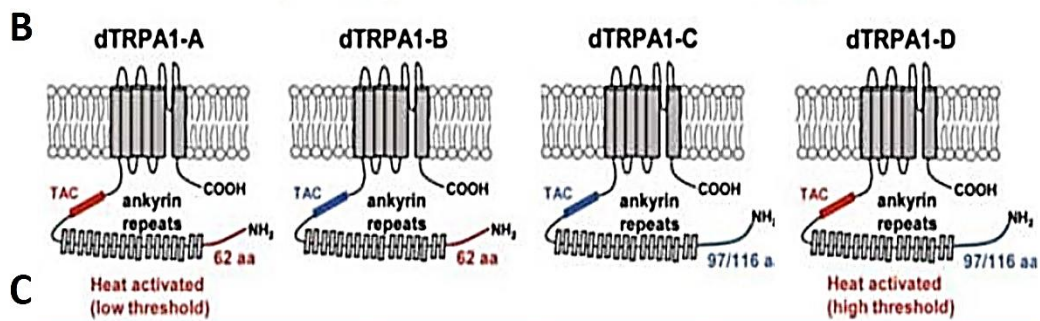
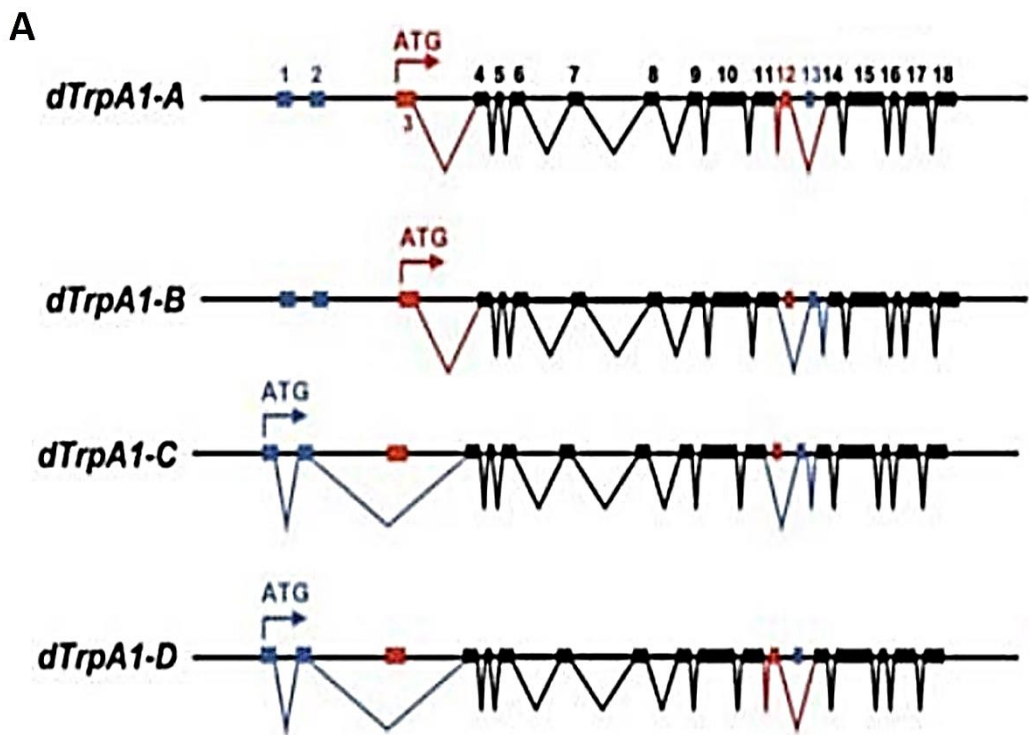
The most unexpected finding of the Vanin (2012) paper was the emergence of the afternoon peak. Green and colleagues (2015) probed further into the A-peak and found it to be dependent on the thermo-sensory gated ion channel TrpA1 (Green *et al.*, 2015). Both *TrpA1* mutants and RNAi knock down of *TrpA1* either via *TrpA1-gal4* or the pan neuronal *elav-gal4* abolishes the A-peak, but RNAi via the clock driver *tim-gal4* and other, more specific clock drivers did not (Green *et al.*, 2015; Das *et al.*, 2015). This suggests that non-clock neurons govern the A-peak. However, mutations in clock genes themselves, such as isogenised *tim<sup>01</sup>*, *Clk<sup>Jrk</sup>*, and the mutants *per<sup>01</sup>* and *per<sup>s</sup>* all showed phenotypical differences in relation to the afternoon peak when compared to wild type flies (Vanin *et al.*, 2012; Menegazzi *et al.*, 2013; Green *et al.*, 2015). This was either through the timing of the peak or the relative size of the A peak. It is therefore likely that although the A peak is reliant on *TrpA1<sup>+</sup>* neurons outside of the clock, the

clock still has a regulatory role on the properties of the A peak, its timing and size.

Mutations in other thermal and photo sensory proteins such as Trp, pyrexia, glass and PLC- $\beta$  did not suppress the A-peak but did however decrease the relative amplitude of the M and E components (Green *et al.*, 2015). Interestingly, disruption of photoreceptor cell morphology via the *glass*<sup>60j</sup> mutant or inhibition of photoreceptor signalling via the *norpA*<sup>P41</sup> mutant showed a slight increase in activity during the afternoon at the expense of reduced morning and evening activity. This suggests that there is subtle suppression of the A peak in summer-like conditions via the visual system (Green *et al.*, 2015). Nonetheless, the afternoon component seems to be mostly regulated by temperature via TrpA1.

TrpA1 is a part of the Transient receptor potential (TRP) family of receptors which allow the influx of Ca<sup>2+</sup> and Na<sup>+</sup> ions (Fowler and Montell, 2013). TrpA1 exists as four isoforms (TrpA1-A, B, C, & D) in which *TrpA1-A* and *TrpA1-B* are under the control of one promoter and *TrpA1-C* and *TrpA1-D* are under the control of another (Zhong *et al.*, 2012). Each isoform has a different composition of exons which changes its overall function as a mature channel (**Figure 6-2**).

The TrpA1 protein has 6 transmembrane repeats and 13 ankyrin repeat units on the intracellular N-terminus (Viswanath *et al.*, 2003). The regions flanking the 13 ankyrin repeats differ between the 4 TrpA1 isoforms, and also determine the TrpA1 temperature-sensing properties (Luo *et al.*, 2017). *TrpA1-A* and *TrpA1-B* begin transcription prior to exon 3, thus missing exons 1 and 2. *TrpA1-C* and *TrpA1-D* begin transcription prior to exon 1 (which contains an alternative ATG site), thus retaining both exons 1 and 2, but exon 3 is spliced out. *TrpA1-A* and *TrpA1-D* both retain exon 12 but splice out exon 13, whereas *TrpA1-B* and *TrpA1-C* both splice out exon 12 and retain exon 13 (Zhong *et al.*, 2012).



**C**

Isoform	Exon 1	Exon 2	Exon 3	Exon 12	Exon 13
TrpA1-A	-	-	+	+	-
TrpA1-B	-	-	+	-	+
TrpA1-C	+	+	-	-	+
TrpA1-D	+	+	-	+	-
TrpA1-E	+	+	-	-	-

Heat activated (low threshold)  
Heat activated (high threshold)

**Figure 6-2.** The alternatively-spliced exon composition of each isoform of TrpA1. **A)** A schematic representation of the *TrpA1* gene in the genome. **B)** A schematic representation of the protein structure situated in the plasma membrane. **A & B)** The TrpA1-A&B isoforms start transcription at exon 3, which encodes a 62 aa N-terminus tail (**red**). TrpA1-B&C start transcription at exon 1, meaning that exon 1 and 2 are included but exon 3 is spliced out. This generates a 97 aa N-terminus tail (**blue**). TrpA1-A&D splice out exon 13 but retain exon 12 creating a 37 aa TAC region (**red**). TrpA1-B&C splice out exon 12 but retain exon 13 creating a 36 aa TAC region (**blue**). **C)** A summary of the inclusion or exclusion of the alternatively spliced exons of each TrpA1 isoform. (**A&B** were adapted from Roessingh et al., 2017).

A 5<sup>th</sup> isoform, *TrpA1-E* has been proposed which like *TrpA1-C* and *D* contains exons 1 and 2 with exon 3 spliced out, however, *TrpA1-E* splices out both exon 12 and exon 13. So far *TrpA1-E* has only been identified in larvae where it has low expression levels. It also does not appear to be a functional protein, emphasising the importance of the TAC domain which links the ankyrin repeats to the transmembrane domain (Gu et al., 2019). Therefore, the role of *TrpA1-E*, particularly in adults, remains unclear.

The TAC region appears to be the crucial part of the TrpA1 protein in determining its thermo-sensitive properties. Only the TrpA1-A and D isoforms which contain the 12th exon in the TAC region, are temperature sensitive. The TrpA1-B and C isoforms lack this exon but instead express exon 13 and are non-responsive to temperature both *in vitro* and *in vivo* (Kang et al., 2012; Zhong et al., 2012; Luo et al., 2017). However, an *in vitro* study by Gu et al (2019) found that TrpA1-B and TrpA1-C are also receptive to heat when expressed at high levels, but this has not been verified *in vivo* and has not been replicated by other laboratories. The exact threshold temperatures seem to differ slightly between studies, although, in general, TrpA1-A seems to be active at temperatures above 27°C and TrpA1-D above 34°C (Luo et al., 2017).

TrpA1 has a diverse expression pattern and has been implicated in several biological process in both the larval and adult fly (Fowler and Montell, 2013). This includes the avoidance of UV light (Guntur et al., 2015), visual light (Xiang et al., 2010), harmful chemicals (Kwon et al., 2010; Kim et al., 2010;

Kang *et al.*, 2010) and touch (Zhong *et al.*, 2012). Its most well studied function however is in thermosensation, particularly in the avoidance of noxious temperatures and the setting of a preferred temperature (Hamada *et al.*, 2008; Rosenzweig *et al.*, 2005; Kaneko *et al.*, 2012; Sokabe *et al.*, 2016).

In addition to sensing absolute temperature, TrpA1 is also needed to sense the rate of temperature change. In larvae this is via the TrpA1-A isoform (Luo *et al.*, 2017). There is also evidence that the thermo-insensitive isoforms are still important in thermosensation but indirectly. TrpA1-C was found to be important in the avoidance of noxiously high temperatures in larvae (Zhong *et al.*, 2012). This isoform does not contain the temperature-sensitive 12<sup>th</sup> exon, so temperature-dependent signalling via TrpA1-C must occur downstream of temperature sensation. Furthermore, TrpA1 signalling can be activated independently of temperature via G<sub>q</sub> and PLC (Kwon *et al.*, 2008), highlighting the versatility of the receptor.

Although TrpA1 has not been found to be able to entrain the circadian clock in rectangular light studies (Roessingh *et al.*, 2015; Das *et al.*, 2016), TrpA1 has been found to be involved in temperature sensation, which is itself rhythmic (Kaneko *et al.*, 2012). This is via the TrpA1<sup>+</sup> AC neurons which communicate to the s-LNvs via serotonin release. The s-LNvs then signal to the DN2s which set the temperature preference (Kaneko *et al.*, 2012; Tang *et al.*, 2017). The preferred temperature cycles between 24°C (in the late night/ pre-morning) to 27°C (in the late-afternoon) (Kaneko *et al.*, 2012).

TrpA1 has also been implicated in the control of sleep and the siesta. Under warm temperature cycles (29:20°C rectangular temperature cycles in DD) mutation of TrpA1 decreases sleep and increases activity during the siesta period (Roessingh *et al.*, 2015; Roessingh *et al.*, 2017). However, at higher temperatures >30°C, and in LD, the opposite effect is seen. Wild type flies seem to reduce the amount of sleep during the siesta due to increased morning activity, whereas TrpA1 mutant flies have a more pronounced siesta period (Lamaze *et al.*, 2017). This is via two distinct populations of

TrpA1<sup>+</sup> neurons: non-clock *TrpA1<sup>SH</sup>-gal4* expressing neurons, and *ppk-gal4* expressing AC neurons which interact with the DN1 cells (Lamaze *et al.*, 2017). TrpA1-dependent control of the siesta was also found to be true in LD at constant 30°C and the phenotype is isoform specific via TrpA1-A and TrpA1-B (Das *et al.*, 2016; Jiang *et al.*, 2017). However, in LD, this phenotype is due to the timing of the evening and morning peaks rather than the amplitude of sleep/siesta, suggesting that TrpA1 works slightly differently in LD than in DD (Das *et al.*, 2016).

The relationship of TrpA1 with adult fly behaviour is clearly very complex and appears to be governing multiple circuits to control multiple, sometimes opposing behaviours (Kwon *et al.*, 2008; Menegazzi *et al.*, 2012; Zhong *et al.*, 2012; Das *et al.*, 2016; Jiang *et al.*, 2017). Furthermore, these behaviours seem to be very dynamic and the role TrpA1 plays changes under different environmental conditions, both in laboratory and in more natural studies (Menegazzi *et al.*, 2013; Green *et al.*, 2015; Das *et al.*, 2015; Roessingh *et al.*, 2017).

## 6.2 Aims

The initial aims of this chapter were to validate findings relating to the TrpA1-controlled afternoon peak and to investigate the circuitry of this behaviour. However, validation proved complicated and the aims had to take a step backwards. It was found that the TrpA1 driver used in the Green *et al.* study (2015) had been wrongly labelled. This chapter identifies the actual TrpA1 driver line used in the study, and tests the ability of other TrpA1 drivers to knock down the afternoon peak under simulated “natural” environmental conditions. Validation of other TrpA1 drivers within this chapter also identified misconceptions that had been made by another study (Das *et al.*, 2015). Using a more in-depth genetic dissection than these two initial papers (Das *et al.*, 2015; Green *et al.*, 2015), the promoter-specificity and isoform-specificity of TrpA1 was identified. Furthermore, visual mutants were previously found to have a minor contribution to the afternoon peak. As such, the contribution of rhodopsin mutations on the afternoon peak were investigated and the relative influence of temperature and light assessed.

## 6.3 Materials and Methods

### 6.3.1 *Drosophila* Stocks

In this chapter several transgenic and mutant lines generated by various laboratories were used. These included existing laboratory stocks TrpA1<sup>IRJF</sup> 02461 (UAS-RNAi), UAS-Valium20, and TrpA1-gal4 (48951) originally from Janelia Farm (cited by Green *et al.*, 2015). Existing laboratory stocks donated from other laboratories: TrpA1<sup>27593</sup>-gal4 donated by Ralph Stanewsky and a line donated by Younseok Lee which is cited as either TrpA1<sup>gal4</sup>-gal4 or TrpA1<sup>K1</sup>-gal4 in the literature (Kim *et al.*, 2010; Das *et al.*, 2015; Roessingh *et al.*, 2017). The Rhodopsin mutants Rh3<sup>1</sup>, Rh4<sup>1</sup>, Rh5<sup>2</sup>, Rh6<sup>1</sup> were donated by Giorgio Fedele who had previously crossed them into a CS background. The following stocks were also pre-existing laboratory

stocks: *UAS-hid,rpr* (expressed on the 2<sup>nd</sup> chromosome, in a *w<sup>1118</sup>* background), TrpA1<sup>NP0002</sup>-gal4, and TrpA1<sup>SH</sup>-gal4. The following stocks were purchased from the Bloomington stock centre: TrpA1<sup>48948</sup>-gal4 TrpA1<sup>49862</sup>-gal4 and TrpA1<sup>49842</sup>-gal4 which were all originally from Janelia Farm (Janett *et al.*, 2012); UAS-TrpA1-A (61504), UAS-TrpA1-B (61505), TrpA1<sup>AB</sup>-gal4 (67131), TrpA1<sup>CD</sup>-gal4 (67133), TrpA1<sup>ACD</sup>-gal4 (67135). These lines were crossed into CyO;Tm6b (CS) to remove irrelevant transgenes.

### 6.3.2 Simulation of semi-natural light and temperature profiles

The same semi-natural light and semi-natural temperature profiles used by Green *et al.* 2015 were used in this study (photo/thermoperiod of 15:9, mimicking a mid-summers day in Treviso Italy). Temperature profiles were created via the Memmert IPP500 peltier incubator systems Celsius software, explained in detail in **Chapter 5**. A gradual and smooth natural-like temperature cycle without any “steps” that oscillates from 25°C to 35°C over a 24-hour period was used.

The simulated light profiles were created via a bespoke custom-built light simulator created by Stefano Bastianello, Euritmi, Venetian Institute of Molecular Medicine, Padova, Italy, referenced in Green *et al.* 2015, and explained in detail in **Chapter 5**.

### 6.3.3 Locomotor activity

Flies were reared at 25°C LD 12:12 and 3-day old males were used to study locomotor activity as described in Material and Methods 2.3. Flies were entrained for 5 days before locomotor activity recordings were taken. The first 3 days after entrainment were used and the average activity across the 3 days for each 30-minute bin was plotted and analysed.

#### **6.3.4 Calculation of $A_{onset}$ and $A_{max}$**

The  $A_{onset}$  and  $A_{max}$  for each fly in each experiment was calculated in accordance to Vanin *et al.* 2012.  $A_{onset}$  was considered as the first 30-minute bin in which activity rises after a period of rest and continues to rise in subsequent bins until it reaches a peak which is determined as  $A_{max}$  and then gradually decreases again. Only activity peaks that occur after or 1 hour prior to the rise in temperature and light in the morning were considered. If two bouts of activity occur during the day then the first would be considered the A component and the second the E component, as long as the E component occurred after midday. Only activity components that were characterised by continuous activity with a steady increase and decrease in amplitude were considered.

$A_{onset}$  and  $A_{max}$  quantification are presented separately alongside the locomotor activity profiles. This is because subtle timings in the average  $A_{onset}$  and  $A_{max}$  can be masked and difficult to observe when presented as an activity profile made from the averaged data of >32 flies: particularly if the activity profiles of individual flies is less synchronous and the  $A_{onset}/A_{max}$  not normally distributed.

## 6.4 Results

### 6.4.1 Identification of the *TrpA1-gal4* driver used in the Green et al. (2015) study

The validity of the *TrpA1-gal4* driver used by Green et al. (2015) was assessed before novel investigations began. The *TrpA1-gal4* driver (*TrpA1<sup>48951</sup>-gal4*) was crossed to the same *TrpA1* RNAi strain used in the original paper (*UAS-TrpA1-IR<sup>JF02461</sup>*), to *UAS-hid,rpr* to induced apoptosis in *TrpA1*<sup>+</sup> cells, and to *UAS-Valium20* as an empty vector control, and subjected to simulated natural light and temperature cycles. Unexpectedly, the resultant locomotor activity profiles show that suppression of the A-peak was not achieved in flies either expressing RNAi of *TrpA1* (green), or ablation of *TrpA1*<sup>+</sup> cells (red), via the *TrpA1<sup>48951</sup>-gal4* promoter (**Figure 6-3A**).

There were two other *TrpA1-gal4* lines that were available in the laboratory during the experiments cited in the Green et al. (2015) paper. These lines were *TrpA1<sup>27593</sup>-gal4* donated by Ralph Stanewsky and a line donated by Younseok Lee which is cited as either *TrpA1<sup>gal4</sup>-gal4* or *TrpA1<sup>K1</sup>-gal4* in the literature (Kim et al., 2010; Das et al., 2015; Roessingh et al., 2017). To avoid confusion, this line will be referred to as *TrpA1<sup>K1</sup>-gal4* in this thesis. It is possible that a mis-labelling or mis-citing had occurred in the write up of the Green et al (2015) paper. To investigate this, the experiment was repeated using these two *TrpA1-gal4* lines (**Figures 6-3C & 6-3B** respectively). Knockdown of *TrpA1* via RNAi driven by the *TrpA1<sup>27593</sup>-gal4* could not abolish the A peak (green). Ablation of *TrpA1<sup>27593</sup>-gal4*<sup>+</sup> neurons (red) resulted in a decrease in the amplitude of the A peak when compared to the empty vector control (blue) but was not completely abolished. However, either RNAi knockdown of *TrpA1*, or *hid,rpr*-induced ablation via *TrpA1<sup>K1</sup>-gal4* was sufficient to completely abolish the A peak (**Figure 6-3B**). Therefore, it is most likely that this was the strain used in the original publication and an error in labelling the fly vials may have led to the mistake.

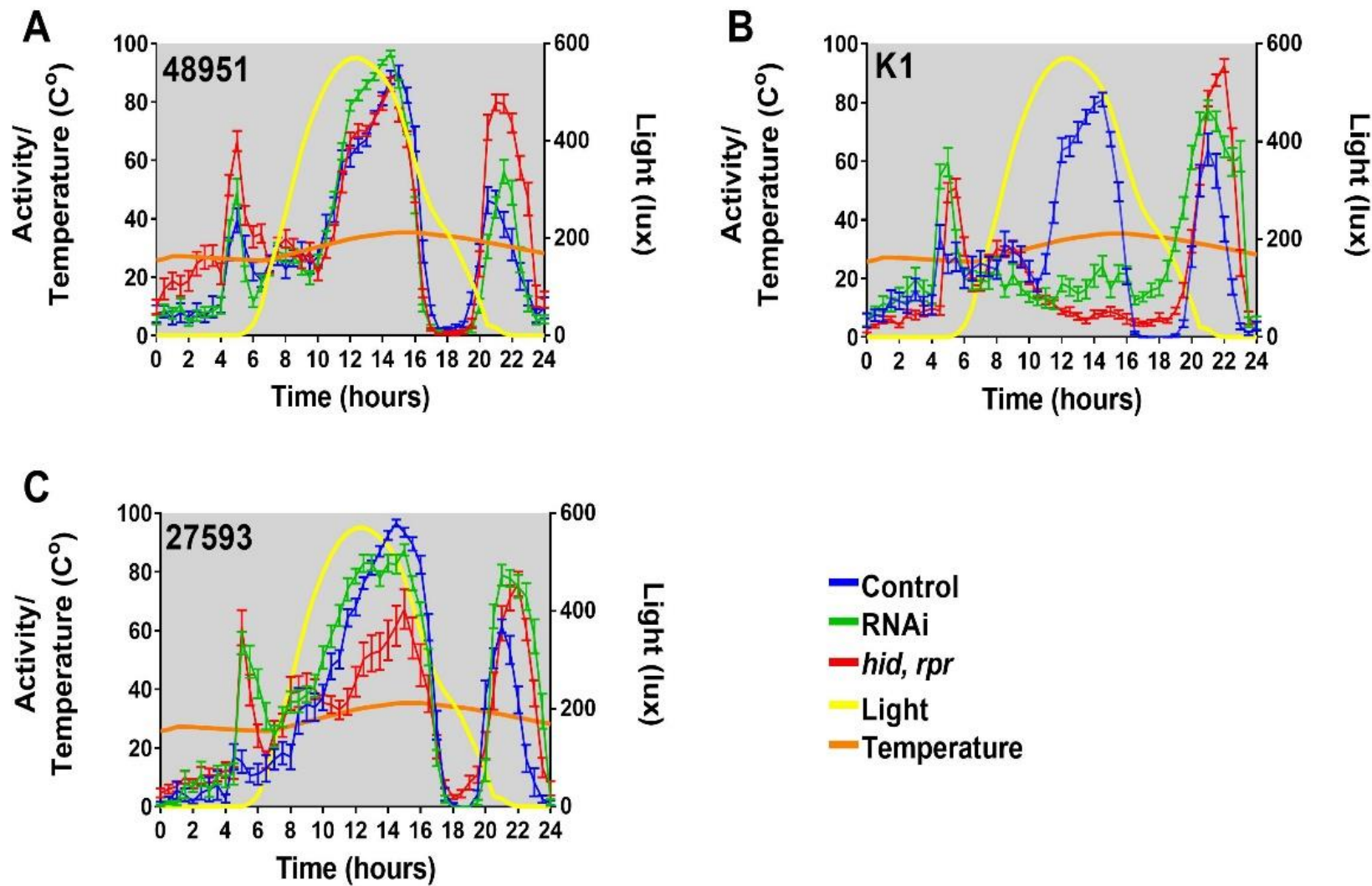


**Figure 6-3.** Locomotor profiles of *TrpA1-gal4* drivers present in our laboratory preceding publication of the Green *et al.* paper (2015). These drivers were *TrpA1<sup>148951</sup>-gal4* (**A**), *TrpA1<sup>K1</sup>-gal4* (**B**), and *TrpA1<sup>127593</sup>-gal4* (**C**). Each driver was crossed to either *UAS-TrpA1-RNAi* (green), the corresponding empty vector control *UAS-Valium20* (blue), or to the *UAS-hid,rpr* (red). The semi-natural light and temperature profiles are presented as yellow and orange respectively. In total, locomotor profiles for 435 flies were used. As the phenotype is clear and obvious, statistical testing of significance was redundant

#### **6.4.2 Investigation of the ability of other *TrpA1-gal4* lines to target the TrpA1<sup>+</sup> neurons responsible for regulating the A peak.**

Not all of the *TrpA1-gal4* drivers that were available in our laboratory were able to drive an observable phenotype in relation to the A peak (**Figure 6-3**). This suggests that differing *TrpA1* drivers have differing expression patterns. There are several other *TrpA1-gal4* drivers that are available from stock centres or in use in laboratories across the field. It has already been documented that the expression patterns of these drivers differ and that certain biological phenotypes are specific to certain drivers (Roessingh *et al.*, 2017). Therefore, it was of interest to test these drivers for their ability to target *TrpA1<sup>+</sup>* A peak-regulating neurons (**Figure 6-4**). This would also help with the identification of such neurons in future ICC experiments.

The *TrpA1<sup>NP0002</sup>-gal4* (**Figure 6-4A**) and *TrpA1<sup>SH</sup>-gal4* (**Figure 6-4B**) lines were made by individual research laboratories and are widely used in the literature (Roessingh *et al.*, 2017). The *TrpA1<sup>148948</sup>-gal4* (**Figure 6-4C**), *TrpA1<sup>149862</sup>-gal4* (**Figure 6-4D**), and *TrpA1<sup>149842</sup>-gal4* (**Figure 6-4E**) lines were made by the Janelia Research Campus as a research tool for the *Drosophila* community. Surprisingly, neither of these *TrpA1-gal4* drivers could inhibit the afternoon component when driving RNAi of *TrpA1* (green) compared to driving the empty vector control *UAS-Valium20* (blue) (**Figure 6-4**). Both *TrpA1<sup>NP0002</sup>-gal4* and *TrpA1<sup>SH</sup>-gal4* showed a very slight reduction in the A component

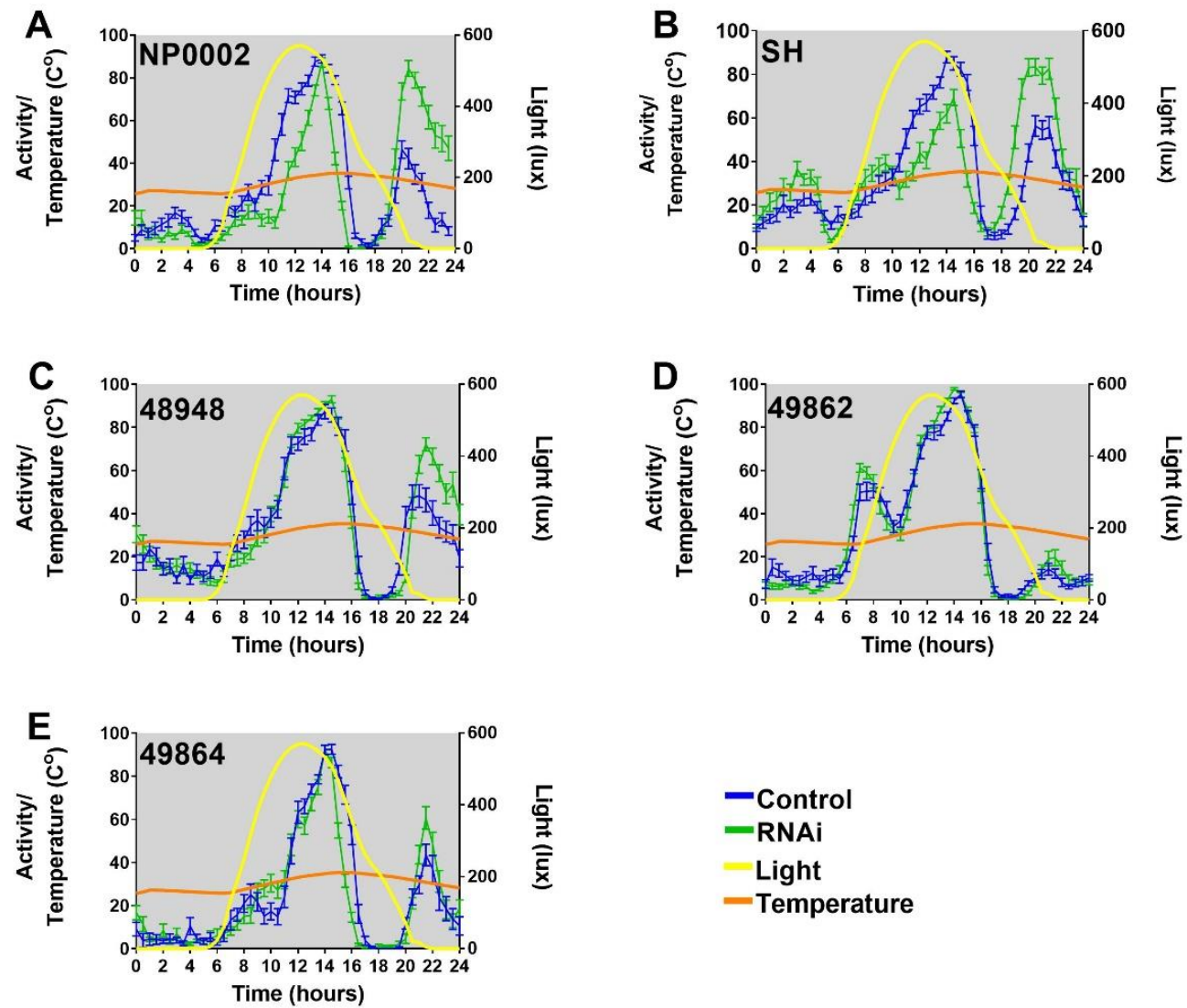


**Figure 6-4.** Locomotor profiles of *TrpA1-gal4* drivers used in the literature or available from stock centres. These drivers were *TrpA1<sup>NP0002</sup>-gal4* (**A**), *TrpA1<sup>SH</sup>-gal4* (**B**), *TrpA1<sup>48948</sup>-gal4* (**C**), *TrpA1<sup>49862</sup>-gal4* (**D**), *TrpA1<sup>49864</sup>-gal4* (**E**). Each driver was crossed to either *UAS-TrpA1-RNAi* (green), or the corresponding empty vector *UAS-Valium20* (blue). The semi-natural light and temperature profiles are presented in yellow and orange respectively. In total, locomotor profiles for 475 flies were used.

#### 6.4.3 *TrpA1* promoter and isoform specificity in regulation of the A component

Of the eight *TrpA1-gal4* drivers tested, only *TrpA1<sup>K1</sup>-gal4* is able to drive knockdown of the A peak via RNAi of TrpA1 (**Figure 6-3 & 6-4**). This driver is a knock-in *gal-4* driver, whereby *gal-4* fused to *mini-white* has been inserted into the intrinsic *TrpA1* genome via homologous recombination (Kim *et al.*, 2010). Interestingly, this line was created before the discovery of the four isoforms of *TrpA1* or its two distinct promoters (Zhong *et al.*, 2012). Consequently, *gal-4* was inserted after the *TrpA1-A/B* specific ATG site (exon 3). Therefore, this allele results in no *TrpA1-A* or *TrpA1-B* expression but will instead express *gal-4* in the relevant tissues driven by the promoter. However, this insertion still allows intrinsic expression of *TrpA1-C* and *TrpA1-D* which start transcription further upstream, from exon 1 (**Figure 6-5**). Therefore, this may suggest that the afternoon peak is *TrpA1-A/B* promoter specific (**Figure 6-3**).

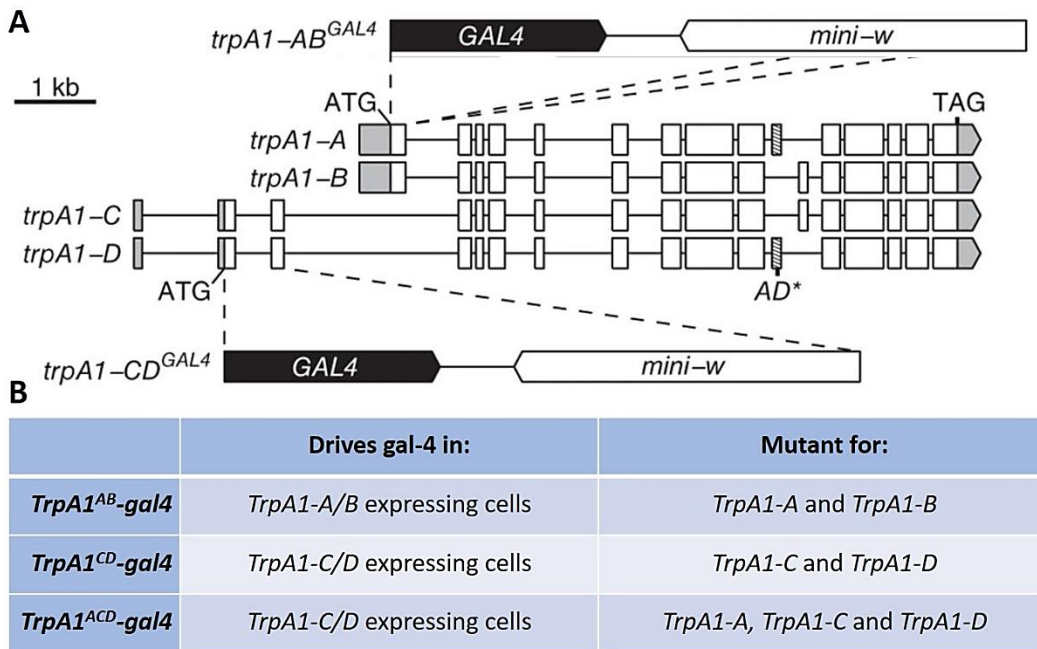
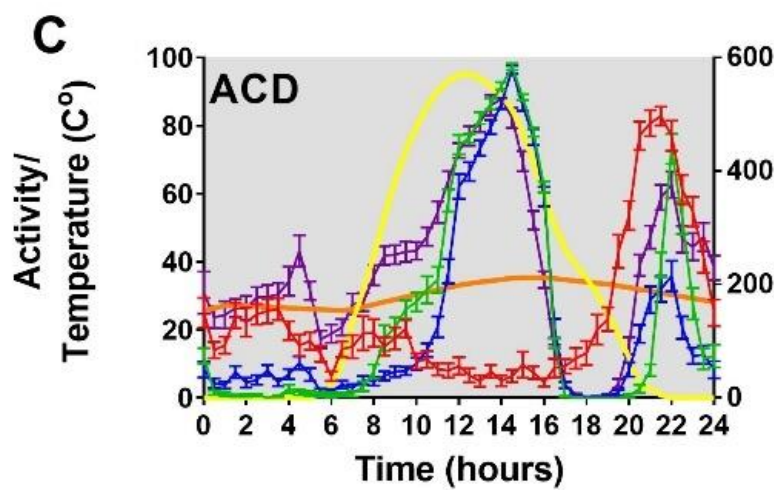
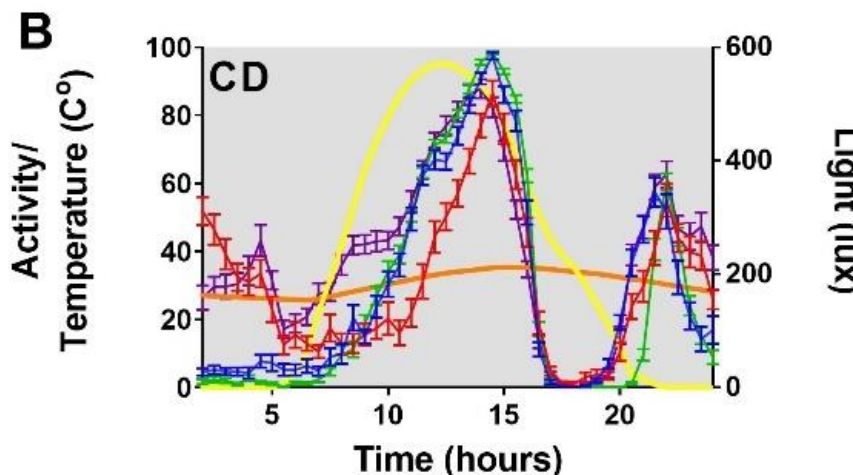
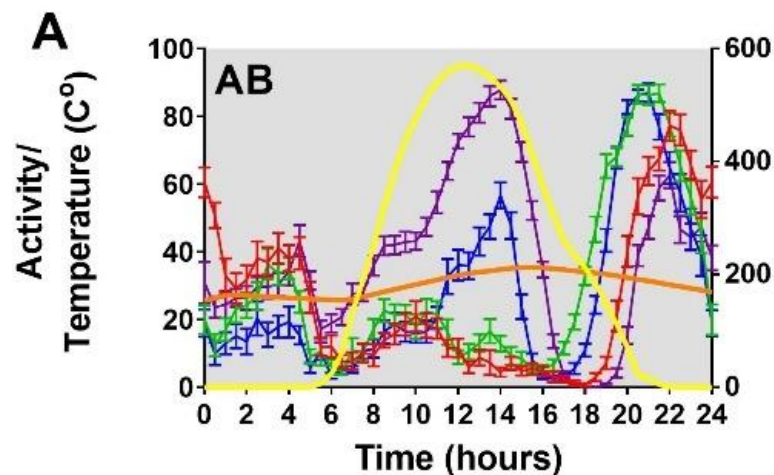


**Figure 6-5.** **A)** Schematic representation of the different *TrpA1* promoter-specific *gal4* lines made by Luo *et al.* (2017). A *gal4* fused to *mini-white* is inserted either in exon 3 to generate a *TrpA1<sup>AB</sup>-gal4* that is mutant for *TrpA1-A* and *TrpA1-B*, or in exon 1 to generate a *TrpA1<sup>CD</sup>-gal4* that is mutant for *TrpA1-C* and *TrpA1-D*. To generate *TrpA1<sup>ACD</sup>-gal4*, the 12<sup>th</sup> exon was mutated with a 2bp deletion (AD\*) in the *TrpA1<sup>CD</sup>-gal4* allele (Adapted from Luo *et al.*, 2017). **B)** A summary of the expression pattern of each *gal4* driver and the *TrpA1* isoforms that are mutated due to its insertion site.

The Montell laboratory created two new *TrpA1-gal4* lines based on the original *TrpA1<sup>K1</sup>-gal4* line (Luo *et al.*, 2017) (**Figure 6-5**). The first was *TrpA1<sup>CD</sup>-gal4* which contains a knock-in insertion of *gal-4* fused to *mini-white* just after the *TrpA1-C/D* promoter ATG (exon 1). This allele is the opposite of the *TrpA1<sup>K1</sup>-gal4* line. *TrpA1-C* and *TrpA1-D* are not expressed but instead *gal-4* is driven by the upstream promoter. However, it still allows intrinsic expression of *TrpA1-A* and *TrpA1-B*. The second line made was identical to the *TrpA1<sup>CD</sup>-gal4* line except for a two-nucleotide frame-shift deletion in the 12<sup>th</sup> exon (shared by *TrpA1-A* and *TrpA1-D*). This generates a line with the same properties as *TrpA1<sup>CD</sup>-gal4* but the *TrpA1-A* isoform is also mutated so that only the *TrpA1-B* isoform is expressed. This line was termed *TrpA1<sup>ACD</sup>-gal4*. Luo and colleagues (2017) also renamed the original *TrpA1<sup>K1</sup>-gal4* line as *TrpA1<sup>AB</sup>-gal4* which they crossed into the same background as the two novel lines (**Figure 6-5**).

The  $TrpA1^{AB}$ -*gal4* ( $TrpA1^{k1}$ -*gal4*),  $TrpA1^{CD}$ -*gal4*,  $TrpA1^{ACD}$ -*gal4* drivers were either crossed to themselves (red) to generate homozygous mutants, crossed to the *Valium20* empty vector (blue) to generate heterozygous mutants, or crossed to *UAS-TrpA1-RNAi* (green), which not only creates a heterozygous mutant for the corresponding isoform, but also knocks-down all *TrpA1* expression of all four isoforms in a promoter-specific manner. As a reference and to act as a wild-type control, *Valium20* expressing flies were also crossed to the *Canton-S* (CS) wild-type strain (purple) (**Figure 6-6**). For this experiment, the  $TrpA1^{AB}$ -*gal4* strain used by the Montell laboratory (Luo *et al.*, 2017) was used instead of the  $TrpA1^{k1}$ -*gal4* strain used in the previous experiments and the Green *et al.* (2015) paper. This was to ensure that the genetic backgrounds were identical, ensuring a more accurate comparison between promoters.

As expected, Knockdown of *TrpA1* in  $TrpA1^{AB+}$  cells via  $TrpA1^{AB}$ -*gal4* (green) or the homozygous *gal4* knock-in mutant of  $TrpA1^{AB}$  (red) completely abolished the afternoon peak (**Figure 6-6A**). This is consistent with what was observed with the  $TrpA1^{k1}$ -*gal4* line used previously in this thesis chapter (**Figure 6-3B**). The heterozygous mutant of  $TrpA1^{AB}$  (blue) also shows a reduced A-peak when compared to the wild-type control (purple), but does not completely abolish it (**Figure 6-6A**). When observing the results from the use of the  $TrpA1^{CD}$ -*gal4* promoter (**Figure 6-6B**), neither the heterozygous mutant, homozygous mutant, or RNAi knock-down of *TrpA1* in  $TrpA1^{CD+}$  cells was capable of altering the A peak. However, when using the  $TrpA1^{ACD}$ -*gal4* promoter (**Figure 6-6C**), the homozygous mutant of  $TrpA1^{ACD}$  is capable of abolishing the A peak (red). The heterozygous  $TrpA1^{ACD}$  mutant or RNAi knock-down of *TrpA1* using this driver were unable to inhibit the A peak.



- Wild-type control
- Heterozygous mutant
- Homozygous mutant
- RNAi
- Light
- Temperature

**Figure 6-6.** Locomotor profiles of promoter-specific *TrpA1-gal4* drivers/mutants. The *TrpA1-A/B* specific driver, *TrpA1<sup>AB</sup>-gal4* (**A**), and the *TrpA1-C/D* specific drivers *TrpA1<sup>CD</sup>-gal4* (**B**) and *TrpA1<sup>ACD</sup>-gal4* (**C**) were crossed to *UAS-TrpA1-RNAi* to knock-down *TrpA1* in promoter-specific tissue (green). Each *TrpA1-gal4* is a knock-in line and therefore an isoform-specific mutant. *TrpA1<sup>ACD</sup>-gal4* has an additional mutation in the 12<sup>th</sup> exon to create a mutant for all the isoforms except for *TrpA1-B* (**C**). Each driver was also crossed to itself to generate a homozygous mutant (red), and to *UAS-Valium20* to generate a heterozygous mutant (blue). As a wild-type control, *UAS-Valium20* was also crossed to CS (purple). The semi-natural light and temperature profiles are presented in yellow and orange respectively. In total, locomotor profiles for 328 flies were used.

#### 6.4.4 Overexpression of *TrpA1-A* or *TrpA1-B* in a promoter-specific manner

The isoform-specificity of the Afternoon peak appears to be mostly via *TrpA1-A*, and mutation of *TrpA1-A*, or both *TrpA1A* and *TrpA1-B*, or knock down via RNAi of *TrpA1* in *TrpA1-AB* expressing tissue resulted in an abolishment of the A peak (**Figure 6-6**). To investigate the effects of overexpressing *TrpA1* in these tissues either *UAS-TrpA1-A* (green) or *UAS-TrpA1-B* (red) were overexpressed via *TrpA1<sup>AB</sup>-gal4* (**Figure 6-7A**) or the *TrpA1<sup>CD</sup>-gal4* promoter (**Figure 6-7B**), and compared to the corresponding promoter crossed to the empty vector control *UAS-Valium20* (blue). When either isoform is overexpressed via the *TrpA1<sup>AB</sup>-gal4* promoter the amplitude of the A peak increases (**Figure 6-7A**). Additionally, the peak of the afternoon component ( $A_{max}$ ) is advanced by ~4.4 hours for *TrpA1-A* ( $P<0.0001$ ) and by ~3.7 hours for *TrpA1-B* ( $P<0.0001$ ) (**Figure 6-8Bi**). This is due to a steep increase in activity as temperature rises, not due to an advanced onset of the A peak ( $A_{onset}$ ) (**Figure 6-8Ai**). Interestingly, an advanced  $A_{max}$  is also seen when *TrpA1-A* and *TrpA1-B* are overexpressed via the *TrpA1<sup>CD</sup>-gal4* promoter (**Figure 6-7B**) albeit to a lesser effect (~0.9hours and ~1.6 respectively) (**Figure 6-8Bii**).

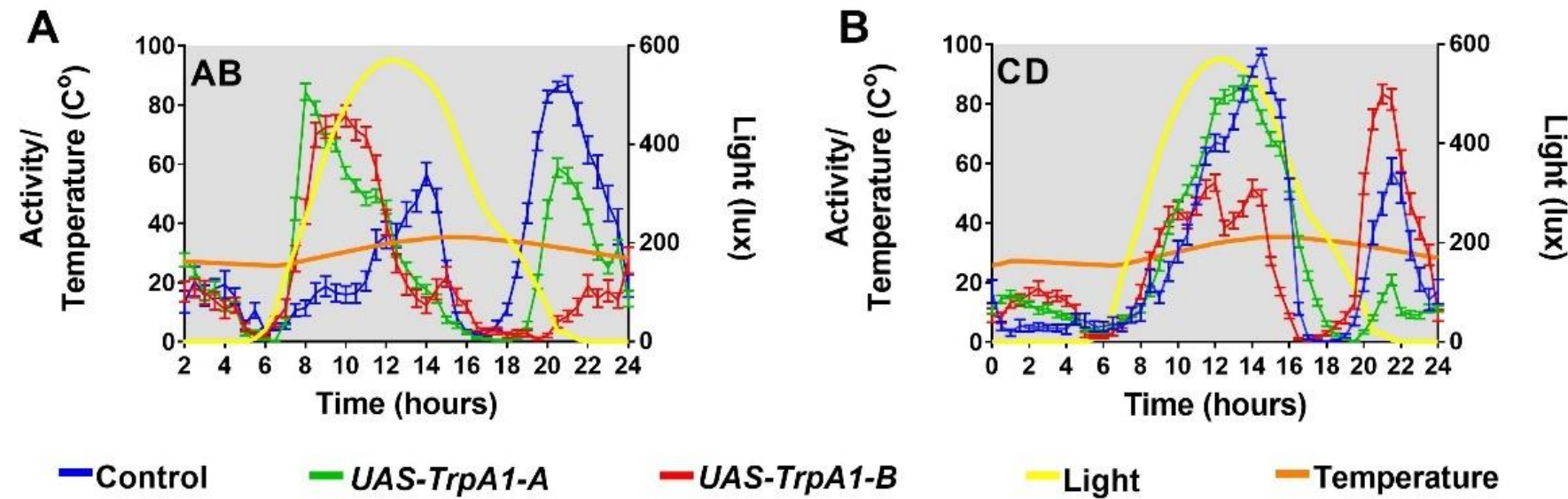


**Figure 6-7.** Locomotor profiles of flies overexpressing TrpA1 in an isoform and promotor-specific manner. The *TrpA1-gal4* drivers *TrpA1<sup>AB</sup>-gal4* (A), and *TrpA1<sup>CD</sup>-gal4* (B) were crossed to either the *UAS-Valium20* empty vector (blue), to *UAS-TrpA1-A* (green), or to *UAS-TrpA1-B* (red) to drive overexpression of TrpA1. The semi-natural light and temperature profiles are presented in yellow and orange respectively. For statistical analysis of A component properties see Figure 6-8.

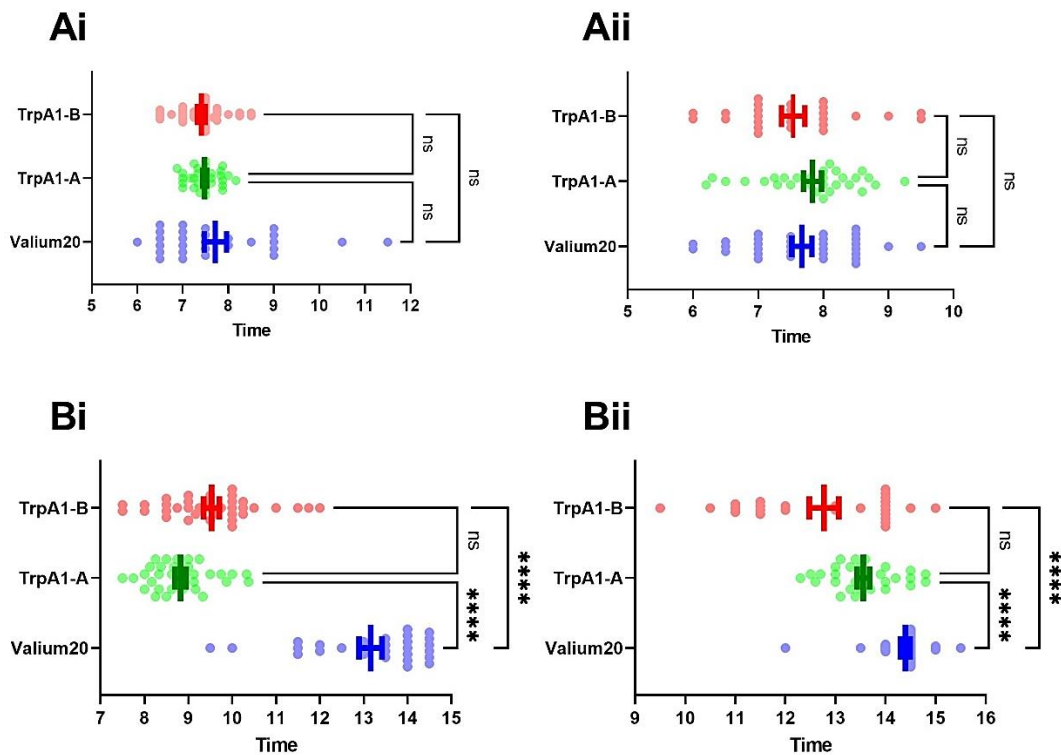


**Figure 6-8.** Analysis of the onset of the A peak ( $A_{\text{onset}}$ ) (A), and the time at which the A component reaches its peak ( $A_{\text{max}}$ ) (B). Either *TrpA1<sup>AB</sup>-gal4* (i) or *TrpA1<sup>CD</sup>-gal4* (ii) were crossed to *UAS-TrpA1-A* (red), *UAS-TrpA1-B* (green), or the empty vector control *UAS-Valium20* (blue). Dots represent individual flies, bars represent Mean  $\pm$  SEM. Significance was calculated via Kruskal-Wallis one-way ANOVA followed by Dunn's multiple comparison test (See appendix 8-6-1 & 8-6-2), \* =  $P < 0.05$ , \*\* =  $P < 0.01$ , \*\*\* =  $P < 0.001$ , \*\*\*\* =  $P < 0.0001$ .

#### 6.4.5 Investigating a function of rhodopsins in regulating the A peak

A possible role of the visual system in regulating the A peak has been suggested (Green *et al.*, 2015). Mutation of *glass* which is essential for photoreceptor morphology, or inhibition of photoreceptor signalling via the *norpA<sup>P41</sup>* mutant showed an enhanced A peak (Green *et al.*, 2015). Therefore, the role of the visual system in control of the A peak was investigated further, specifically the role of rhodopsins. The R7 and R8 photoreceptor cells have been implicated in several independent light-input pathways to entrain and regulate the circadian clock. (Veleri *et al.*, 2007; Hanai and Ishida, 2009; Szular *et al.*, 2012; Schlichting *et al.*, 2015; Ogueta

*et al.*, 2018;). Therefore, flies mutant for rhodopsins that express in the R7 and R8 photoreceptor cells were assessed for their effects on the A peak: Rh3 (UV-blue light sensitive), Rh4 (UV-blue light sensitive), Rh5 (blue light sensitive), and Rh6 (green light sensitive) (**Figure 6-10**).

Flies had previously been backcrossed into a CS background by Giorgio Fedele in our laboratory. Nonetheless, each line had been kept in the laboratory separately for several years. To ensure the backgrounds of the mutants to their controls were comparable, each rhodopsin mutant line was either assessed as a homozygous mutant (red) or crossed to the original CS stock once to generate a heterozygous mutant (green), or the mutation was crossed out with CS to generate a wild-type control (blue) (**Figure 6-9**).

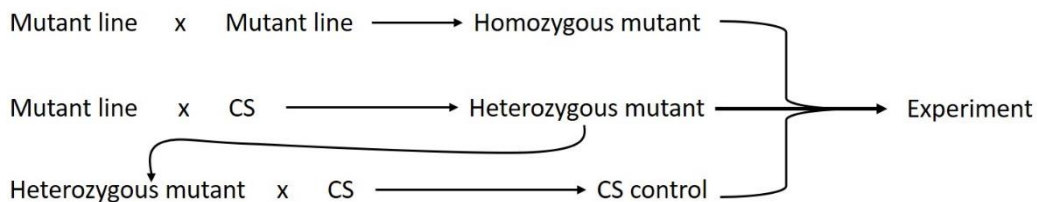


**Figure 9.** Cross scheme for generation of Rhodopsin mutant fly lines and their respective controls.

*rh4* mutant flies were healthy when reared at 25°C, but did not survive the experiment when kept at the high temperatures required to elicit the A peak (25°C - 35°C). The other three mutants however were viable at these temperatures (**Figure 6-10**). Flies expressing *rh5* both as a heterozygous or homozygous mutant did not show any change in the A peak when compared to wild-type flies (**Figure 6-10B, 6-11B**). Flies that were either heterozygous or homozygous mutant for *rh3* showed a slight delay of  $A_{\text{onset}}$  (~0.75h) compared to wild-type flies ( $P=0.0013$ ,  $p=0.0008$  respectively) (**Figure 6-11Bi**). Furthermore, the  $A_{\text{max}}$  was advanced by ~1h in homozygous *rh3* mutants compared to wild-type flies ( $P<0.0001$ ) (**Figure 6-11Bii**). *rh3* heterozygous mutant flies also display a slight advancement of  $A_{\text{max}}$  (~0.75h) but this was not significant when compared to wild type flies ( $P=0.1745$ ). However, when compared to the homozygous mutant flies

there is a significant difference ( $P=0.0220$ ). Flies that were either heterozygous or homozygous mutant for *rh6* also showed a delay in  $A_{\text{onset}}$  (~1.5h, ~2h respectively) compared to the wild-type control flies ( $P<0.0001$ ) (**Figure 6-11Ci**). The  $A_{\text{max}}$  was delayed in *rh6* mutant flies, but curiously, more so in the heterozygous mutant flies (~0.7h,  $P=0.0054$ ) than the homozygous mutant flies (~0.6,  $P=0.1243$ ) (**Figure 6-11Cii**).

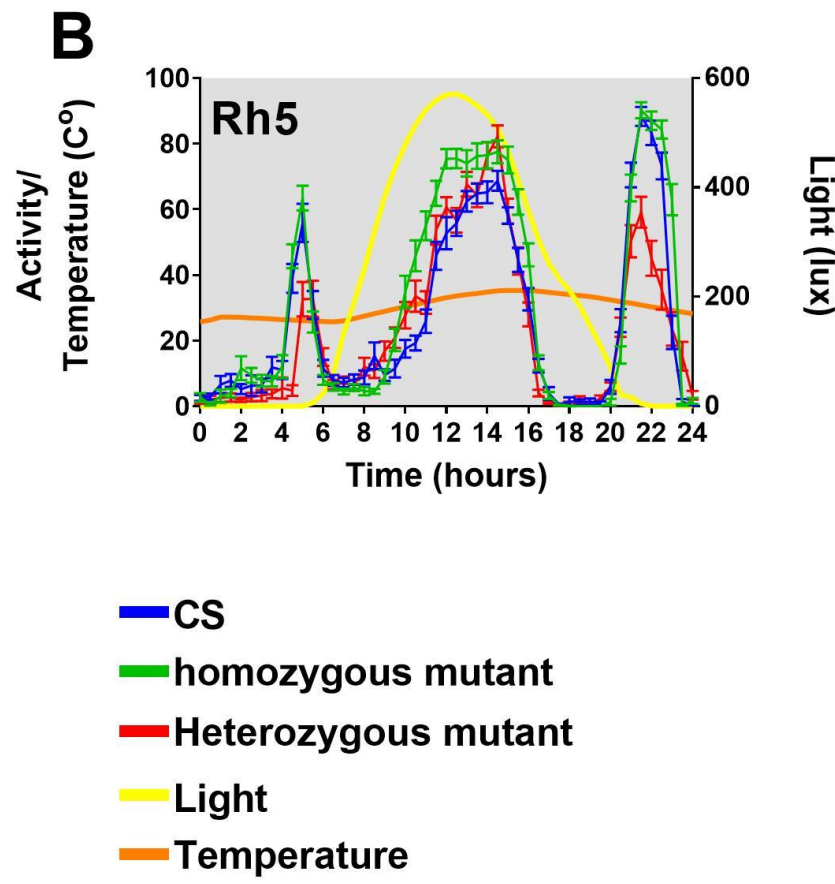
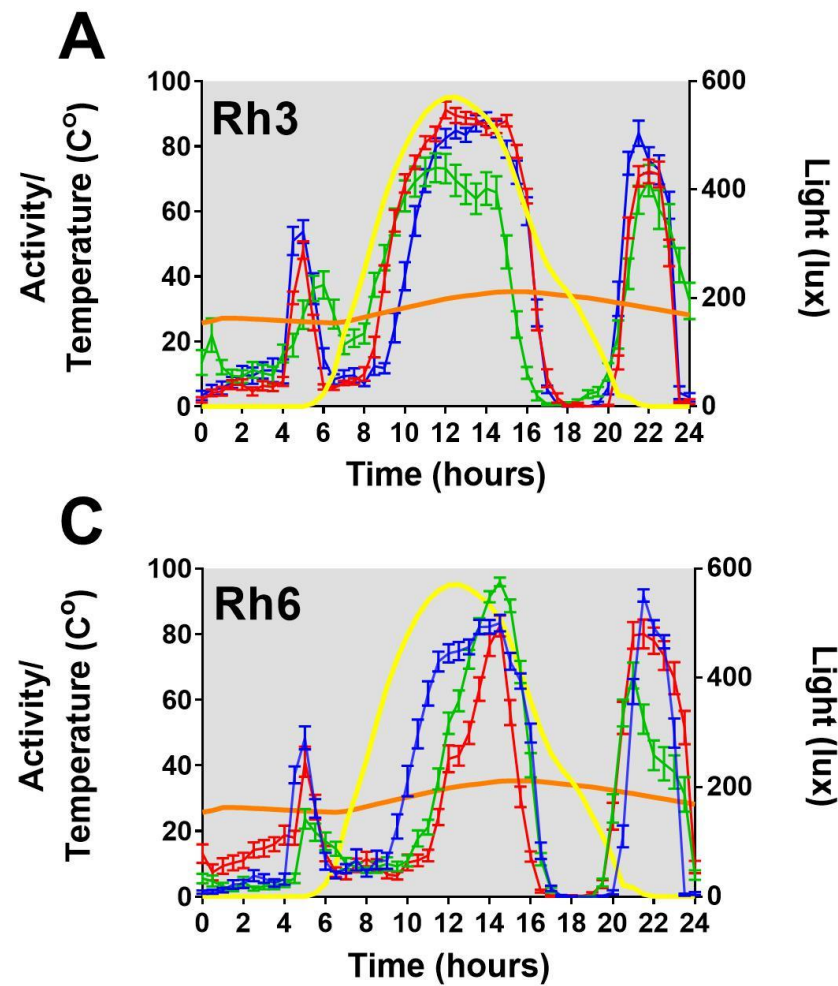


**Figure 6-10.** Locomotor profiles of flies mutant for specific rhodopsins. Flies mutant for either *rh3* (**A**), *rh5* (**B**), and *rh6* (**C**) were crossed to themselves to generate homozygous mutants (red), or to CS flies to generate heterozygous mutants (green) or the mutant crossed out to generate wild-type CS controls (blue). The semi-natural light and temperature profiles are presented in yellow and orange respectively. For statistical analysis of A component properties see Figure 6-11.

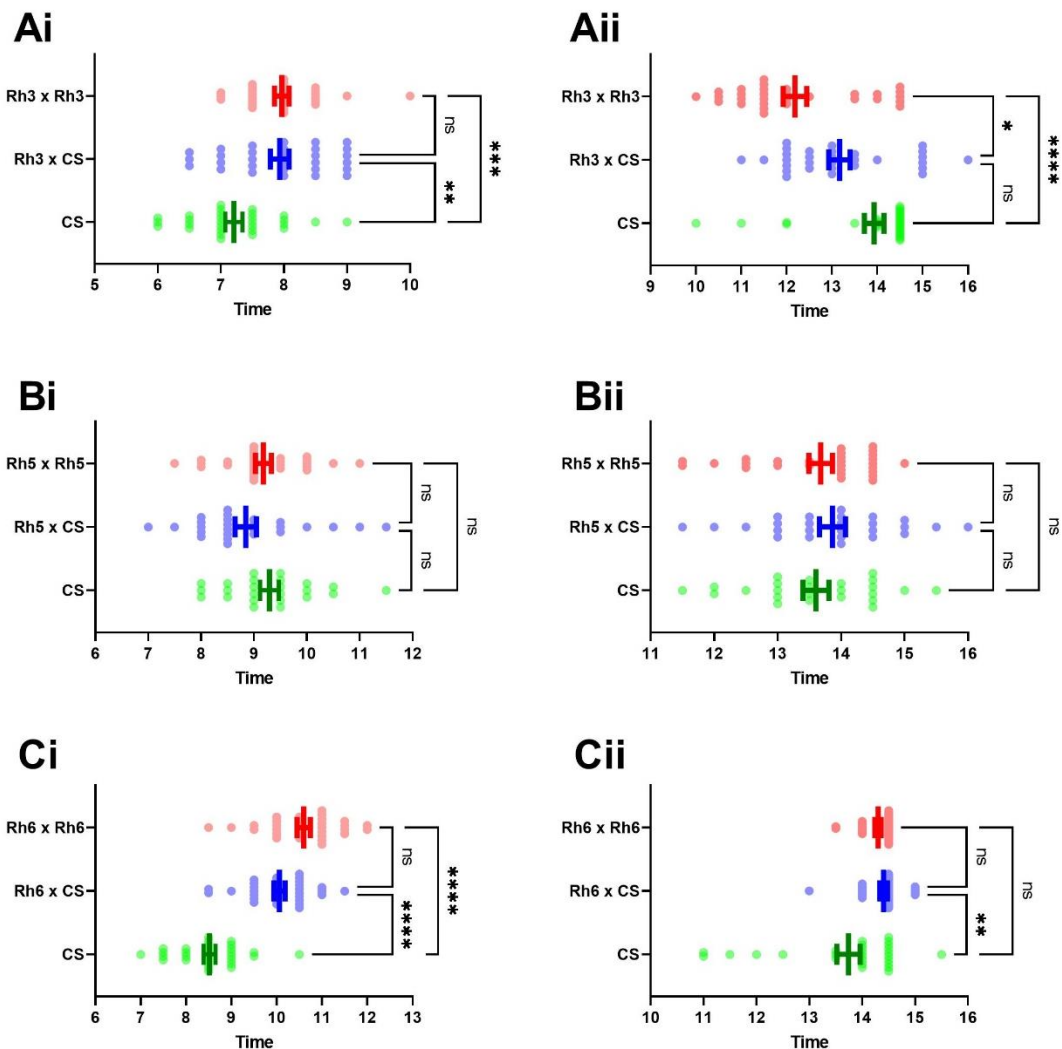


**Figure 6-11.** Analysis of the onset of the A peak ( $A_{\text{onset}}$ ) (**i**), and the time at which the A component reaches its peak ( $A_{\text{max}}$ ) (**ii**) of flies either homozygous mutant (red) or heterozygous mutant (blue) for either *rh3* (**A**), *rh5* (**B**) or *rh6* (**C**) compared to their respective CS controls (green). Dots represent individual flies, bars represent Mean  $\pm$  SEM. Significance was calculated via Kruskal-Wallis one-way ANOVA followed by Dunn's multiple comparison test (See appendix 8-6-3, 6-4 & 8-6-5), \* =  $P<0.05$ , \*\* =  $P<0.01$ , \*\*\* =  $P<0.001$ , \*\*\*\* =  $P<0.0001$ .

#### **6.4.6 The effect of rhodopsin mutants on the A peak when temperature and light are un-coupled**

Temperature has the larger influence on the A peak in comparison to light, and is dependent on the expression of the thermosensitive channel TrpA1. However, it had previously been shown that light has a potentially inhibitory role in regulation of the A peak (Green *et al.*, 2015) and results from this thesis chapter have implicated that the timing of the A peak is also influenced by the visual system via Rh3 and Rh6 (**Figures 6-10 & 6-11**). Therefore, to test the relationship between temperature and light and their relative regulatory properties, the light cycle and the temperature cycle were uncoupled (**Figure 6-12**). Both the thermal and photo cycles corresponded to the same 15:9 sunset-sundown length, identical to that of all previous experiments in this chapter. However, whereas ordinarily temperature begins to increase at the same time as light (6am) and naturally peaks ~4hs later than light intensity peaks (Vanin *et al* 2012), in this experiment the thermocycle was advanced by 4 hrs. This meant that temperature begins to increase 4 hrs. before light, and reaches its peak at the same time as light does (**Figure 6-12**).

Homozygous mutant flies for either of the three viable rhodopsins (green) as well as their corresponding CS controls (red) were subjected to the aforementioned “uncoupled” thermal and photo cycles. The activity profiles of homozygous mutants under “coupled” light and temperature profiles (blue) (data from **Figure 6-10**) were overlaid to act as a reference. In mutants for either of the Rhodopsins, Rh3 (**Figure 6-12A**), Rh5 (**Figure 6-12B**), and Rh6 (**Figure 6-12C**), the timing of both  $A_{onset}$  and  $A_{max}$  is identical to that of their relevant CS controls with no statistically significant differences (**Figure 6-13**). Furthermore, the A peak has advanced in line with the advanced temperature profile so that it occurs 4hs earlier than if the temperature and light cycles were “coupled”.

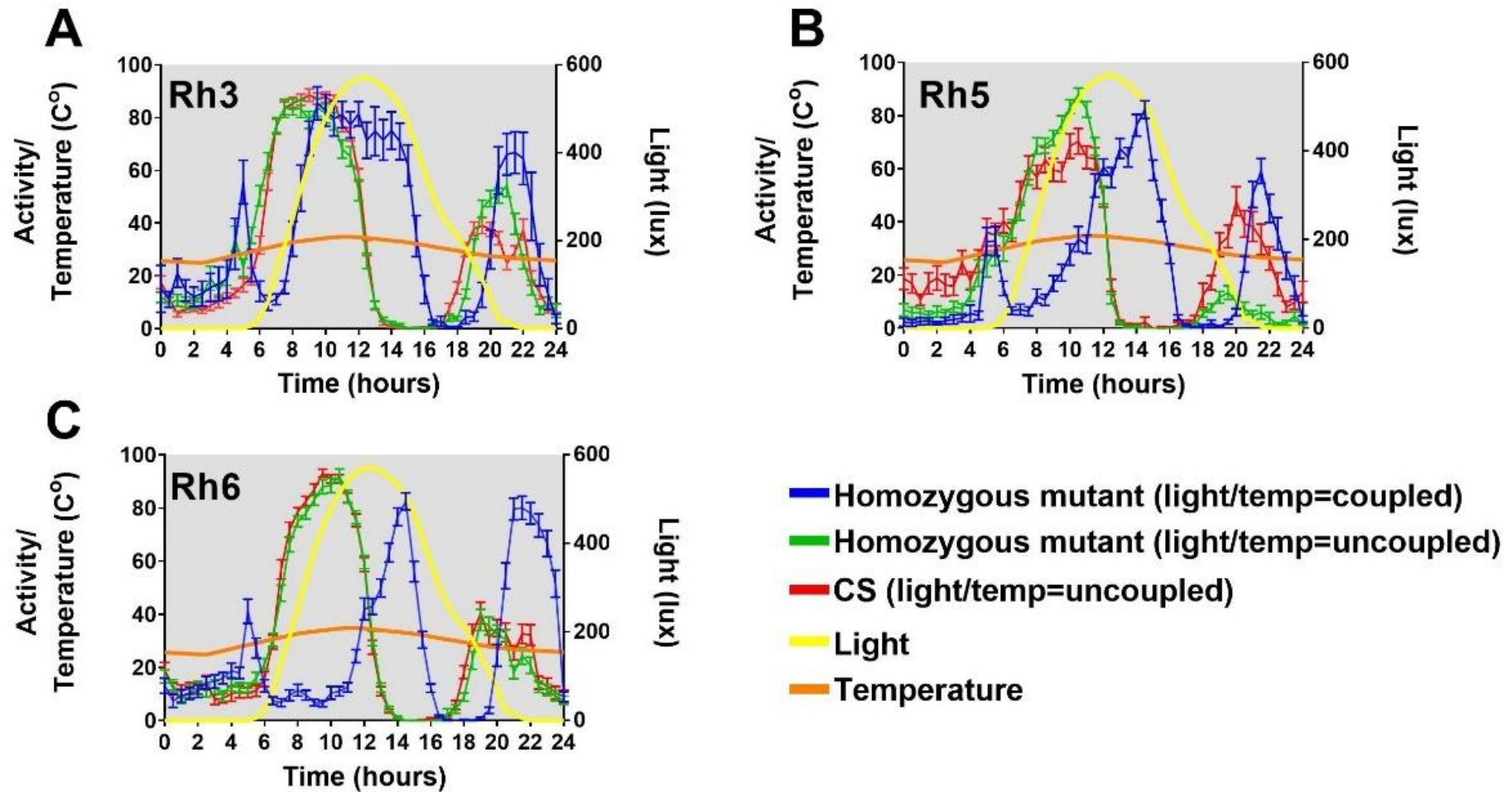


**Figure 6-12.** Locomotor profiles of flies mutant for specific rhodopsins under uncoupled light and temperature cycles. Both wild-type CS flies (red) and homozygous mutant flies (green) for either *rh3* (A), *rh5* (B), or *rh6* (C) were exposed to light and temperature cycles that were uncoupled from one another so that the increase in temperature starts 4hs earlier than the increase in light. As a reference, homozygous mutant flies for each rhodopsin which had been kept in “coupled” light and temperature cycles was included (blue). The semi-natural light and temperature profiles are presented in yellow and orange respectively.

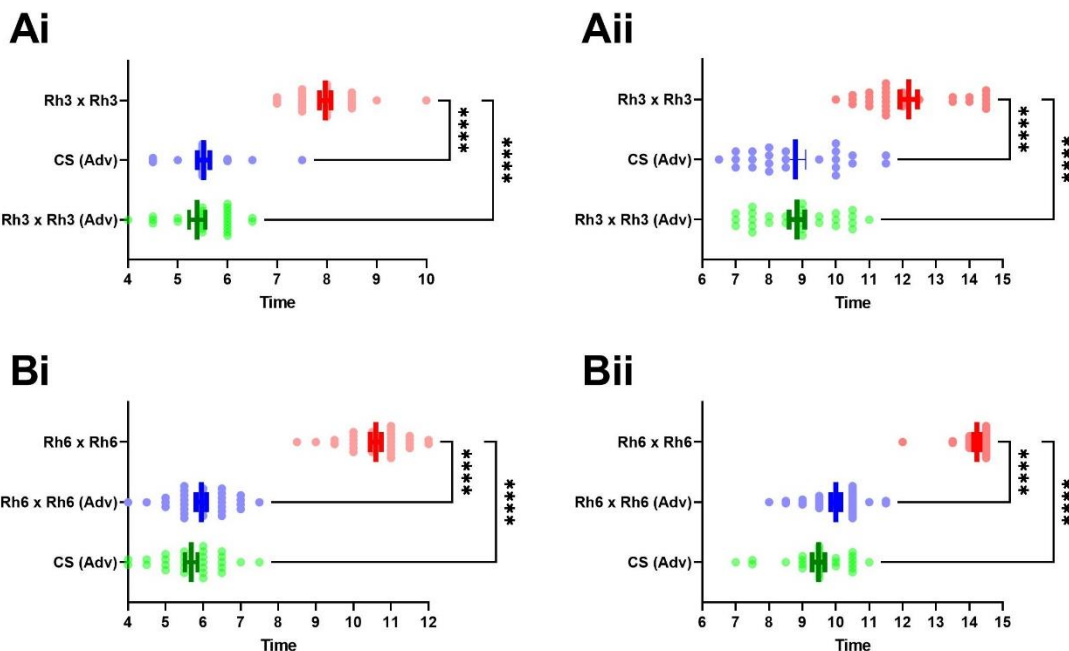


**Figure 13.** Analysis of ( $A_{\text{onset}}$ ) (i), and ( $A_{\text{max}}$ ) (ii) of flies either homozygous mutant (red) or heterozygous mutant (blue) for either Rh3 (A) or Rh6 (B) compared to their respective CS controls (green). Dots represent individual flies, bars represent Mean  $\pm$  SEM. Significance was calculated via Kruskal-Wallis one-way ANOVA followed by Dunn's multiple comparison test (See appendix 8-6-6 & 8-6-7), \* =  $P < 0.05$ , \*\* =  $P < 0.01$ , \*\*\* =  $P < 0.001$ , \*\*\*\* =  $P < 0.0001$ .

## 6.5 Discussion

The involvement of TrpA1 in control of the A peak has been well documented (Green *et al.*, 2015; Das *et al.*, 2015). However, the role TrpA1 plays in regards to the circadian clock, sleep, locomotor activity, and heat avoidance vary significantly depending on the precise experimental conditions used (Kwon *et al.*, 2008; Menegazzi *et al.*, 2012; Zhong *et al.*,

2012; Roessingh *et al.*, 2015; Das *et al.*, 2016; Roessingh *et al.*, 2017; Lamaze *et al.*, 2017; Jiang *et al.*, 2017). This is also partly due to the differing *TrpA1-gal4* promoters used in these studies (Rosenzweig *et al.*, 2005; Hamada *et al.*, 2008; Kim *et al.*, 2010; Zhong *et al.*, 2012; Luo *et al.*, 2017). The promoter-specificity of TrpA1-related behaviours also became apparent from the results of this thesis chapter in relation to the A peak.

The initial paper linking TrpA1 to the A peak came from our laboratory (Green *et al.*, 2015). However, the results of that study could not be replicated (**Figure 6-3**). The driver originally cited was unable to abolish the A peak when driving either RNAi knock down of *TrpA1* or ablation of TrpA1<sup>+</sup> cells via *UAS-hid,rpr*. The experiment was repeated with other *TrpA1-gal4* drivers that were available in the laboratory at the time the experiment for the 2015 paper was conducted (**Figure 6-3**). Only the *TrpA1<sup>K1</sup>-gal4* line, also known as *TrpA1<sup>gal4</sup>-gal4*, was able to replicate the results from the Green study. Therefore, it is highly likely that there was an error during the publication of the Green paper in which the wrong driver was cited, and the *TrpA1<sup>K1</sup>-gal4* line was in fact the line used. Furthermore, only 1 out of 3 lines from the laboratory stocks were able to drive a phenotype, indicating a specificity of the A peak to a promoter-specific subset of TrpA1<sup>+</sup> cells.

Other *TrpA1-gal4* drivers were used to drive RNAi of TrpA1 under the same conditions as the previous experiments. Surprisingly, none of these lines were able to abolish the A peak (**Figure 6-4**). From the eight lines tested, only the *TrpA1<sup>K1</sup>-gal4* line was capable of reducing the A peak (**Figure 6-3 & 6-4**). One of the lines that was unable to knockdown the A peak was the commonly cited *TrpA1<sup>SH</sup>-gal4*. Interesting, overexpression of *TrpA1-A* via *TrpA1<sup>SH</sup>-gal4* had been found to enhance the A peak in wild-type flies, or to rescue the loss of the A peak in *TrpA1* mutant flies (Das *et al.*, 2015). This is contradictory to our results that show that *TrpA1<sup>SH</sup>-gal4*<sup>+</sup> neurons do not regulate the A peak (**Figure 6-4**). However, In the simulated natural conditions used by Das and colleagues (2015), light and temperature “cycle” in a step-wise manner with sharp increases and decreases between

steps. By their own admission, small bouts of activity in wild-type flies are observed at each step increase, and the ‘A’ peak is observed as a very steep peak when the step-up for T-max occurs (30 – 32°C). All activity then ceases immediately after the step-down from T-max occurs. This creates an “A” peak that lasts just over ~1 hour in which the flies go from almost inactivity pre-step-up to maximum activity in response to the step-up (Das *et al.*, 2015).

In incubators that are able to generate smooth continuous temperature cycles (Green *et al.*, 2015; and **figures 6-3 & 6-4** of this thesis), the “A” peak lasts several hours and is characterised by a gradual increase in activity as temperature rises. In larvae, the *TrpA1-A* isoform is not only important in sensing rapid changes in temperature, but also, independently, is able to sense gradual temperature changes that occur over time (Luo *et al.*, 2017). Therefore, it is likely that the results of Das *et al.* (2015) are due to a *TrpA1<sup>SH</sup>-gal4* specific startle response to sudden changes in temperature, whereas results from this chapter (**Figure 6-3 & 6-4**) and by Green *et al.* (2015) are due to gradual changes in temperature. Das and colleagues (2015) did find that using the *TrpA1<sup>K1</sup>-gal4* as a homozygous mutant for *TrpA1* was sufficient to abolish their startle response. The *TrpA1<sup>SH</sup>-gal4* line has a more limited expression pattern than the *TrpA1<sup>K1</sup>-gal4* line and it is expected that *TrpA1<sup>SH+</sup>* neurons overlap with *TrpA1<sup>K1+</sup>* neurons (Shih *et al.*, 2011; Lee *et al.*, 2013) (see also **Figure 6-14**). Therefore, it is likely that the startle response observed by Das *et al.* (2015) is regulated by non-clock *TrpA1<sup>SH</sup>* expressing neurons that overlap with *TrpA1<sup>K1</sup>*, and the natural A peak is regulated by non-clock *TRPA1<sup>K1</sup>* expressing neurons that do not overlap with *TrpA1<sup>SH</sup>*.

Upon closer inspection of the *TrpA1-gal4* lines tested (**Figure 6-3 & 6-4**), there is a clear difference between the *TrpA1<sup>K1</sup>-gal4* line and the others, including *TrpA1<sup>SH</sup>-gal4*. The other seven lines used are all transgenes, and use a fragment of only a few kb of the *TrpA1* gene and its surrounding genome to drive *gal4* (**Figure 6-14**: an example of the *TrpA1<sup>SH</sup>-gal4*

transgene). On the otherhand,  $TrpA1^{K1}$ -*gal4* is not a transgene but instead is a knock-in insertion. This means that when crossed to the  $TrpA1$ -RNAi line it generates a heterozygous mutant. It also means that all intrinsic enhancer and activation sequences that ordinarily regulate  $TrpA1$  expression are present to drive the expression of *gal4*. Consequently, there may be two explanations to why only  $TrpA1^{K1}$ -*gal4* was able to abolish the A peak in the affermentioned experiments whereby none of the other  $TrpA1$ -*gal4* lines could (Figure 6-3 & 6-4). Either the level of  $TrpA1$  knock-down by RNAi is not sufficient unless one copy of the  $TrpA1$  gene is mutated, or the other drivers are missing key regulatory elements that prevent a correct expression pattern. However,  $TrpA1^{SH}$ -*gal4* had sufficient expression levels to elicit the startle response under similar conditions (Das et al., 2015) and both  $TrpA1^{SH}$ -*gal4* and  $TrpA1^{NP0002}$ -*gal4* have been shown to effectively knock-down  $TrpA1$  in studies conducted at lower temperatures where *gal4* expression is expected to be less (Rosenzweig et al., 2005; Hamada et al., 2008). Therefore, it is more likely that the differing expression patterns between promotores is the reason why only  $TrpA1^{K1}$ -*gal4* could abolish the A peak.

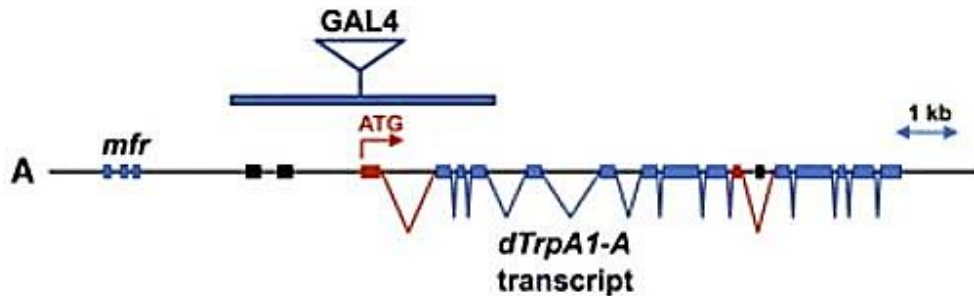


**Figure 6-14.** A genomic map of *TrpA1* and the *TrpA1<sup>SH</sup>-gal4* transgene. The alternatively spliced exons of *TrpA1* are coloured in either red or black and the splicing pattern is representative of *TrpA1-A*. The blue bar above the *TrpA1* transcript shows the portion of the *TrpA1* sequence that is cloned into the *TrpA1<sup>SH</sup>-gal4* transgene with a *gal4* gene inserted in the middle of it. (Taken from Zhong et al., 2012)

The insertion site of  $TrpA1^{K1}$ -*gal4* is at the beginning of exon 3 meaning that it creates a  $TrpA1$ -A and  $TrpA1$ -B null mutation.(Figure 6-5). Therefore, regulation of the A peak may be promoter or isoform specific. Homozygous mutant flies of the  $TrpA1$ -A & B isoforms resulted in an abolition of the A

peak whereas homozygous mutants of the C & D isoforms did not (**Figure 6-6A & B**). Furthermore, flies homozygous mutant for the A, C & D isoforms also resulted in an abolition of the A peak (**Figure 6-6C**). This implies that regulation of the A peak is via the *TrpA1-A* isoform. However, heterozygous mutation of *TrpA1-A,C,D* resulted in a wild-type A peak (**Figure 6-6C**), whereas heterozygous mutation of *TrpA1-A,B* results in a decreased amplitude of  $A_{\max}$  by almost half (**Figure 6-6A**). Furthermore, RNAi knockdown of *TrpA1* using the *TrpA1-C/D*-specific promoter did not affect the afternoon peak (**Figure 6-6B & 6-C**) but did when driven by the *TrpA1-A/B*-specific promoter (**Figure 6-6A**). This suggests that there is no overlap in expression between the two promoters in relation to A peak-regulating *TrpA1-A<sup>+</sup>* neurons. Therefore, although *TrpA1-A* is essential for regulating the A peak (**Figure 6-6C**), *TrpA1-B* must also be having a functional role (**Figure 6-6A**), possibly through amplification of *TrpA1-A* signalling.

It is curious that regulation of the A peak is *TrpA1-A* isoform specific because its activation threshold is expected to be between 24-29°C. This would imply that it was almost consistently active during the experiments of this chapter (25°C – 35°C). However, differing expression levels of *TrpA1-D* (and therefore possibly other isoforms) leads to differing temperature thresholds (Gu *et al.*, 2019). Indeed, Luo *et al.*, found that overexpressing *TrpA1-A* in larvae resulted in a significantly lowered activation threshold (Luo *et al.*, 2017). Therefore, it is possible that *TrpA1-A* is expressed at low levels in cells that regulate the A peak and this raises the activation threshold. This would also explain why the calculated activation threshold of *TrpA1-A* differs between studies (Viswanath *et al.*, 2003; Hamada *et al.*, 2008; Zhong *et al.*, 2012; Tang *et al.*, 2013). It is also possible that *TrpA1* is constitutively active at these experimental conditions, but it is the accumulation and summation of signals at a neuronal level that govern the behavioural response.

Alternatively, *TrpA1-A<sup>+</sup>* neurons may be acting downstream of temperature sensation, this would also explain the supporting role that *TrpA1-B* seems

to play (**Figure 6-6A**). PYX<sup>+</sup> neurons in the antennae send temperature input to TRPA1 expressing AC neurons in the brain. The AC neurons then propagate the signal to the posterior antennal lobe (PAL) which acts as a centre to collate temperature and humidity information from the periphery. This information is then transmitted to the DN1s which set the temperature entrainment of the clock (Tang *et al.*, 2013; Frank *et al.*, 2015). The antennae were removed from flies in an attempt to investigate the relevance of this circuit in regulating the A peak but almost all flies did not survive the high temperatures of the experiment. Of the few flies that did survive, the A peak was present (**Figure 6-15**). Therefore, this circuit is unlikely to be involved in regulation of the A peak, but does not rule out other possible roles for *TrpA1*-A downstream of temperature sensation.

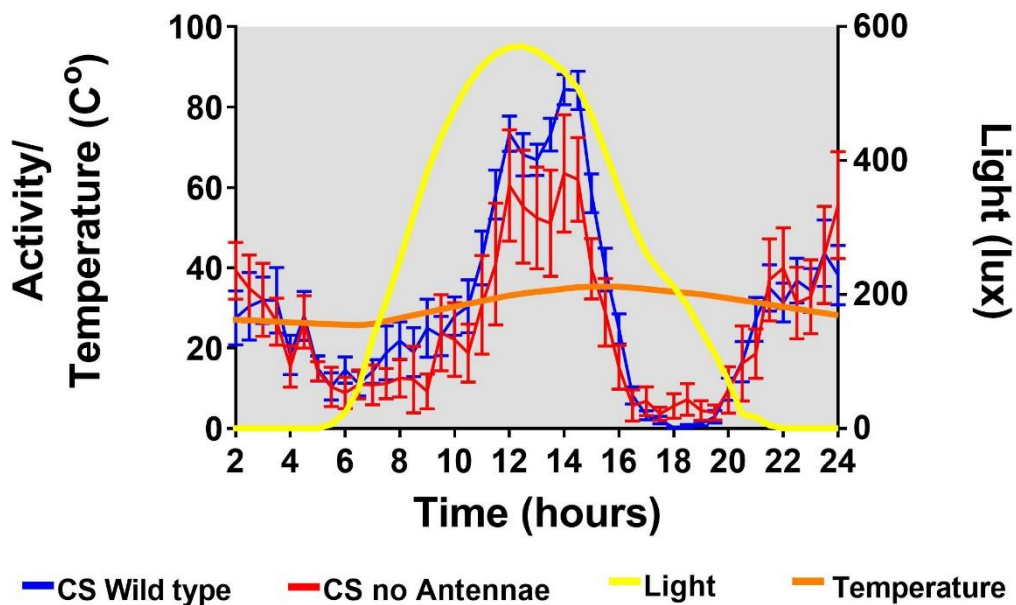


**Figure 6-15.** Locomotor profiles of CS flies in which their antennae have either been removed (red) or left untouched (blue). The semi-natural light and temperature profiles are presented in yellow and orange respectively. CS wild-type flies n=58, CS no Antennae flies n=6.

A phenotype was also observed when overexpressing either *TrpA1*-A or *TrpA1*-B via the *TrpA1* promoter-specific *gal4* drivers (**Figure 6-7**). Overexpression of either isoform via the *TrpA1<sup>AB</sup>* driver resulted in an advanced A peak that begins immediately after temperature starts to rise.

Interestingly, this was not due to an advanced  $A_{onset}$  but due to a greatly advanced  $A_{max}$  of up to 4.4hs (**Figure 6-8**). Therefore, the flies are overreacting to the increase in temperature through a steeper increase in activity. Unexpectedly, overexpression of either isoform via the *TrpA1<sup>CD</sup>* driver also resulted in an advanced  $A_{max}$  although to a considerably lesser extent (~0.9-1.6hs) (**Figure 6-8**). As discussed, the A-peak relevant expression of the AB specific promoter and expression of the CD specific promoter do not overlap (**Figure 6-6**). Therefore, overexpressing the TrpA1-A/B isoforms in tissue that they are not intrinsically expressed may have forced the phenotype seen (**Figures 6-7 & 6-8**).

Overexpression of either isoform in TrpA1-A/B<sup>+</sup> neurons resulted in an advanced  $A_{max}$  that begins immediately after temperature rises. This suggests that the advanced  $A_{max}$  may be due to an over-sensitisation to temperature increases. This could be because of a lowered activation threshold due to overexpression of the channel, as seen by Luo *et al.* (2017). However, TrpA1-B lacks the crucial 12<sup>th</sup> exon, and is unable to sense temperature. *UAS-TrpA1-A/B* were not expressed in a homozygous *TrpA1* mutant background. Therefore, endogenous TrpA1-A will still be expressed. It is possible that TrpA1-A acts as the temperature sensor in these cells and the overexpressed TrpA1-B amplifies the downstream signalling cascade through its own signalling capabilities, or by providing a scaffold for more efficient signalling of activated TrpA1-A. This would also explain why the advancement in  $A_{max}$  is greater when overexpressing TrpA1-A than when overexpressing TrpA1-B. Indeed, rhodopsin expression in TrpA1<sup>+</sup> neurons has been linked to correct temperature preference in larvae (Shen *et al.*, 2011; Sokabe *et al.*, 2016) and in the larval Cho neurons rhodopsins act as scaffolding proteins for Trp channels closely related to TrpA1 (Zanini *et al.*, 2018). If TrpA1 is able to scaffold with rhodopsins, it is possible it can scaffold to other TrpA1 channels.

Another possible explanation for the relationship of TrpA1-A and TrpA1-B could be that temperature sensation occurs upstream of TrpA1 when

regulating the A peak. As previously discussed, TrpA1<sup>+</sup> AC neurons act downstream of temperature sensation in the adult fly (Tang *et al.*, 2013). Moreover, TrpA1-C has been found to be needed for nociception in larvae (Zhong *et al.*, 2012). This channel also does not contain the 12<sup>th</sup> exon so its role in nociception is likely downstream of temperature sensation. It is possible that *TrpA1-A* and/or *TrpA1-B* may be acting as downstream signalling propagators and not direct temperature sensors in regulating the A peak. It is also possible that in the TrpA1<sup>+</sup> neurons necessary for regulating the afternoon peak, the TrpA1-A isoform is endogenously expressed at greater levels than TrpA1-B (which is why when this isoform is mutated the A peak is abolished (**Figure 6-6**), and why A<sub>max</sub> is advanced further when overexpressed compared to *TrpA1-B* (**Figures 6-7 & 6-8**)). Therefore, when either *TrpA1-A* or *TrpA1-B* is overexpressed, an over-sensitive signalling cascade is created resulting in an advanced A<sub>max</sub>.

Unfortunately, a *TrpA1-B*-specific mutant was not tested, and does not exist as a knock-in *gal4* driver. It would be interesting to see the effects on the A peak of mutation of the TrpA1-B isoform only or *TrpA1-B* specific RNAi, as well as repeating the *TrpA1-A/B* overexpression experiments but in a *TrpA1* homozygous mutant background. Both of these experiments will help to understand TpA1 control of the A peak further. Furthermore, identification of the TrpA1<sup>+</sup> neurones responsible for the A peak is yet to be achieved. A LexA version of the *TrpA1<sup>AB</sup>-gal4* driver exists. Combining the LexA system with the *UAS-gal4* system would enable expression of one fluorophore in *TrpA1<sup>AB+</sup>* cells and a different fluorophore via other drivers that do not affect the A peak, such as *TrpA1<sup>SH</sup>-gal4* or *TrpA1<sup>CD</sup>-gal4*. This was attempted, but a contamination in one of the reagents resulted in a failed ICC. Unfortunately, due to time constraints, it could not be repeated.

The relationship between the visual system and temperature sensation is complex, as discussed previously and in the general introduction. The visual system has also been directly linked to control of the A peak under semi-natural conditions via *norpA* (Green *et al.*, 2015). Results from this chapter

(**Figures 6-10 & 6-11**) indicate a role for rhodopsins in the timing of the A peak. Mutation of UV-blue-light sensitive Rh3 resulted in an advanced A peak, whereas mutation of green-light sensitive Rh6 resulted in a delayed A-peak (**Figure 6-10**). For *rh3* mutants this was due to a significantly advanced  $A_{\max}$  (of up to ~1.75 hrs.), albeit with a slightly delayed  $A_{\text{onset}}$  (of ~0.7 hrs.) (**Figure 6-11A**). Whereas, in *rh6* mutants the delayed A peak was due to a significantly delayed  $A_{\text{onset}}$  (of up to ~2 hrs.), as well as a slightly delayed  $A_{\max}$  (~0.7 hrs), albeit with a large variation lowering statistical significance (**Figure 6-11C**). The cell fate determination of the photoreceptors of the compound eye, and the relative rhodopsin expression pattern is complex and involves several feedback mechanisms. This complex expression pattern may explain the opposing phenotypes of Rh3 and Rh6 mutant flies (**Figure 6-16**).

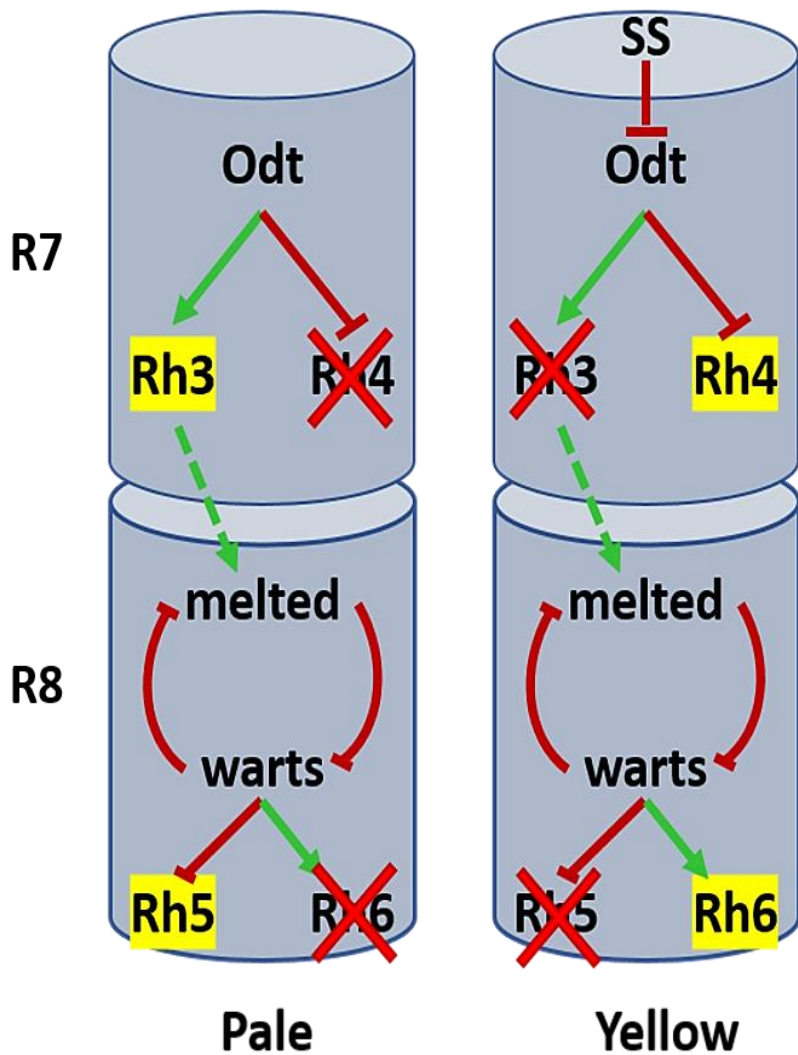


**Figure 6-16.** Visualisation of pale and yellow ommatidia fate determination. Pale ommatidia express pale-specific transcription factors such as Odt in R7 photoreceptors which enables *rh3* expression but inhibits *rh4* expression. Rh3 activates melted in the R8 cells resulting in an inhibition of warts. Warts is unable to repress *rh5* or activate *rh6* resulting in expression of Rh5. In yellow ommatidia SS is expressed in R7 cells resulting in a repression of Odt. *rh3* transcription is no longer activated and *rh4*, now derepressed, is expressed. No signal is sent to melted in the R8 so warts dominates the double-negative feedback loop resulting in Rh6 expression.

The R7 and R8 cells of each ommatidia are stacked upon each other and each pair interact through signalling cascades to determine the correct rhodopsin expression pattern (**Figure 6-16**). Yellow ommatidia express Rh4 and Rh6, whereas Pale ommatidia express Rh3 and Rh5. The majority of R7 cells express *spineless* (Ss) during early pupal development which ultimately marks these ommatidia as yellow fated through inhibition of pale-

specific transcription factors such as Orthodenticle (Odt) which activates *rh3* and *rh5* transcription (Tahayato *et al.*, 2003). The remaining R7 cells with absent *spineless* expression will become pale ommatidia (Wernet *et al.*, 2006). The normal fate of the ommatidia is thus pale, and in the absence of *ss* the R7 photoreceptor represses *rh4* and promotes *rh3* transcription. The R7 cell subsequently communicates to the R8 cell via an unknown mechanism to activate the growth factor, *melted*. The *melted-warts* double negative feedback loop then regulates determination of either *rh5* or *rh6* in the R8 cells (Mikeladze-Dvali *et al.*, 2005) (**Figure 6-16**).

The opposing phenotype of *rh3* and *rh6* mutants in the timing of the A peak (**Figures 6-10 & 6-11**) may be explained via the signalling-dependency of *rh6* expression. If *rh3* is mutated then *melted* is not activated and Rh6 rather than Rh5 becomes the default Rhodopsin expressed in the R8 photoreceptor cells. Therefore, the *rh3* mutant flies overexpress Rh6. The advancement in the A peak in *rh3* mutant flies may actually be due to Rh6 overexpression rather than loss of Rh3, consistent with a delayed A peak in *rh6* mutant flies. To prove this, spatial-temporal knock down of *rh3* and ***rh6*** will need to be conducted to bypass developmental fate-determination. However even this may not be sufficient as Rhodopsin expression has been found to be regulated and maintained post-differentiation, particularly in the R8 cells (Vasiliauskas *et al.*, 2011). Alternatively, programming the natural-light simulators to only omit light within the blue-light spectra or within the green-light spectra may mimic a *rh6* or *rh3* mutant without changing protein expression or signalling at the cellular level. Repeating these experiments under these light parameters would truly uncover the individual characteristics of Rh3 vs Rh6. Particularly as their light-sensitivities are on opposite ends of the *D. melanogaster* light-sensitivity spectra (peak sensitivity of 331nm and 515nm respectively).

Clearly, the visual system, and in particular the Rhodopsins have a regulatory role in determining the properties of the A peak. However, it is unclear if this is light or temperature-dependent. Are they acting as

signalling proteins downstream of temperature sensation, acting as scaffolding proteins for TrpA1, or are they acting independently via their own light-dependent signalling properties? To test this the photoperiodic and thermoperiodic cycles were uncoupled from one another.

Interestingly, the effects of *rh3* and *rh6* mutants on the timing of  $A_{onset}$  and  $A_{max}$  do not persist when the photoperiodic cycle and thermal cycle are uncoupled (**Figures 6-12 & 6-13**). Flies mutant for either rhodopsin show identical A peaks compared to their wild-type controls. Interestingly, the timing of the A peak in these experiments advances in line with temperature, occurring ~4 hrs earlier than when temperature and light were coupled (**Figure 6-11**). These data imply that the Rhodopsins are acting in a light-dependent manner, but temperature is the overriding regulator. However, when both light and temperature cycles are coupled, overall photoreceptor signalling via NORPA suppresses the amplitude of the A peak (Green *et al.*, 2015) and the Rhodopsins aid in setting the correct timing of the  $A_{onset}$  and  $A_{max}$  of the A component (**Figures 6-10 & 6-11**).

It would be interesting to repeat the rhodopsin experiments in a *TrpA1* mutant background to examine whether the evening and morning peaks still follow the thermocycle or are they more influenced by light. It would also be of interest to uncouple the thermo and photocycles further. Is temperature still dominant over light if the temperature cycle is advanced further by a full 12 hours? Under these conditions would flies still display an ‘afternoon’ peak but which is now in the middle of the night? If so, would these flies still display a morning and evening peak or would they display complete nocturnal activity? These would be interesting questions to answer to further understand the relationship of the temperature and light responses of *D. melanogaster* during the intensities of warm summer months. It would also be of interest to investigate any relationship the other rhodopsins have in relation to the A peak (Rh1, Rh2, and Rh7), and to investigate further the role of NORPA signalling.

This chapter has attempted to correct discrepancies in the study of the A peak using TrpA1 constructs and to help further understand the role of temperature and light in the regulation of the A peak. Parisky *et al.* (2016) found that sleep is independent from the circadian clock, and that both temperature and light work in opposing directions for regulation of day-time sleep but that light is the dominant component and thus the flies “siesta” (Parisky *et al.*, 2016). In semi-natural conditions, it could be that this is true (via NORPA) until temperatures get too high and the temperature-dependent element takes over. This may be via TrpA1 as is seen in studies under rectangular laboratory conditions whereby TrpA1 has opposing roles at <30°C and >30°C (Menegazzi *et al.*, 2012; Roessingh *et al.*, 2015; Roessingh *et al.*, 2017; Lamaze *et al.*, 2017). This would also help explain why the A peak is only present at high temperature cycles (Vanin *et al.*, 2012).

The overall findings of this chapter can be summarised as follows:

- *TrpA1<sup>K1</sup>-gal4* not *TrpA1<sup>48951</sup>-gal4* was used to abolish the A peak in the original Green *et al.* paper (2015).
- The TrpA1-dependent A peak is regulated by the *TrpA1-AB* promoter and not the *TrpA1-CD* promoter.
- Mutation of the *TrpA1-A* isoform is sufficient to abolish the A peak, but *TrpA1-B* also has regulatory functionality.
- The “A peak” identified in two independent studies are likely due to two alternative TrpA1-dependent mechanisms. The first is a true “A peak” (Green *et al.*, 2015) and was studied further in this chapter. The second is likely a TrpA1-dependent startle response due to experimental artefacts (Das *et al.*, 2015).
- Rh6 expression regulates the timings of the A peak. The role of Rh3 in A-peak timing is not clear. It may be working independently to regulate the A-peak in an opposing manner to Rh6, or its mutation may indirectly lead to an overexpression of Rh6.
- Temperature is the overriding contributor to the A peak.

## 7. GENERAL DISCUSSION

The work presented in this thesis was centred around the adaptations of *D. melanogaster* to the unfavourable conditions experienced during winter or the height of summer. In particular, the main focus of this study has been on the latter, and the pre-emptive diapause response. The involvement of the two main components of the molecular clock PER and TIM were investigated and in doing so revealed two new regulatory mechanisms for diapause control. These included key roles for the long forgotten 0.9 kb gene, and of an increasingly multi-purposed *miRNA*, *miR-276b*. In regards to adaptation to long, hot summer days, *TrpA1* was further investigated in regulating the A peak, by uncovering the promoter and isoform specificity underlying the A component. A role for the visual system was also probed by uncovering a functional role for the Rhodopsins specifically Rh6 and Rh3 in regulating A component timing.

The importance of experimental procedure was also highlighted by this study, both in relation to diapause and to locomotor behaviour at high temperatures. The use of natural-like environmental parameters produced differing phenotypes than that of standard laboratory parameters. Furthermore, the traditional method of scoring diapause was readdressed and an alternative trialled. The relationship and contribution of temperature and light was also investigated in relation to diapause and the A component, either through genetic dissection or changes in environmental parameters.

This chapter will discuss and summarise the main findings of this study and attempt to put them into perspective.

## 7.1 Evaluation of the diapause scoring methodology

Diapause has traditionally been scored in *Drosophila* females whose egg chambers are previtellogenic (stages 0-7 according to King's classification (King, 1970)). This is because after stage 7 yolk protein is produced and builds up in the egg chambers (vitellogenesis). This would be a logical stage to initiate diapause in order to conserve as much energy as possible. However, some groups have observed that *Drosophila* actually blocks its oogenesis pre-stage 10 (Tatar *et al.*, 2001; Lee *et al.*, 2011). Yolk protein pre-stage 10 is made by the eggs themselves represents only a relatively small amount compared to the fully matured eggs (Brennan *et al.*, 1982). In contrast, at post stage 9 of oogenesis the fat bodies make vast amounts of yolk protein that is deposited into the eggs contributing to an exponential increase in egg size (He *et al.*, 2011). Additionally, flies have been shown to continue to produce yolk protein in the fat bodies even when diapausing but to a lesser extent, and this is not deposited into the egg chambers (Richard *et al.*, 2001). Therefore, stage 10 may be the defining point of diapause induction and not stage 8, characterised by an increase in yolk production in the fat bodies and its subsequent deposition into the egg chambers. Lirakis *et al* (2018) proposed that the most accurate scoring method would be to count the total number of eggs at each stage. This however makes an already time-consuming experiment even more so. As such in this study two methods of scoring for diapause were used: a) scoring diapause using the traditional method (Saunders *et al.*, 1989) which was applied to experiments conducted at earlier stages of this project. b) scoring diapause from both stage < 8 and < 10, thus providing twice as much information for very little extra effort/time.

Upon analysing the two scoring methods it is clear that the trend is always consistent between each scoring method, if diapause levels increase from one genotype to another scoring from egg stage <8 the same will be true scoring from stage <10. However, the relative strength of the phenotype

between scoring methods changes from experiment to experiment and chapter to chapter. In **chapter 5**, in general, there is a greater photoperiodic and thermoperiodic effect when scoring from stage <8, but a greater population effect when scoring from stage <10. In **chapter 4**, in general, there were greater significance across phenotypes scored via stage <10 compared to stage <8. However, in **chapter 3**, phenotypes were marginally more significant scoring from <8 than scoring from <10.

Consequently, which scoring method is used has little impact on the study of the diapause phenotype. Scoring and recording both methods simultaneously, as was conducted in this study, seems to be the most appropriate procedure to take. It requires very little extra time and provides twice as much data, even if this extra data may not always provide much additional information. However, the scoring of diapause is still imperfect. It involves a subjective decision based on the human eye. This lends itself to error and makes it difficult to compare between studies. The Chiu laboratory have proposed using image J software to calculate ovary surface area as a measure of diapause (Abrieux *et al.*, 2020). However, this too is imperfect as it does not take into account size differences between individuals or populations. This will make this method particularly unsuitable for studying clines in diapause amongst natural populations. It also does not account at all for yolk protein which is of course the characterising component of diapausing ovaries (Saunders *et al.*, 1989). A smaller sized population may have smaller eggs, but have larger amounts of yolk within eggs. An alternative method could be to assay for total yolk protein via a yolk-synthesis specific *gal4* driver expressing an assayable marker such as a fluorophore. To avoid detection of yolk protein accumulated in the fat bodies and haemolymph (Richard *et al.*, 2001) this would have to be done after isolation of whole ovaries. However, there would still have to be a way of accounting for size variation between individuals and populations, possibly by normalising against ovary mass. A combination of the two methods would be the most accurate, but this would be very time consuming as each individual ovary would have to be imaged and then assayed

separately for its yolk content. Clearly, a better method is yet to be thought of and in the meantime the subjective scoring method will suffice.

## 7.2 The role of the circadian clock in diapause regulation

The two main components of the molecular clock PER and TIM were investigated for relevance in diapause in **Chapter 4** and **Chapter 3** respectively. The role of PER in diapause regulation has been a topic for debate. Findings from our laboratory find that *per<sup>0</sup>* flies show a reduced diapause incidence compared to wild type flies (Gesto, 2011; Collins, 2014) contradictory to findings by Saunders and colleagues (1989) that suggested that *per* has no influence on diapause. Concurrent with Gesto and Collins, results from this current study (**Chapter 4**) show that in a *per<sup>0</sup>* background, flies overexpressing a wild-type *UAS-per* rescue display higher diapause levels than flies overexpressing an empty vector. However, the splicing event of *dmp18* which has been shown to have wide-ranging effects for seasonal adaptations for circadian phenotypes (Majercak *et al.*, 1999; Collins *et al.*, 2004; Majercak *et al.*, 2004; Low *et al.*, 2008; Low *et al.*, 2012; Yang and Edery, 2019; Breda *et al.*, 2020) was found to only have an effect if overexpressed via *tim-gal4* but not if under intrinsic expression via the *per* promoter (**Chapter 4**). As already discussed, this may be due to experimental sub-optimum temperature levels. Nonetheless, overexpression (via *tim-gal4*) of a splice-locked unspliced *perA* isoform results in a decrease in diapause compared to overexpression of the spliced *perB* isoform.

The role of TIM in diapause regulation is also controversial. Although it is widely accepted that TIM regulates diapause, the direction in which it regulates it is debated (Tauber *et al.*, 2007; Gesto, 2011; Zonato *et al.*, 2017; Martin Anduaga, 2018; Abrieux *et al.*, 2020). In **Chapter 3**, inhibition of *tim* via *miR-276b* was found to result in an increase in diapause levels, consistent with *tim* mutants from Tauber *et al.* 2007 and Gesto, 2011 but

contradictory to Abrieux *et al* 2020. However, Abrieux and colleagues used an alternative method to characterise diapause via ovary size (as previously discussed).

Consequently, an inhibition of PER via overexpression of *perA*, known to slowdown *per* accumulation (Majercak *et al.*, 2004), or mutation of PER leads to a decrease in diapause, whereas inhibition of *tim* via *miR-276b* results in an increase in diapause. The apparently opposing effects of *per* and *tim* on diapause (at least in this study) may imply clock-independent pleiotropy. On the other hand, it can also be supportive of a clock-dependent role when compared to a study by Menegazzi *et al.* 2013. They found that in both nature and laboratory conditions, the peak in TIM expression precedes the peak in PER expression. Furthermore, the relative time distance between peaks increases as photoperiod/thermoperiod increases. In the approach to winter, the two peaks are close together, whereas in the summer they are far apart (Menegazzi *et al.*, 2013). It was suggested that this is reminiscent of an internal coincidence model for diapause control (Menegazzi *et al.*, 2013).

If this model for diapause induction is correct, then the opposing effects of inhibiting PER and TIM bare more logic. Internal coincidence models suggest that the two peaks in protein must occur close to each other in order to elicit a diapause effect (**Figure 7-1A**). If PER accumulation is inhibited/slowed (via overexpression of *perA*) this causes the PER peak to lag even further, resulting in a greater distance between the two peaks and consequently less diapause (**Figure 7-1B**). However, as the TIM peak precedes PER, inhibition of *tim* (via *miR-276b* expression) may delay TIM accumulation so that it is more in line with PER and thus increase diapause further (**Figure 7-1C**). Unfortunately, a *tim* null mutant was not tested. As already discussed, *tim*<sup>0</sup> mutants provide differing results in the literature (Tauber *et al.*, 2007; Gesto, 2011; Marin Anduaga, 2018; Abrieux *et al.*, 2020). However, it would be expected that this would result in a decrease in diapause as it would remove the clock-control element, in a similar

manner as the *per<sup>0</sup>* mutant did. However, the proposed model (**Figure 7-1**) is entirely speculative and requires much more experimental dissection.

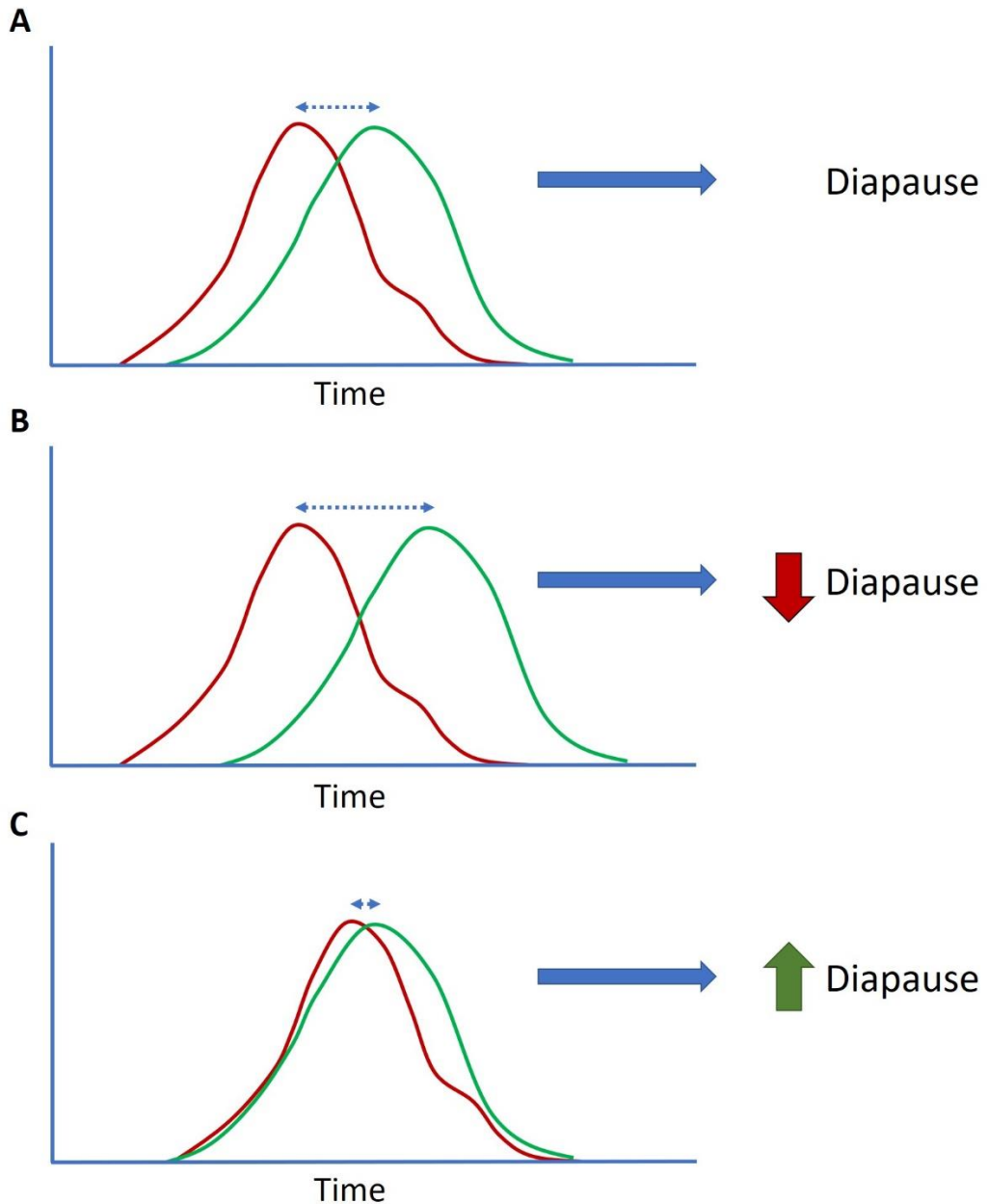


**Figure 7-1.** An internal coincidence model for diapause regulation via TIM (red) and PER (green). **A)** under diapause inducing conditions the two peaks of TIM and PER are close together resulting in relatively high diapause induction. **B)** inhibition of PER accumulation delays the PER peak further causing a further distance between the two peaks, and consequently, a decrease in diapause levels. **C)** Inhibition of *tim* delays the TIM peak so that both peaks are even closer together resulting in an enhancement of diapause levels.

In addition to results from this thesis indicating a circadian role in diapause regulation, albeit via a speculative model, data from other studies

strengthen this hypothesis: The previously believed absence of a functional circadian clock at low temperatures has been recently challenged (Montelli *et al.*, 2015; Abrieux *et al.*, 2020; Ralf Stanewsky, pers comm). Moreover, *miR-276b* is not only itself under circadian control (Chen and Rosbash, 2016) but also has several other circadian targets (*npf1*, *CK2* & *DopR1*) (Yang *et al.*, 2008; Zhang *et al.*, 2021). Furthermore, in addition to PER and TIM, mutation of CLK, CYC or CRY have also proven to influence diapause levels (Gesto, 2011; Martin Anduaga, 2018). Clock-related neuronal circuits have also been implicated in diapause-related phenotypes. A decrease in diapause is observed when PDF and sNPF signalling from the sLNvs to the IPCs is blocked (Nagy *et al.*, 2019). Also, the DN1s, DN2s, and the circadian-linked compound eye have also all been implicated in diapause-relevant pathways, although the actual diapause-inducing properties are only partly explored (Barber *et al.*, 2016; Tang *et al.*, 2013; Wolfgang *et al.*, 2013; Roessingh *et al.*, 2019; Abrieux *et al.*, 2020). All these data imply that the clock as a module regulates diapause, rather than the pleiotropic roles of individual components. However, there may also be pleiotropy amongst some clock components running in parallel.

## 7.3 The relationship between temperature and light in diapause regulation

As discussed previously (**Chapters 1.3 & 5**), the photoperiodicity of diapause is a debatable topic. Under artificial laboratory conditions with rectangular light and temperature profiles, the photoperiodic response appears to be weak (Emerson *et al.*, 2009b; Anduaga *et al.*, 2018; Nagy *et al.*, 2019) particularly when taking into account artificial thermoperiods accidentally created in most studies (Pegoraro *et al.*, 2014; Anduaga *et al.*, 2018). However, using more natural-like light profiles, the photoperiodic response is strong (Nagy *et al.*, 2019), albeit without a temperature cycle.

The overriding role of temperature over photoperiod in rectangular light and constant temperature profiles has been identified as a possible cause for

discrepancies in the role of *dmp18* splicing in this thesis (**Chapter 4**) due to differing optimum experimental temperatures. It may also account for many other discrepancies between studies in the literature (Saunders, 1990; Saunders and Gilbert, 1990; Tatar *et al.*, 2001; Tauber *et al.*, 2007; Emerson *et al.*, 2009b; Gesto, 2011; Lee *et al.*, 2011; Collins, 2014; Pegoraro *et al.*, 2014; Schiesari *et al.*, 2016; Pegoraro *et al.*, 2017; Zonato *et al.*, 2017; Anduaga *et al.*, 2018; Nagy *et al.*, 2018; Larikis *et al.*, 2018; Abrieux *et al.*, 2020). Furthermore, the rearing conditions of parental flies, and experimental flies pre-eclosion also has an influence on the ability of flies to respond to winter-like conditions, affecting their diapause inducibility, metabolic response and cold-shock survival rate (Pegoraro *et al.*, 2014; Anduaga *et al.*, 2018). Clearly, temperature has a profound influence on diapause inducibility and experimental parameters must be carefully considered when assaying for diapause.

**Chapter 5** studied the role of both temperature and light under simulated natural conditions to try to better understand what appears to be a complex relationship. A new model is proposed in which *D. melanogaster* is able to sense the rate of change in temperature and light and compare the synchronicity of these inputs. Only if they match is the fly able to interpret other diapausing cues to enter dormancy or not. The synchronicity of these two factors seem to override any individual photoperiodic or thermoperiodic effects, albeit an experiment investigating natural-like thermoperiods in LL or DD is yet to be conducted. Nevertheless, these findings reassess yet again the strength of the photoperiodic response, which is minimal if not coupled to a correct thermoperiod.

The gradual cyclic oscillation of temperature and light is absent from traditional laboratory studies of diapause so it is therefore difficult to model previous findings based on this new model. However, both in adult flies and in larvae, the rate of temperature change has been found to be important for several processes, such as setting of temperature preference/avoidance and in sleep/arousal (Luo *et al.*, 2017; Roessingh *et al.*, 2017). Furthermore,

a role for the visual system in regulating the A component of locomotor rhythms in long summer days has been found to be most likely due to the measurement of a rate in temperature change in the morning (**Chapter 6**). It is possible that these same circuits are responsible for diapause control. Moreover, the control of TIM expression via EYA has been shown to regulate diapause induction in response to differing environmental cues via a circuit from the compound eye to the IPCs (Abrieux *et al.*, 2020). However, whether this is in response to light or temperature is unclear (see **chapter 3**), and these experiments were not conducted under natural-like conditions. Nonetheless, it may represent a complete circuit from environmental input to diapause control via the clock. Investigation of clock, visual, and thermosensory mutants under simulated natural conditions is the next logical step to understand how environmental input is conveyed to elicit diapause in nature.

## **7.4 The Afternoon component and the startle response under semi-natural summer conditions**

Temperature had already been implied as the overriding regulator of the A component due to the essential dependence of the thermosensory channel TrpA1 (Green *et al.*, 2015). Das and colleagues (2015) also proposed that this was isoform specific via TrpA1-A (Das *et al.*, 2015). However, results from this thesis (**Chapter 6**) and inspection of the experimental parameters and subsequent data in Das *et al.* (2015), reveal that there are two separate mechanisms dictating day-time activity at high temperatures. The first is a startle response that responds to sharp step-ups in temperature, which is assayed for in the Das study (Das *et al.*, 2015), and the second is a more physiological component responsive to smooth gradual changes in temperature over time. The latter is the true A component observed in nature (Vanin *et al.*, 2012). This was found to be regulated by the TrpA1<sup>AB</sup> specific promoter rather than TrpA1<sup>CD</sup>, and both isoforms TrpA1-A and TrpA1-B have a regulatory role, although TrpA1-A more so. The timing of the A peak is dependent on the expression of these

isoforms, as overexpression leads to an over sensitisation and an advanced A peak. Whether these isoforms sense temperature directly or act downstream is still unknown.

Another consideration between these two studies (Das *et al.*, 2015; **Chapter 6**) is the experimental set up. Although the A peak has been studied in outside arenas (Vanin *et al.*, 2012; Das *et al.*, 2016) study of TrpA1 has been done so in “simulated” natural conditions. The quality of the temperature simulation has already demonstrated a distinction between phenotypes (discussed previously), but the method of measuring activity may also play a part. Inside incubator systems, using trikinetics software, flies must be kept as individuals in small glass tubes. This of course is not true to a fly’s experience in nature. Therefore, repeating these results in open field experiments would strengthen the findings of this chapter.

## 7.5 The relationship between temperature and light in regulating the A component

Overexpression of the TrpA1-A/B isoforms advanced the  $A_{\max}$  of the A component but the onset of the A peak was not advanced. The gradual ramp up in activity characterising the A peak always starts as temperature and light begin to rise. To further uncover the relationship of the A component with light and temperature, several of the light-sensitive rhodopsins were investigated. The visual system had previously been implicated in regulating the A component as complete shutdown of photoreceptor signalling capabilities enhances the relative size of the A component (Green *et al.*, 2015). Furthermore, a synergistic role between Rhodopsin signalling and TrpA1 signalling has already been found to be important for temperature sensation, whereby each channel scaffolds the other (Shen *et al.*, 2011; Sokabe *et al.*, 2016). Indeed, in **Chapter 6**, it was found that mutation of Rh3 or Rh6 had opposing effects on the timing of the A peak, by changing either  $A_{\max}$  or  $A_{\text{onset}}$ . Rh3 mutants resulted in an advanced A peak whereas Rh6 mutants resulted in a delayed A peak.

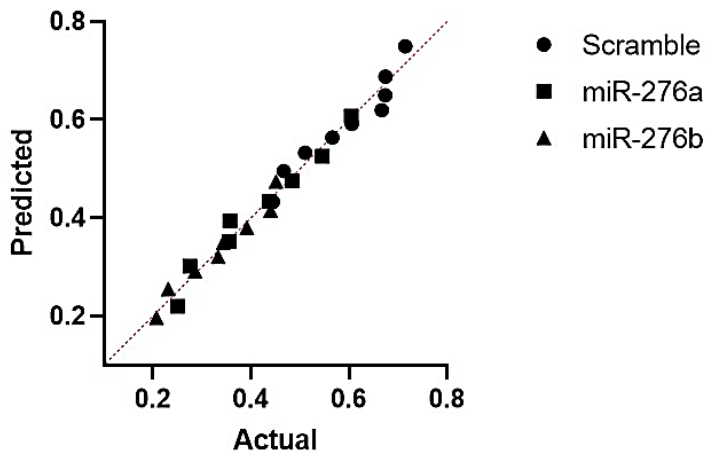
Uncoupling of the light cycle from the thermocycle indicated that the Rhodopsin-dependent regulation on the timing of the A component was light-dependent. Furthermore, it was found that the A peak itself follows the temperature cycle not the light cycle. As such, temperature is the overriding contributor to *D. melanogaster* diurnal activity under simulated hot summer days. However, if both light and temperature inputs are coupled, the rhodopsin-dependent visual system is able to fine tune the A component and set its properties.

## 7.6 Summary

This thesis has highlighted the importance of experimental set up and how subtle discrepancies in environmental conditions can have unexpected and sometimes misinterpreted results. The relationship between light and temperature in regulating behavioural adaptation to harsh winters or harsh summers has also revealed that in both cases temperature is the main component. However, both light and temperature synergise to finetune each adaptation and that this is more prevalent under natural-like environmental conditions. Indeed, the way in which *D. melanogaster* interprets environmental cues in either season appears to be different between laboratory rectangular conditions and semi-natural cyclic conditions. The importance of sensing gradual changes in the environment rather than absolute temperature and light inputs is a key difference. Therefore, studies conducted in the laboratory should always be considered with a level of caution when extrapolating findings to nature. Finally, a role of the circadian molecular clock in diapause control has been strengthened through findings in this thesis. However, these findings were conducted in restrictive laboratory settings. It would be of interest to explore these findings further in a more natural-like experimental set up.

## 8. Appendix

### 8.1 Appendix, Chapter 3



Anderson-Darling test			
A2*	0.3725	0.1950	0.2055
P value	0.3364	0.8349	0.8013
Passed normality test (alpha=0.05)?	Yes	Yes	Yes
P value summary	ns	ns	ns
D'Agostino & Pearson test			
K2	1.976	0.7485	0.8838
P value	0.3723	0.6878	0.6428
Passed normality test (alpha=0.05)?	Yes	Yes	Yes
P value summary	ns	ns	ns
Number of values	9	8	8

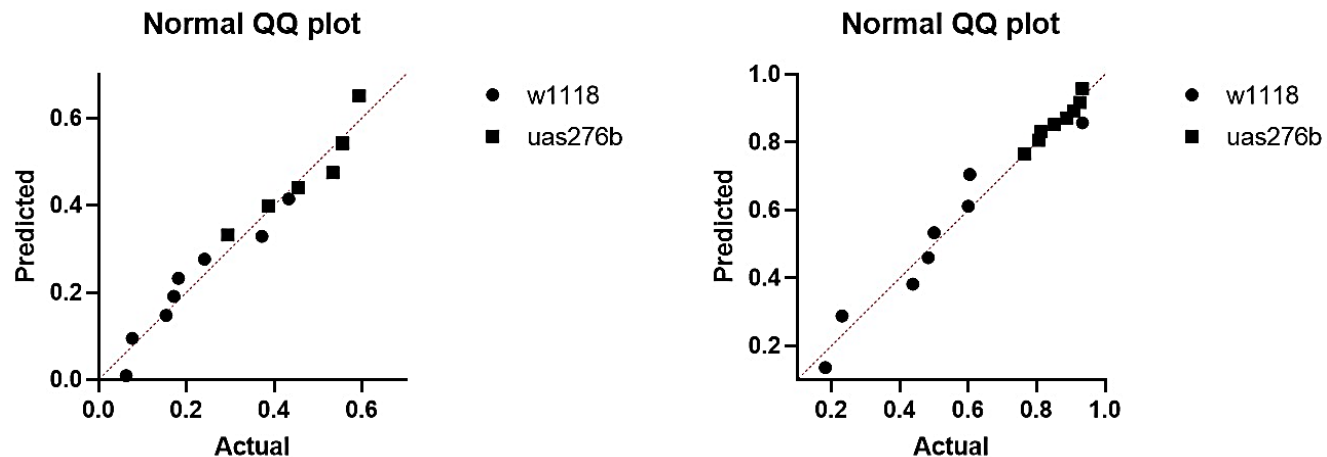
**Figure 8-3-1.** Normal distribution tests for diapause data created from Knock-down of miR-276a and miR-276b expression via miRNA-sponges. Top: QQ normality plot for each of the three data sets (*tim-gal4 x uas-scramble<sup>sponge</sup>/ miR-276a<sup>sponge</sup>./ miR-276b<sup>sponge</sup>*). Bottom: Anderson-Darling and D'Agostino & Pearson tests for normality.

<b>ANOVA table</b>	<b>SS</b>	<b>DF</b>	<b>MS</b>	<b>F (DFn, DFd)</b>	<b>P value</b>
Treatment (between columns)	0.2957	2	0.1478	F (2, 22) = 13.11	P=0.0002
Residual (within columns)	0.2481	22	0.01128		
Total	0.5438	24			

<b>Tukey's multiple comparisons test</b>	<b>Mean Diff.</b>	<b>95.00% CI of diff.</b>	<b>Below threshold?</b>	<b>Summary</b>	<b>Adjusted P Value</b>
Scramble vs. miR-276a	0.1778	0.04815 to 0.3074	Yes	**	0.0063
Scramble vs. miR-276b	0.2561	0.1265 to 0.3858	Yes	***	0.0002
miR-276a vs. miR-276b	0.07835	-0.05504 to 0.2117	No	ns	0.3216

**Figure 8-3-2.** Statistical analysis for diapause data created from Knock-down of miR-276a and miR-276b expression via miRNA-sponges. Top: one-way ANOVA. Bottom: Tukey's *post hoc* multiple comparison test



Anderson-Darling test			
A2*	0.3508	0.6087	
P value	0.3704	0.0728	
Passed normality test (alpha=0.05)?	Yes	Yes	
P value summary	ns	ns	
D'Agostino & Pearson test			
K2	1.037	2.579	
P value	0.5954	0.2754	
Passed normality test (alpha=0.05)?	Yes	Yes	
P value summary	ns	ns	
Number of values	8	8	

Anderson-Darling test			
A2*	0.2992	0.2860	
P value	0.5039	0.5269	
Passed normality test (alpha=0.05)?	Yes	Yes	
P value summary	ns	ns	
D'Agostino & Pearson test			
K2	1.050	1.360	
P value	0.5916	0.5067	
Passed normality test (alpha=0.05)?	Yes	Yes	
P value summary	ns	ns	
Number of values	8	8	

**Figure 8-3-3.** Normal distribution tests for diapause data created from overexpressing *miR-276b* via *tim-gal4* scored from either egg stage <8 (left) or egg stage <10 (right). Top: QQ normality plot for each of the two data sets (*tim-gal4* x *uas-miR-276b*/ *w<sup>1118</sup>*). Bottom: Anderson-Darling and D'Agostino & Pearson tests for normality.

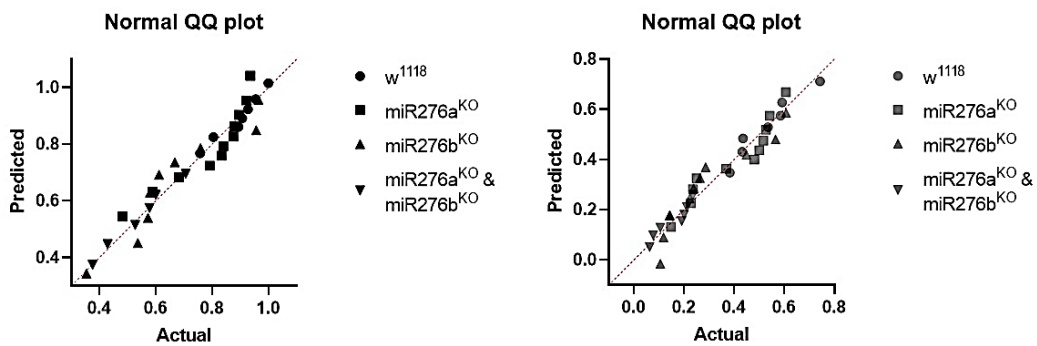
**Unpaired t test with Welch's correction**

P value	0.0004
P value summary	***
Significantly different ( $P < 0.05$ )?	Yes
One- or two-tailed P value?	Two-tailed
Welch-corrected t, df	t=4.704, df=13.27

**Unpaired t test with Welch's correction**

P value	0.0028
P value summary	**
Significantly different ( $P < 0.05$ )?	Yes
One- or two-tailed P value?	Two-tailed
Welch-corrected t, df	t=4.249, df=7.981

**Figure 8-3-4.** Unpaired t test with Welch's correction for diapause data created from overexpressing *miR-276b* via *tim-gal4* scored from either egg stage <8 (top) or egg stage <10 (bottom)



Anderson-Darling test				
A2*	N too small	0.5953	0.6352	N too small
P value		0.0915	0.0715	
Passed normality test (alpha=0.05)?		Yes	Yes	
P value summary		ns	ns	
D'Agostino & Pearson test				
K2	N too small	3.111	2.088	N too small
P value		0.2110	0.3520	
Passed normality test (alpha=0.05)?		Yes	Yes	
P value summary		ns	ns	
Shapiro-Wilk test				
W	0.9333	0.8897	0.8608	0.8715
P value	0.5797	0.1379	0.0589	0.1912
Passed normality test (alpha=0.05)?	Yes	Yes	Yes	Yes
P value summary	ns	ns	ns	ns
Kolmogorov-Smirnov test				
KS distance	0.2052	0.2384	0.2264	0.2665
P value	>0.1000	0.0809	>0.1000	>0.1000
Passed normality test (alpha=0.05)?	Yes	Yes	Yes	Yes
P value summary	ns	ns	ns	ns
Number of values	7	11	11	7

**Figure 8-3-5.** Normal distribution tests for diapause data created from heterozygous mutants for either *miR-276a*, *miR-276b* or both, scored from either egg stage <8 (left) or egg stage <10 (right). Top: QQ normality plot for each of the two data sets (*tim-gal4 x uas-miR-276b/ w<sup>1118</sup>*). Bottom: Anderson-Darling, D'Agostino & Pearson, Shapiro-Wilk, and Kolmogorov-Smirnov tests for normality.

<b>ANOVA table</b>	<b>SS</b>	<b>DF</b>	<b>MS</b>	<b>F (DFn, DFd)</b>	<b>P value</b>
Treatment (between columns)	0.7138	3	0.2379	F (3, 32) = 9.090	P=0.0002
Residual (within columns)	0.8376	32	0.02617		
Total	1.551	35			

<b>Tukey's multiple comparisons test</b>	<b>Mean Diff.</b>	<b>95.00% CI of diff.</b>	<b>Below threshold?</b>	<b>Summary</b>	<b>Adjusted P Value</b>
w1118 vs. mir276aKO x w1118	0.1381	-0.07388 to 0.3500	No	ns	0.3085
w1118 vs. mir276bKO x w1118	0.2672	0.05531 to 0.4792	Yes	**	0.0090
w1118 vs. mir276aKO x mir276bKO	0.4214	0.1871 to 0.6557	Yes	***	0.0002
mir276aKO x w1118 vs. mir276bKO x w1118	0.1292	-0.05772 to 0.3161	No	ns	0.2597
mir276aKO x w1118 vs. mir276aKO x mir276bKO	0.2833	0.07140 to 0.4953	Yes	**	0.0053
mir276bKO x w1118 vs. mir276aKO x mir276bKO	0.1541	-0.05779 to 0.3661	No	ns	0.2202

<b>ANOVA table</b>	<b>SS</b>	<b>DF</b>	<b>MS</b>	<b>F (DFn, DFd)</b>	<b>P value</b>
Treatment (between columns)	0.8447	3	0.2816	F (3, 32) = 8.444	P=0.0003
Residual (within columns)	1.067	32	0.03334		
Total	1.912	35			

<b>Tukey's multiple comparisons test</b>	<b>Mean Diff.</b>	<b>95.00% CI of diff.</b>	<b>Below threshold?</b>	<b>Summary</b>	<b>Adjusted P Value</b>
w1118 vs. mir276aKO x w1118	0.1534	-0.08581 to 0.3926	No	ns	0.3217
w1118 vs. mir276bKO x w1118	0.3108	0.07161 to 0.5500	Yes	**	0.0069
w1118 vs. mir276aKO x mir276bKO	0.4497	0.1853 to 0.7142	Yes	***	0.0003
mir276aKO x w1118 vs. mir276bKO x w1118	0.1574	-0.05354 to 0.3684	No	ns	0.2013
mir276aKO x w1118 vs. mir276aKO x mir276bKO	0.2963	0.05714 to 0.5355	Yes	*	0.0105
mir276bKO x w1118 vs. mir276aKO x mir276bKO	0.1389	-0.1003 to 0.3781	No	ns	0.4075

**Figure 8-3-6.** One-way ANOVA followed by Tukey's *post hoc* multiple comparison test for diapause data from heterozygous mutants for either *miR-276a*, *miR-276b* or both, scored from either egg stage <8 (top) or egg stage <10 (bottom).

Data analyzed	Rhythmic	Arythmic	Total	P value and statistical significance	
♀ wt 16	150	0	150	Test	Chi-square
♀ aKO	104	8	112	Chi-square, df	11.05, 1
Total	254	8	262	z	3.324
				P value	0.0009
				P value summary	***
				One- or two-sided	Two-sided
				Statistically significant ( $P < 0.05$ )?	Yes
Data analyzed	Rhythmic	Arythmic	Total	P value and statistical significance	
♀ wt 16	150	0	150	Test	Chi-square
♀ bKO	83	3	86	Chi-square, df	5.300, 1
Total	233	3	236	z	2.302
				P value	0.0213
				P value summary	*
				One- or two-sided	Two-sided
				Statistically significant ( $P < 0.05$ )?	Yes
Data analyzed	Rhythmic	Arythmic	Total	P value and statistical significance	
♀ wt 16	150	0	150	Test	Chi-square
♀ aKO x bKO	88	22	110	Chi-square, df	32.77, 1
Total	238	22	260	z	5.725
				P value	<0.0001
				P value summary	****
				One- or two-sided	Two-sided
				Statistically significant ( $P < 0.05$ )?	Yes
Data analyzed	Rhythmic	Arythmic	Total	P value and statistical significance	
♀ wt 16	150	0	150	Test	Chi-square
♀ UAS	42	75	117	Chi-square, df	133.7, 1
Total	192	75	267	z	11.56
				P value	<0.0001
				P value summary	****
				One- or two-sided	Two-sided
				Statistically significant ( $P < 0.05$ )?	Yes

Figure continues onto next page

Data analyzed	Rhythmic	Arythmic	Total	P value and statistical significance	
				Test	Chi-square
♂ wt 16	144	1	145	Chi-square, df	8.903, 1
♂ aKO	54	5	59	z	2.984
Total	198	6	204	P value	0.0028
				P value summary	**
				One- or two-sided	Two-sided
				Statistically significant ( $P < 0.05$ )?	Yes
Data analyzed	Rhythmic	Arythmic	Total	P value and statistical significance	
				Test	Chi-square
♂ wt 16	144	1	145	Chi-square, df	3.540, 1
♂ bKO	90	4	94	z	1.881
Total	234	5	239	P value	0.0599
				P value summary	ns
				One- or two-sided	Two-sided
				Statistically significant ( $P < 0.05$ )?	No
Data analyzed	Rhythmic	Arythmic	Total	P value and statistical significance	
				Test	Chi-square
♂ wt 16	144	1	145	Chi-square, df	38.282, 1
♂ aKO X bKO	62	22	84	z	6.1873
Total	206	23	229	P value	<0.0001
				P value summary	****
				One- or two-sided	Two-sided
				Statistically significant ( $P < 0.05$ )?	Yes
Data analyzed	Rhythmic	Arythmic	Total	P value and statistical significance	
				Test	Chi-square
♂ wt 16	144	1	145	Chi-square, df	122.4, 1
♂ UAS	47	77	124	z	11.06
Total	191	78	269	P value	<0.0001
				P value summary	****
				One- or two-sided	Two-sided
				Statistically significant ( $P < 0.05$ )?	Yes

Figure continues onto next page

Data analyzed	Rhythmic	Arythmic	Total	P value and statistical significance	
♀ wt 25	83	4	87	Test	Chi-square
♀ aKO	51	7	58	Chi-square, df	2.771, 1
Total	134	11	145	z	1.665
				P value	0.0960
				P value summary	ns
				One- or two-sided	Two-sided
				Statistically significant ( $P < 0.05$ )?	No
Data analyzed	Rhythmic	Arythmic	Total	P value and statistical significance	
♀ wt 25	83	4	87	Test	Chi-square
♀ bKO	81	10	91	Chi-square, df	2.507, 1
Total	164	14	178	z	1.583
				P value	0.1133
				P value summary	ns
				One- or two-sided	Two-sided
				Statistically significant ( $P < 0.05$ )?	No
Data analyzed	Rhythmic	Arythmic	Total	P value and statistical significance	
♀ wt 25	83	4	87	Test	Chi-square
♀ aKO x bKO	48	10	58	Chi-square, df	6.378, 1
Total	131	14	145	z	2.525
				P value	0.0116
				P value summary	*
				One- or two-sided	Two-sided
				Statistically significant ( $P < 0.05$ )?	Yes
Data analyzed	Rhythmic	Arythmic	Total	P value and statistical significance	
♀ wt 25	83	4	87	Test	Chi-square
♀ UAS	45	46	91	Chi-square, df	46.49, 1
Total	128	50	178	z	6.819
				P value	<0.0001
				P value summary	****
				One- or two-sided	Two-sided
				Statistically significant ( $P < 0.05$ )?	Yes

Figure continues onto next page

Data analyzed	Rhythmic	Arythmic	Total	P value and statistical significance
♂ wt 25	41	5	46	Test
♂ aKO	27	1	28	Chi-square, df
Total	68	6	74	z
				P value
				P value summary
				One- or two-sided
				Statistically significant ( $P < 0.05$ )?
				Chi-square
				1.244, 1
				1.115
				0.2647
				ns
				Two-sided
				No
Data analyzed	Rhythmic	Arythmic	Total	P value and statistical significance
♂ wt 25	41	5	46	Test
♂ bKO	88	8	96	Chi-square, df
Total	129	13	142	z
				P value
				P value summary
				One- or two-sided
				Statistically significant ( $P < 0.05$ )?
				Chi-square
				0.2405, 1
				0.4904
				0.6238
				ns
				Two-sided
				No
Data analyzed	Rhythmic	Arythmic	Total	P value and statistical significance
♂ wt 25	41	5	46	Test
♂ aKO x bKO	33	26	59	Chi-square, df
Total	74	31	105	z
				P value
				P value summary
				One- or two-sided
				Statistically significant ( $P < 0.05$ )?
				Chi-square
				13.69, 1
				3.700
				0.0002
				***
				Two-sided
				Yes
Data analyzed	Rhythmic	Arythmic	Total	P value and statistical significance
♂ wt 25	41	5	46	Test
♂ UAS	23	40	63	Chi-square, df
Total	64	45	109	z
				P value
				P value summary
				One- or two-sided
				Statistically significant ( $P < 0.05$ )?
				Chi-square
				30.37, 1
				5.511
				<0.0001
				****
				Two-sided
				Yes

**Figure 8-3-7.** Chi-square analysis of locomotor data collected from flies under differing genetic manipulation of *miR-276a* and *miR-276b*.

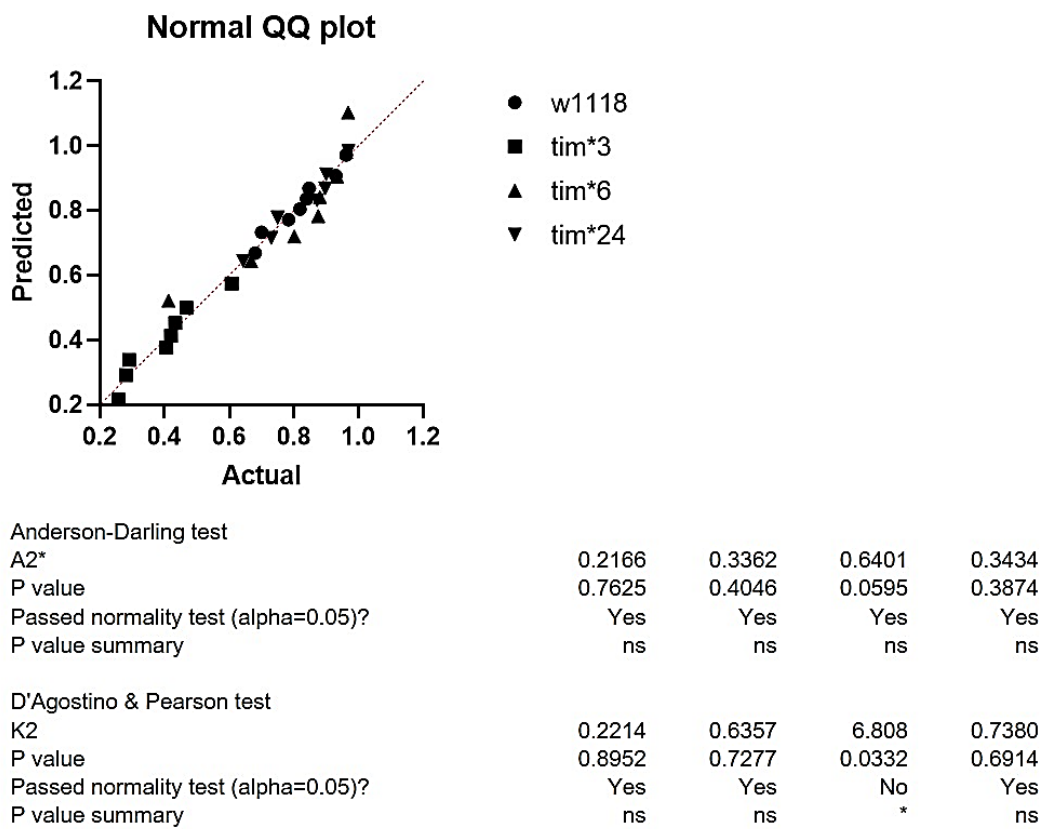


**Figure 8-3-8.** Normal distribution tests for diapause data created from mutants of the the *miR-276b* seed-site binding region of *tim*. Top: QQ normality plot for each of the four data sets (*w<sup>1118</sup>*, *tim<sup>\*3</sup>*, *tim<sup>\*6</sup>*, and *tim<sup>\*24</sup>*). Bottom: Anderson-Darling and D'Agostino & Pearson tests for normality.

<b>ANOVA table</b>	<b>SS</b>	<b>DF</b>	<b>MS</b>	<b>F (DFn, DFd)</b>	<b>P value</b>
Treatment (between columns)	1.059	3	0.3529	F (3, 28) = 19.74	P<0.0001
Residual (within columns)	0.5005	28	0.01787		
Total	1.559	31			

<b>Tukey's multiple comparisons test</b>	<b>Mean Diff.</b>	<b>95.00% CI of diff.</b>	<b>Below threshold?</b>	<b>Summary</b>	<b>Adjusted P Value</b>
w1118 vs. tim*3	0.4245	0.2420 to 0.6071	Yes	****	<0.0001
w1118 vs. tim*6	0.007599	-0.1749 to 0.1901	No	ns	0.9995
w1118 vs. tim*24	0.005989	-0.1765 to 0.1885	No	ns	0.9997
tim*3 vs. tim*6	-0.4170	-0.5995 to -0.2344	Yes	****	<0.0001
tim*3 vs. tim*24	-0.4186	-0.6011 to -0.2360	Yes	****	<0.0001
tim*6 vs. tim*24	-0.001610	-0.1841 to 0.1809	No	ns	>0.9999

**Figure 8-3-9.** Statistical analysis for diapause data created from mutants of the the *miR-276b* seed-site binding region of *tim*. Top: one-way ANOVA. Bottom: Tukey's *post hoc* multiple comparison test

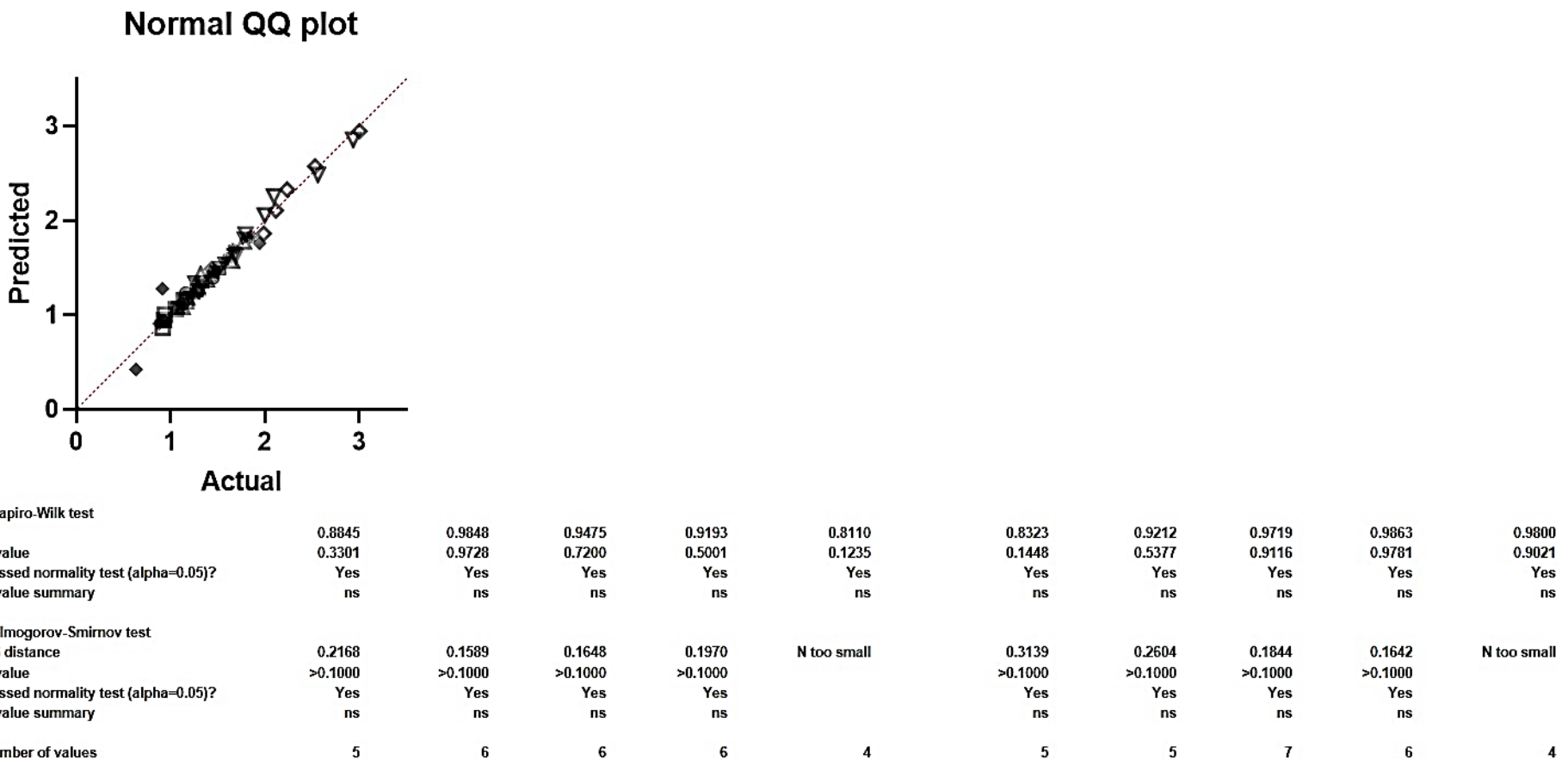


**Figure 8-3-9.** Statistical analysis for diapause data created from mutants of the the *miR-276b* seed-site binding region of *tim*. Top: one-way ANOVA. Bottom: Tukey's *post hoc* multiple comparison test

ANOVA table	SS (Type III)	DF	MS	F (DFn, DFd)	P value
Interaction	1.547	4	0.3867	F (4, 44) = 3.165	P=0.0227
Genotype	4.260	4	1.065	F (4, 44) = 8.717	P<0.0001
Tissue	2.457	1	2.457	F (1, 44) = 20.11	P<0.0001
Residual	5.376	44	0.1222		

Test details	Predicted (LS) mean 1	Predicted (LS) mean 2	Predicted (LS) mean diff.	SE of diff.	N1	N2	q	DF
<b>Head</b>								
w1118 vs. UAS:miR-276b x miR-276b-Gal4	1.114	1.212	-0.09778	0.2117	5	6	0.4620	44.00
w1118 vs. miR-276a <sup>KO</sup> x w1118	1.114	1.266	-0.1526	0.2117	5	6	0.7211	44.00
w1118 vs. miR-276b <sup>KO</sup> x w1118	1.114	1.493	-0.3791	0.2117	5	6	1.791	44.00
w1118 vs. miR-276a <sup>KO</sup> x miR-276b <sup>KO</sup>	1.114	1.090	0.02343	0.2345	5	4	0.09991	44.00
<b>Body</b>								
w1118 vs. UAS:miR-276b x miR-276b-Gal4	0.9998	1.430	-0.4307	0.2211	5	5	1.948	44.00
w1118 vs. miR-276a <sup>KO</sup> x w1118	0.9998	2.051	-1.052	0.2047	5	7	5.138	44.00
w1118 vs. miR-276b <sup>KO</sup> x w1118	0.9998	2.215	-1.215	0.2117	5	6	5.741	44.00
w1118 vs. miR-276a <sup>KO</sup> x miR-276b <sup>KO</sup>	0.9998	1.644	-0.6446	0.2345	5	4	2.749	44.00

**Figure 8-3-11.** Two-way ANOVA followed by Tukey's *post hoc* multiple comparison test for data created from *tim* mRNA levels of flies under differing genetic manipulation of *miR-276a* and *miR-276b*.

#### Normality of Residuals

Test name	Statistics	P value	Passed normality test (alpha=0.05)?	P value summary
Anderson-Darling (A2*)	0.2004	0.8673	Yes	ns
D'Agostino-Pearson omnibus (K2)	2.783	0.2487	Yes	ns
Shapiro-Wilk (W)	0.9757	0.8059	Yes	ns
Kolmogorov-Smirnov (distance)	0.07979	0.1000	Yes	ns

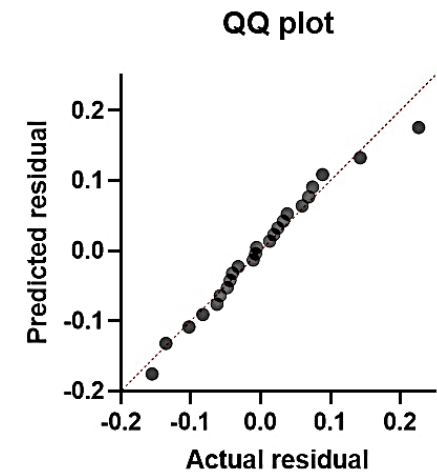


**Figure 8-3-14.** Normal distribution tests for data created from *miR-276b* microRNA levels of flies kept at differing temperatures. Left: QQ normality plot. Right: Anderson-Darling and D'Agostino & Pearson tests for normality.

ANOVA table	SS (Type III)	DF	MS	F (DFn, DFd)	P value
Interaction	0.01242	1	0.01242	F (1, 20) = 1.451	P=0.2424
Tissue	0.05591	1	0.05591	F (1, 20) = 6.536	P=0.0188
Temperature	0.005004	1	0.005004	F (1, 20) = 0.5850	P=0.4533
Residual	0.1711	20	0.008554		

Tukey's multiple comparisons test	Predicted (LS) mean diff.	95.00% CI of diff.	Below threshold?	Summary	Adjusted P Value
Head:11.5 vs. Head:25	0.01705	-0.1270 to 0.1611	No	ns	0.9871
Head:11.5 vs. Body:11.5	-0.05239	-0.1908 to 0.08598	No	ns	0.7171
Head:11.5 vs. Body:25	-0.1287	-0.2910 to 0.03353	No	ns	0.1518
Head:25 vs. Body:11.5	-0.06944	-0.2135 to 0.07458	No	ns	0.5438
Head:25 vs. Body:25	-0.1458	-0.3129 to 0.02132	No	ns	0.1011
Body:11.5 vs. Body:25	-0.07633	-0.2386 to 0.08592	No	ns	0.5634

**Figure 8-3-15.** One-way ANOVA followed by Tukey's *post hoc* multiple comparison test for data created from *miR-276b* microRNA levels of flies kept at differing temperatures.

Head				
w1118	uas-miR276b	miR-276aKO	miR-276bKO	miR-276aKO x miR276bKO
26.64	22.38	26.04	27.44	26.55
25.38	22.94	26.29	26.10	27.08
26.17	21.82	26.14	26.09	25.77
25.31	23.08	26.35	26.39	26.66
26.03	22.11	26.35	29.27	
27.68	23.05	25.83	25.33	
<hr/>				
26.20	22.56	26.17	26.77	26.52

#### Anova: Single Factor

##### SUMMARY

Groups	Count	Sum	Average	Variance
Column 1	6	157.22	26.20	0.78
Column 2	6	135.38	22.56	0.29
Column 3	6	156.99	26.17	0.04
Column 4	6	160.63	26.77	1.97
Column 5	4	106.06	26.52	0.30

##### ANOVA

Source of Variation	SS	df	MS	F	P-value	F crit
Between Groups	71.0057	4	17.75143	25.0804236	0.8	4.2E-08
Within Groups	16.2789	23	0.70778			
Total	87.2847	27				

**Figure 8-3-16.** Absolute *perA* levels in fly heads under different genetic manipulation of *miR-276a/b*. Table of results (right) followed by ANOVA one-way analysis (left)

Body				
w1118	uas-miR276b	miR-276aKO	miR-276bKO	miR-276aKO x miR276bKO
27.68	25.27	26.92	24.76	27.57
25.41	26.29	24.26	26.38	27.46
26.64	25.77	25.82	25.61	25.55
28.03	24.84	24.05	24.94	26.72
26.11	26.18	23.71	24.96	
22.17		26.69		
		24.63		
26.01	25.67	25.16	25.33	26.82

#### Anova: Single Factor

##### SUMMARY

Groups	Count	Sum	Average	Variance
Column 1	6	156.04	26.01	4.48
Column 2	5	128.34	25.67	0.38
Column 3	7	176.09	25.16	1.71
Column 4	5	126.65	25.33	0.45
Column 5	4	107.29	26.82	0.86

##### ANOVA

Source of Variation	SS	df	MS	F	P-value	F crit
Between Groups	8.34273	4	2.085683	1.18855549	0.34344	2.816708
Within Groups	38.6057	22	1.754805			
Total	46.9484	26				

**Figure 8-3-17.** Absolute *perA* levels in fly bodies under different genetic manipulation of *miR-276a/b*. Table of results (right) followed by ANOVA one-way analysis (left)

## 8.2 Appendix, Chapter 4

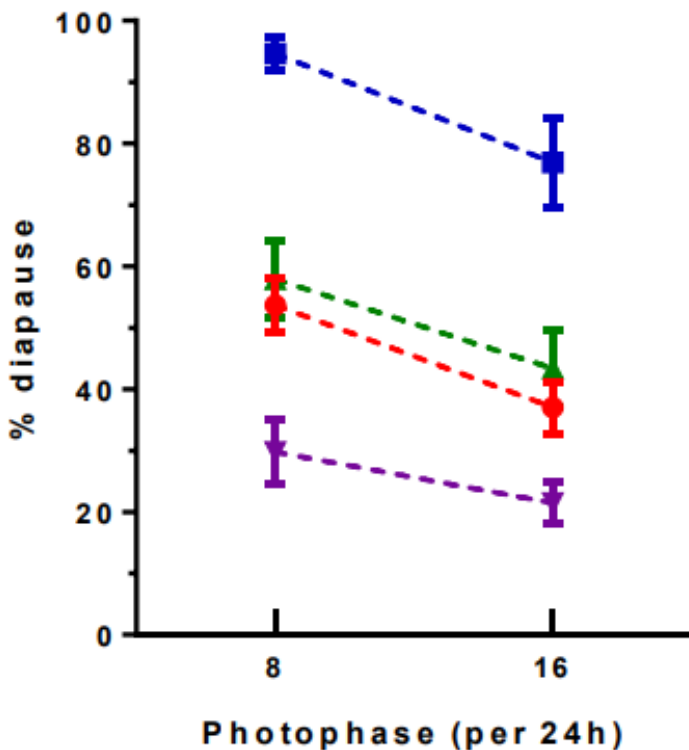


**Figure 8-4-1.** Photoperiodic response of *per* variants VT1.1 and VT1.2 natural lines. Comparing long and short photoperiods of VT1.1a (red), VT1.1b (blue), VT1.2a (green) and VT1.2b (purple). Mean ±SEM. (Taken from Collins, 2014).

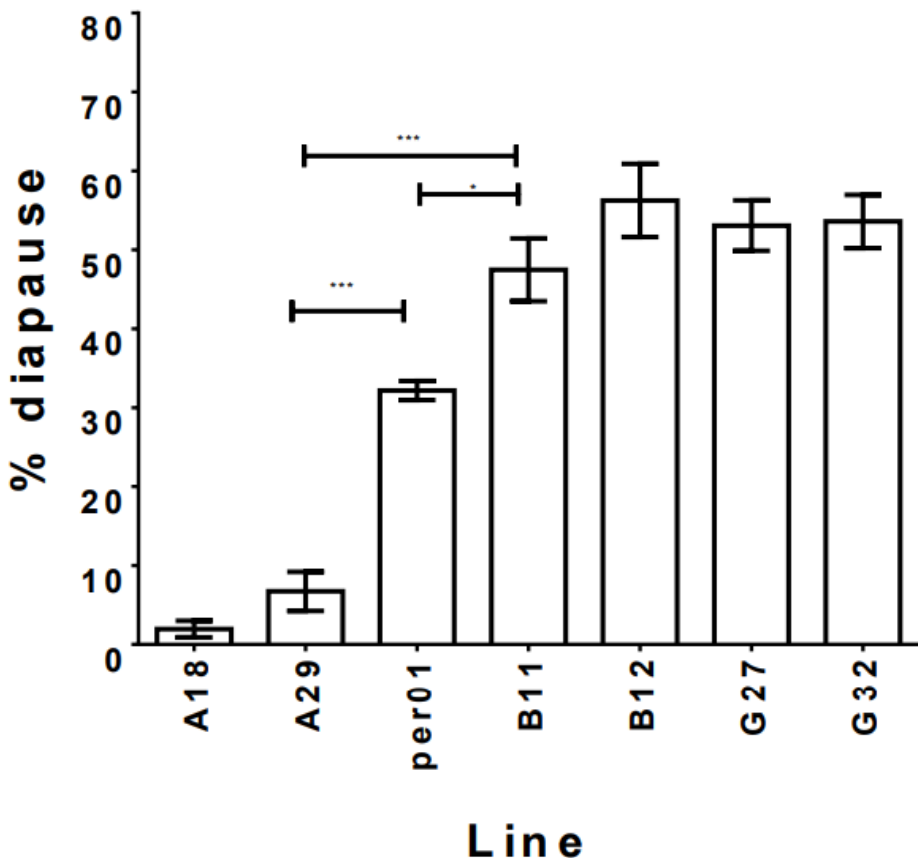


**Figure 8-4-2.** Diapause levels of splice-locked transgenic flies. A=unspliced, B=spliced, G=intrinsic splicing. Mean  $\pm$ SEM. (Taken from Collins, 2014).

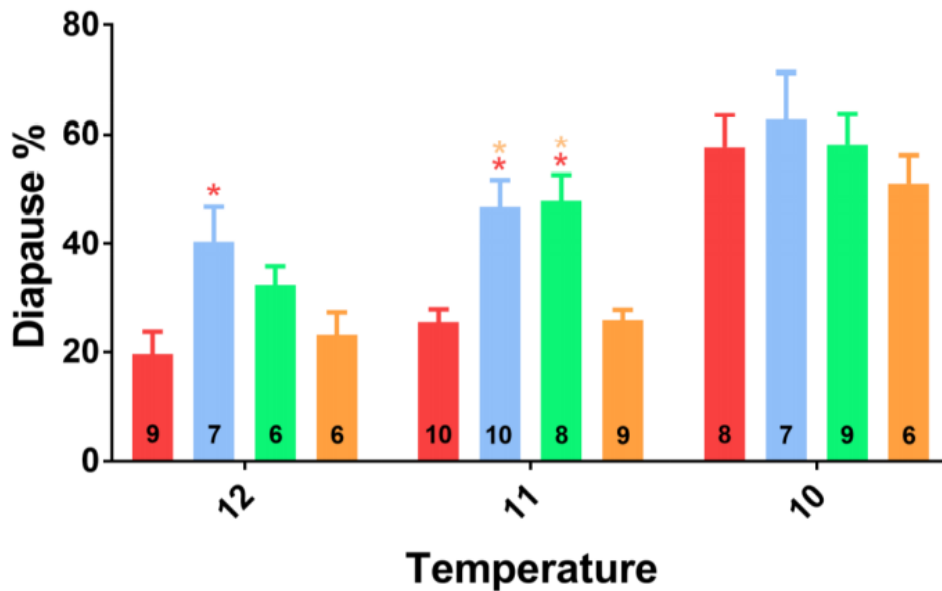


**Figure 8-4-3.** Diapause levels of *UAS* splice-locked transgenic flies crossed to *tim-gal4*. perA=unspliced (red), perB=spliced (blue), G=intrinsic splicing (green), empty attB vector control (orange). Mean  $\pm$ SEM. (Taken from Martin Anduaga, 2018).

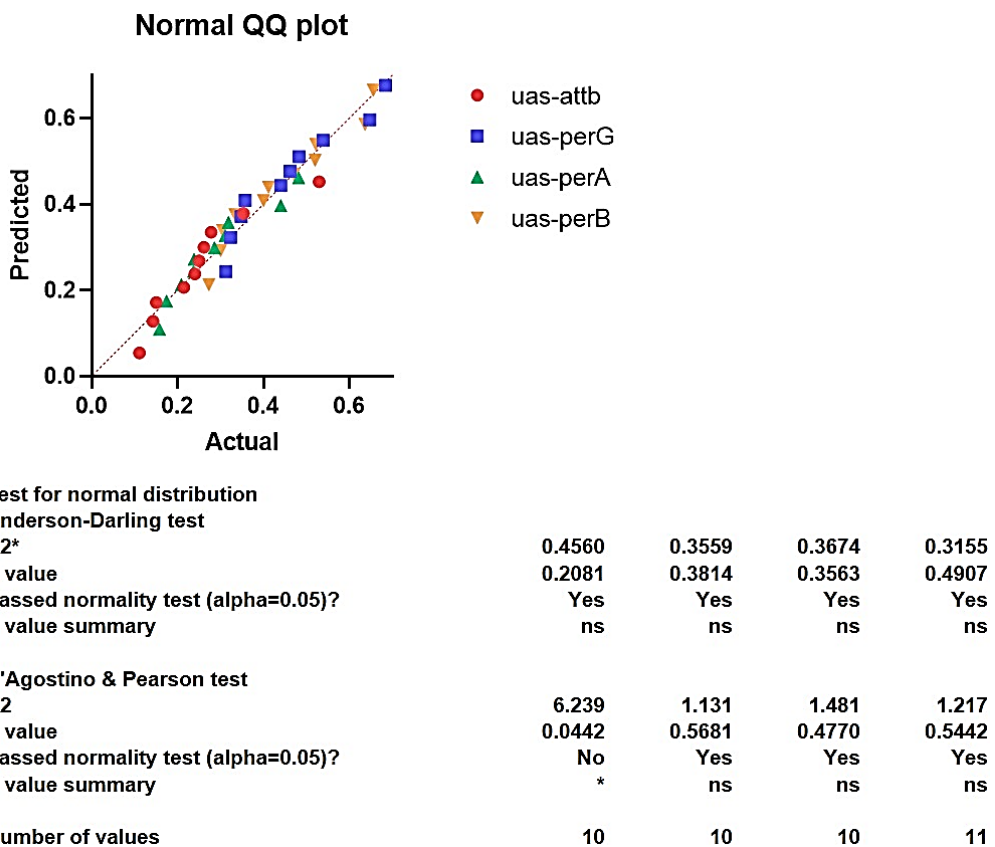
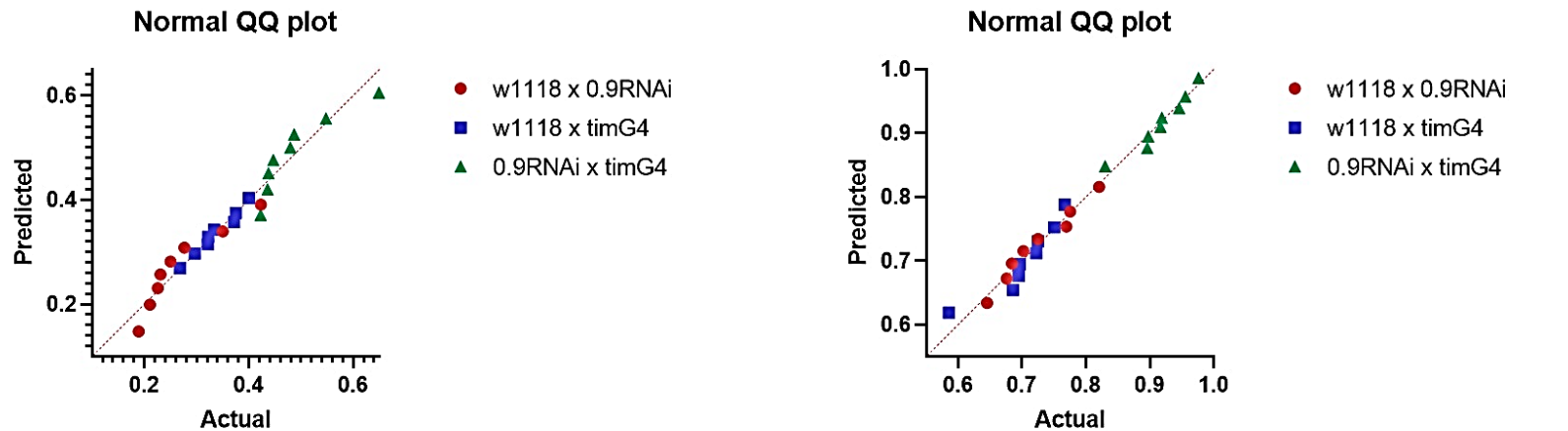


**Figure 8-4-4.** Normal distribution tests for diapause data created from *UAS-perA/B/G/attB* flies crossed to *tim-gal4*. Top: QQ normality plot. Bottom: Anderson-Darling and D'Agostino & Pearson tests for normality.

ANOVA table	SS	DF	MS	F (DFn, DFd)	P value
Treatment (between columns)	0.3986	3	0.1329	F (3, 37) = 7.648	P=0.0004
Residual (within columns)	0.6428	37	0.01737		
Total	1.041	40			
Tukey's multiple comparisons test	Mean Diff.	95.00% CI of diff.	Below threshold?	Summary	Adjusted P Value
uas-attb (control) vs. uas-perG	-0.2258	-0.3844 to -0.06729	Yes	**	0.0026
uas-attb (control) vs. uas-perA	-0.03929	-0.1978 to 0.1192	No	ns	0.9089
uas-attb (control) vs. uas-perB	-0.2039	-0.3588 to -0.04902	Yes	**	0.0058
uas-perG vs. uas-perA	0.1865	0.02800 to 0.3451	Yes	*	0.0157
uas-perG vs. uas-perB	0.02192	-0.1330 to 0.1768	No	ns	0.9809
uas-perA vs. uas-perB	-0.1646	-0.3195 to -0.009721	Yes	*	0.0336

**Figure 8-4-5.** One-way ANOVA followed by Tukey's *post hoc* multiple comparison test for diapause data created from *UAS-perA/B/G/attb* flies crossed to *tim-gal4*.



Test for normal distribution				Test for normal distribution			
Anderson-Darling test				Anderson-Darling test			
A2*	0.4981	0.2117	0.6425	A2*	0.2122	0.4749	0.2671
P value	0.1459	0.7799	0.0586	P value	0.7781	0.1698	0.5781
Passed normality test (alpha=0.05)?	Yes	Yes	Yes	Passed normality test (alpha=0.05)?	Yes	Yes	Yes
P value summary	ns	ns	ns	P value summary	ns	ns	ns
D'Agostino & Pearson test				D'Agostino & Pearson test			
K2	3.324	0.1992	6.606	K2	0.5493	6.701	1.994
P value	0.1898	0.9052	0.0368	P value	0.7598	0.0351	0.3691
Passed normality test (alpha=0.05)?	Yes	Yes	No	Passed normality test (alpha=0.05)?	Yes	No	Yes
P value summary	ns	ns	*	P value summary	ns	*	ns
Number of values	8	8	8	Number of values	8	8	8

**Figure 8-4-6.** Normal distribution tests for diapause data created from *tim-gal4* flies crossed either *UAS-0.9* or *w<sup>1118</sup>* scoring diapause from either egg stage <8 (left) or egg stage <10 (right). Top: QQ normality plot. Bottom: Anderson-Darling and D'Agostino & Pearson tests for normality.

<b>ANOVA table</b>	<b>SS</b>	<b>DF</b>	<b>MS</b>	<b>F (DFn, DFd)</b>	<b>P value</b>
Treatment (between columns)	0.2008	2	0.1004	$F(2, 21) = 21.51$	$P < 0.0001$
Residual (within columns)	0.09801	21	0.004667		
Total	0.2988	23			

<b>Tukey's multiple comparisons test</b>	<b>Mean Diff.</b>	<b>95.00% CI of diff.</b>	<b>Below threshold?</b>	<b>Summary</b>	<b>Adjusted P Value</b>
w1118 x 0.9RNAi vs. w1118 x timG4	-0.06648	-0.1526 to 0.01962	No	ns	0.1507
w1118 x 0.9RNAi vs. 0.9RNAi x timG4	-0.2185	-0.3046 to -0.1324	Yes	****	<0.0001
w1118 x timG4 vs. 0.9RNAi x timG4	-0.1521	-0.2382 to -0.06597	Yes	***	0.0006

<b>ANOVA table</b>	<b>SS</b>	<b>DF</b>	<b>MS</b>	<b>F (DFn, DFd)</b>	<b>P value</b>
Treatment (between columns)	0.2218	2	0.1109	$F(2, 21) = 38.68$	$P < 0.0001$
Residual (within columns)	0.06020	21	0.002867		
Total	0.2820	23			

<b>Tukey's multiple comparisons test</b>	<b>Mean Diff.</b>	<b>95.00% CI of diff.</b>	<b>Below threshold?</b>	<b>Summary</b>	<b>Adjusted P Value</b>
w1118 x 0.9RNAi vs. w1118 x timG4	0.02133	-0.04615 to 0.08880	No	ns	0.7092
w1118 x 0.9RNAi vs. 0.9RNAi x timG4	-0.1924	-0.2599 to -0.1249	Yes	****	<0.0001
w1118 x timG4 vs. 0.9RNAi x timG4	-0.2138	-0.2812 to -0.1463	Yes	****	<0.0001

**Figure 8-4-7.** One-way ANOVA followed by Tukey's *post hoc* multiple comparison test for diapause data created from *tim-gal4* flies crossed either *UAS-0.9* or *w<sup>1118</sup>* scoring diapause from either egg stage <8 (top) or egg stage <10 (bottom).

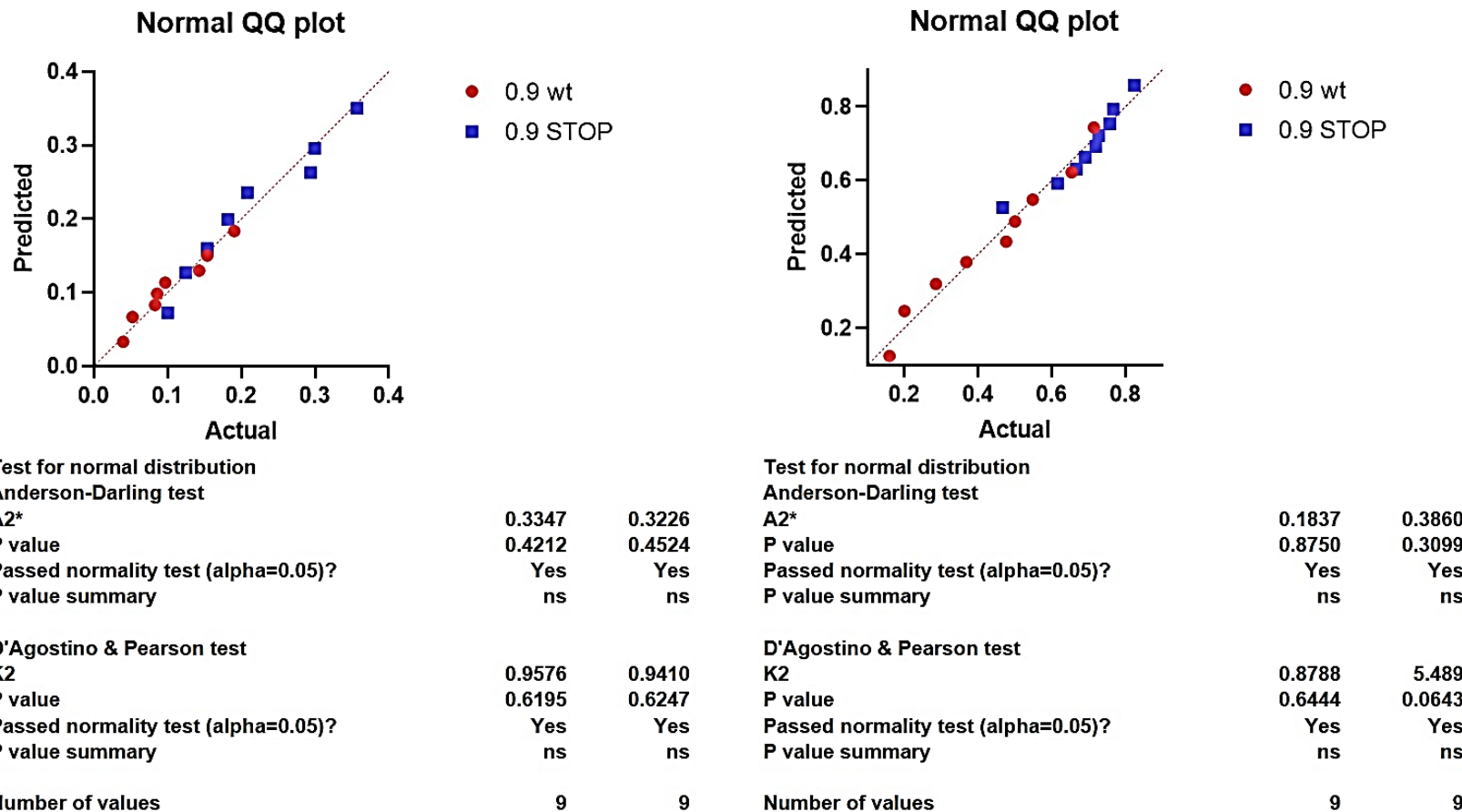


**Figure 8-4-8.** Normal distribution tests for diapause data created from transgenic flies overexpressing either the wild-type 0.9 transgene or a mutant 0.9 transgene, scoring diapause from either egg stage <8 (left) or egg stage <10 (right). Top: QQ normality plot. Bottom: Anderson-Darling and D'Agostino & Pearson tests for normality.

<b>Unpaired t test with Welch's correction</b>		<b>Unpaired t test with Welch's correction</b>	
<b>P value</b>	<b>0.0055</b>	<b>P value</b>	<b>0.0041</b>
<b>P value summary</b>	<b>**</b>	<b>P value summary</b>	<b>**</b>
<b>Significantly different (<math>P &lt; 0.05</math>)?</b>	<b>Yes</b>	<b>Significantly different (<math>P &lt; 0.05</math>)?</b>	<b>Yes</b>
<b>One- or two-tailed P value?</b>	<b>Two-tailed</b>	<b>One- or two-tailed P value?</b>	<b>Two-tailed</b>
<b>Welch-corrected t, df</b>	<b>t=3.312, df=13.26</b>	<b>Welch-corrected t, df</b>	<b>t=3.518, df=12.23</b>

**Figure 8-4-9.** Unpaired t test with Welch's correction test for diapause data created from transgenic flies overexpressing either the wild-type 0.9 transgene or a mutant 0.9 transgene, scoring diapause from either egg stage <8 (left) or egg stage <10 (right).

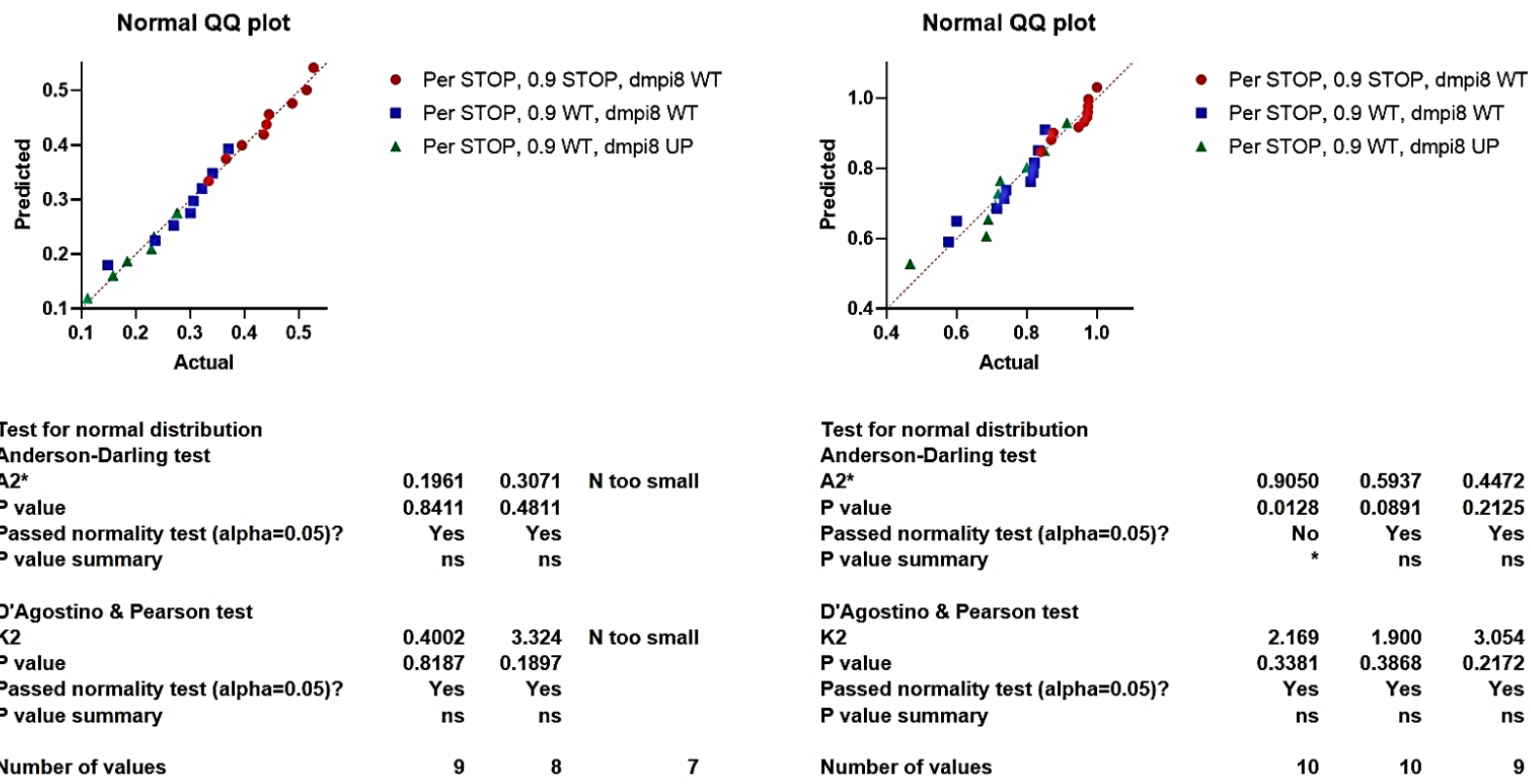


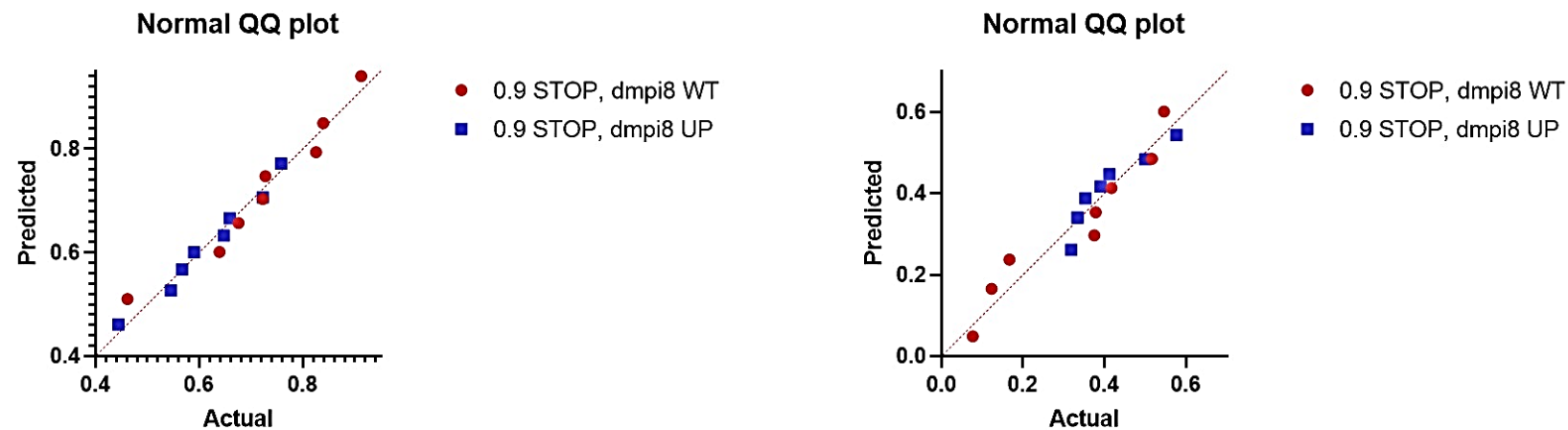
**Figure 8-4-10.** Normal distribution tests for diapause data created from transgenic flies overexpressing either the wild-type 0.9 transgene or a mutant 0.9 transgene, and either wild-type *dmp18* splicing or enhanced *dmp18* splicing, in a *per* mutant background, scoring diapause from either egg stage <8 (left) or egg stage <10 (right). Top: QQ normality plot. Bottom: Anderson-Darling and D'Agostino & Pearson tests for normality.

<b>ANOVA table</b>	<b>SS</b>	<b>DF</b>	<b>MS</b>	<b>F (DFn, DFd)</b>	<b>P value</b>
Treatment (between columns)	0.2193	2	0.1097	F (2, 21) = 25.43	P<0.0001
Residual (within columns)	0.09055	21	0.004312		
Total	0.3099	23			
<b>Tukey's multiple comparisons test</b>					
	<b>Mean Diff.</b>	<b>95.00% CI of diff.</b>	<b>Below threshold?</b>	<b>Summary</b>	<b>Adjusted P Value</b>
Per STOP, 0.9 STOP, dmp18 WT vs. Per STOP, 0.9 WT, dmp18 WT	0.1514	0.07100 to 0.2319	Yes	***	0.0003
Per STOP, 0.9 STOP, dmp18 WT vs. Per STOP, 0.9 WT, dmp18 UP	0.2282	0.1448 to 0.3117	Yes	****	<0.0001
Per STOP, 0.9 WT, dmp18 WT vs. Per STOP, 0.9 WT, dmp18 UP	0.07682	-0.008845 to 0.1625	No	ns	0.0841

<b>ANOVA table</b>	<b>SS</b>	<b>DF</b>	<b>MS</b>	<b>F (DFn, DFd)</b>	<b>P value</b>
Treatment (between columns)	0.6148	2	0.3074	F (2, 26) = 19.01	P<0.0001
Residual (within columns)	0.4204	26	0.01617		
Total	1.035	28			
<b>Tukey's multiple comparisons test</b>					
	<b>Mean Diff.</b>	<b>95.00% CI of diff.</b>	<b>Below threshold?</b>	<b>Summary</b>	<b>Adjusted P Value</b>
Per STOP, 0.9 STOP, dmp18 WT vs. Per STOP, 0.9 WT, dmp18 WT	0.2958	0.1545 to 0.4371	Yes	****	<0.0001
Per STOP, 0.9 STOP, dmp18 WT vs. Per STOP, 0.9 WT, dmp18 UP	0.3169	0.1717 to 0.4620	Yes	****	<0.0001
Per STOP, 0.9 WT, dmp18 WT vs. Per STOP, 0.9 WT, dmp18 UP	0.02103	-0.1241 to 0.1662	No	ns	0.9312

**Figure 8-4-11.** One-way ANOVA followed by Tukey's *post hoc* multiple comparison test for diapause data created from transgenic flies overexpressing either the wild-type 0.9 transgene or a mutant 0.9 transgene, and either wild-type *dmp18* splicing or enhanced *dmp18* splicing, in a *per* mutant background, scoring diapause from either egg stage <8 (top) or egg stage <10 (bottom).



Test for normal distribution		
Anderson-Darling test		
A2*	0.3844	0.5304
P value	0.3015	0.1177
Passed normality test (alpha=0.05)?	Yes	Yes
P value summary	ns	ns

D'Agostino & Pearson test		
K2	1.882	2.756
P value	0.3902	0.2521
Passed normality test (alpha=0.05)?	Yes	Yes
P value summary	ns	ns

Number of values

8	8
---	---

Test for normal distribution		
Anderson-Darling test		
A2*	0.2332	0.1547
P value	0.7006	0.9256
Passed normality test (alpha=0.05)?	Yes	Yes
P value summary	ns	ns

D'Agostino & Pearson test		
K2	1.354	0.1398
P value	0.5083	0.9325
Passed normality test (alpha=0.05)?	Yes	Yes
P value summary	ns	ns

Number of values

**Figure 8-4-12.** Normal distribution tests for diapause data created from transgenic flies overexpressing either wild-type *dmp18* splicing or enhanced *dmp18* splicing, in a 0.9 mutant background, scoring diapause from either egg stage <8 (left) or egg stage <10 (right). Top: QQ normality plot. Bottom: Anderson-Darling and D'Agostino & Pearson tests for normality.

**Unpaired t test with Welch's correction**

P value **0.3037**  
P value summary ns  
Significantly different ( $P < 0.05$ )? No  
One- or two-tailed P value? Two-tailed  
Welch-corrected t, df **t=1.082, df=10.41**

**Unpaired t test with Welch's correction**

P value **0.0990**  
P value summary ns  
Significantly different ( $P < 0.05$ )? No  
One- or two-tailed P value? Two-tailed  
Welch-corrected t, df **t=1.780, df=12.74**

**Figure 8-4-13.** Unpaired t test with Welch's correction for diapause data created from transgenic flies overexpressing either wild-type *dmp18* splicing or enhanced *dmp18* splicing, in a 0.9 mutant background, scoring diapause from either egg stage <8 (left) or egg stage <10 (right)

## 8.3 Appendix, Chapter 5

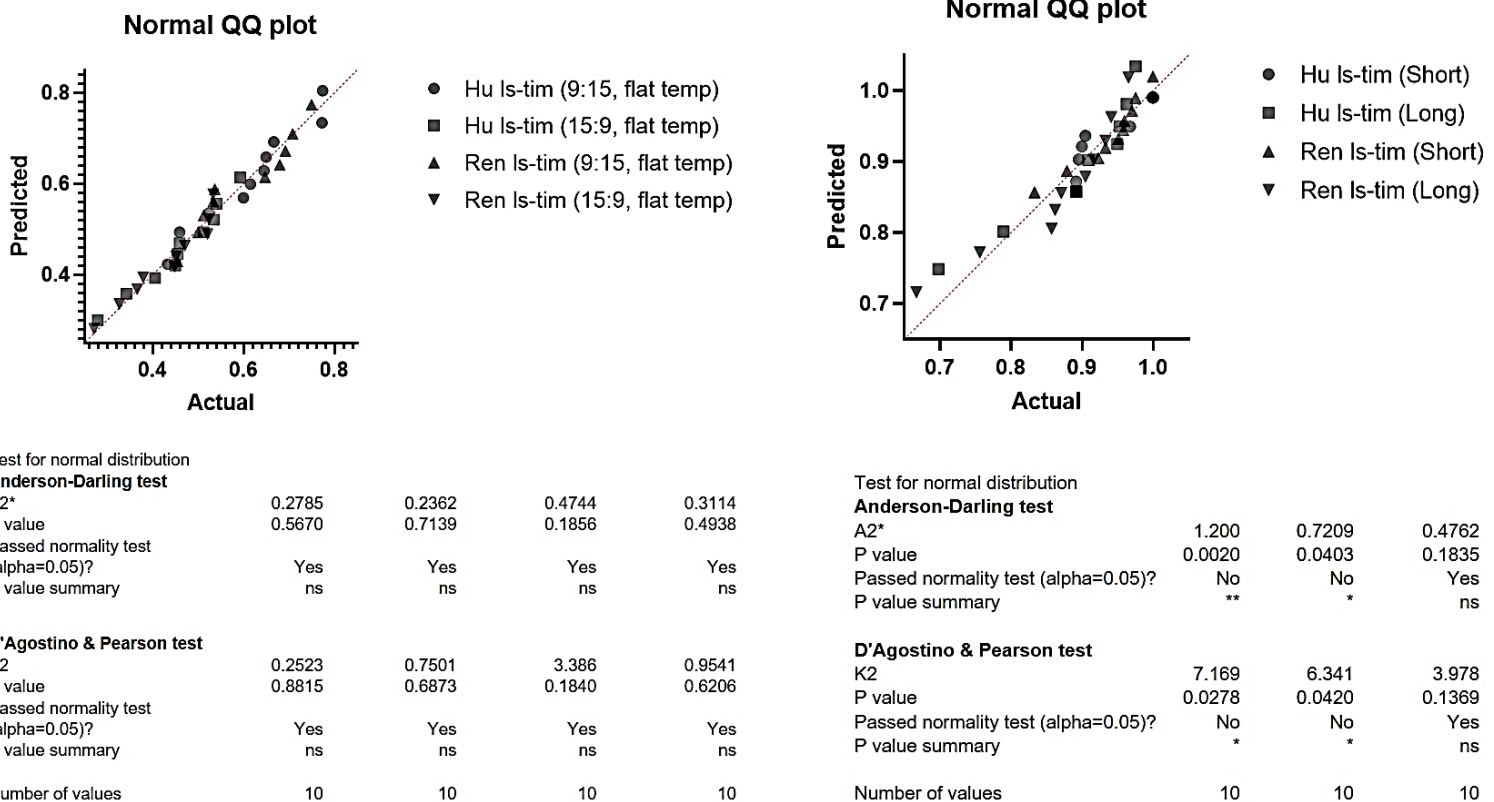


**Figure 8-5-1.** Normal distribution tests for diapause data created from naturally caught fly populations from either Houten or Rende, subjected to either a short photoperiod or long photoperiod, kept at a constant 11.5°C temperature. Diapause was scored from either egg stage <8 (left) or egg stage <10 (right). Top: QQ normality plot. Bottom: Anderson-Darling and D'Agostino & Pearson tests for normality.

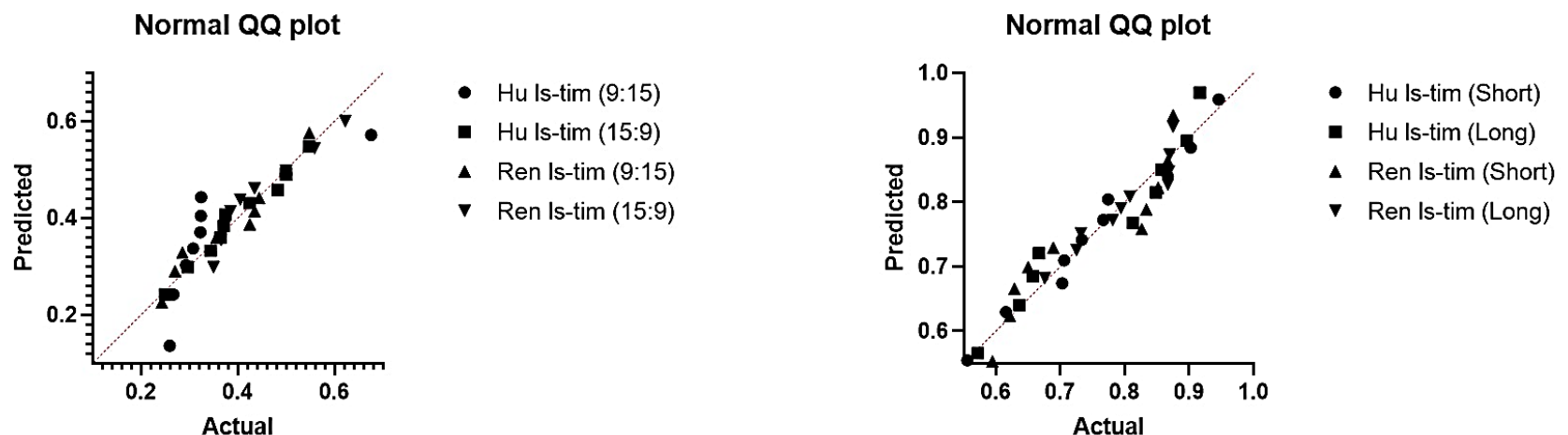
<b>ANOVA table</b>	<b>SS</b>	<b>DF</b>	<b>MS</b>	<b>F (DFn, DFd)</b>	<b>P value</b>
Interaction	0.0005924	1	0.0005924	F (1, 36) = 0.05694	P=0.8128
Photoperiod	0.2711	1	0.2711	F (1, 36) = 26.05	P<0.0001
population	0.004115	1	0.004115	F (1, 36) = 0.3955	P=0.5334
Residual	0.3746	36	0.01040		

<b>Tukey's multiple comparisons test</b>	<b>Mean Diff.</b>	<b>95.00% CI of diff.</b>	<b>Below threshold?</b>	<b>Summary</b>	<b>Adjusted P Value</b>
short (9:15) light:Houten vs. short (9:15) light:Rende	0.01259	-0.1103 to 0.1354	No	ns	0.9925
short (9:15) light:Houten vs. long (15:9) light:Houten	0.1569	0.03409 to 0.2798	Yes	**	0.0077
short (9:15) light:Houten vs. long (15:9) light:Rende	0.1849	0.06207 to 0.3078	Yes	**	0.0014
short (9:15) light:Rende vs. long (15:9) light:Houten	0.1444	0.02150 to 0.2672	Yes	*	0.0159
short (9:15) light:Rende vs. long (15:9) light:Rende	0.1723	0.04948 to 0.2952	Yes	**	0.0031
long (15:9) light:Houten vs. long (15:9) light:Rende	0.02798	-0.09488 to 0.1508	No	ns	0.9272

<b>ANOVA table</b>	<b>SS</b>	<b>DF</b>	<b>MS</b>	<b>F (DFn, DFd)</b>	<b>P value</b>
Interaction	0.003870	1	0.003870	F (1, 36) = 0.2107	P=0.6490
photoperiod	0.2210	1	0.2210	F (1, 36) = 12.03	P=0.0014
population	0.03602	1	0.03602	F (1, 36) = 1.961	P=0.1700
Residual	0.6613	36	0.01837		

<b>Tukey's multiple comparisons test</b>	<b>Mean Diff.</b>	<b>95.00% CI of diff.</b>	<b>Below threshold?</b>	<b>Summary</b>	<b>Adjusted P Value</b>
short (9:15) light:Houten vs. short (9:15) light:Rende	0.07969	-0.08356 to 0.2429	No	ns	0.5598
short (9:15) light:Houten vs. long (15:9) light:Houten	0.1683	0.005090 to 0.3316	Yes	*	0.0412
short (9:15) light:Houten vs. long (15:9) light:Rende	0.2087	0.04543 to 0.3719	Yes	**	0.0077
short (9:15) light:Rende vs. long (15:9) light:Houten	0.08865	-0.07460 to 0.2519	No	ns	0.4701
short (9:15) light:Rende vs. long (15:9) light:Rende	0.1290	-0.03425 to 0.2922	No	ns	0.1636
long (15:9) light:Houten vs. long (15:9) light:Rende	0.04034	-0.1229 to 0.2036	No	ns	0.9093

**Figure 8-5-2.** Two-way ANOVA followed by Tukey's *post hoc* multiple comparison test for diapause data created from naturally caught fly populations from either Houten or Rende, subjected to either a short photoperiod or long photoperiod, kept at a constant 11.5°C temperature. Diapause was scored from either egg stage <8 (top) or egg stage <10 (bottom).



#### Test for normal distribution

##### Anderson-Darling test

A2*	1.337	0.2168	0.3438	0.4181
P value	0.0009	0.7830	0.4093	0.2628
Passed normality test ( $\alpha=0.05$ )?	No	Yes	Yes	Yes
P value summary	***	ns	ns	ns

##### D'Agostino & Pearson test

K2	12.34	0.2455	1.643	1.400
P value	0.0021	0.8845	0.4398	0.4966
Passed normality test ( $\alpha=0.05$ )?	No	Yes	Yes	Yes
P value summary	**	ns	ns	ns

Number of values

10      10      10      10

#### Test for normal distribution

##### Anderson-Darling test

A2*	0.1902	0.5005	0.7484	0.4489
P value	0.8642	0.1574	0.0339	0.2175
Passed normality test ( $\alpha=0.05$ )?	Yes	Yes	No	Yes
P value summary	ns	ns	*	ns

##### D'Agostino & Pearson test

K2	0.09788	2.422	7.070	1.203
P value	0.9522	0.2979	0.0292	0.5481
Passed normality test ( $\alpha=0.05$ )?	Yes	Yes	No	Yes
P value summary	ns	ns	*	ns

Number of values

10      10      10      10

**Figure 8-5-3.** Normal distribution tests for diapause data created from naturally caught fly populations from either Houten or Rende, subjected to either a short photoperiod and thermoperiod or a long photoperiod and thermoperiod. Diapause was scored from either egg stage <8 (left) or egg stage <10 (right). Top: QQ normality plot. Bottom: Anderson-Darling and D'Agostino & Pearson tests for normality.

<b>ANOVA table</b>	<b>SS</b>	<b>DF</b>	<b>MS</b>	<b>F (DFn, DFd)</b>	<b>P value</b>
Interaction	0.0001480	1	0.0001480	$F(1, 36) = 0.01214$	$P=0.9129$
Environmental parameters	0.02280	1	0.02280	$F(1, 36) = 1.870$	$P=0.1800$
population	0.02736	1	0.02736	$F(1, 36) = 2.244$	$P=0.1428$
Residual	0.4389	36	0.01219		

<b>Tukey's multiple comparisons test</b>	<b>Mean Diff.</b>	<b>95.00% CI of diff.</b>	<b>Below threshold?</b>	<b>Summary</b>	<b>Adjusted P Value</b>
short (9:15):Houten vs. short (9:15):Rende	-0.04846	-0.1814 to 0.08452	No	ns	0.7608
short (9:15):Houten vs. long (15:9):Houten	-0.04390	-0.1769 to 0.08909	No	ns	0.8105
short (9:15):Houten vs. long (15:9):Rende	-0.1001	-0.2330 to 0.03293	No	ns	0.1974
short (9:15):Rende vs. long (15:9):Houten	0.004562	-0.1284 to 0.1375	No	ns	0.9997
short (9:15):Rende vs. long (15:9):Rende	-0.05159	-0.1846 to 0.08139	No	ns	0.7245
long (15:9):Houten vs. long (15:9):Rende	-0.05615	-0.1891 to 0.07683	No	ns	0.6693

<b>ANOVA table</b>	<b>SS</b>	<b>DF</b>	<b>MS</b>	<b>F (DFn, DFd)</b>	<b>P value</b>
Interaction	0.006573	1	0.006573	$F(1, 36) = 0.3658$	$P=0.5491$
environmental parameters	0.01351	1	0.01351	$F(1, 36) = 0.7519$	$P=0.3916$
population	0.0003499	1	0.0003499	$F(1, 36) = 0.01947$	$P=0.8898$
Residual	0.6470	36	0.01797		

<b>Tukey's multiple comparisons test</b>	<b>Mean Diff.</b>	<b>95.00% CI of diff.</b>	<b>Below threshold?</b>	<b>Summary</b>	<b>Adjusted P Value</b>
short (9:15):Houten vs. short (9:15):Rende	0.01972	-0.1417 to 0.1812	No	ns	0.9875
short (9:15):Houten vs. long (15:9):Houten	-0.01112	-0.1726 to 0.1503	No	ns	0.9977
short (9:15):Houten vs. long (15:9):Rende	-0.04268	-0.2041 to 0.1188	No	ns	0.8917
short (9:15):Rende vs. long (15:9):Houten	-0.03085	-0.1923 to 0.1306	No	ns	0.9551
short (9:15):Rende vs. long (15:9):Rende	-0.06240	-0.2239 to 0.09907	No	ns	0.7269
long (15:9):Houten vs. long (15:9):Rende	-0.03155	-0.1930 to 0.1299	No	ns	0.9522

**Figure 8-5-4.** Two-way ANOVA followed by Tukey's *post hoc* multiple comparison test for diapause data created from naturally caught fly populations from either Houten or Rende, subjected to either a short photoperiod and thermoperiod or a long photoperiod and thermoperiod. Diapause was scored from either egg stage <8 (top) or egg stage <10 (bottom)

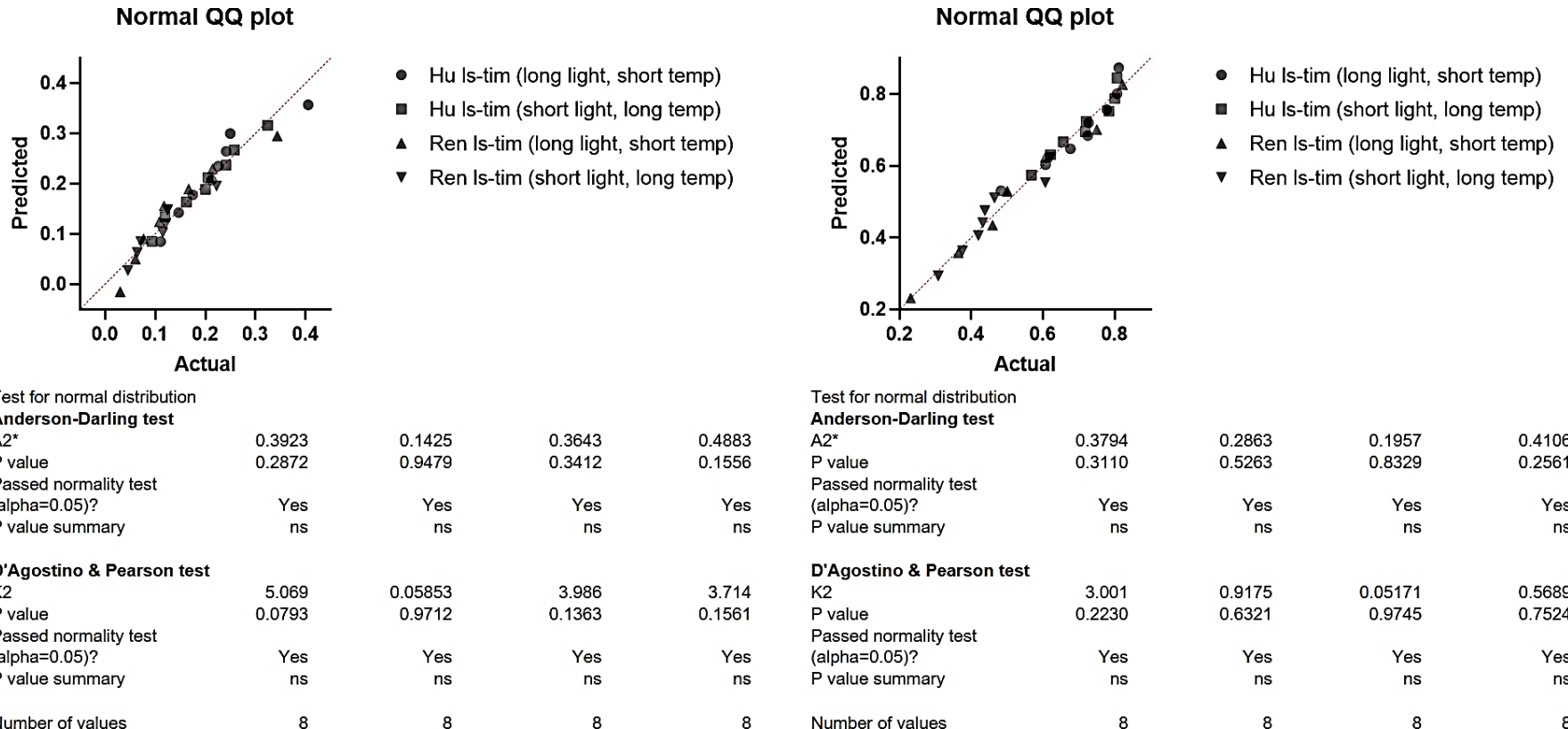


**Figure 8-5-5.** Normal distribution tests for diapause data created from naturally caught fly populations from either Houten or Rende, subjected to either a short photoperiod but a long thermoperiod or a long photoperiod but short thermoperiod. Diapause was scored from either egg stage <8 (left) or egg stage <10 (right). Top: QQ normality plot. Bottom: Anderson-Darling and D'Agostino & Pearson tests for normality.

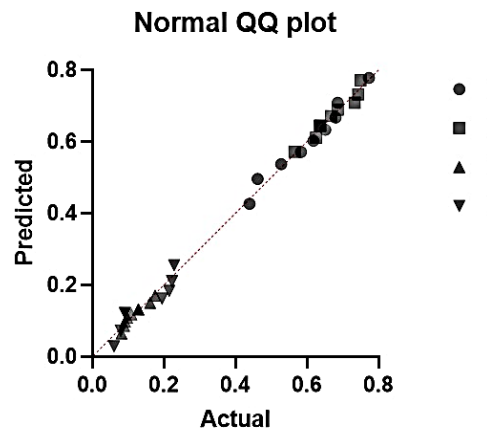
<b>ANOVA table</b>	<b>SS</b>	<b>DF</b>	<b>MS</b>	<b>F (DFn, DFd)</b>	<b>P value</b>
Interaction	0.0001320	1	0.0001320	$F(1, 28) = 0.01975$	$P=0.8892$
Environmental parameter	0.004781	1	0.004781	$F(1, 28) = 0.7152$	$P=0.4049$
Population	0.05816	1	0.05816	$F(1, 28) = 8.699$	$P=0.0064$
Residual	0.1872	28	0.006685		

<b>Tukey's multiple comparisons test</b>	<b>Mean Diff.</b>	<b>95.00% CI of diff.</b>	<b>Below threshold?</b>	<b>Summary</b>	<b>Adjusted P Value</b>
short temp, long light:Houten vs. short temp, long light:Rende	0.08120	-0.03042 to 0.1928	No	ns	0.2172
short temp, long light:Houten vs. long temp, short light:Houten	0.02038	-0.09124 to 0.1320	No	ns	0.9587
short temp, long light:Houten vs. long temp, short light:Rende	0.1097	-0.001913 to 0.2213	No	ns	0.0554
short temp, long light:Rende vs. long temp, short light:Houten	-0.06081	-0.1724 to 0.05081	No	ns	0.4581
short temp, long light:Rende vs. long temp, short light:Rende	0.02851	-0.08311 to 0.1401	No	ns	0.8972
long temp, short light:Houten vs. long temp, short light:Rende	0.08932	-0.02230 to 0.2009	No	ns	0.1522

<b>ANOVA table</b>	<b>SS</b>	<b>DF</b>	<b>MS</b>	<b>F (DFn, DFd)</b>	<b>P value</b>
Interaction	0.01226	1	0.01226	$F(1, 28) = 0.7070$	$P=0.4076$
Environmental parameters	0.008078	1	0.008078	$F(1, 28) = 0.4657$	$P=0.5006$
Population	0.3594	1	0.3594	$F(1, 28) = 20.72$	$P<0.0001$
Residual	0.4856	28	0.01734		

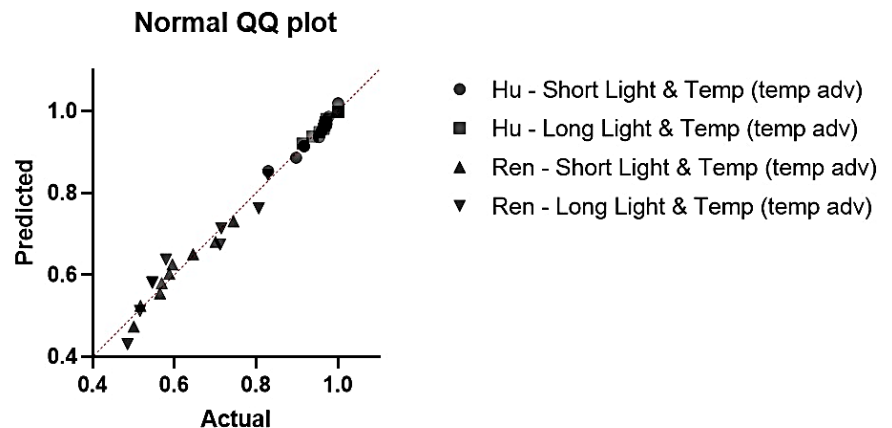
<b>Tukey's multiple comparisons test</b>	<b>Mean Diff.</b>	<b>95.00% CI of diff.</b>	<b>Below threshold?</b>	<b>Summary</b>	<b>Adjusted P Value</b>
short temp, long light:Houten vs. short temp, long light:Rende	0.1728	-0.006997 to 0.3526	No	ns	0.0630
short temp, long light:Houten vs. long temp, short light:Houten	-0.007376	-0.1872 to 0.1724	No	ns	0.9995
short temp, long light:Houten vs. long temp, short light:Rende	0.2437	0.06393 to 0.4235	Yes	**	0.0049
short temp, long light:Rende vs. long temp, short light:Houten	-0.1802	-0.3600 to -0.0003792	Yes	*	0.0494
short temp, long light:Rende vs. long temp, short light:Rende	0.07093	-0.1089 to 0.2507	No	ns	0.7060
long temp, short light:Houten vs. long temp, short light:Rende	0.2511	0.07131 to 0.4309	Yes	**	0.0036

**Figure 8-5-6.** Two-way ANOVA followed by Tukey's *post hoc* multiple comparison test for diapause data created from naturally caught fly populations from either Houten or Rende, subjected to either a short photoperiod but a long thermoperiod or a long photoperiod but short thermoperiod. Diapause was scored from either egg stage <8 (top) or egg stage <10 (bottom).



Test for normal distribution				
Anderson-Darling test				
A2*	0.1961	0.2932	0.3953	0.8646
P value	0.8410	0.5217	0.2929	0.0154
Passed normality test (alpha=0.05)?				
Yes	Yes	Yes	No	
P value summary	ns	ns	ns	*

D'Agostino & Pearson test				
K2	0.3085	0.3297	1.287	6.373
P value	0.8570	0.8480	0.5254	0.0413
Passed normality test (alpha=0.05)?				
Yes	Yes	Yes	No	
P value summary	ns	ns	ns	*
Number of values	9	9	9	9



Test for normal distribution				
Anderson-Darling test				
A2*	0.3304	0.3233	0.2798	0.4749
P value	0.4321	0.4505	0.5536	0.1782
Passed normality test (alpha=0.05)?				
Yes	Yes	Yes	Yes	Yes
P value summary	ns	ns	ns	ns
Number of values	9	9	9	9

**Figure 8-5-7.** Normal distribution tests for diapause data created from naturally caught fly populations from either Houten or Rende, subjected to either photoperiod and thermoperiod or a long photoperiod and thermoperiod. The thermoperiod was advanced by 12 hours in relation to the photoperiod. Diapause was scored from either egg stage <8 (left) or egg stage <10 (right). Top: QQ normality plot. Bottom: Anderson-Darling and D'Agostino & Pearson tests for normality.

<b>ANOVA table</b>	<b>SS</b>	<b>DF</b>	<b>MS</b>	<b>F (DFn, DFd)</b>	<b>P value</b>
Interaction	0.004133	1	0.004133	F (1, 32) = 0.5390	P=0.4682
Environmental parameters	0.02214	1	0.02214	F (1, 32) = 2.888	P=0.0990
population	2.870	1	2.870	F (1, 32) = 374.3	P<0.0001
Residual	0.2453	32	0.007667		

<b>Tukey's multiple comparisons test</b>	<b>Mean Diff.</b>	<b>95.00% CI of diff.</b>	<b>Below threshold?</b>	<b>Summary</b>	<b>Adjusted P Value</b>
short-day, adv temp:Houten vs. short-day, adv temp:Rende	0.5433	0.4314 to 0.6551	Yes	****	<0.0001
short-day, adv temp:Houten vs. long-day, adv temp:Houten	-0.07102	-0.1829 to 0.04081	No	ns	0.3299
short-day, adv temp:Houten vs. long-day, adv temp:Rende	0.5151	0.4033 to 0.6269	Yes	****	<0.0001
short-day, adv temp:Rende vs. long-day, adv temp:Houten	-0.6143	-0.7261 to -0.5025	Yes	****	<0.0001
short-day, adv temp:Rende vs. long-day, adv temp:Rende	-0.02817	-0.1400 to 0.08366	No	ns	0.9030
long-day, adv temp:Houten vs. long-day, adv temp:Rende	0.5861	0.4743 to 0.6980	Yes	****	<0.0001

<b>ANOVA table</b>	<b>SS</b>	<b>DF</b>	<b>MS</b>	<b>F (DFn, DFd)</b>	<b>P value</b>
Interaction	8.626e-005	1	8.626e-005	F (1, 32) = 0.01287	P=0.9104
Environmental Parameters	0.008886	1	0.008886	F (1, 32) = 1.326	P=0.2581
Population	0.9838	1	0.9838	F (1, 32) = 146.8	P<0.0001
Residual	0.2145	32	0.006703		

<b>Tukey's multiple comparisons test</b>	<b>Mean Diff.</b>	<b>95.00% CI of diff.</b>	<b>Below threshold?</b>	<b>Summary</b>	<b>Adjusted P Value</b>
short-day, adv temp:Houten vs. short-day, adv temp:Rende	0.3337	0.2292 to 0.4383	Yes	****	<0.0001
short-day, adv temp:Houten vs. long-day, adv temp:Houten	-0.02833	-0.1329 to 0.07624	No	ns	0.8827
short-day, adv temp:Houten vs. long-day, adv temp:Rende	0.2992	0.1946 to 0.4038	Yes	****	<0.0001
short-day, adv temp:Rende vs. long-day, adv temp:Houten	-0.3621	-0.4666 to -0.2575	Yes	****	<0.0001
short-day, adv temp:Rende vs. long-day, adv temp:Rende	-0.03452	-0.1391 to 0.07005	No	ns	0.8078
long-day, adv temp:Houten vs. long-day, adv temp:Rende	0.3275	0.2230 to 0.4321	Yes	****	<0.0001

**Figure 8-5-8.** Two-way ANOVA followed by Tukey's *post hoc* multiple comparison test for diapause data created from naturally caught fly populations from either Houten or Rende, subjected to either photoperiod and thermoperiod or a long photoperiod and thermoperiod. The thermoperiod was advanced by 12 hours in relation to the photoperiod. Diapause was scored from either egg stage <8 (top) or egg stage <10 (bottom).

<b>ANOVA table</b>	<b>SS (Type III)</b>	<b>DF</b>	<b>MS</b>	<b>F (DFn, DFd)</b>	<b>P value</b>
Thermoperiod	1.497	3	0.4991	F (3, 132) = 57.14	P<0.0001
Population	0.7250	1	0.7250	F (1, 132) = 83.01	P<0.0001
Photoperiod	0.005386	1	0.005386	F (1, 132) = 0.6166	P=0.4337
Thermoperiod x Population	1.624	3	0.5414	F (3, 132) = 61.99	P<0.0001
Thermoperiod x Photoperiod	1.257	3	0.4190	F (3, 132) = 47.97	P<0.0001
Population x Photoperiod	0.001176	1	0.001176	F (1, 132) = 0.1346	P=0.7143
Thermoperiod x Population x Photoperiod	0.08617	3	0.02872	F (3, 132) = 3.289	P=0.0228
Residual	1.153	132	0.008734		

<b>Tukey's multiple comparisons test</b>	<b>Predicted (LS) mean diff.</b>	<b>95.00% CI of diff.</b>	<b>Below threshold?</b>	<b>Summary</b>	<b>Adjusted P Value</b>
Flat Temperature:Hu photoperiod 9:15 vs. Flat Temperature:Hu photoperiod 15:9	0.1569	0.01675 to 0.2971	Yes	*	0.0177
Flat Temperature:Hu photoperiod 9:15 vs. Thermoperiod 9:15:Hu photoperiod 9:15	0.2601	0.1199 to 0.4003	Yes	****	<0.0001
Flat Temperature:Hu photoperiod 9:15 vs. Thermoperiod 9:15:Hu photoperiod 15:9	0.3930	0.2443 to 0.5417	Yes	****	<0.0001
Flat Temperature:Hu photoperiod 9:15 vs. Thermoperiod 15:9:Hu photoperiod 9:15	0.4134	0.2647 to 0.5621	Yes	****	<0.0001
Flat Temperature:Hu photoperiod 9:15 vs. Thermoperiod 15:9:Hu photoperiod 15:9	0.2186	0.07836 to 0.3587	Yes	***	0.0002
Flat Temperature:Hu photoperiod 9:15 vs. Advanced (12h):Hu photoperiod 9:15	0.01192	-0.1321 to 0.1560	No	ns	>0.9999
Flat Temperature:Hu photoperiod 9:15 vs. Advanced (12h):Hu photoperiod 15:9	-0.05726	-0.2013 to 0.08677	No	ns	0.9153
Flat Temperature:Hu photoperiod 15:9 vs. Thermoperiod 9:15:Hu photoperiod 9:15	0.1032	-0.03702 to 0.2434	No	ns	0.3073
Flat Temperature:Hu photoperiod 15:9 vs. Thermoperiod 9:15:Hu photoperiod 15:9	0.2361	0.08740 to 0.3848	Yes	***	0.0001
Flat Temperature:Hu photoperiod 15:9 vs. Thermoperiod 15:9:Hu photoperiod 9:15	0.2565	0.1078 to 0.4052	Yes	****	<0.0001
Flat Temperature:Hu photoperiod 15:9 vs. Thermoperiod 15:9:Hu photoperiod 15:9	0.06161	-0.07858 to 0.2018	No	ns	0.8650
Flat Temperature:Hu photoperiod 15:9 vs. Advanced (12h):Hu photoperiod 9:15	-0.1450	-0.2891 to -0.0009925	Yes	*	0.0473
Flat Temperature:Hu photoperiod 15:9 vs. Advanced (12h):Hu photoperiod 15:9	-0.2142	-0.3582 to -0.07017	Yes	***	0.0004
Thermoperiod 9:15:Hu photoperiod 9:15 vs. Thermoperiod 9:15:Hu photoperiod 15:9	0.1329	-0.01577 to 0.2816	No	ns	0.1131
Thermoperiod 9:15:Hu photoperiod 9:15 vs. Thermoperiod 15:9:Hu photoperiod 9:15	0.1533	0.004614 to 0.3020	Yes	*	0.0386
Thermoperiod 9:15:Hu photoperiod 9:15 vs. Thermoperiod 15:9:Hu photoperiod 15:9	-0.04157	-0.1818 to 0.09862	No	ns	0.9822
Thermoperiod 9:15:Hu photoperiod 9:15 vs. Advanced (12h):Hu photoperiod 9:15	-0.2482	-0.3922 to -0.1042	Yes	****	<0.0001
Thermoperiod 9:15:Hu photoperiod 9:15 vs. Advanced (12h):Hu photoperiod 15:9	-0.3174	-0.4614 to -0.1733	Yes	****	<0.0001
Thermoperiod 9:15:Hu photoperiod 15:9 vs. Thermoperiod 15:9:Hu photoperiod 9:15	0.02038	-0.1364 to 0.1771	No	ns	>0.9999
Thermoperiod 9:15:Hu photoperiod 15:9 vs. Thermoperiod 15:9:Hu photoperiod 15:9	-0.1745	-0.3232 to -0.02579	Yes	*	0.0107
Thermoperiod 9:15:Hu photoperiod 15:9 vs. Advanced (12h):Hu photoperiod 9:15	-0.3811	-0.5334 to -0.2288	Yes	****	<0.0001
Thermoperiod 9:15:Hu photoperiod 15:9 vs. Advanced (12h):Hu photoperiod 15:9	-0.4503	-0.6026 to -0.2980	Yes	****	<0.0001
Thermoperiod 15:9:Hu photoperiod 9:15 vs. Thermoperiod 15:9:Hu photoperiod 15:9	-0.1949	-0.3436 to -0.04618	Yes	**	0.0028
Thermoperiod 15:9:Hu photoperiod 9:15 vs. Advanced (12h):Hu photoperiod 9:15	-0.4015	-0.5538 to -0.2492	Yes	****	<0.0001
Thermoperiod 15:9:Hu photoperiod 9:15 vs. Advanced (12h):Hu photoperiod 15:9	-0.4707	-0.6230 to -0.3184	Yes	****	<0.0001
Thermoperiod 15:9:Hu photoperiod 15:9 vs. Advanced (12h):Hu photoperiod 9:15	-0.2066	-0.3507 to -0.06260	Yes	***	0.0007
Thermoperiod 15:9:Hu photoperiod 15:9 vs. Advanced (12h):Hu photoperiod 15:9	-0.2758	-0.4198 to -0.1318	Yes	****	<0.0001
Advanced (12h):Hu photoperiod 9:15 vs. Advanced (12h):Hu photoperiod 15:9	-0.06918	-0.2169 to 0.07860	No	ns	0.8226

Figure continues onto next page

Flat Temperature:Ren photoperiod 9:15 vs. Flat Temperature:Ren photoperiod 15:9	0.1723	0.05160 to 0.2931	Yes	***	0.0008
Flat Temperature:Ren photoperiod 9:15 vs. Thermoperiod 9:15:Ren photoperiod 9:15	0.2008	0.08003 to 0.3215	Yes	****	<0.0001
Flat Temperature:Ren photoperiod 9:15 vs. Thermoperiod 9:15:Ren photoperiod 15:9	0.4616	0.3336 to 0.5897	Yes	****	<0.0001
Flat Temperature:Ren photoperiod 9:15 vs. Thermoperiod 15:9:Ren photoperiod 9:15	0.4902	0.3621 to 0.6182	Yes	****	<0.0001
Flat Temperature:Ren photoperiod 9:15 vs. Thermoperiod 15:9:Ren photoperiod 15:9	0.1518	0.03103 to 0.2725	Yes	**	0.0047
Flat Temperature:Ren photoperiod 9:15 vs. Advanced (12h):Ren photoperiod 9:15	0.4838	0.3598 to 0.6079	Yes	****	<0.0001
Flat Temperature:Ren photoperiod 9:15 vs. Advanced (12h):Ren photoperiod 15:9	0.4601	0.3361 to 0.5842	Yes	****	<0.0001
Flat Temperature:Ren photoperiod 15:9 vs. Thermoperiod 9:15:Ren photoperiod 9:15	0.02844	-0.09230 to 0.1492	No	ns	0.9955
Flat Temperature:Ren photoperiod 15:9 vs. Thermoperiod 9:15:Ren photoperiod 15:9	0.2893	0.1612 to 0.4174	Yes	****	<0.0001
Flat Temperature:Ren photoperiod 15:9 vs. Thermoperiod 15:9:Ren photoperiod 9:15	0.3178	0.1898 to 0.4459	Yes	****	<0.0001
Flat Temperature:Ren photoperiod 15:9 vs. Thermoperiod 15:9:Ren photoperiod 15:9	-0.02057	-0.1413 to 0.1002	No	ns	0.9994
Flat Temperature:Ren photoperiod 15:9 vs. Advanced (12h):Ren photoperiod 9:15	0.3115	0.1875 to 0.4355	Yes	****	<0.0001
Flat Temperature:Ren photoperiod 15:9 vs. Advanced (12h):Ren photoperiod 15:9	0.2878	0.1637 to 0.4118	Yes	****	<0.0001
Thermoperiod 9:15:Ren photoperiod 9:15 vs. Thermoperiod 9:15:Ren photoperiod 15:9	0.2609	0.1328 to 0.3889	Yes	****	<0.0001
Thermoperiod 9:15:Ren photoperiod 9:15 vs. Thermoperiod 15:9:Ren photoperiod 9:15	0.2894	0.1613 to 0.4174	Yes	****	<0.0001
Thermoperiod 9:15:Ren photoperiod 9:15 vs. Thermoperiod 15:9:Ren photoperiod 15:9	-0.04901	-0.1697 to 0.07173	No	ns	0.9064
Thermoperiod 9:15:Ren photoperiod 9:15 vs. Advanced (12h):Ren photoperiod 9:15	0.2831	0.1590 to 0.4071	Yes	****	<0.0001
Thermoperiod 9:15:Ren photoperiod 9:15 vs. Advanced (12h):Ren photoperiod 15:9	0.2594	0.1353 to 0.3834	Yes	****	<0.0001
Thermoperiod 9:15:Ren photoperiod 15:9 vs. Thermoperiod 15:9:Ren photoperiod 9:15	0.02851	-0.1065 to 0.1635	No	ns	0.9977
Thermoperiod 9:15:Ren photoperiod 15:9 vs. Thermoperiod 15:9:Ren photoperiod 15:9	-0.3099	-0.4379 to -0.1818	Yes	****	<0.0001
Thermoperiod 9:15:Ren photoperiod 15:9 vs. Advanced (12h):Ren photoperiod 9:15	0.02219	-0.1090 to 0.1534	No	ns	0.9995
Thermoperiod 9:15:Ren photoperiod 15:9 vs. Advanced (12h):Ren photoperiod 15:9	-0.001525	-0.1327 to 0.1297	No	ns	>0.9999
Thermoperiod 15:9:Ren photoperiod 9:15 vs. Thermoperiod 15:9:Ren photoperiod 15:9	-0.3384	-0.4665 to -0.2103	Yes	****	<0.0001
Thermoperiod 15:9:Ren photoperiod 9:15 vs. Advanced (12h):Ren photoperiod 9:15	-0.006322	-0.1375 to 0.1249	No	ns	>0.9999
Thermoperiod 15:9:Ren photoperiod 9:15 vs. Advanced (12h):Ren photoperiod 15:9	-0.03003	-0.1612 to 0.1012	No	ns	0.9962
Thermoperiod 15:9:Ren photoperiod 15:9 vs. Advanced (12h):Ren photoperiod 9:15	0.3321	0.2080 to 0.4561	Yes	****	<0.0001
Thermoperiod 15:9:Ren photoperiod 15:9 vs. Advanced (12h):Ren photoperiod 15:9	0.3084	0.1843 to 0.4324	Yes	****	<0.0001
Advanced (12h):Ren photoperiod 9:15 vs. Advanced (12h):Ren photoperiod 15:9	-0.02371	-0.1510 to 0.1036	No	ns	0.9990

**Figure 8-5-9.** Three-way ANOVA followed by Tukey's *post hoc* multiple comparison test for diapause data scored from egg stage <8, created from naturally caught fly populations from either Houten or Rende subjected to various thermoperiods and photoperiods

**ANOVA table**

	<b>SS (Type III)</b>	<b>DF</b>	<b>MS</b>	<b>F (DFn, DFd)</b>	<b>P value</b>
Thermoperiod	1.465	3	0.4883	F (3, 132) = 46.13	P<0.0001
Population	0.7824	1	0.7824	F (1, 132) = 73.90	P<0.0001
Photoperiod	5.166e-006	1	5.166e-006	F (1, 132) = 0.0004880	P=0.9824
Thermoperiod x Population	0.4886	3	0.1629	F (3, 132) = 15.38	P<0.0001
Thermoperiod x Photoperiod	0.4729	3	0.1576	F (3, 132) = 14.89	P<0.0001
Population x Photoperiod	0.002272	1	0.002272	F (1, 132) = 0.2146	P=0.6440
Thermoperiod x Population x Photoperiod	0.1649	3	0.05498	F (3, 132) = 5.193	P=0.0020
Residual	1.397	132	0.01059		

**Tukey's multiple comparisons test**

	<b>Predicted (LS) mean diff.</b>	<b>95.00% CI of diff.</b>	<b>Below threshold?</b>	<b>Summary</b>	<b>Adjusted P Value</b>
Flat Temperature:Hu photoperiod 9:15 vs. Flat Temperature:Hu photoperiod 15:9	0.06459	-0.06107 to 0.1903	No	ns	0.7432
Flat Temperature:Hu photoperiod 9:15 vs. Thermoperiod 9:15:Hu photoperiod 9:15	0.1991	0.07346 to 0.3248	Yes	***	0.0001
Flat Temperature:Hu photoperiod 9:15 vs. Thermoperiod 9:15:Hu photoperiod 15:9	0.2543	0.1210 to 0.3876	Yes	****	<0.0001
Flat Temperature:Hu photoperiod 9:15 vs. Thermoperiod 15:9:Hu photoperiod 9:15	0.2469	0.1136 to 0.3802	Yes	****	<0.0001
Flat Temperature:Hu photoperiod 9:15 vs. Thermoperiod 15:9:Hu photoperiod 15:9	0.1884	0.06279 to 0.3141	Yes	***	0.0004
Flat Temperature:Hu photoperiod 9:15 vs. Advanced (12h):Hu photoperiod 9:15	0.02019	-0.1089 to 0.1493	No	ns	0.9997
Flat Temperature:Hu photoperiod 9:15 vs. Advanced (12h):Hu photoperiod 15:9	-0.008138	-0.1372 to 0.1210	No	ns	>0.9999
Flat Temperature:Hu photoperiod 15:9 vs. Thermoperiod 9:15:Hu photoperiod 9:15	0.1345	0.008861 to 0.2602	Yes	*	0.0275
Flat Temperature:Hu photoperiod 15:9 vs. Thermoperiod 9:15:Hu photoperiod 15:9	0.1897	0.05640 to 0.3230	Yes	***	0.0008
Flat Temperature:Hu photoperiod 15:9 vs. Thermoperiod 15:9:Hu photoperiod 9:15	0.1823	0.04903 to 0.3156	Yes	**	0.0015
Flat Temperature:Hu photoperiod 15:9 vs. Thermoperiod 15:9:Hu photoperiod 15:9	0.1239	-0.001807 to 0.2495	No	ns	0.0562
Flat Temperature:Hu photoperiod 15:9 vs. Advanced (12h):Hu photoperiod 9:15	-0.04441	-0.1735 to 0.08470	No	ns	0.9595
Flat Temperature:Hu photoperiod 15:9 vs. Advanced (12h):Hu photoperiod 15:9	-0.07273	-0.2018 to 0.05637	No	ns	0.6463
Thermoperiod 9:15:Hu photoperiod 9:15 vs. Thermoperiod 9:15:Hu photoperiod 15:9	0.05517	-0.07812 to 0.1884	No	ns	0.8973
Thermoperiod 9:15:Hu photoperiod 9:15 vs. Thermoperiod 15:9:Hu photoperiod 9:15	0.04779	-0.08549 to 0.1811	No	ns	0.9496
Thermoperiod 9:15:Hu photoperiod 9:15 vs. Thermoperiod 15:9:Hu photoperiod 15:9	-0.01067	-0.1363 to 0.1150	No	ns	>0.9999
Thermoperiod 9:15:Hu photoperiod 9:15 vs. Advanced (12h):Hu photoperiod 9:15	-0.1789	-0.3080 to -0.04982	Yes	**	0.0012
Thermoperiod 9:15:Hu photoperiod 9:15 vs. Advanced (12h):Hu photoperiod 15:9	-0.2073	-0.3364 to -0.07815	Yes	***	0.0001
Thermoperiod 9:15:Hu photoperiod 15:9 vs. Thermoperiod 15:9:Hu photoperiod 9:15	-0.007376	-0.1479 to 0.1331	No	ns	>0.9999
Thermoperiod 9:15:Hu photoperiod 15:9 vs. Thermoperiod 15:9:Hu photoperiod 15:9	-0.06583	-0.1991 to 0.06745	No	ns	0.7796
Thermoperiod 9:15:Hu photoperiod 15:9 vs. Advanced (12h):Hu photoperiod 9:15	-0.2341	-0.3706 to -0.09756	Yes	****	<0.0001
Thermoperiod 9:15:Hu photoperiod 15:9 vs. Advanced (12h):Hu photoperiod 15:9	-0.2624	-0.3990 to -0.1259	Yes	****	<0.0001
Thermoperiod 15:9:Hu photoperiod 9:15 vs. Thermoperiod 15:9:Hu photoperiod 15:9	-0.05846	-0.1917 to 0.07482	No	ns	0.8661
Thermoperiod 15:9:Hu photoperiod 9:15 vs. Advanced (12h):Hu photoperiod 9:15	-0.2267	-0.3632 to -0.09018	Yes	****	<0.0001
Thermoperiod 15:9:Hu photoperiod 9:15 vs. Advanced (12h):Hu photoperiod 15:9	-0.2550	-0.3916 to -0.1185	Yes	****	<0.0001
Thermoperiod 15:9:Hu photoperiod 15:9 vs. Advanced (12h):Hu photoperiod 9:15	-0.1683	-0.2974 to -0.03916	Yes	**	0.0030
Thermoperiod 15:9:Hu photoperiod 15:9 vs. Advanced (12h):Hu photoperiod 15:9	-0.1966	-0.3257 to -0.06748	Yes	***	0.0003
Advanced (12h):Hu photoperiod 9:15 vs. Advanced (12h):Hu photoperiod 15:9	-0.02833	-0.1608 to 0.1041	No	ns	0.9975

Figure continues onto next page

Flat Temperature:Ren photoperiod 9:15 vs. Flat Temperature:Ren photoperiod 15:9	0.07099	-0.08933 to 0.2313	No	ns	0.8604
Flat Temperature:Ren photoperiod 9:15 vs. Thermoperiod 9:15:Ren photoperiod 9:15	0.1948	0.03445 to 0.3551	Yes	**	0.0072
Flat Temperature:Ren photoperiod 9:15 vs. Thermoperiod 9:15:Ren photoperiod 15:9	0.4095	0.2395 to 0.5796	Yes	****	<0.0001
Flat Temperature:Ren photoperiod 9:15 vs. Thermoperiod 15:9:Ren photoperiod 9:15	0.4804	0.3104 to 0.6505	Yes	****	<0.0001
Flat Temperature:Ren photoperiod 9:15 vs. Thermoperiod 15:9:Ren photoperiod 15:9	0.1993	0.03893 to 0.3596	Yes	**	0.0055
Flat Temperature:Ren photoperiod 9:15 vs. Advanced (12h):Ren photoperiod 9:15	0.3363	0.1716 to 0.5011	Yes	****	<0.0001
Flat Temperature:Ren photoperiod 9:15 vs. Advanced (12h):Ren photoperiod 15:9	0.3018	0.1371 to 0.4665	Yes	****	<0.0001
Flat Temperature:Ren photoperiod 15:9 vs. Thermoperiod 9:15:Ren photoperiod 9:15	0.1238	-0.03654 to 0.2841	No	ns	0.2507
Flat Temperature:Ren photoperiod 15:9 vs. Thermoperiod 9:15:Ren photoperiod 15:9	0.3385	0.1685 to 0.5086	Yes	****	<0.0001
Flat Temperature:Ren photoperiod 15:9 vs. Thermoperiod 15:9:Ren photoperiod 9:15	0.4094	0.2394 to 0.5795	Yes	****	<0.0001
Flat Temperature:Ren photoperiod 15:9 vs. Thermoperiod 15:9:Ren photoperiod 15:9	0.1283	-0.03206 to 0.2886	No	ns	0.2119
Flat Temperature:Ren photoperiod 15:9 vs. Advanced (12h):Ren photoperiod 9:15	0.2654	0.1006 to 0.4301	Yes	***	0.0001
Flat Temperature:Ren photoperiod 15:9 vs. Advanced (12h):Ren photoperiod 15:9	0.2308	0.06613 to 0.3956	Yes	**	0.0011
Thermoperiod 9:15:Ren photoperiod 9:15 vs. Thermoperiod 9:15:Ren photoperiod 15:9	0.2147	0.04470 to 0.3848	Yes	**	0.0045
Thermoperiod 9:15:Ren photoperiod 9:15 vs. Thermoperiod 15:9:Ren photoperiod 9:15	0.2857	0.1156 to 0.4557	Yes	****	<0.0001
Thermoperiod 9:15:Ren photoperiod 9:15 vs. Thermoperiod 15:9:Ren photoperiod 15:9	0.004484	-0.1558 to 0.1648	No	ns	>0.9999
Thermoperiod 9:15:Ren photoperiod 9:15 vs. Advanced (12h):Ren photoperiod 9:15	0.1416	-0.02313 to 0.3063	No	ns	0.1439
Thermoperiod 9:15:Ren photoperiod 9:15 vs. Advanced (12h):Ren photoperiod 15:9	0.1071	-0.05765 to 0.2718	No	ns	0.4673
Thermoperiod 9:15:Ren photoperiod 15:9 vs. Thermoperiod 15:9:Ren photoperiod 9:15	0.07093	-0.1083 to 0.2502	No	ns	0.9172
Thermoperiod 9:15:Ren photoperiod 15:9 vs. Thermoperiod 15:9:Ren photoperiod 15:9	-0.2103	-0.3803 to -0.04021	Yes	**	0.0058
Thermoperiod 9:15:Ren photoperiod 15:9 vs. Advanced (12h):Ren photoperiod 9:15	-0.07316	-0.2474 to 0.1010	No	ns	0.8901
Thermoperiod 9:15:Ren photoperiod 15:9 vs. Advanced (12h):Ren photoperiod 15:9	-0.1077	-0.2819 to 0.06651	No	ns	0.5326
Thermoperiod 15:9:Ren photoperiod 9:15 vs. Thermoperiod 15:9:Ren photoperiod 15:9	-0.2812	-0.4512 to -0.1111	Yes	****	<0.0001
Thermoperiod 15:9:Ren photoperiod 9:15 vs. Advanced (12h):Ren photoperiod 9:15	-0.1441	-0.3183 to 0.03011	No	ns	0.1785
Thermoperiod 15:9:Ren photoperiod 9:15 vs. Advanced (12h):Ren photoperiod 15:9	-0.1786	-0.3528 to -0.004413	Yes	*	0.0405
Thermoperiod 15:9:Ren photoperiod 15:9 vs. Advanced (12h):Ren photoperiod 9:15	0.1371	-0.02762 to 0.3018	No	ns	0.1726
Thermoperiod 15:9:Ren photoperiod 15:9 vs. Advanced (12h):Ren photoperiod 15:9	0.1026	-0.06213 to 0.2673	No	ns	0.5230
Advanced (12h):Ren photoperiod 9:15 vs. Advanced (12h):Ren photoperiod 15:9	-0.03452	-0.2035 to 0.1345	No	ns	0.9981

**Figure 8-5-10.** Three-way ANOVA followed by Tukey's *post hoc* multiple comparison test for diapause data scored from egg stage <10, created from naturally caught fly populations from either Houten or Rende subjected to various thermoperiods and photoperiods.

## 8.4 Appendix, Chapter 6

Kruskal-Wallis test		Dunn's multiple comparisons test					
		Mean rank diff,	Significant?	Summary	Adjusted P Value		
P value	0,8101						
Exact or approximate P value?	Approximate	Valium20 vs. TrpA1-A	-3,317	No	ns	>0,9999	
P value summary	ns						
Do the medians vary signif. (P < 0,05)?	No	Valium20 vs. TrpA1-B	0,8532	No	ns	>0,9999	
Number of groups	3						
Kruskal-Wallis statistic	0,4212	TrpA1-A vs. TrpA1-B	4,170	No	ns	>0,9999	
Kruskal-Wallis test		Dunn's multiple comparisons test					
		Mean rank diff,	Significant?	Summary	Adjusted P Value		
P value	<0,0001						
Exact or approximate P value?	Approximate	Valium20 vs. TrpA1-A	53,59	Yes	****	<0,0001	
P value summary	***						
Do the medians vary signif. (P < 0,05)?	Yes	Valium20 vs. TrpA1-B	38,56	Yes	****	<0,0001	
Number of groups	3						
Kruskal-Wallis statistic	58,29	TrpA1-A vs. TrpA1-B	-15,03	No	ns	0,0786	

**Figure 8-6-1.** Kruskal-Wallis test (left) followed by Dunns' multiple comparison test (right) of the timing of  $A_{\text{onset}}$  (top) and  $A_{\text{max}}$  (bottom) from  $\text{TrpA1}^{AB}\text{-gal4}$  flies crossed to either *UAS-TrpA1-A*, *UAS-TrpA1-B*, or *UAS-Valium20*.

<b>Kruskal-Wallis test</b>		<b>Dunn's multiple comparisons test</b>					
		Mean rank diff,	Significant?	Summary	Adjusted P	Value	
P value	0,2511						
Exact or approximate P value?	Approximate	Valium20 vs. TrpA1-A	-5,570	No	ns	>0,9999	
P value summary	ns						
Do the medians vary signif. (P < 0,05)?	No	Valium20 vs. TrpA1-B	5,690	No	ns	>0,9999	
Number of groups	3						
Kruskal-Wallis statistic	2,764	TrpA1-A vs. TrpA1-B	11,26	No	ns	0,2896	
<b>Kruskal-Wallis test</b>		<b>Dunn's multiple comparisons test</b>					
		Mean rank diff,	Significant?	Summary	Adjusted P	Value	
P value	<0,0001						
Exact or approximate P value?	Approximate	Valium20 vs. TrpA1-A	28,07	Yes	****	<0,0001	
P value summary	****						
Do the medians vary signif. (P < 0,05)?	Yes	Valium20 vs. TrpA1-B	35,62	Yes	****	<0,0001	
Number of groups	3						
Kruskal-Wallis statistic	34,02	TrpA1-A vs. TrpA1-B	7,553	No	ns	0,7954	

**Figure 8-6-2.** Kruskal-Wallis test (left) followed by Dunn's multiple comparison test (right) of the timing of A<sub>onset</sub> (top) and A<sub>max</sub> (bottom) from TrpA1<sup>CD</sup>-gal4 flies crossed to either UAS-TrpA1-A, UAS-TrpA1-B, or UAS-Valium20.

Kruskal-Wallis test		Dunn's multiple comparisons test				
		Mean rank diff,	Significant?	Summary	Adjusted P Value	
P value	0,0002					
Exact or approximate P value?	Approximate	Rh3 x CS vs. CS	23,30	Yes	**	0,0013
P value summary	***					
Do the medians vary signif. (P < 0,05)?	Yes	Rh3 x CS vs. Rh3 x Rh3	-0,7167	No	ns	>0,9999
Number of groups	3					
Kruskal-Wallis statistic	16,99	CS vs. Rh3 x Rh3	-24,01	Yes	***	0,0008
Kruskal-Wallis test		Dunn's multiple comparisons test				
		Mean rank diff, Significant?		Summary	Adjusted P Value	
P value	<0,0001					
Exact or approximate P value?	Approximate	Rh3 x CS vs. CS	-12,58	No	ns	0,1745
P value summary	****					
Do the medians vary signif. (P < 0,05)?	Yes	Rh3 x CS vs. Rh3 x Rh3	17,65	Yes	*	0,0220
Number of groups	3					
Kruskal-Wallis statistic	20,96	CS vs. Rh3 x Rh3	30,23	Yes	****	<0,0001

**Figure 8-6-3.** Kruskal-Wallis test (left) followed by Dunn's multiple comparison test (right) of the timing of  $A_{onset}$  (top) and  $A_{max}$  (bottom) of either CS flies, or flies that are either heterozygous mutant for *Rh3* or homozygous mutant for *Rh3*.

Kruskal-Wallis test		Dunn's multiple comparisons test					
		Mean rank diff,	Significant?	Summary	Adjusted P	Value	
P value	0,0882						
Exact or approximate P value?	Approximate	CS vs. Rh5 x CS	12,79	No	ns	0,1277	
P value summary	ns						
Do the medians vary signif. (P < 0,05)?	No	CS vs. Rh5 x Rh5	2,110	No	ns	>0,9999	
Number of groups	3						
Kruskal-Wallis statistic	4,857	Rh5 x CS vs. Rh5 x Rh5	-10,68	No	ns	0,2353	
Kruskal-Wallis test		Dunn's multiple comparisons test					
		Mean rank diff,	Significant?	Summary	Adjusted P	Value	
P value	0,7245						
Exact or approximate P value?	Approximate	CS vs. Rh5 x CS	-5,071	No	ns	>0,9999	
P value summary	ns						
Do the medians vary signif. (P < 0,05)?	No	CS vs. Rh5 x Rh5	-2,720	No	ns	>0,9999	
Number of groups	3						
Kruskal-Wallis statistic	0,6447	Rh5 x CS vs. Rh5 x Rh5	2,350	No	ns	>0,9999	

**Figure 8-6-4.** Kruskal-Wallis test (left) followed by Dunns multiple comparison test (right) of the timing of  $A_{onset}$  (top) and  $A_{max}$  (bottom) of either CS flies, or flies that are either heterozygous mutant for *Rh5* or homozygous mutant for *Rh5*.

Kruskal-Wallis test		Dunn's multiple comparisons test		Mean rank diff, Significant?	Summary	Adjusted P Value
P value	<0,0001					
Exact or approximate P value?	Approximate	CS vs. Rh6 x CS		-34,85	Yes	****
P value summary	****					<0,0001
Do the medians vary signif. (P < 0,05)?	Yes	CS vs. Rh6 x Rh6		-48,33	Yes	****
Number of groups	3					<0,0001
Kruskal-Wallis statistic	52,85	Rh6 x CS vs. Rh6 x Rh6		-13,48	No	ns
						0,1369
Kruskal-Wallis test		Dunn's multiple comparisons test		Mean rank diff, Significant?	Summary	Adjusted P Value
P value	0,0070					
Exact or approximate P value?	Approximate	CS vs. Rh6 x CS		-19,12	Yes	**
P value summary	**					0,0054
Do the medians vary signif. (P < 0,05)?	Yes	CS vs. Rh6 x Rh6		-12,68	No	ns
Number of groups	3					0,1243
Kruskal-Wallis statistic	9,933	Rh6 x CS vs. Rh6 x Rh6		6,435	No	ns
						0,8401

**Figure 8-6-5.** Kruskal-Wallis test (left) followed by Dunn's multiple comparison test (right) of the timing of  $A_{onset}$  (top) and  $A_{max}$  (bottom) of either CS flies, or flies that are either heterozygous mutant for *Rh6* or homozygous mutant for *Rh6*.

Kruskal-Wallis test		Dunn's multiple comparisons test					
			Mean rank diff,	Significant?	Summary	Adjusted P	Value
P value	<0,0001						
Exact or approximate P value?	Approximate	CS (Adv) vs. Rh3 x Rh3 (Adv)	-1,759	No	ns	>0,9999	
P value summary	****						
Do the medians vary signif. (P < 0.05)?	Yes	CS (Adv) vs. Rh3 x Rh3	-41,58	Yes	****	<0,0001	
Number of groups	3	Rh3 x Rh3 (Adv) vs. Rh3 x Rh3	-39,82	Yes	****	<0,0001	
Kruskal-Wallis statistic	57,33						

Kruskal-Wallis test		Dunn's multiple comparisons test					
			Mean rank diff,	Significant?	Summary	Adjusted P	Value
P value	<0,0001						
Exact or approximate P value?	Approximate	CS (Adv) vs. Rh3 x Rh3 (Adv)	-0,3571	No	ns	>0,9999	
P value summary	****						
Do the medians vary signif. (P < 0.05)?	Yes	CS (Adv) vs. Rh3 x Rh3	-38,62	Yes	****	<0,0001	
Number of groups	3	Rh3 x Rh3 (Adv) vs. Rh3 x Rh3	-38,26	Yes	****	<0,0001	
Kruskal-Wallis statistic	49,89						

**Figure 8-6-6.** Kruskal-Wallis test (left) followed by Dunns multiple comparison test (right) of the timing of  $A_{onset}$  (top) and  $A_{max}$  (bottom) of either CS flies, or flies that are or homozygous mutant for *Rh3*, subjected to an uncoupled photoperiod and thermoperiod in which temperature begins to increase 4 hours prior to light, and flies homozygous mutant for *Rh3* but were subjected to a coupled photoperiod and thermoperiod

<b>Kruskal-Wallis test</b>		<b>Dunn's multiple comparisons test</b>	<b>Mean rank diff, Significant?</b>	<b>Summary</b>	<b>Adjusted P Value</b>
P value	<0,0001				
Exact or approximate P value?	Approximate	CS (Adv) vs. Rh6 x Rh6 (Adv)	-5,156	No	ns >0,9999
P value summary	****				
Do the medians vary signif. (P < 0,05)?	Yes	CS (Adv) vs. Rh6 x Rh6	-47,80	Yes	**** <0,0001
Number of groups	3				
Kruskal-Wallis statistic	61,57	Rh6 x Rh6 (Adv) vs. Rh6 x Rh6	-42,64	Yes	**** <0,0001
<b>Kruskal-Wallis test</b>		<b>Dunn's multiple comparisons test</b>	<b>Mean rank diff, Significant?</b>	<b>Summary</b>	<b>Adjusted P Value</b>
P value	<0,0001				
Exact or approximate P value?	Approximate	CS (Adv) vs. Rh6 x Rh6 (Adv)	-8,809	No	ns 0,5718
P value summary	****				
Do the medians vary signif. (P < 0,05)?	Yes	CS (Adv) vs. Rh6 x Rh6	-49,78	Yes	**** <0,0001
Number of groups	3				
Kruskal-Wallis statistic	63,75	Rh6 x Rh6 (Adv) vs. Rh6 x Rh6	-40,97	Yes	**** <0,0001

**Figure 8-6-7.** Kruskal-Wallis test (left) followed by Dunn's multiple comparison test (right) of the timing of  $A_{onset}$  (top) and  $A_{max}$  (bottom) of either CS flies, or flies that are homozygous mutant for *Rh6*, subjected to an uncoupled photoperiod and thermoperiod in which temperature begins to increase 4 hours prior to light, and flies homozygous mutant for *Rh6* but were subjected to a coupled photoperiod and thermoperiod

## 9. References

- Abrieux, A., Xue, Y., Cai, Y., Lewald, K.M., Nguyen, H.N., Zhang, Y. and Chiu, J.C., 2020. EYES ABSENT and TIMELESS integrate photoperiodic and temperature cues to regulate seasonal physiology in *Drosophila*. *Proceedings of the National Academy of Sciences*, 117(26), pp.15293-15304.
- Adams, M.D., Celtniker, S.E., Holt, R.A., Evans, C.A., Gocayne, J.D., Amanatides, P.G., Scherer, S.E., Li, P.W., Hoskins, R.A., Galle, R.F. and George, R.A., 2000. The genome sequence of *Drosophila melanogaster*. *Science*, 287(5461), pp.2185-2195.
- Akten, B., Jauch, E., Genova, G.K., Kim, E.Y., Edery, I., Raabe, T. and Jackson, F.R., 2003. A role for CK2 in the *Drosophila* circadian oscillator. *Nature neuroscience*, 6(3), pp.251-257.
- Alejevski, F., Saint-Charles, A., Michard-Vanhée, C., Martin, B., Galant, S., Vasiliauskas, D. and Rouyer, F., 2019. The HisCl1 histamine receptor acts in photoreceptors to synchronize *Drosophila* behavioural rhythms with light-dark cycles. *Nature communications*, 10(1), pp.1-10.
- Allada, R., White, N.E., So, W.V., Hall, J.C. and Rosbash, M., 1998. A mutant *Drosophila* homolog of mammalian Clock disrupts circadian rhythms and transcription of period and timeless. *Cell*, 93(5), pp.791-804.
- Allebrandt, K.V., Amin, N., Müller-Myhsok, B., Esko, T., Teder-Laving, M., Azevedo, R.V.D.M., Hayward, C., Van Mill, J., Vogelzangs, N., Green, E.W. and Melville, S.A., 2013. AK ATP channel gene effect on sleep duration: from genome-wide association studies to function in *Drosophila*. *Molecular psychiatry*, 18(1), pp.122-132.
- Allemand, R. and David, J.R., 1984. Genetic analysis of the circadian oviposition rhythm in *Drosophila melanogaster*: Effects of drift in laboratory strains. *Behavior genetics*, 14(1), pp.31-43.
- Alpert, M.H., Frank, D.D., Kaspi, E., Flourakis, M., Zaharieva, E.E., Allada, R., Para, A. and Gallio, M., 2020. A circuit encoding absolute cold temperature in *Drosophila*. *Current Biology*, 30(12), pp.2275-2288.
- Andreatta, G., Kyriacou, C.P., Flatt, T. and Costa, R., 2018. Aminergic signalling controls ovarian dormancy in *Drosophila*. *Scientific reports*, 8(1), pp.1-14.
- Anduaga, A.M., Evental, N., Patop, I.L., Bartok, O., Weiss, R. and Kadener, S., 2019. Thermosensitive alternative splicing senses and mediates temperature adaptation in *Drosophila*. *Elife*, 8, p.e44642.

Anduaga, A.M., Nagy, D., Costa, R. and Kyriacou, C.P., 2018. Diapause in *Drosophila melanogaster*—Photoperiodicity, cold tolerance and metabolites. *Journal of insect physiology*, 105, pp.46-53.

Ayrinhac, A., Debat, V., Gibert, P., Kister, A.G., Legout, H., Moreteau, B., Vergilino, R. and David, J.R., 2004. Cold adaptation in geographical populations of *Drosophila melanogaster*: phenotypic plasticity is more important than genetic variability. *Functional Ecology*, 18(5), pp.700-706.

Azevedo, R.V.D.M.D., Hansen, C., Chen, K.F., Rosato, E. and Kyriacou, C.P., 2020. Disrupted glutamate signalling in *Drosophila* generates locomotor rhythms in constant light. *Frontiers in physiology*, 11, p.145.

Bachleitner, W., Kempinger, L., Wülbbeck, C., Rieger, D. and Helfrich-Förster, C., 2007. Moonlight shifts the endogenous clock of *Drosophila melanogaster*. *Proceedings of the National Academy of Sciences*, 104(9), pp.3538-3543.

Bai, H., Gelman, D.B. and Palli, S.R., 2010. Mode of action of methoprene in affecting female reproduction in the African malaria mosquito, *Anopheles gambiae*. *Pest management science*, 66(9), pp.936-943.

Bai, H., Kang, P. and Tatar, M., 2012. *Drosophila insulin-like peptide-6* (dilp6) expression from fat body extends lifespan and represses secretion of *Drosophila insulin-like peptide-2* from the brain. *Aging cell*, 11(6), pp.978-985.

Bai, J. and Montell, D., 2002. Eyes absent, a key repressor of polar cell fate during *Drosophila* oogenesis. *Development*, 129(23), pp.5377-5388.

Barber, A.F., Erion, R., Holmes, T.C. and Sehgal, A., 2016. Circadian and feeding cues integrate to drive rhythms of physiology in *Drosophila* insulin-producing cells. *Genes & development*, 30(23), pp.2596-2606.

Bauer, J., Antosh, M., Chang, C., Schorl, C., Kolli, S., Neretti, N. and Helfand, S.L., 2010. Comparative transcriptional profiling identifies takeout as a gene that regulates life span. *Aging (Albany NY)*, 2(5), p.298.

Beckwith, E.J. and Ceriani, M.F., 2015. Experimental assessment of the network properties of the *Drosophila* circadian clock. *Journal of Comparative Neurology*, 523(6), pp.982-996.

Behm-Ansmant, I., Rehwinkel, J., Doerks, T., Stark, A., Bork, P. and Izaurralde, E., 2006. mRNA degradation by miRNAs and GW182 requires both CCR4: NOT deadenylase and DCP1: DCP2 decapping complexes. *Genes & development*, 20(14), pp.1885-1898.

Behnia, R. and Desplan, C., 2015. Visual circuits in flies: beginning to see the whole picture. *Current opinion in neurobiology*, 34, pp.125-132.

- Bellivier, F., Geoffroy, P.A., Etain, B. and Scott, J., 2015. Sleep-and circadian rhythm-associated pathways as therapeutic targets in bipolar disorder. *Expert opinion on therapeutic targets*, 19(6), pp.747-763.
- Benito, J., Hoxha, V., Lama, C., Lazareva, A.A., Ferveur, J.F., Hardin, P.E. and Dauwalder, B., 2010. The circadian output gene takeout is regulated by Pdp1 $\epsilon$ . *Proceedings of the National Academy of Sciences*, 107(6), pp.2544-2549.
- Benito, J., Zheng, H. and Hardin, P.E., 2007. PDP1 $\epsilon$  functions downstream of the circadian oscillator to mediate behavioural rhythms. *Journal of Neuroscience*, 27(10), pp.2539-2547.
- Bhadra, U., Thakkar, N., Das, P. and Bhadra, M.P., 2017. Evolution of circadian rhythms: from bacteria to human. *Sleep medicine*, 35, pp.49-61.
- Bieber, C. and Ruf, T., 2009. Summer dormancy in edible dormice (*Glis glis*) without energetic constraints. *Naturwissenschaften*, 96(1), pp.165-171.
- Bonini, N.M., Leiserson, W.M. and Benzer, S., 1993. The eyes absent gene: genetic control of cell survival and differentiation in the developing *Drosophila* eye. *Cell*, 72(3), pp.379-395.
- Boulan, L., Andersen, D., Colombani, J., Boone, E. and Léopold, P., 2019. Inter-organ growth coordination is mediated by the Xrp1-Dilp8 axis in *Drosophila*. *Developmental cell*, 49(5), pp.811-818.
- Bownes, M., 1982. Hormonal and genetic regulation of vitellogenesis in *Drosophila*. *The Quarterly Review of Biology*, 57(3), pp.247-274.
- Bradshaw, W.E. and Holzapfel, C.M., 2001. Genetic shift in photoperiodic response correlated with global warming. *Proceedings of the National Academy of Sciences*, 98(25), pp.14509-14511.
- Bradshaw, W.E. and Holzapfel, C.M., 2010. What season is it anyway? Circadian tracking vs. photoperiodic anticipation in insects. *Journal of Biological Rhythms*, 25(3), pp.155-165.
- Breda, C., Rosato, E. and Kyriacou, C.P., 2020. Norpa signalling and the seasonal circadian locomotor phenotype in *Drosophila*. *Biology*, 9(6), p.130.
- Brennan, M.D., Weiner, A.J., Goralski, T.J. and Mahowald, A.P., 1982. The follicle cells are a major site of vitellogenin synthesis in *Drosophila melanogaster*. *Developmental biology*, 89(1), pp.225-236.
- Brogiolo, W., Stocker, H., Ikeya, T., Rintelen, F., Fernandez, R. and Hafen, E., 2001. An evolutionarily conserved function of the *Drosophila* insulin receptor and insulin-like peptides in growth control. *Current biology*, 11(4), pp.213-221.
- Broughton, S.J., Piper, M.D., Ikeya, T., Bass, T.M., Jacobson, J., Driege, Y., Martinez, P., Hafen, E., Withers, D.J., Leevers, S.J. and Partridge, L., 2005. Longer lifespan, altered

metabolism, and stress resistance in *Drosophila* from ablation of cells making insulin-like ligands. *Proceedings of the National Academy of Sciences*, 102(8), pp.3105-3110.

Buch, S., Melcher, C., Bauer, M., Katzenberger, J. and Pankratz, M.J., 2008. Opposing effects of dietary protein and sugar regulate a transcriptional target of *Drosophila* insulin-like peptide signalling. *Cell metabolism*, 7(4), pp.321-332.

Busza, A., Emery-Le, M., Rosbash, M. and Emery, P., 2004. Roles of the two *Drosophila* CRYPTOCHROME structural domains in circadian photoreception. *Science*, 304(5676), pp.1503-1506.

Busza, A., Murad, A. and Emery, P., 2007. Interactions between circadian neurons control temperature synchronization of *Drosophila* behaviour. *Journal of Neuroscience*, 27(40), pp.10722-10733.

Buszczak, M., Freeman, M.R., Carlson, J.R., Bender, M., Cooley, L. and Segraves, W.A., 1999. Ecdysone response genes govern egg chamber development during mid-oogenesis in *Drosophila*. *Development*, 126(20), pp.4581-4589.

Cao, W. and Edery, I., 2015. A novel pathway for sensory-mediated arousal involves splicing of an intron in the period clock gene. *Sleep*, 38(1), pp.41-51.

Carlsson, M.A., Enell, L.E. and Nässel, D.R., 2013. Distribution of short neuropeptide F and its receptor in neuronal circuits related to feeding in larval *Drosophila*. *Cell and tissue research*, 353(3), pp.511-523.

Carney, G.E. and Bender, M., 2000. The *Drosophila* ecdysone receptor (EcR) gene is required maternally for normal oogenesis. *Genetics*, 154(3), pp.1203-1211.

Chamseddin, K.H., Khan, S.Q., Nguyen, M.L., Antosh, M., Morris, S.N.S., Kolli, S., Neretti, N., Helfand, S.L. and Bauer, J.H., 2012. takeout-dependent longevity is associated with altered Juvenile Hormone signalling. *Mechanisms of ageing and development*, 133(11-12), pp.637-646.

Chang, V. and Meuti, M.E., 2020. Circadian transcription factors differentially regulate features of the adult overwintering diapause in the Northern house mosquito, *Culex pipiens*. *Insect biochemistry and molecular biology*, 121, p.103365.

Chasin, L.A., 2008. Searching for splicing motifs. *Advances in Experimental Medicine & Biology*, 623, p.85.

Chen, C., Buhl, E., Xu, M., Croset, V., Rees, J.S., Lilley, K.S., Benton, R., Hodge, J.J. and Stanewsky, R., 2015. *Drosophila* Ionotropic Receptor 25a mediates circadian clock resetting by temperature. *Nature*, 527(7579), pp.516-520.

Chen, C., Xu, M., Anantaprakorn, Y., Rosing, M. and Stanewsky, R., 2018. nocte is required for integrating light and temperature inputs in circadian clock neurons of *Drosophila*. *Current Biology*, 28(10), pp.1595-1605.

- Chen, C., Xu, M., Correa, P. and Stanewsky, R., 2020. A temperature-dependent molecular switch to adjust behaviour to changing environmental conditions. *bioRxiv*.
- Chen, K.F., Possidente, B., Lomas, D.A. and Crowther, D.C., 2014a. The central molecular clock is robust in the face of behavioural arrhythmia in a *Drosophila* model of Alzheimer's disease. *Disease models & mechanisms*, 7(4), pp.445-458.
- Chen, W., Liu, Z., Li, T., Zhang, R., Xue, Y., Zhong, Y., Bai, W., Zhou, D. and Zhao, Z., 2014b. Regulation of *Drosophila* circadian rhythms by miRNA let-7 is mediated by a regulatory cycle. *Nature communications*, 5(1), pp.1-13.
- Chen, X. and Rosbash, M., 2016. mir-276a strengthens *Drosophila* circadian rhythms by regulating timeless expression. *Proceedings of the National Academy of Sciences*, 113(21), pp.E2965-E2972.
- Cheng, Y., Gvakharia, B. and Hardin, P.E., 1998. Two alternatively spliced transcripts from the *Drosophila* period gene rescue rhythms having different molecular and behavioral characteristics. *Molecular and cellular biology*, 18(11), pp.6505-6514.
- Chiu, J.C., Vanselow, J.T., Kramer, A. and Edery, I., 2008. The phospho-occupancy of an atypical SLIMB-binding site on PERIOD that is phosphorylated by DOUBLETIME controls the pace of the clock. *Genes & development*, 22(13), pp.1758-1772.
- Chou, W.H., Hall, K.J., Wilson, D.B., Wideman, C.L., Townson, S.M., Chadwell, L.V. and Britt, S.G., 1996. Identification of a novel *Drosophila* opsin reveals specific patterning of the R7 and R8 photoreceptor cells. *Neuron*, 17(6), pp.1101-1115.
- Chou, W.H., Huber, A., Bentrop, J., Schulz, S., Schwab, K., Chadwell, L.V., Paulsen, R. and Britt, S.G., 1999. Patterning of the R7 and R8 photoreceptor cells of *Drosophila*: evidence for induced and default cell-fate specification. *Development*, 126(4), pp.607-616.
- Citri, Y., Colot, H.V., Jacquier, A.C., Yu, Q., Hall, J.C., Baltimore, D. and Rosbash, M., 1987. A family of unusually spliced biologically active transcripts encoded by a *Drosophila* clock gene. *Nature*, 326(6108), pp.42-47.
- Claeys, I., Simonet, G., Poels, J., Van Loy, T., Vercammen, L., De Loof, A. and Broeck, J.V., 2002. Insulin-related peptides and their conserved signal transduction pathway. *Peptides*, 23(4), pp.807-816.
- Clancy, D.J., Gems, D., Harshman, L.G., Oldham, S., Stocker, H., Hafen, E., Leevers, S.J. and Partridge, L., 2001. Extension of life-span by loss of CHICO, a *Drosophila* insulin receptor substrate protein. *Science*, 292(5514), pp.104-106.
- Collins, B.H., Dissel, S., Gaten, E., Rosato, E. and Kyriacou, C.P., 2005. Disruption of Cryptochrome partially restores circadian rhythmicity to the arrhythmic period mutant of *Drosophila*. *Proceedings of the National Academy of Sciences*, 102(52), pp.19021-19026.]

- Collins, B.H., Rosato, E. and Kyriacou, C.P., 2004. Seasonal behavior in *Drosophila melanogaster* requires the photoreceptors, the circadian clock, and phospholipase C. *Proceedings of the National Academy of Sciences*, 101(7), pp.1945-1950.
- Collins, L.A., 2014. *Genetic analyses of circadian and seasonal phenotypes in Drosophila* (Doctoral dissertation, University of Leicester).
- Colombani, J., Andersen, D.S. and Léopold, P., 2012. Secreted peptide Dilp8 coordinates *Drosophila* tissue growth with developmental timing. *Science*, 336(6081), pp.582-585.
- Cyran, S.A., Buchsbaum, A.M., Reddy, K.L., Lin, M.C., Glossop, N.R., Hardin, P.E., Young, M.W., Storti, R.V. and Blau, J., 2003. vrille, Pdp1, and dClock form a second feedback loop in the *Drosophila* circadian clock. *Cell*, 112(3), pp.329-341.
- Czarna, A., Berndt, A., Singh, H.R., Grudziecki, A., Ladurner, A.G., Timinszky, G., Kramer, A. and Wolf, E., 2013. Structures of *Drosophila* cryptochrome and mouse cryptochrome1 provide insight into circadian function. *Cell*, 153(6), pp.1394-1405.
- Czech, B., Malone, C.D., Zhou, R., Stark, A., Schlingeheyde, C., Dus, M., Perrimon, N., Kellis, M., Wohlschlegel, J.A., Sachidanandam, R. and Hannon, G.J., 2008. An endogenous small interfering RNA pathway in *Drosophila*. *Nature*, 453(7196), pp.798-802.
- Da Lage, J.L., Capy, P. and David, J.R., 1990. Starvation and desiccation tolerance in *Drosophila melanogaster*: differences between European, North African and Afrotropical populations. *Genetics Selection Evolution*, 22(4), pp.381-391.
- Da Ros, V.G., Gutierrez-Perez, I., Ferres-Marco, D. and Dominguez, M., 2013. Dampening the signals transduced through hedgehog via microRNA miR-7 facilitates notch-induced tumourigenesis. *PLoS Biol*, 11(5), p.e1001554.
- Daan, S., Spoelstra, K., Albrecht, U., Schmutz, I., Daan, M., Daan, B., Rienks, F., Poletaeva, I., Dell'omo, G., Vyssotski, A. and Lipp, H.P., 2011. Lab mice in the field: unorthodox daily activity and effects of a dysfunctional circadian clock allele. *Journal of Biological Rhythms*, 26(2), pp.118-129.
- Danks, H.V., 1987, Ottawa: Biological Survey of Canada (Terrestrial Arthropods). *Insect dormancy: an ecological perspective* (Vol. 1, pp. 439-439).
- Darlington, T.K., Wager-Smith, K., Ceriani, M.F., Staknis, D., Gekakis, N., Steeves, T.D., Weitz, C.J., Takahashi, J.S. and Kay, S.A., 1998. Closing the circadian loop: CLOCK-induced transcription of its own inhibitors per and tim. *Science*, 280(5369), pp.1599-1603.
- Das, A., Holmes, T.C. and Sheeba, V., 2015. dTRPA1 modulates afternoon peak of activity of fruit flies *Drosophila melanogaster*. *PloS one*, 10(7), p.e0134213.
- Das, A., Holmes, T.C. and Sheeba, V., 2016. dTRPA1 in non-circadian neurons modulates temperature-dependent rhythmic activity in *Drosophila melanogaster*. *Journal of biological rhythms*, 31(3), pp.272-288.

- David, J.R. & Capy, P., 1988. Genetic variation of *Drosophila melanogaster* natural populations. *Trends in Genetics*, 4, 106-111.
- David, J.R. and Bocquet, C., 1975. Evolution in a cosmopolitan species: genetic latitudinal clines in *Drosophila melanogaster* wild populations. *Experientia*, 31(2), pp.164-166.
- David, J.R., Allemand, R., Capy, P., Chakir, M., Gibert, P., Pétavy, G. and Moreteau, B., 2004. Comparative life histories and ecophysiology of *Drosophila melanogaster* and *D. simulans*. *Drosophila melanogaster, Drosophila simulans: So Similar, So Different*, pp.151-163.
- De Wilde, J., Duintjer, C.S. and Mook, L., 1959. Physiology of diapause in the adult Colorado beetle (*Leptinotarsa decemlineata* Say)—I The photoperiod as a controlling factor. *Journal of Insect Physiology*, 3(2), pp.75-85.
- De, J., Varma, V., Saha, S., Sheeba, V. and Sharma, V.K., 2013. Significance of activity peaks in fruit flies, *Drosophila melanogaster*, under seminatural conditions. *Proceedings of the National Academy of Sciences*, 110(22), pp.8984-8989.
- Delventhal, R., O'Connor, R.M., Pantalia, M.M., Ulgherait, M., Kim, H.X., Basturk, M.K., Canman, J.C. and Shirasu-Hiza, M., 2019. Dissection of central clock function in *Drosophila* through cell-specific CRISPR-mediated clock gene disruption. *Elife*, 8, p.e48308.
- Denlinger, D.L., 1986. Dormancy in tropical insects. *Annual review of entomology*, 31(1), pp.239-264.
- Denlinger, D.L., 2008. Why study diapause?. *Entomological Research*, 38(1), pp.1-9.
- Dissel, S., Hansen, C.N., Özkaya, Ö., Hemsley, M., Kyriacou, C.P. and Rosato, E., 2014. The logic of circadian organization in *Drosophila*. *Current Biology*, 24(19), pp.2257-2266.
- Dowse, H.B., Hall, J.C. and Ringo, J.M., 1987. Circadian and ultradian rhythms in period mutants of *Drosophila melanogaster*. *Behaviour genetics*, 17(1), pp.19-35.
- Duchen, P., Živković, D., Hutter, S., Stephan, W. and Laurent, S., 2013. Demographic inference reveals African and European admixture in the North American *Drosophila melanogaster* population. *Genetics*, 193(1), pp.291-301.
- Durmaz, E., Benson, C., Kapun, M., Schmidt, P. and Flatt, T., 2018. An inversion supergene in *Drosophila* underpins latitudinal clines in survival traits. *Journal of evolutionary biology*, 31(9), pp.1354-1364.
- Durmaz, E., Rajpurohit, S., Betancourt, N., Fabian, D.K., Kapun, M., Schmidt, P. and Flatt, T., 2019. A clinal polymorphism in the insulin signalling transcription factor foxo contributes to life-history adaptation in *Drosophila*. *Evolution*, 73(9), pp.1774-1792.

- Dweck, H.K., Ebrahim, S.A., Kromann, S., Bown, D., Hillbur, Y., Sachse, S., Hansson, B.S. and Stensmyr, M.C., 2013. Olfactory preference for egg laying on citrus substrates in *Drosophila*. *Current Biology*, 23(24), pp.2472-2480.
- Dyar, K.A. and Eckel-Mahan, K.L., 2017. Circadian metabolomics in time and space. *Frontiers in neuroscience*, 11, p.369.
- Eckel-Mahan, K. and Sassone-Corsi, P., 2013. Metabolism and the circadian clock converge. *Physiological reviews*, 93(1), pp.107-135.
- Egevang, C., Stenhouse, I.J., Phillips, R.A., Petersen, A., Fox, J.W. and Silk, J.R., 2010. Tracking of Arctic terns *Sterna paradisaea* reveals longest animal migration. *Proceedings of the National Academy of Sciences*, 107(5), pp.2078-2081.
- Emerson, K.J., Bradshaw, W.E. and Holzapfel, C.M., 2009a. Complications of complexity: integrating environmental, genetic and hormonal control of insect diapause. *Trends in Genetics*, 25(5), pp.217-225.
- Emerson, K.J., Uyemura, A.M., McDaniel, K.L., Schmidt, P.S., Bradshaw, W.E. and Holzapfel, C.M., 2009b. Environmental control of ovarian dormancy in natural populations of *Drosophila melanogaster*. *Journal of Comparative Physiology A*, 195(9), pp.825-829.
- Emery, P., So, W.V., Kaneko, M., Hall, J.C. and Rosbash, M., 1998. CRY, a *Drosophila* clock and light-regulated cryptochrome, is a major contributor to circadian rhythm resetting and photosensitivity. *Cell*, 95(5), pp.669-679.
- Enell, L.E., Kapan, N., Söderberg, J.A., Kahsai, L. and Nässel, D.R., 2010. Insulin signalling, lifespan and stress resistance are modulated by metabotropic GABA receptors on insulin producing cells in the brain of *Drosophila*. *PloS one*, 5(12), p.e15780.
- Ersahin, T., Tuncbag, N. and Cetin-Atalay, R., 2015. The PI3K/AKT/mTOR interactive pathway. *Molecular BioSystems*, 11(7), pp.1946-1954.
- Evans, A.L., Singh, N.J., Friebe, A., Arnemo, J.M., Laske, T.G., Fröbert, O., Swenson, J.E. and Blanc, S., 2016. Drivers of hibernation in the brown bear. *Frontiers in zoology*, 13(1), pp.1-14.
- Fabian, D.K., Kapun, M., Nolte, V., Kofler, R., Schmidt, P.S., Schlötterer, C. and Flatt, T., 2012. Genome-wide patterns of latitudinal differentiation among populations of *Drosophila melanogaster* from North America. *Molecular ecology*, 21(19), pp.4748-4769.
- Fabian, D.K., Lack, J.B., Mathur, V., Schlötterer, C., Schmidt, P.S., Pool, J.E. and Flatt, T., 2015. Spatially varying selection shapes life history clines among populations of *Drosophila melanogaster* from sub-Saharan Africa. *Journal of evolutionary biology*, 28(4), pp.826-840.
- Fan, J.Y., Agyekum, B., Venkatesan, A., Hall, D.R., Keightley, A., Bjes, E.S., Bouyain, S. and Price, J.L., 2013. Noncanonical FK506-binding protein BDBT binds DBT to enhance its circadian function and forms foci at night. *Neuron*, 80(4), pp.984-996.

Fancy, S.G., Pank, L.F., Whitten, K.R. and Regelin, W.L., 1989. Seasonal movements of caribou in arctic Alaska as determined by satellite. *Canadian Journal of Zoology*, 67(3), pp.644-650.

Fang, Y., Sathyaranayanan, S. and Sehgal, A., 2007. Post-translational regulation of the *Drosophila* circadian clock requires protein phosphatase 1 (PP1). *Genes & development*, 21(12), pp.1506-1518.

Farshadi, Elham, Gijsbertus TJ van Der Horst, and Inês Chaves. "Molecular Links between the Circadian Clock and the Cell Cycle." *Journal of Molecular Biology* (2020).

Fernández, M.P., Berni, J. and Ceriani, M.F., 2008. Circadian remodelling of neuronal circuits involved in rhythmic behaviour. *PLoS Biol*, 6(3), p.e69.

Fernandez, M.P., Pettibone, H.L., Bogart, J.T., Roell, C.J., Davey, C.E., Pranevicius, A., Huynh, K.V., Lennox, S.M., Kostadinov, B.S. and Shafer, O.T., 2020. Sites of circadian clock neuron plasticity mediate sensory integration and entrainment. *Current Biology*, 30(12), pp.2225-2237.

Flatt, T. and Kawecki, T.J., 2007. Juvenile hormone as a regulator of the trade-off between reproduction and life span in *Drosophila melanogaster*. *Evolution*, 61(8), pp.1980-1991.

Flatt, T., 2020. Life-history evolution and the genetics of fitness components in *Drosophila melanogaster*. *Genetics*, 214(1), pp.3-48.

Flatt, T., Tu, M.P. and Tatar, M., 2005. Hormonal pleiotropy and the juvenile hormone regulation of *Drosophila* development and life history. *Bioessays*, 27(10), pp.999-1010.

Foronda, D., Weng, R., Verma, P., Chen, Y.W. and Cohen, S.M., 2014. Coordination of insulin and Notch pathway activities by microRNA miR-305 mediates adaptive homeostasis in the intestinal stem cells of the *Drosophila* gut. *Genes & development*, 28(21), pp.2421-2431.

Fowler, M.A. and Montell, C., 2013. *Drosophila* TRP channels and animal behavior. *Life sciences*, 92(8-9), pp.394-403.

Frank, D.D., Jouandet, G.C., Kearney, P.J., Macpherson, L.J. and Gallio, M., 2015. Temperature representation in the *Drosophila* brain. *Nature*, 519(7543), pp.358-361.

Frydenberg, J., Hoffmann, A.A. and Loeschke, V., 2003. DNA sequence variation and latitudinal associations in hsp23, hsp26 and hsp27 from natural populations of *Drosophila melanogaster*. *Molecular Ecology*, 12(8), pp.2025-2032.

Fryxell, K.J. and Meyerowitz, E.M., 1987. An opsin gene that is expressed only in the R7 photoreceptor cell of *Drosophila*. *The EMBO journal*, 6(2), p.443.

Fujiwara, Y., Hermann-Luibl, C., Katsura, M., Sekiguchi, M., Ida, T., Helfrich-Förster, C. and Yoshii, T., 2018. The CCHamide1 neuropeptide expressed in the anterior dorsal

neuron 1 conveys a circadian signal to the ventral lateral neurons in *Drosophila melanogaster*. *Frontiers in physiology*, 9, p.1276.

Fulga, T.A., McNeill, E.M., Binari, R., Yelick, J., Blanche, A., Booker, M., Steinkraus, B.R., Schnall-Levin, M., Zhao, Y., DeLuca, T. and Bejarano, F., 2015. A transgenic resource for conditional competitive inhibition of conserved *Drosophila* microRNAs. *Nature communications*, 6(1), pp.1-10.

Gabaldón, C., Legüe, M., Palomino, M.F., Verdugo, L., Gutzwiller, F. and Calixto, A., 2020. Intergenerational Pathogen-Induced Diapause in *Caenorhabditis elegans* Is Modulated by mir-243. *Mbio*, 11(5), pp.e01950-20.

Garaulet, D.L., Sun, K., Li, W., Wen, J., Panzarino, A.M., O'Neil, J.L., Hiesinger, P.R., Young, M.W. and Lai, E.C., 2016. miR-124 regulates diverse aspects of rhythmic behavior in *Drosophila*. *Journal of Neuroscience*, 36(12), pp.3414-3421.

Garelli, A., Heredia, F., Casimiro, A.P., Macedo, A., Nunes, C., Garcez, M., Dias, A.R., Volonte, Y.A., Uhlmann, T., Caparros, E. and Koyama, T., 2015. Dilp8 requires the neuronal relaxin receptor Lgr3 to couple growth to developmental timing. *Nat. Commun.* 6: 8732.

Gattermann, R., Johnston, R.E., Yigit, N., Fritzsche, P., Larimer, S., Özkurt, S., Neumann, K., Song, Z., Colak, E., Johnston, J. and McPhee, M.E., 2008. Golden hamsters are nocturnal in captivity but diurnal in nature. *Biology letters*, 4(3), pp.253-255.

Gebert, L.F. and MacRae, I.J., 2019. Regulation of microRNA function in animals. *Nature reviews Molecular cell biology*, 20(1), pp.21-37.

Geffen, E. and Mendelssohn, H., 1989. Activity patterns and thermoregulatory behavior of the Egyptian tortoise *Testudo kleinmanni* in Israel. *Journal of Herpetology*, pp.404-409.

Géminard, C., Rulifson, E.J. and Léopold, P., 2009. Remote control of insulin secretion by fat cells in *Drosophila*. *Cell metabolism*, 10(3), pp.199-207.

Gentile, C., Sehadova, H., Simoni, A., Chen, C. and Stanewsky, R., 2013. Cryptochrome antagonizes synchronization of *Drosophila*'s circadian clock to temperature cycles. *Current Biology*, 23(3), pp.185-195.

Gesto, J.S.M., 2011. *Circadian clock genes and seasonal behaviour* (Doctoral dissertation, University of Leicester).

Glaser, F.T. and Stanewsky, R., 2005. Temperature synchronization of the *Drosophila* circadian clock. *Current Biology*, 15(15), pp.1352-1363.

Glossop, N.R., Houl, J.H., Zheng, H., Ng, F.S., Dudek, S.M. and Hardin, P.E., 2003. VRILLE feeds back to control circadian transcription of Clock in the *Drosophila* circadian oscillator. *Neuron*, 37(2), pp.249-261.

- Glossop, N.R., Lyons, L.C. and Hardin, P.E., 1999. Interlocked feedback loops within the *Drosophila* circadian oscillator. *Science*, 286(5440), pp.766-768.
- Golden, S.S., Ishiura, M., Johnson, C.H. and Kondo, T., 1997. Cyanobacterial circadian rhythms. *Annual review of plant biology*, 48(1), pp.327-354.
- Gorostiza, E.A., Depetris-Chauvin, A., Frenkel, L., Pérez, N. and Ceriani, M.F., 2014. Circadian pacemaker neurons change synaptic contacts across the day. *Current Biology*, 24(18), pp.2161-2167.
- Goto, M., Sekine, Y., Outa, H., Hujikura, M. and Suzuki, K., 2001. Relationships between cold hardiness and diapause, and between glycerol and free amino acid contents in overwintering larvae of the oriental corn borer, *Ostrinia furnacalis*. *Journal of Insect Physiology*, 47(2), pp.157-165.
- Green, E.W., O'Callaghan, E.K., Hansen, C.N., Bastianello, S., Bhutani, S., Vanin, S., Armstrong, J.D., Costa, R. and Kyriacou, C.P., 2015. *Drosophila* circadian rhythms in seminatural environments: summer afternoon component is not an artifact and requires TrpA1 channels. *Proceedings of the National Academy of Sciences*, 112(28), pp.8702-8707.
- Grima, B., Chélot, E., Xia, R. and Rouyer, F., 2004. Morning and evening peaks of activity rely on different clock neurons of the *Drosophila* brain. *Nature*, 431(7010), p.869.
- Grima, B., Lamouroux, A., Chelot, E. and Papin, C., 2002. The F-box protein slimb controls the levels of clock proteins period and timeless. *Nature*, 420(6912), p.178.
- Grönke, S., Clarke, D.F., Broughton, S., Andrews, T.D. and Partridge, L., 2010. Molecular evolution and functional characterization of *Drosophila* insulin-like peptides. *PLoS Genet*, 6(2), p.e1000857.
- Gruntenko, N.E., Laukhina, O.V. and Rauschenbach, I.Y., 2012. Role of D1-and D2-like receptors in age-specific regulation of juvenile hormone and 20-hydroxyecdysone levels by dopamine in *Drosophila*. *Journal of insect physiology*, 58(12), pp.1534-1540.
- Gu, P., Gong, J., Shang, Y., Wang, F., Ruppell, K.T., Ma, Z., Sheehan, A.E., Freeman, M.R. and Xiang, Y., 2019. Polymodal nociception in *Drosophila* requires alternative splicing of TrpA1. *Current Biology*, 29(23), pp.3961-3973.
- Guerra, P.A., Gegear, R.J. and Reppert, S.M., 2014. A magnetic compass aids monarch butterfly migration. *Nature communications*, 5(1), pp.1-8.
- Guntur, A.R., Gu, P., Takle, K., Chen, J., Xiang, Y. and Yang, C.H., 2015. *Drosophila* TRPA1 isoforms detect UV light via photochemical production of H<sub>2</sub>O<sub>2</sub>. *Proceedings of the National Academy of Sciences*, 112(42), pp.E5753-E5761.
- Guo, F., Cerullo, I., Chen, X. and Rosbash, M., 2014. PDF neuron firing phase-shifts key circadian activity neurons in *Drosophila*. *ELife*, 3, p.e02780.

- Guo, F., Holla, M., Díaz, M.M. and Rosbash, M., 2018. A circadian output circuit controls sleep-wake arousal in *Drosophila*. *Neuron*, 100(3), pp.624-635.
- Hamada, F.N., Rosenzweig, M., Kang, K., Pulver, S.R., Ghezzi, A., Jegla, T.J. and Garrity, P.A., 2008. An internal thermal sensor controlling temperature preference in *Drosophila*. *Nature*, 454(7201), pp.217-220.
- Hamblen, M., Zehring, W.A., Kyriacou, C.P., Reddy, P., Yu, Q., Wheeler, D.A., Zwiebel, L.J., Konopka, R.J., Rosbash, M. and Hall, J.C., 1986. Germ-line transformation involving DNA from the period locus in *Drosophila melanogaster*: overlapping genomic fragments that restore circadian and ultradian rhythmicity to per<sup>0</sup> and per<sup>-</sup> mutants. *Journal of neurogenetics*, 3(5), pp.249-291.
- Han, K.A., Millar, N.S., Grotewiel, M.S. and Davis, R.L., 1996. DAMB, a novel dopamine receptor expressed specifically in *Drosophila* mushroom bodies. *Neuron*, 16(6), pp.1127-1135.
- Hanai, S. and Ishida, N., 2009. Entrainment of *Drosophila* circadian clock to green and yellow light by Rh1, Rh5, Rh6 and CRY. *Neuroreport*, 20(8), pp.755-758.
- Hanai, S., Hamasaka, Y. and Ishida, N., 2008. Circadian entrainment to red light in *Drosophila*: requirement of Rhodopsin 1 and Rhodopsin 6. *Neuroreport*, 19(14), pp.1441-1444.
- Hao, H., Allen, D.L. and Hardin, P.E., 1997. A circadian enhancer mediates PER-dependent mRNA cycling in *Drosophila melanogaster*. *Molecular and cellular biology*, 17(7), pp.3687-3693.
- Hardie, R.C. and Juusola, M., 2015. Phototransduction in *Drosophila*. *Current opinion in neurobiology*, 34, pp.37-45.
- Hardin, P.E., Hall, J.C. and Rosbash, M., 1990. Feedback of the *Drosophila* period gene product on circadian cycling of its messenger RNA levels. *Nature*, 343(6258), pp.536-540.
- Hardin, P.E., 2011. Molecular genetic analysis of circadian timekeeping in *Drosophila*. *Advances in genetics*, 74, pp.141-173.
- Haspel, J.A., Anafi, R., Brown, M.K., Cermakian, N., Depner, C., Desplats, P., Gelman, A.E., Haack, M., Jelic, S., Kim, B.S. and Laposky, A.D., 2020. Perfect timing: circadian rhythms, sleep, and immunity—an NIH workshop summary. *JCI insight*, 5(1).
- He, C., Cong, X., Zhang, R., Wu, D., An, C. and Zhao, Z., 2013a. Regulation of circadian locomotor rhythm by neuropeptide Y-like system in *Drosophila melanogaster*. *Insect molecular biology*, 22(4), pp.376-388.
- He, C., Yang, Y., Zhang, M., Price, J.L. and Zhao, Z., 2013b. Regulation of sleep by neuropeptide Y-like system in *Drosophila melanogaster*. *PLoS One*, 8(9), p.e74237.

- He, J., Chen, Q., Wei, Y., Jiang, F., Yang, M., Hao, S., Guo, X., Chen, D. and Kang, L., 2016. MicroRNA-276 promotes egg-hatching synchrony by up-regulating brm in locusts. *Proceedings of the National Academy of Sciences*, 113(3), pp.584-589.
- He, L., Wang, X. and Montell, D.J., 2011. Shining light on *Drosophila* oogenesis: live imaging of egg development. *Current opinion in genetics & development*, 21(5), pp.612-619.
- He, Q., Wu, B., Price, J.L. and Zhao, Z., 2017. Circadian Rhythm Neuropeptides in *Drosophila*: Signals for Normal Circadian Function and Circadian Neurodegenerative Disease. *International journal of molecular sciences*, 18(4), p.886.
- Helfrich, C. and Engelmann, W., 1987. Evidences for circadian rhythmicity in the per mutant of *Drosophila melanogaster*. *Zeitschrift für Naturforschung C*, 42(11-12), pp.1335-1338.
- Helfrich-förster, C., 2009. Neuropeptide PDF plays multiple roles in the circadian clock of *Drosophila melanogaster*. *Sleep and Biological Rhythms*, 7(3), pp.130-143.
- Helfrich-Förster, C., Edwards, T., Yasuyama, K., Wisotzki, B., Schneuwly, S., Stanewsky, R., Meinertzhagen, I.A. and Hofbauer, A., 2002. The extraretinal eyelet of *Drosophila*: development, ultrastructure, and putative circadian function. *Journal of Neuroscience*, 22(21), pp.9255-9266.
- Helfrich-Förster, C., Shafer, O.T., Wülbeck, C., Grieshaber, E., Rieger, D. and Taghert, P., 2007. Development and morphology of the clock-gene-expressing lateral neurons of *Drosophila melanogaster*. *Journal of Comparative Neurology*, 500(1), pp.47-70.
- Helfrich-Förster, C., Winter, C., Hofbauer, A., Hall, J.C. and Stanewsky, R., 2001. The circadian clock of fruit flies is blind after elimination of all known photoreceptors. *Neuron*, 30(1), pp.249-261.
- Herzog, E.D., 2007. Neurons and networks in daily rhythms. *Nature reviews. Neuroscience*, 8(10), p.790.
- Hidayat, P. and Goodman, W.G., 1994. Juvenile hormone and haemolymph juvenile hormone binding protein titers and their interaction in the haemolymph of fourth stadium *Manduca sexta*. *Insect biochemistry and molecular biology*, 24(7), pp.709-715.
- Hoang, N., Schleicher, E., Kacprzak, S., Bouly, J.P., Picot, M., Wu, W., Berndt, A., Wolf, E., Bittl, R. and Ahmad, M., 2008. Human and *Drosophila* cryptochromes are light activated by flavin photoreduction in living cells. *PLoS biology*, 6(7), p.e160.
- Hobson, K.A., Anderson, R.C., Soto, D.X. and Wassenaar, L.I., 2012. Isotopic evidence that dragonflies (*Pantala flavescens*) migrating through the Maldives come from the northern Indian subcontinent. *PLoS one*, 7(12), p.e52594.
- Hoffmann, A.A., 2010. Physiological climatic limits in *Drosophila*: patterns and implications. *Journal of Experimental Biology*, 213(6), pp.870-880. Izquierdo, J.I., 1991.

How does *Drosophila melanogaster* overwinter?. *Entomologia Experimentalis et Applicata*, 59(1), pp.51-58.

Hoffmann, A.A., Shirriffs, J. and Scott, M., 2005. Relative importance of plastic vs genetic factors in adaptive differentiation: geographical variation for stress resistance in *Drosophila melanogaster* from eastern Australia. *Functional Ecology*, 19(2), pp.222-227.

Hori, S., Kaneko, K., Saito, T.H., Takeuchi, H. and Kubo, T., 2011. Expression of two microRNAs, ame-mir-276 and-1000, in the adult honeybee (*Apis mellifera*) brain. *Apidologie*, 42(1), pp.89-102.

Huber, A., Schulz, S., Bentrop, J., Groell, C., Wolfrum, U. and Paulsen, R., 1997. Molecular cloning of *Drosophila* Rh6 rhodopsin: the visual pigment of a subset of R8 photoreceptor cells. *FEBS letters*, 406(1-2), pp.6-10.

Hunt, T. and Sassone-Corsi, P., 2007. Riding tandem: circadian clocks and the cell cycle. *Cell*, 129(3), pp.461-464.

Izquierdo, J.I., 1991. How does *Drosophila melanogaster* overwinter?. *Entomologia Experimentalis et Applicata*, 59(1), pp.51-58.

Jenett, A., Rubin, G.M., Ngo, T.T., Shepherd, D., Murphy, C., Dionne, H., Pfeiffer, B.D., Cavallaro, A., Hall, D., Jeter, J. and Iyer, N., 2012. A GAL4-driver line resource for *Drosophila* neurobiology. *Cell reports*, 2(4), pp.991-1001.

Jaubert, S., Mereau, A., Antoniewski, C. and Tagu, D., 2007. MicroRNAs in *Drosophila*: the magic wand to enter the Chamber of Secrets?. *Biochimie*, 89(10), pp.1211-1220.

Jenett, A., Rubin, G.M., Ngo, T.T., Shepherd, D., Murphy, C., Dionne, H., Pfeiffer, B.D., Cavallaro, A., Hall, D., Jeter, J. and Iyer, N., 2012. A GAL4-driver line resource for *Drosophila* neurobiology. *Cell reports*, 2(4), pp.991-1001.

Jiang, C., Yadlapalli, S., Bahle, A., Reddy, P., Meyhofer, E. and Shafer, O., 2017. Temperature Sensation and Integration in the *Drosophila* Circadian Clock. *Biophysical Journal*, 112(3), p.135a.

Johnston, J.G. and Pollock, D.M., 2018. Circadian regulation of renal function. *Free Radical Biology and Medicine*, 119, pp.93-107.

Jui-Ming, L., Kilman, V.L., Keegan, K. and Paddock, B., 2002. A role for casein kinase 2alpha in the *Drosophila* circadian clock. *Nature*, 420(6917), p.816.

Jünger, M.A., Rintelen, F., Stocker, H., Wasserman, J.D., Végh, M., Radimerski, T., Greenberg, M.E. and Hafen, E., 2003. The *Drosophila* forkhead transcription factor FOXO mediates the reduction in cell number associated with reduced insulin signalling. *Journal of biology*, 2(3), pp.1-17.

Kadener, S., Menet, J.S., Sugino, K., Horwich, M.D., Weissbein, U., Nawathean, P., Vagin, V.V., Zamore, P.D., Nelson, S.B. and Rosbash, M., 2009. A role for microRNAs in the *Drosophila* circadian clock. *Genes & development*, 23(18), pp.2179-2191.

- Kadener, S., Stoleru, D., McDonald, M., Nawathean, P. and Rosbash, M., 2007. Clockwork Orange is a transcriptional repressor and a new *Drosophila* circadian pacemaker component. *Genes & development*, 21(13), pp.1675-1686.
- Kaneko, H., Head, L.M., Ling, J., Tang, X., Liu, Y., Hardin, P.E., Emery, P. and Hamada, F.N., 2012. Circadian rhythm of temperature preference and its neural control in *Drosophila*. *Current Biology*, 22(19), pp.1851-1857.
- Kaneko, M. and Hall, J.C., 2000. Neuroanatomy of cells expressing clock genes in *Drosophila*: transgenic manipulation of the period and timeless genes to mark the perikarya of circadian pacemaker neurons and their projections. *Journal of Comparative Neurology*, 422(1), pp.66-94.
- Kaneko, M., Hamblen, M.J. and Hall, J.C., 2000. Involvement of the period gene in developmental time-memory: effect of the perShort mutation on phase shifts induced by light pulses delivered to *Drosophila* larvae. *Journal of biological rhythms*, 15(1), pp.13-30.
- Kaneko, M., Helfrich-Förster, C. and Hall, J.C., 1997. Spatial and Temporal Expression of the period andtimeless Genes in the Developing Nervous System of*Drosophila*: Newly Identified Pacemaker Candidates and Novel Features of Clock Gene Product Cycling. *Journal of Neuroscience*, 17(17), pp.6745-6760.
- Kang, K., Panzano, V.C., Chang, E.C., Ni, L., Dainis, A.M., Jenkins, A.M., Regna, K., Muskavitch, M.A. and Garrity, P.A., 2012. Modulation of TRPA1 thermal sensitivity enables sensory discrimination in *Drosophila*. *Nature*, 481(7379), pp.76-80.
- Kang, K., Pulver, S.R., Panzano, V.C., Chang, E.C., Griffith, L.C., Theobald, D.L. and Garrity, P.A., 2010. Analysis of *Drosophila* TRPA1 reveals an ancient origin for human chemical nociception. *Nature*, 464(7288), pp.597-600.
- Kao, J.Y., Zubair, A., Salomon, M.P., Nuzhdin, S.V. and Campo, D., 2015. Population genomic analysis uncovers African and European admixture in *Drosophila melanogaster* populations from the south-eastern United States and Caribbean Islands. *Molecular ecology*, 24(7), pp.1499-1509.
- Kapan, N., Lushchak, V., Luo, J. and Nässel, D.R., 2012. Identified peptidergic neurons in the *Drosophila* brain regulate insulin-producing cells, stress responses and metabolism by coexpressed short neuropeptide F and corazonin. *Cellular and Molecular Life Sciences*, 69(23), pp.4051-4066.
- Kapun, M., Fabian, D.K., Goudet, J. and Flatt, T., 2016a. Genomic evidence for adaptive inversion clines in *Drosophila melanogaster*. *Molecular biology and evolution*, 33(5), pp.1317-1336.
- Kapun, M., Schmidt, C., Durmaz, E., Schmidt, P.S. and Flatt, T., 2016b. Parallel effects of the inversion In (3R) Payne on body size across the North American and Australian clines in *Drosophila melanogaster*. *Journal of evolutionary biology*, 29(5), pp.1059-1072.

Keller, A., 2007. *Drosophila melanogaster's* history as a human commensal. *Current biology*, 17(3), pp.R77-R81.

Kennerdell, J. R., & Carthew, R. W. (1998). Use of dsRNA-mediated genetic interference to demonstrate that frizzled and frizzled 2 act in the wingless pathway. *Cell*, 95(7), 1017-1026.

Khaper, N., Bailey, C.D., Ghugre, N.R., Reitz, C., Awosanmi, Z., Waines, R. and Martino, T.A., 2018. Implications of disturbances in circadian rhythms for cardiovascular health: A new frontier in free radical biology. *Free Radical Biology and Medicine*, 119, pp.85-92.

Kim, I.H., Castillo, J.C., Aryan, A., Martin-Martin, I., Nouzova, M., Noriega, F.G., Barletta, A.B.F., Calvo, E., Adelman, Z.N., Ribeiro, J.M. and Andersen, J.F., 2020. A mosquito juvenile hormone binding protein (mJHBP) regulates the activation of innate immune defenses and hemocyte development. *PLoS pathogens*, 16(1), p.e1008288.

Kim, S.H., Lee, Y., Akitake, B., Woodward, O.M., Guggino, W.B. and Montell, C., 2010. Drosophila TRPA1 channel mediates chemical avoidance in gustatory receptor neurons. *Proceedings of the National Academy of Sciences*, 107(18), pp.8440-8445.

King, R.C., 1970. Ovarian development in *Drosophila melanogaster* (No. 595.774 K5).

Kiselev, A. and Subramaniam, S., 1994. Activation and regeneration of rhodopsin in the insect visual cycle. *Science*, 266(5189), pp.1369-1373.

Kistenpfennig, C., Hirsh, J., Yoshii, T. and Helfrich-Förster, C., 2012. Phase-shifting the fruit fly clock without cryptochrome. *Journal of biological rhythms*, 27(2), pp.117-125.

Klepsatel, P., Gálíková, M., De Maio, N., Ricci, S., Schlotterer, C. and Flatt, T., 2013. Reproductive and post-reproductive life history of wild-caught *Drosophila melanogaster* under laboratory conditions. *Journal of Evolutionary Biology*, 26(7), pp.1508-1520.

Kloss, B., Rothenfluh, A., Young, M.W. and Saez, L., 2001. Phosphorylation of period is influenced by cycling physical associations of double-time, period, and timeless in the Drosophila clock. *Neuron*, 30(3), pp.699-706.

Ko, H.W., Jiang, J. and Edery, I., 2002. Role for Slimb in the degradation of Drosophila Period protein phosphorylated by Doubletime. *Nature*, 420(6916), p.673.

Koh, K., Zheng, X. and Sehgal, A., 2006. JETLAG resets the Drosophila circadian clock by promoting light-induced degradation of TIMELESS. *Science*, 312(5781), pp.1809-1812.

Kong, Y., Liang, X., Liu, L., Zhang, D., Wan, C., Gan, Z. and Yuan, L., 2015a. High throughput sequencing identifies microRNAs mediating α-synuclein toxicity by targeting neuroactive-ligand receptor interaction pathway in early stage of drosophila parkinson's disease model. *PLoS One*, 10(9), p.e0137432.

- Kong, Y., Wu, J., Zhang, D., Wan, C. and Yuan, L., 2015b. The role of miR-124 in Drosophila Alzheimer's Disease model by targeting delta in notch signalling pathway. *Current molecular medicine*, 15(10), pp.980-989.
- Konopka, R.J. and Benzer, S., 1971. Clock mutants of Drosophila melanogaster. *Proceedings of the National Academy of Sciences*, 68(9), pp.2112-2116.
- Koressaar, T. and Remm, M., 2007. Enhancements and modifications of primer design program Primer3. *Bioinformatics*, 23(10), pp.1289-1291.
- Koštál, V., 2006. Eco-physiological phases of insect diapause. *Journal of insect physiology*, 52(2), pp.113-127.
- Koyama, T., Rodrigues, M.A., Athanasiadis, A., Shingleton, A.W. and Mirth, C.K., 2014. Nutritional control of body size through FoxO-Ultraspiracle mediated ecdysone biosynthesis. *Elife*, 3, p.e03091.
- Kramer, J.M., Davidge, J.T., Lockyer, J.M. and Staveley, B.E., 2003. Expression of Drosophila FOXO regulates growth and can phenocopy starvation. *BMC developmental biology*, 3(1), pp.1-14.
- Kistenpfennig, C., Hirsh, J., Yoshii, T. and Helfrich-Förster, C., 2012. Phase-shifting the fruit fly clock without cryptochrome. *Journal of biological rhythms*, 27(2), pp.117-125.
- Kubrak, O.I., Kučerová, L., Theopold, U. and Nässel, D.R., 2014. The sleeping beauty: how reproductive diapause affects hormone signalling, metabolism, immune response and somatic maintenance in Drosophila melanogaster. *PLoS One*, 9(11), p.e113051.
- Kume, K., Kume, S., Park, S.K., Hirsh, J. and Jackson, F.R., 2005. Dopamine is a regulator of arousal in the fruit fly. *Journal of Neuroscience*, 25(32), pp.7377-7384.
- Kwon, Y., Kim, S.H., Ronderos, D.S., Lee, Y., Akitake, B., Woodward, O.M., Guggino, W.B., Smith, D.P. and Montell, C., 2010. Drosophila TRPA1 channel is required to avoid the naturally occurring insect repellent citronellal. *Current Biology*, 20(18), pp.1672-1678.
- Kwon, Y., Shim, H.S., Wang, X. and Montell, C., 2008. Control of thermotactic behavior via coupling of a TRP channel to a phospholipase C signalling cascade. *Nature neuroscience*, 11(8), p.871.
- Lachaise, D., Cariou, M.L., David, J.R., Lemeunier, F., Tsacas, L. and Ashburner, M., 1988. Historical biogeography of the Drosophila melanogaster species subgroup. *Evolutionary biology*, pp.159-225.
- LaFever, L. and Drummond-Barbosa, D., 2005. Direct control of germline stem cell division and cyst growth by neural insulin in Drosophila. *Science*, 309(5737), pp.1071-1073.
- Lamaze, A., Öztürk-Çolak, A., Fischer, R., Peschel, N., Koh, K. and Jepson, J.E., 2017. Regulation of sleep plasticity by a thermo-sensitive circuit in Drosophila. *Scientific reports*, 7, p.40304.

- Lampe, L., Jentzsch, M., Kierszniewska, S. and Levashina, E.A., 2019. Metabolic balancing by miR-276 shapes the mosquito reproductive cycle and Plasmodium falciparum development. *Nature communications*, 10(1), pp.1-10.
- Laurent, S.J., Werzner, A., Excoffier, L. and Stephan, W., 2011. Approximate Bayesian analysis of *Drosophila melanogaster* polymorphism data reveals a recent colonization of Southeast Asia. *Molecular biology and evolution*, 28(7), pp.2041-2051.
- Lazareva, A.A., Roman, G., Mattox, W., Hardin, P.E. and Dauwalder, B., 2007. A role for the adult fat body in *Drosophila* male courtship behavior. *PLoS genetics*, 3(1), p.e16.
- Lear, B.C., Merrill, C.E., Lin, J.M., Schroeder, A., Zhang, L. and Allada, R., 2005. A novel G-protein coupled receptor, groom-of-PDF, is required for PDF neuron action in circadian behavior. *Neuron*, 48, p.221.
- Lee, C., Bae, K. and Edery, I., 1999. PER and TIM Inhibit the DNA Binding Activity of aDrosophila CLOCK-CYC/dBMAL1 Heterodimer without Disrupting Formation of the Heterodimer: a Basis for Circadian Transcription. *Molecular and cellular biology*, 19(8), pp.5316-5325
- Lee, J., Yoo, E., Lee, H., Park, K., Hur, J.H. and Lim, C., 2017. LSM12 and ME31B/DDX6 Define Distinct Modes of Posttranscriptional Regulation by ATAXIN-2 Protein Complex in *Drosophila* Circadian Pacemaker Neurons. *Molecular Cell*, 66(1), pp.129-140.
- Lee, R.C., Feinbaum, R.L. and Ambros, V., 1993. The *C. elegans* heterochronic gene lin-4 encodes small RNAs with antisense complementarity to lin-14. *cell*, 75(5), pp.843-854.
- Lee, S.F., Sgro, C.M., Shirriffs, J., Wee, C.W., Rako, L.E.A., Van Heerwaarden, B. and Hoffmann, A.A., 2011. Polymorphism in the couch potato gene clines in eastern Australia but is not associated with ovarian dormancy in *Drosophila melanogaster*. *Molecular ecology*, 20(14), pp.2973-2984.
- Lee, T. and Luo, L., 1999. Mosaic analysis with a repressible cell marker for studies of gene function in neuronal morphogenesis. *Neuron*, 22(3), pp.451-461.
- Lee, Y. and Montell, C., 2013. *Drosophila* TRPA1 functions in temperature control of circadian rhythm in pacemaker neurons. *Journal of Neuroscience*, 33(16), pp.6716-6725.
- Lee, Y., 2013. Contribution of *Drosophila* TRPA1-expressing neurons to circadian locomotor activity patterns. *PLoS one*, 8(12), p.e85189.
- Lee, Y., Ahn, C., Han, J., Choi, H., Kim, J., Yim, J., Lee, J., Provost, P., Rådmark, O., Kim, S. and Kim, V.N., 2003. The nuclear RNase III Drosha initiates microRNA processing. *Nature*, 425(6956), pp.415-419.

- Lee, Y., Jeon, K., Lee, J.T., Kim, S. and Kim, V.N., 2002. MicroRNA maturation: stepwise processing and subcellular localization. *The EMBO journal*, 21(17), pp.4663-4670.
- Lees, A.D., 1973. Photoperiodic time measurement in the aphid Megoura viciae. *Journal of Insect Physiology*, 19(12), pp.2279-2316.
- Leever, S.J., Weinkove, D., MacDougall, L.K., Hafen, E. and Waterfield, M.D., 1996. The *Drosophila* phosphoinositide 3-kinase Dp110 promotes cell growth. *The EMBO journal*, 15(23), pp.6584-6594.
- Leonard, D.E., 1968. Diapause in the gypsy moth. *Journal of Economic Entomology*, 61(3), pp.596-598.
- Lewis, B.P., Burge, C.B. and Bartel, D.P., 2005. Conserved seed pairing, often flanked by adenosines, indicates that thousands of human genes are microRNA targets. *cell*, 120(1), pp.15-20.
- Li, H. and Stephan, W., 2006. Inferring the demographic history and rate of adaptive substitution in *Drosophila*. *PLoS genetics*, 2(10), p.e166.
- Li, L. and Liu, Y., 2011. Diverse small non-coding RNAs in RNA interference pathways. *Therapeutic Oligonucleotides*, pp.169-182.
- Li, M.T., Cao, L.H., Xiao, N., Tang, M., Deng, B., Yang, T., Yoshii, T. and Luo, D.G., 2018. Hub-organized parallel circuits of central circadian pacemaker neurons for visual photoentrainment in *Drosophila*. *Nature communications*, 9(1), pp.1-14.
- Li, W., Cressy, M., Qin, H., Fulga, T., Van Vactor, D. and Dubnau, J., 2013. MicroRNA-276a functions in ellipsoid body and mushroom body neurons for naive and conditioned olfactory avoidance in *Drosophila*. *Journal of Neuroscience*, 33(13), pp.5821-5833.
- Liang, X., Holy, T.E. and Taghert, P.H., 2016. Synchronous *Drosophila* circadian pacemakers display nonsynchronous Ca<sup>2+</sup> rhythms in vivo. *Science*, 351(6276), pp.976-981.
- Liang, X., Holy, T.E. and Taghert, P.H., 2017. A Series of Suppressive Signals within the *Drosophila* Circadian Neural Circuit Generates Sequential Daily Outputs. *Neuron*.
- Lim, C. and Allada, R., 2013. ATAXIN-2 activates PERIOD translation to sustain circadian rhythms in *Drosophila*. *Science*, 340(6134), pp.875-879.
- Lim, C., Lee, J., Choi, C., Kilman, V.L., Kim, J., Park, S.M., Jang, S.K., Allada, R. and Choe, J., 2011. twenty-four defines a critical translational step in the *Drosophila* clock. *Nature*, 470(7334), p.399.
- Lin, J.M., Kilman, V.L., Keegan, K., Paddock, B., Emery-Le, M., Rosbash, M. and Allada, R., 2002. A role for casein kinase 2α in the *Drosophila* circadian clock. *Nature*, 420(6917), pp.816-820.

- Linz, J., Baschwitz, A., Strutz, A., Dweck, H.K., Sachse, S., Hansson, B.S. and Stensmyr, M.C., 2013. Host plant-driven sensory specialization in *Drosophila erecta*. *Proceedings of the Royal Society B: Biological Sciences*, 280(1760), p.20130626.
- Lirakis, M., Dolezal, M. and Schloetterer, C., 2018. Redefining reproductive dormancy in *Drosophila* as a general stress response to cold temperatures. *Journal of insect physiology*, 107, pp.175-185.
- Liu, Y., Liao, S., Veenstra, J.A. and Nässel, D.R., 2016. *Drosophila* insulin-like peptide 1 (DILP1) is transiently expressed during non-feeding stages and reproductive dormancy. *Scientific reports*, 6(1), pp.1-15.
- Lorenz, L.J., Hall, J.C. and Rosbash, M.I.C.H.A.E.L., 1989. Expression of a *Drosophila* mRNA is under circadian clock control during pupation. *Development*, 107(4), pp.869-880.
- Low, K.H., Chen, W.F., Yildirim, E. and Edery, I., 2012. Natural variation in the *Drosophila melanogaster* clock gene period modulates splicing of its 3'-terminal intron and mid-day siesta. *PloS one*, 7(11), p.e49536.
- Low, K.H., Lim, C., Ko, H.W. and Edery, I., 2008. Natural variation in the splice site strength of a clock gene and species-specific thermal adaptation. *Neuron*, 60(6), pp.1054-1067.
- Luo, J., Becnel, J., Nichols, C.D. and Nässel, D.R., 2012. Insulin-producing cells in the brain of adult *Drosophila* are regulated by the serotonin 5-HT 1A receptor. *Cellular and Molecular Life Sciences*, 69(3), pp.471-484.
- Luo, J., Lushchak, V., Goergen, P., Williams, M.J. and Nässel, D.R., 2014. *Drosophila* insulin-producing cells are differentially modulated by serotonin and octopamine receptors and affect social behavior. *PloS one*, 9(6), p.e99732.
- Luo, J., Shen, W.L. and Montell, C., 2017. TRPA1 mediates sensing the rate of temperature change in *Drosophila* larvae. *Nature neuroscience*, 20(1), p.34.
- Luo, W. and Sehgal, A., 2012. microRNA-279 acts through the JAK/STAT pathway to regulate circadian behavioural output in *Drosophila*. *Cell*, 148(4), p.765.
- Majercak, J., Chen, W.F. and Edery, I., 2004. Splicing of the period gene 3'-terminal intron is regulated by light, circadian clock factors, and phospholipase C. *Molecular and Cellular Biology*, 24(8), pp.3359-3372.
- Majercak, J., Sidote, D., Hardin, P.E. and Edery, I., 1999. How a circadian clock adapts to seasonal decreases in temperature and day length. *Neuron*, 24(1), pp.219-230.
- Mansourian, S., Enjin, A., Jirle, E.V., Ramesh, V., Rehermann, G., Becher, P.G., Pool, J.E. and Stensmyr, M.C., 2018. Wild African *Drosophila melanogaster* are seasonal specialists on marula fruit. *Current Biology*, 28(24), pp.3960-3968.
- Martin Anduaga, A., 2018. Diapause And The Circadian Clock In *Drosophila Melanogaster* (*Doctoral dissertation, University of Leicester*).

- Martinek, S., Inonog, S., Manoukian, A.S. and Young, M.W., 2001. A role for the segment polarity gene shaggy/GSK-3 in the Drosophila circadian clock. *Cell*, 105(6), pp.769-779.
- Mazzoni, E.O., Celik, A., Wernet, M.F., Vasilisiuskas, D., Johnston, R.J., Cook, T.A., Pichaud, F. and Desplan, C., 2008. Iroquois complex genes induce co-expression of rhodopsins in Drosophila. *PLoS biology*, 6(4), p.e97.
- McKenzie, J. A., and P. A. Parsons. "Alcohol tolerance: an ecological parameter in the relative success of *Drosophila melanogaster* and *Drosophila simulans*." *Oecologia* 10, no. 4 (1972): 373-388.
- McMillan, I., Fitz-Earle, M. and Robson, D.S., 1970. Quantitative genetics of fertility I. Lifetime egg production of *Drosophila melanogaster*—theoretical. *Genetics*, 65(2), p.349.
- Means, J.C., Venkatesan, A., Gerdes, B., Fan, J.Y., Bjes, E.S. and Price, J.L., 2015. Drosophila spaghetti and doubletime link the circadian clock and light to caspases, apoptosis and tauopathy. *PLoS genetics*, 11(5), p.e1005171.
- Menegazzi, P., Vanin, S., Yoshii, T., Rieger, D., Hermann, C., Dusik, V., Kyriacou, C.P., Helfrich-Förster, C. and Costa, R., 2013. Drosophila clock neurons under natural conditions. *Journal of biological rhythms*, 28(1), pp.3-14.
- Menegazzi, P., Yoshii, T. and Helfrich-Förster, C., 2012. Laboratory versus nature: the two sides of the Drosophila circadian clock. *Journal of Biological Rhythms*, 27(6), pp.433-442.
- Merlin, C., liams, S.E. and Lugena, A.B., 2020. Monarch butterfly migration moving into the genetic era. *Trends in Genetics*.
- Metaxakis, A., Tain, L.S., Grönke, S., Hendrich, O., Hinze, Y., Birras, U. and Partridge, L., 2014. Lowered insulin signalling ameliorates age-related sleep fragmentation in Drosophila. *PLoS Biol*, 12(4), p.e1001824.
- Meuti, M.E., Bautista-Jimenez, R. and Reynolds, J.A., 2018. Evidence that microRNAs are part of the molecular toolkit regulating adult reproductive diapause in the mosquito, *Culex pipiens*. *PloS one*, 13(11), p.e0203015.
- Mikeladze-Dvali, T., Wernet, M.F., Pistillo, D., Mazzoni, E.O., Teleman, A.A., Chen, Y.W., Cohen, S. and Desplan, C., 2005. The growth regulators warts/lats and melted interact in a bistable loop to specify opposite fates in Drosophila R8 photoreceptors. *Cell*, 122(5), pp.775-787.
- Mingardi, J., Musazzi, L., De Petro, G. and Barbon, A., 2018. miRNA editing: new insights into the fast control of gene expression in health and disease. *Molecular neurobiology*, 55(10), pp.7717-7727.
- Mirth, C.K., Tang, H.Y., Makohon-Moore, S.C., Salhadar, S., Gokhale, R.H., Warner, R.D., Koyama, T., Riddiford, L.M. and Shingleton, A.W., 2014. Juvenile hormone regulates

body size and perturbs insulin signalling in *Drosophila*. *Proceedings of the National Academy of Sciences*, 111(19), pp.7018-7023.

Mitrovski, P. and Hoffmann, A.A., 2001. Postponed reproduction as an adaptation to winter conditions in *Drosophila melanogaster*: evidence for clinal variation under semi-natural conditions. *Proceedings of the Royal Society of London. Series B: Biological Sciences*, 268(1481), pp.2163-2168.

Miyasako, Y., Umezaki, Y. and Tomioka, K., 2007. Separate sets of cerebral clock neurons are responsible for light and temperature entrainment of *Drosophila* circadian locomotor rhythms. *Journal of biological rhythms*, 22(2), pp.115-126.

Møller, M., Lund-Andersen, C., Rovsing, L., Sparre, T., Bache, N., Roepstorff, P. and Vorum, H., 2010. Proteomics of the photoneuroendocrine circadian system of the brain. *Mass spectrometry reviews*, 29(2), pp.313-325.

Montell, C., Jones, K., Zuker, C. and Rubin, G., 1987. A second opsin gene expressed in the ultraviolet-sensitive R7 photoreceptor cells of *Drosophila melanogaster*. *Journal of Neuroscience*, 7(5), pp.1558-1566.

Montelli, S., Mazzotta, G., Vanin, S., Caccin, L., Corrà, S., De Pittà, C., Boothroyd, C., Green, E.W., Kyriacou, C.P. and Costa, R., 2015. period and timeless mRNA splicing profiles under natural conditions in *Drosophila melanogaster*. *Journal of biological rhythms*, 30(3), pp.217-227.

Morgan, T.H., 1910. Sex limited inheritance in *Drosophila*. *Science*, 32(812), pp.120-122.

Musiek, E.S., Xiong, D.D. and Holtzman, D.M., 2015. Sleep, circadian rhythms, and the pathogenesis of Alzheimer disease. *Experimental & molecular medicine*, 47(3), p.e148.

Nagy, D., Andreatta, G., Bastianello, S., Martín Anduaga, A., Mazzotta, G., Kyriacou, C.P. and Costa, R., 2018. A semi-natural approach for studying seasonal diapause in *Drosophila melanogaster* reveals robust photoperiodicity. *Journal of biological rhythms*, 33(2), pp.117-125.

Nagy, D., Cusumano, P., Andreatta, G., Anduaga, A.M., Hermann-Luibl, C., Reinhard, N., Gesto, J., Wegener, C., Mazzotta, G., Rosato, E. and Kyriacou, C.P., 2019. Peptidergic signalling from clock neurons regulates reproductive dormancy in *Drosophila melanogaster*. *PLoS genetics*, 15(6), p.e1008158.

Nahvi, A., Shoemaker, C.J. and Green, R., 2009. An expanded seed sequence definition accounts for full regulation of the hid 3' UTR by bantam miRNA. *Rna*, 15(5), pp.814-822.

Ni, J.D., Baik, L.S., Holmes, T.C. and Montell, C., 2017. A rhodopsin in the brain functions in circadian photoentrainment in *Drosophila*. *Nature*, 545(7654), pp.340-344.

- Nian, X., Chen, W., Bai, W. and Zhao, Z., 2020. Regulation of circadian locomotor rhythm by miR-263a. *Biological Rhythm Research*, pp.1-11.
- Nian, X., Chen, W., Bai, W., Zhao, Z. and Zhang, Y., 2019. miR-263b controls circadian behavior and the structural plasticity of pacemaker neurons by regulating the LIM-only protein Beadex. *Cells*, 8(8), p.923.
- Niu, Y., Liu, Z., Nian, X., Xu, X. and Zhang, Y., 2019. miR-210 controls the evening phase of circadian locomotor rhythms through repression of Fasciclin 2. *PLoS genetics*, 15(7), p.e1007655.
- Nunes, M.V. and Saunders, D., 1999. Photoperiodic time measurement in insects: a review of clock models. *Journal of Biological Rhythms*, 14(2), pp.84-104.
- Ogienko, A.A., Fedorova, S.A. and Baricheva, E.M., 2007. Basic aspects of ovarian development in *Drosophila melanogaster*. *Russian Journal of Genetics*, 43(10), pp.1120-1134.
- Ogueta, M., Hardie, R.C. and Stanewsky, R., 2018. Non-canonical phototransduction mediates synchronization of the *Drosophila melanogaster* circadian clock and retinal light responses. *Current Biology*, 28(11), pp.1725-1735.
- Okamoto, N. and Yamanaka, N., 2015. Nutrition-dependent control of insect development by insulin-like peptides. *Current opinion in insect science*, 11, pp.21-30.
- Okamoto, N. and Yamanaka, N., 2020. Steroid hormone entry into the brain requires a membrane transporter in *Drosophila*. *Current Biology*, 30(2), pp.359-366.
- Okamoto, N., Yamanaka, N., Yagi, Y., Nishida, Y., Kataoka, H., O'Connor, M.B. and Mizoguchi, A., 2009. A fat body-derived IGF-like peptide regulates postfeeding growth in *Drosophila*. *Developmental cell*, 17(6), pp.885-891.
- O'Tousa, J.E., Baehr, W., Martin, R.L., Hirsh, J., Pak, W.L. and Applebury, M.L., 1985. The *Drosophila ninaE* gene encodes an opsin. *Cell*, 40(4), pp.839-850.
- Ozturk, N., Selby, C.P., Annayev, Y., Zhong, D. and Sancar, A., 2011. Reaction mechanism of *Drosophila* cryptochrome. *Proceedings of the National Academy of Sciences*, 108(2), pp.516-521.
- Ozturk, N., VanVickle-Chavez, S.J., Akileswaran, L., Van Gelder, R.N. and Sancar, A., 2013. Ramshackle (Brwd3) promotes light-induced ubiquitylation of *Drosophila* Cryptochrome by DDB1-CUL4-ROC1 E3 ligase complex. *Proceedings of the National Academy of Sciences*, 110(13), pp.4980-4985.
- Paaby, A.B., Bergland, A.O., Behrman, E.L. and Schmidt, P.S., 2014. A highly pleiotropic amino acid polymorphism in the *Drosophila* insulin receptor contributes to life-history adaptation. *Evolution*, 68(12), pp.3395-3409.

- Papatsenko, D., Sheng, G. and Desplan, C., 1997. A new rhodopsin in R8 photoreceptors of *Drosophila*: evidence for coordinate expression with Rh3 in R7 cells. *Development*, 124(9), pp.1665-1673.
- Parisky, K.M., Rivera, J.L.A., Donelson, N.C., Kotecha, S. and Griffith, L.C., 2016. Reorganization of sleep by temperature in *Drosophila* requires light, the homeostat, and the circadian clock. *Current Biology*, 26(7), pp.882-892.
- Pasquinelli, A.E., Reinhart, B.J., Slack, F., Martindale, M.Q., Kuroda, M.I., Maller, B., Hayward, D.C., Ball, E.E., Degnan, B., Müller, P. and Spring, J., 2000. Conservation of the sequence and temporal expression of let-7 heterochronic regulatory RNA. *Nature*, 408(6808), pp.86-89.
- Pegoraro, M. and Tauber, E., 2018. Photoperiod-dependent expression of MicroRNA in *Drosophila*. *bioRxiv*, p.464180.
- Pegoraro, M., Gesto, J.S., Kyriacou, C.P. and Tauber, E., 2014. Role for circadian clock genes in seasonal timing: testing the Bünning hypothesis. *PLoS Genet*, 10(9), p.e1004603.
- Pegoraro, M., Zonato, V., Tyler, E.R., Fedele, G., Kyriacou, C.P. and Tauber, E., 2017. Geographical analysis of diapause inducibility in European *Drosophila melanogaster* populations. *Journal of insect physiology*, 98, pp.238-244.
- Peng, J., Wang, C., Wan, C., Zhang, D., Li, W., Li, P., Kong, Y. and Yuan, L., 2015. miR-184 is Critical for the motility-related PNS development in *Drosophila*. *International journal of developmental neuroscience: the official journal of the International Society for Developmental Neuroscience*, 46, pp.100-107.
- Peng, X., Wang, S., Huang, L., Su, S. and Chen, M., 2021. Characterization of *Rhopalosiphum padi* takeout-like genes and their role in insecticide susceptibility. *Pesticide Biochemistry and Physiology*, 171, p.104725.
- Peng, Y., Stoleru, D., Levine, J.D., Hall, J.C. and Rosbash, M., 2003. *Drosophila* free-running rhythms require intercellular communication. *PLoS biology*, 1(1), p.e13.
- Peschel, N., Chen, K.F., Szabo, G. and Stanewsky, R., 2009. Light-dependent interactions between the *Drosophila* circadian clock factors cryptochrome, jetlag, and timeless. *Current biology*, 19(3), pp.241-247.
- Petryk, A., Warren, J.T., Marqués, G., Jarcho, M.P., Gilbert, L.I., Kahler, J., Parvy, J.P., Li, Y., Dauphin-Villemant, C. and O'Connor, M.B., 2003. Shade is the *Drosophila* P450 enzyme that mediates the hydroxylation of ecdysone to the steroid insect molting hormone 20-hydroxyecdysone. *Proceedings of the National Academy of Sciences*, 100(24), pp.13773-13778.

- Picot, M., Klarsfeld, A., Chélot, E., Malpel, S. and Rouyer, F., 2009. A role for blind DN2 clock neurons in temperature entrainment of the *Drosophila* larval brain. *Journal of Neuroscience*, 29(26), pp.8312-8320.
- Pierrehumbert, R., 2019. There is no Plan B for dealing with the climate crisis. *Bulletin of the Atomic Scientists*, 75(5), pp.215-221.
- Pittendrigh, C.S., 1960, January. Circadian rhythms and the circadian organization of living systems. *Cold Spring Harbor symposia on quantitative biology*, 25, pp. 159-184
- Pittendrigh, C.S., 1972. Circadian surfaces and the diversity of possible roles of circadian organization in photoperiodic induction. *Proceedings of the National Academy of Sciences*, 69(9), pp.2734-2737.
- Plautz, J.D., Kaneko, M., Hall, J.C. and Kay, S.A., 1997. Independent photoreceptive circadian clocks throughout *Drosophila*. *Science*, 278(5343), pp.1632-1635.
- Pollock, J.A. and Benzer, S., 1988. Transcript localization of four opsin genes in the three visual organs of *Drosophila*; RH2 is ocellus specific. *Nature*, 333(6175), pp.779-782.
- Prabhakaran, P.M. and Sheeba, V., 2014. Simulating natural light and temperature cycles in the laboratory reveals differential effects on activity/rest rhythm of four Drosophilids. *Journal of Comparative Physiology A*, 200(10), pp.849-862.
- Price, J.L., Blau, J., Rothenfluh, A., Abodeely, M., Kloss, B. and Young, M.W., 1998. double-time is a novel *Drosophila* clock gene that regulates PERIOD protein accumulation. *Cell*, 94(1), pp.83-95.
- Puig, O. and Tjian, R., 2005. Transcriptional feedback control of insulin receptor by dFOXO/FOXO1. *Genes & development*, 19(20), pp.2435-2446.
- Puig, O., Marr, M.T., Ruhf, M.L. and Tjian, R., 2003. Control of cell number by *Drosophila* FOXO: downstream and feedback regulation of the insulin receptor pathway. *Genes & development*, 17(16), pp.2006-2020.
- Pullin, A.S., 1996. Physiological relationships between insect diapause and cold tolerance: Coevolution or coincidence. *European Journal of Entomology*, 93, pp.121-130.
- Rajan, A. and Perrimon, N., 2012. *Drosophila* cytokine unpaired 2 regulates physiological homeostasis by remotely controlling insulin secretion. *Cell*, 151(1), pp.123-137.
- Rajpurohit, S., Gefen, E., Bergland, A.O., Petrov, D.A., Gibbs, A.G. and Schmidt, P.S., 2018. Spatiotemporal dynamics and genome-wide association analysis of desiccation tolerance in *Drosophila melanogaster*. *Molecular ecology*, 27(17), pp.3525-3540.
- Rauschenbach, I.Y., Karpova, E.K., Burdina, E.V., Adonyeva, N.V., Bykov, R.A., Ilinsky, Y.Y., Menshanov, P.N. and Grunenko, N.E., 2017. Insulin-like peptide DILP6 regulates juvenile hormone and dopamine metabolism in *Drosophila* females. *General and comparative endocrinology*, 243, pp.1-9.

Reddy, P., Zehring, W.A., Wheeler, D.A., Pirrotta, V., Hadfield, C., Hall, J.C. and Rosbash, M., 1984. Molecular analysis of the period locus in *Drosophila melanogaster* and identification of a transcript involved in biological rhythms. *Cell*, 38(3), pp.701-710.

Reppert, Steven M., and David R. Weaver. "Molecular analysis of mammalian circadian rhythms." *Annual review of physiology* 63, no. 1 (2001): 647-676.

Reynolds, J.A., Nachman, R.J. and Denlinger, D.L., 2019. Distinct microRNA and mRNA responses elicited by ecdysone, diapause hormone and a diapause hormone analog at diapause termination in pupae of the corn earworm, *Helicoverpa zea*. *General and comparative endocrinology*, 278, pp.68-78.

Reynolds, J.A., Peyton, J.T. and Denlinger, D.L., 2017. Changes in microRNA abundance may regulate diapause in the flesh fly, *Sarcophaga bullata*. *Insect biochemistry and molecular biology*, 84, pp.1-14.

Richard, D.S., Jones, J.M., Barbarito, M.R., Cerula, S., Detweiler, J.P., Fisher, S.J., Brannigan, D.M. and Scheswohl, D.M., 2001. Vitellogenesis in diapausing and mutant *Drosophila melanogaster*: further evidence for the relative roles of ecdysteroids and juvenile hormones. *Journal of Insect Physiology*, 47(8), pp.905-913.

Richard, D.S., Rybczynski, R., Wilson, T.G., Wang, Y., Wayne, M.L., Zhou, Y., Partridge, L. and Harshman, L.G., 2005. Insulin signalling is necessary for vitellogenesis in *Drosophila melanogaster* independent of the roles of juvenile hormone and ecdysteroids: female sterility of the chico1 insulin signalling mutation is autonomous to the ovary. *Journal of Insect Physiology*, 51(4), pp.455-464.

Richard, D.S., Watkins, N.L., Serafin, R.B. and Gilbert, L.I., 1998. Ecdysteroids regulate yolk protein uptake by *Drosophila melanogaster* oocytes. *Journal of insect physiology*, 44(7-8), pp.637-644.

Richier, B., Michard-Vanhée, C., Lamouroux, A., Papin, C. and Rouyer, F., 2008. The clockwork orange *Drosophila* protein functions as both an activator and a repressor of clock gene expression. *Journal of biological rhythms*, 23(2), pp.103-116.

Rieger, D., Fraunholz, C., Popp, J., Bichler, D., Dittmann, R. and Helfrich-Förster, C., 2007. The fruit fly *Drosophila melanogaster* favors dim light and times its activity peaks to early dawn and late dusk. *Journal of biological rhythms*, 22(5), pp.387-399.

Rio, B., 1983. Evolution d'une spécialisation saisonnière chez *Drosophila erecta* (Dipt., Drosophilidae).

Roberts, L., Leise, T.L., Noguchi, T., Galschiodt, A.M., Houl, J.H., Welsh, D.K. and Holmes, T.C., 2015. Light evokes rapid circadian network oscillator desynchrony followed by gradual phase retuning of synchrony. *Current Biology*, 25(7), pp.858-867.

Roditakis, N.E. and Karandinos, M.G., 2001. Effects of photoperiod and temperature on pupal diapause induction of grape berry moth *Lobesia botrana*. *Physiological Entomology*, 26(4), pp.329-340.

Roessingh, S. and Stanewsky, R., 2017. The Drosophila TRPA1 channel and neuronal circuits controlling rhythmic behaviours and sleep in response to environmental temperature. *International journal of molecular sciences*, 18(10), p.2028.

Roessingh, S., Rosing, M., Marunova, M., Ogueta, M., George, R., Lamaze, A. and Stanewsky, R., 2019. Temperature synchronization of the Drosophila circadian clock protein PERIOD is controlled by the TRPA channel PYREXIA. *Communications biology*, 2(1), pp.1-13.

Roessingh, S., Wolfgang, W. and Stanewsky, R., 2015. Loss of Drosophila melanogaster TRPA1 function affects "siesta" behavior but not synchronization to temperature cycles. *Journal of biological rhythms*, 30(6), pp.492-505.

Rosato, E. and Kyriacou, C.P., 2006. Analysis of locomotor activity rhythms in Drosophila. *Nature Protocols*, 1(2), p.559.

Rosenzweig, M., Brennan, K.M., Tayler, T.D., Phelps, P.O., Patapoutian, A. and Garrity, P.A., 2005. The Drosophila ortholog of vertebrate TRPA1 regulates thermotaxis. *Genes & development*, 19(4), pp.419-424.

Rulifson, E.J., Kim, S.K. and Nusse, R., 2002. Ablation of insulin-producing neurons in flies: growth and diabetic phenotypes. *Science*, 296(5570), pp.1118-1120.

Rutila, J.E., Suri, V., Le, M., So, W.V., Rosbash, M. and Hall, J.C., 1998. CYCLE is a second bHLH-PAS clock protein essential for circadian rhythmicity and transcription of Drosophila period and timeless. *Cell*, 93(5), pp.805-814.

Saint-Charles, A., Michard-Vanhée, C., Alejevski, F., Chélot, E., Boivin, A. and Rouyer, F., 2016. Four of the six Drosophila rhodopsin-expressing photoreceptors can mediate circadian entrainment in low light. *Journal of Comparative Neurology*, 524(14), pp.2828-2844.

Salcedo, E., Huber, A., Henrich, S., Chadwell, L.V., Chou, W.H., Paulsen, R. and Britt, S.G., 1999. Blue-and green-absorbing visual pigments of Drosophila: Ectopic expression and physiological characterization of the R8 photoreceptor cell-specific Rh5 and Rh6 rhodopsins. *Journal of Neuroscience*, 19(24), pp.10716-10726.

Sanchez, J.A., Mesquita, D., Ingaramo, M.C., Ariel, F., Milán, M. and Dekanty, A., 2019. Eiger/TNF $\alpha$ -mediated Dilp8 and ROS production coordinate intra-organ growth in Drosophila. *PLoS genetics*, 15(8), p.e1008133.

Sandrelli, F., Tauber, E., Pegoraro, M., Mazzotta, G., Cisotto, P., Landskron, J., Stanewsky, R., Piccin, A., Rosato, E., Zordan, M. and Costa, R., 2007. A molecular basis

for natural selection at the timeless locus in *Drosophila melanogaster*. *Science*, 316(5833), pp.1898-1900.

Sarbassov, D.D., Guertin, D.A., Ali, S.M. and Sabatini, D.M., 2005. Phosphorylation and regulation of Akt/PKB by the rictor-mTOR complex. *Science*, 307(5712), pp.1098-1101.

Sarov-Blat, L., So, W.V., Liu, L. and Rosbash, M., 2000. The *Drosophila* takeout gene is a novel molecular link between circadian rhythms and feeding behavior. *Cell*, 101(6), pp.647-656.

Sathyamaranayanan, S., Zheng, X., Xiao, R. and Sehgal, A., 2004. Posttranslational regulation of *Drosophila* PERIOD protein by protein phosphatase 2A. *Cell*, 116(4), pp.603-615.

Saunders, D.S. and Gilbert, L.I., 1990. Regulation of ovarian diapause in *Drosophila melanogaster* by photoperiod and moderately low temperature. *Journal of Insect Physiology*, 36(3), pp.195-200.

Saunders, D.S., 1990. The circadian basis of ovarian diapause regulation in *Drosophila melanogaster*: is the period gene causally involved in photoperiodic time measurement?. *Journal of biological rhythms*, 5(4), pp.315-331.

Saunders, D.S., 2005. Erwin Bünning and Tony Lees, two giants of chronobiology, and the problem of time measurement in insect photoperiodism. *Journal of Insect Physiology*, 51(6), pp.599-608.

Saunders, D.S., Gillanders, S.W. and Lewis, R.D., 1994. Light-pulse phase response curves for the locomotor activity rhythm in period mutants of *Drosophila melanogaster*. *Journal of Insect Physiology*, 40(11), pp.957-968.

Saunders, D.S., Henrich, V.C. and Gilbert, L.I., 1989. Induction of diapause in *Drosophila melanogaster*: photoperiodic regulation and the impact of arrhythmic clock mutations on time measurement. *Proceedings of the National Academy of Sciences*, 86(10), pp.3748-3752.

Saunders, D.S., Richard, D.S., Applebaum, S.W., Ma, M. and Gilbert, L.I., 1990. Photoperiodic diapause in *Drosophila melanogaster* involves a block to the juvenile hormone regulation of ovarian maturation. *General and comparative endocrinology*, 79(2), pp.174-184.

Saunders, D.S., Sutton, D. and Jarvis, R.A., 1970. The effect of host species on diapause induction in *Nasonia vitripennis*. *Journal of insect physiology*, 16(3), pp.405-416.

Saurabh, S., Vanaphan, N., Wen, W. and Dauwalder, B., 2018. High functional conservation of takeout family members in a courtship model system. *Plos one*, 13(9), p.e0204615.

- Schiesari, L., Andreatta, G., Kyriacou, C.P., O'Connor, M.B. and Costa, R., 2016. The insulin-like proteins dILPs-2/5 determine diapause inducibility in *Drosophila*. *PLoS one*, 11(9), p.e0163680.
- Schllichting, M., Díaz, M.M., Xin, J. and Rosbash, M., 2019. Neuron-specific knockouts indicate the importance of network communication to *Drosophila* rhythmicity. *Elife*, 8, p.e48301.
- Schllichting, M., Menegazzi, P., Rosbash, M. and Helfrich-Förster, C., 2019. A distinct visual pathway mediates high-intensity light adaptation of the circadian clock in *Drosophila*. *Journal of Neuroscience*, 39(9), pp.1621-1630.
- Schllichting, M., Menegazzi, P. and Helfrich-Förster, C., 2015. Normal vision can compensate for the loss of the circadian clock. *Proceedings of the Royal Society B: Biological Sciences*, 282(1815), p.20151846.
- Schllichting, M., Menegazzi, P., Lelito, K.R., Yao, Z., Buhl, E., Dalla Benetta, E., Bahle, A., Denike, J., Hodge, J.J., Helfrich-Förster, C. and Shafer, O.T., 2016. A neural network underlying circadian entrainment and photoperiodic adjustment of sleep and activity in *Drosophila*. *Journal of Neuroscience*, 36(35), pp.9084-9096.
- Schmidt, P.S. and Paaby, A.B., 2008. Reproductive diapause and life-history clines in North American populations of *Drosophila melanogaster*. *Evolution: International Journal of Organic Evolution*, 62(5), pp.1204-1215.
- Schmidt, P.S., Zhu, C.T., Das, J., Batavia, M., Yang, L. and Eanes, W.F., 2008. An amino acid polymorphism in the couch potato gene forms the basis for climatic adaptation in *Drosophila melanogaster*. *Proceedings of the National Academy of Sciences*, 105(42), pp.16207-16211.
- Schmidt, P.S., 2011. Evolution and mechanisms of insect reproductive diapause: a plastic and pleiotropic life history syndrome. *Mechanisms of life history evolution: the genetics and physiology of life history traits and trade-offs*, pp.221-229.
- Schmidt, P.S., Matzkin, L., Ippolito, M. and Eanes, W.F., 2005. Geographic variation in diapause incidence, life-history traits, and climatic adaptation in *Drosophila melanogaster*. *Evolution*, 59(8), pp.1721-1732.
- Schwarz, D.S., Hutvágner, G., Du, T., Xu, Z., Aronin, N. and Zamore, P.D., 2003. Asymmetry in the assembly of the RNAi enzyme complex. *Cell*, 115(2), pp.199-208.
- Sedghifar, A., Saelao, P. and Begun, D.J., 2016. Genomic patterns of geographic differentiation in *Drosophila simulans*. *Genetics*, 202(3), pp.1229-1240.
- Sehadova, H., Glaser, F.T., Gentile, C., Simoni, A., Giesecke, A., Albert, J.T. and Stanewsky, R., 2009. Temperature entrainment of *Drosophila*'s circadian clock involves the gene nocte and signalling from peripheral sensory tissues to the brain. *Neuron*, 64(2), pp.251-266.

Semaniuk, U., Piskovatska, V., Strilbytska, O., Strutynska, T., Burdyliuk, N., Vaiserman, A., Bubalo, V., Storey, K.B. and Lushchak, O., 2021. Drosophila insulin-like peptides: from expression to functions—a review. *Entomologia Experimentalis et Applicata*, 169(2), pp.195-208.

Shafer, O.T., Helfrich-Förster, C., Renn, S.C.P. and Taghert, P.H., 2006. Reevaluation of Drosophila melanogaster's neuronal circadian pacemakers reveals new neuronal classes. *Journal of Comparative Neurology*, 498(2), pp.180-193.

Shafer, O.T., Kim, D.J., Dunbar-Yaffe, R., Nikolaev, V.O., Lohse, M.J. and Taghert, P.H., 2008. Widespread receptivity to neuropeptide PDF throughout the neuronal circadian clock network of Drosophila revealed by real-time cyclic AMP imaging. *Neuron*, 58(2), pp.223-237.

Shakhmantir, I., Nayak, S., Grant, G.R. and Sehgal, A., 2018. Spliceosome factors target timeless (tim) mRNA to control clock protein accumulation and circadian behavior in Drosophila. *Elife*, 7, p.e39821.

Shang, Y., Griffith, L.C. and Rosbash, M., 2008. Light-arousal and circadian photoreception circuits intersect at the large PDF cells of the Drosophila brain. *Proceedings of the National Academy of Sciences*, 105(50), pp.19587-19594.

Shapiro, H., 1932. The rate of oviposition in the fruit fly, Drosophila. *The Biological Bulletin*, 63(3), pp.456-471.

Sharma, V.K. and Chandrashekaran, M.K., 2005. Zeitgebers (time cues) for biological clocks. *Current Science*, pp.1136-1146.

Sheeba, V., Kaneko, M., Sharma, V.K. and Holmes, T.C., 2008. The Drosophila circadian pacemaker circuit: Pas de deux or Tarantella?. *Critical reviews in biochemistry and molecular biology*, 43(1), pp.37-61.

Sheldon, A.L., Zhang, J., Fei, H. and Levitan, I.B., 2011. SLOB, a SLOWPOKE channel binding protein, regulates insulin pathway signalling and metabolism in Drosophila. *PLoS One*, 6(8), p.e23343.

Shen, W.L., Kwon, Y., Adegbola, A.A., Luo, J., Chess, A. and Montell, C., 2011. Function of rhodopsin in temperature discrimination in Drosophila. *Science*, 331(6022), pp.1333-1336.

Shih, H.W. and Chiang, A.S., 2011. Anatomical characterization of thermosensory AC neurons in the adult Drosophila brain. *Journal of neurogenetics*, 25(1-2), pp.1-6.

Shirasu-Hiza, M.M., Dionne, M.S., Pham, L.N., Ayres, J.S. and Schneider, D.S., 2007. Interactions between circadian rhythm and immunity in Drosophila melanogaster. *Current Biology*, 17(10), pp.R353-R355.

- Sim, C., Kang, D.S., Kim, S., Bai, X. and Denlinger, D.L., 2015. Identification of FOXO targets that generate diverse features of the diapause phenotype in the mosquito *Culex pipiens*. *Proceedings of the National Academy of Sciences*, 112(12), pp.3811-3816.
- Siomi, M.C., Saito, K. and Siomi, H., 2008. How selfish retrotransposons are silenced in *Drosophila* germline and somatic cells. *FEBS letters*, 582(17), pp.2473-2478.
- Socha, R., Šula, J., Kodrík, D. and Gelbič, I., 1991. Hormonal control of vitellogenin synthesis in *Pyrrhocoris apterus* (L.) (Heteroptera). *Journal of Insect Physiology*, 37(11), pp.805-816.
- Sokabe, T., Chen, H.C., Luo, J. and Montell, C., 2016. A switch in thermal preference in *Drosophila* larvae depends on multiple rhodopsins. *Cell reports*, 17(2), pp.336-344.
- Soller, M., Bownes, M. and Kubli, E., 1999. Control of oocyte maturation in sexually mature *Drosophila* females. *Developmental biology*, 208(2), pp.337-351.
- Sprengelmeyer, Q.D., Mansourian, S., Lange, J.D., Matute, D.R., Cooper, B.S., Jirle, E.V., Stensmyr, M.C. and Pool, J.E., 2020. Recurrent collection of *Drosophila melanogaster* from wild African environments and genomic insights into species history. *Molecular biology and evolution*, 37(3), pp.627-638.
- Staal, G.B., 1975. Insect growth regulators with juvenile hormone activity. *Annual review of entomology*, 20(1), pp.417-460.
- Stanewsky, R., Kaneko, M., Emery, P., Beretta, B., Wager-Smith, K., Kay, S.A., Rosbash, M. and Hall, J.C., 1998. The cryb mutation identifies cryptochrome as a circadian photoreceptor in *Drosophila*. *Cell*, 95(5), pp.681-692.
- Stark, A., Brennecke, J., Bushati, N., Russell, R.B. and Cohen, S.M., 2005. Animal MicroRNAs confer robustness to gene expression and have a significant impact on 3' UTR evolution. *Cell*, 123(6), pp.1133-1146.
- Stéphanou, A., Fanchon, E., Innominate, P.F. and Ballesta, A., 2018. Systems biology, systems medicine, systems pharmacology: the what and the why. *Acta biotheoretica*, 66(4), pp.345-365.
- Stocker, H. and Hafen, E., 2000. Genetic control of cell size. *Current opinion in genetics & development*, 10(5), pp.529-535.
- Stoleru, D., Peng, Y., Agosto, J. and Rosbash, M., 2004. Coupled oscillators control morning and evening locomotor behaviour of *Drosophila*. *Nature*, 431(7010), p.862.
- Stone, E.F., Fulton, B.O., Ayres, J.S., Pham, L.N., Ziauddin, J. and Shirasu-Hiza, M.M., 2012. The circadian clock protein timeless regulates phagocytosis of bacteria in *Drosophila*. *PLoS pathogens*, 8(1), p.e1002445.
- Sulli, G., Lam, M.T.Y. and Panda, S., 2019. Interplay between circadian clock and cancer: new frontiers for cancer treatment. *Trends in cancer*, 5(8), pp.475-494.

- Sun, K., Jee, D., de Navas, L.F., Duan, H. and Lai, E.C., 2015. Multiple in vivo biological processes are mediated by functionally redundant activities of *Drosophila* mir-279 and mir-996. *PLoS Genet*, 11(6), p.e1005245.
- Szular, J., Sehadova, H., Gentile, C., Szabo, G., Chou, W.H., Britt, S.G. and Stanewsky, R., 2012. Rhodopsin 5-and Rhodopsin 6-Mediated Clock Synchronization in *Drosophila melanogaster* Is Independent of Retinal Phospholipase C- $\beta$  Signaling. *Journal of biological rhythms*, 27(1), pp.25-36.
- Tahayato, A., Sonneville, R., Pichaud, F., Wernet, M.F., Papatsenko, D., Beaufils, P., Cook, T. and Desplan, C., 2003. Otd/Crx, a dual regulator for the specification of ommatidia subtypes in the *Drosophila* retina. *Developmental cell*, 5(3), pp.391-402.
- Tamura, Y., Shintani, M., Nakamura, A., Monden, M. and Shiomi, H., 2005. Phase-specific central regulatory systems of hibernation in Syrian hamsters. *Brain research*, 1045(1-2), pp.88-96.
- Tang, X., Platt, M.D., Lagnese, C.M., Leslie, J.R. and Hamada, F.N., 2013. Temperature integration at the AC thermosensory neurons in *Drosophila*. *Journal of Neuroscience*, 33(3), pp.894-901.
- Tang, X., Roessingh, S., Hayley, S.E., Chu, M.L., Tanaka, N.K., Wolfgang, W., Song, S., Stanewsky, R. and Hamada, F.N., 2017. The role of PDF neurons in setting the preferred temperature before dawn in *Drosophila*. *Elife*, 6, p.e23206.
- Tatar, M., Chien, S.A. and Priest, N.K., 2001. Negligible senescence during reproductive dormancy in *Drosophila melanogaster*. *The American Naturalist*, 158(3), pp.248-258.
- Tauber, E., Zordan, M., Sandrelli, F., Pegoraro, M., Osterwalder, N., Breda, C., Daga, A., Selmin, A., Monger, K., Benna, C. and Rosato, E., 2007. Natural selection favors a newly derived timeless allele in *Drosophila melanogaster*. *science*, 316(5833), pp.1895-1898.
- Taylor, G.K. and Krapp, H.G., 2007. Sensory systems and flight stability: what do insects measure and why?. *Advances in insect physiology*, 34, pp.231-316.
- Teleman, A.A. and Cohen, S.M., 2006. *Drosophila* lacking microRNA miR-278 are defective in energy homeostasis. *Genes & development*, 20(4), pp.417-422.
- Toivonen, J.M. and Partridge, L., 2009. Endocrine regulation of aging and reproduction in *Drosophila*. *Molecular and cellular endocrinology*, 299(1), pp.39-50.
- Tomioka, K., Sakamoto, M., Harui, Y., Matsumoto, N. and Matsumoto, A., 1998. Light and temperature cooperate to regulate the circadian locomotor rhythm of wild type and period mutants of *Drosophila melanogaster*. *Journal of insect physiology*, 44(7), pp.587-596.

- Top, D. and Young, M.W., 2018. Coordination between differentially regulated circadian clocks generates rhythmic behavior. *Cold Spring Harbor perspectives in biology*, 10(7), p.a033589.
- Top, D., Harms, E., Syed, S., Adams, E.L. and Saez, L., 2016. GSK-3 and CK2 kinases converge on timeless to regulate the master clock. *Cell reports*, 16(2), pp.357-367.
- Tu, M.P., Yin, C.M. and Tatar, M., 2005. Mutations in insulin signalling pathway alter juvenile hormone synthesis in *Drosophila melanogaster*. *General and comparative endocrinology*, 142(3), pp.347-356.
- Umina, P.A., Weeks, A.R., Kearney, M.R., McKechnie, S.W. and Hoffmann, A.A., 2005. A rapid shift in a classic clinal pattern in *Drosophila* reflecting climate change. *Science*, 308(5722), pp.691-693.
- United States Naval Observatory (USNO) Astronomy Application Department. *Rise, Set, and Twilight Definitions* ([http://aa.usno.navy.mil/faq/docs/RST\\_defs.php](http://aa.usno.navy.mil/faq/docs/RST_defs.php)) (2017)
- Vaidya, A.T., Top, D., Manahan, C.C., Tokuda, J.M., Zhang, S., Pollack, L., Young, M.W. and Crane, B.R., 2013. Flavin reduction activates *Drosophila* cryptochrome. *Proceedings of the National Academy of Sciences*, 110(51), pp.20455-20460.
- Vanaphan, N., Dauwalder, B. and Zufall, R.A., 2012. Diversification of takeout, a male-biased gene family in *Drosophila*. *Gene*, 491(2), pp.142-148.
- Vanin, S., Bhutani, S., Montelli, S., Menegazzi, P., Green, E.W., Pegoraro, M., Sandrelli, F., Costa, R. and Kyriacou, C.P., 2012. Unexpected features of *Drosophila* circadian behavioural rhythms under natural conditions. *Nature*, 484(7394), p.371.
- Vasiliauskas, D., Mazzoni, E.O., Sprecher, S.G., Brodetskiy, K., Johnston Jr, R.J., Lidder, P., Vogt, N., Celik, A. and Desplan, C., 2011. Feedback from rhodopsin controls rhodopsin exclusion in *Drosophila* photoreceptors. *Nature*, 479(7371), p.108.
- Veleri, S., Rieger, D., Helfrich-Förster, C. and Stanewsky, R., 2007. Hofbauer-Buchner eyelet affects circadian photosensitivity and coordinates TIM and PER expression in *Drosophila* clock neurons. *Journal of biological rhythms*, 22(1), pp.29-42.
- Viswanath, V., Story, G.M., Peier, A.M., Petrus, M.J., Lee, V.M., Hwang, S.W., Patapoutian, A. and Jegla, T., 2003. Opposite thermosensor in fruitfly and mouse. *Nature*, 423(6942), pp.822-823.
- Vodala, S., Pescatore, S., Rodriguez, J., Buescher, M., Chen, Y.W., Weng, R., Cohen, S.M. and Rosbash, M., 2012. The oscillating miRNA 959-964 cluster impacts *Drosophila* feeding time and other circadian outputs. *Cell metabolism*, 16(5), pp.601-612.
- Walker, N.J., 1995. Late Pleistocene and Holocene hunter-gatherers of the Matopos: an archaeological study of change and continuity in Zimbabwe.

- Wei, X., Zheng, C., Peng, T., Pan, Y., Xi, J., Chen, X., Zhang, J., Yang, S., Gao, X. and Shang, Q., 2016. miR-276 and miR-3016-modulated expression of acetyl-CoA carboxylase accounts for spirotetramat resistance in *Aphis gossypii* Glover. *Insect biochemistry and molecular biology*, 79, pp.57-65.
- Wernet, M.F., Mazzoni, E.O., Celik, A., Duncan, D.M., Duncan, I. and Desplan, C., 2006. Stochastic spineless expression creates the retinal mosaic for colour vision. *Nature*, 440(7081).
- Wernet, M.F., Velez, M.M., Clark, D.A., Baumann-Klausener, F., Brown, J.R., Klovstad, M., Labhart, T. and Clandinin, T.R., 2012. Genetic dissection reveals two separate retinal substrates for polarization vision in *Drosophila*. *Current Biology*, 22(1), pp.12-20.
- Wheeler, D.A., Hamblen-Coyle, M.J., Dushay, M.S. and Hall, J.C., 1993. Behavior in light-dark cycles of *Drosophila* mutants that are arrhythmic, blind, or both. *Journal of Biological Rhythms*, 8(1), pp.67-94.
- Wilczek, A.M., Burghardt, L.T., Cobb, A.R., Cooper, M.D., Welch, S.M. and Schmitt, J., 2010. Genetic and physiological bases for phenological responses to current and predicted climates. *Philosophical Transactions of the Royal Society of London B: Biological Sciences*, 365(1555), pp.3129-3147.
- Williams, G.E., 2000. Geological constraints on the Precambrian history of Earth's rotation and the Moon's orbit. *Reviews of Geophysics*, 38(1), pp.37-59.
- Williams, K.D., Bustos, M., Suster, M.L., So, A.K.C., Ben-Shahar, Y., Leavers, S.J. and Sokolowski, M.B., 2006. Natural variation in *Drosophila melanogaster* diapause due to the insulin-regulated PI3-kinase. *Proceedings of the National Academy of Sciences*, 103(43), pp.15911-15915.
- Wilson, R.C. and Doudna, J.A., 2013. Molecular mechanisms of RNA interference. *Annual review of biophysics*, 42, pp.217-239.
- Wolff, C.A. and Esser, K.A., 2019. Exercise timing and circadian rhythms. *Current opinion in physiology*, 10, pp.64-69.
- Wolfgang, W., Simoni, A., Gentile, C. and Stanewsky, R., 2013. The Pyrexia transient receptor potential channel mediates circadian clock synchronization to low temperature cycles in *Drosophila melanogaster*. *Proceedings of the Royal Society of London B: Biological Sciences*, 280(1768), p.20130959.
- Wolschin, F. and Gadau, J., 2009. Deciphering proteomic signatures of early diapause in *Nasonia*. *PloS one*, 4(7), p.e6394.
- Xia, X., Fu, X., Du, J., Wu, B., Zhao, X., Zhu, J. and Zhao, Z., 2020. Regulation of circadian rhythm and sleep by miR-375-timeless interaction in *Drosophila*. *The FASEB Journal*, 34(12), pp.16536-16551.

- Xiang, Y., Yuan, Q., Vogt, N., Looger, L.L., Jan, L.Y. and Jan, Y.N., 2010. Light-avoidance-mediating photoreceptors tile the Drosophila larval body wall. *Nature*, 468(7326), pp.921-926.
- Xiong, X.P., Kurthkoti, K., Chang, K.Y., Li, J.L., Ren, X., Ni, J.Q., Rana, T.M. and Zhou, R., 2016. miR-34 modulates innate immunity and ecdysone signalling in Drosophila. *PLoS pathogens*, 12(11), p.e1006034.
- Xu, P., Vernooy, S.Y., Guo, M. and Hay, B.A., 2003. The Drosophila microRNA Mir-14 suppresses cell death and is required for normal fat metabolism. *Current Biology*, 13(9), pp.790-795.
- Yadlapalli, S., Jiang, C., Bahle, A., Reddy, P., Meyhofer, E. and Shafer, O.T., 2018. Circadian clock neurons constantly monitor environmental temperature to set sleep timing. *Nature*, 555(7694), pp.98-102.
- Yamaguchi, S., Wolf, R., Desplan, C. and Heisenberg, M., 2008. Motion vision is independent of color in Drosophila. *Proceedings of the National Academy of Sciences*, 105(12), pp.4910-4915.
- Yamashita, Okitsugu. "Diapause hormone of the silkworm, Bombyx mori: structure, gene expression and function." *Journal of insect physiology* 42, no. 7 (1996): 669-679.
- Yang, C.H., Belawat, P., Hafen, E., Jan, L.Y. and Jan, Y.N., 2008a. Drosophila egg-laying site selection as a system to study simple decision-making processes. *Science*, 319(5870), pp.1679-1683.
- Yang, M., Lee, J.E., Padgett, R.W. and Edery, I., 2008b. Circadian regulation of a limited set of conserved microRNAs in Drosophila. *BMC genomics*, 9(1), pp.1-11.
- Yang, Y. and Edery, I., 2019. Daywake, an anti-siesta gene linked to a splicing-based thermostat from an adjoining clock gene. *Current Biology*, 29(10), pp.1728-1734.
- Yao, Z. and Shafer, O.T., 2014. The Drosophila circadian clock is a variably coupled network of multiple peptidergic units. *Science*, 343(6178), pp.1516-1520.
- Yenush, L., Fernandez, R., Myers Jr, M.G., Grammer, T.C., Sun, X.J., Blenis, J., Pierce, J.H., Schlessinger, J. and White, M.F., 1996. The Drosophila insulin receptor activates multiple signalling pathways but requires insulin receptor substrate proteins for DNA synthesis. *Molecular and Cellular Biology*, 16(5), pp.2509-2517.
- Yoshii, T., Hermann, C. and Helfrich-Förster, C., 2010. Cryptochrome-positive and-negative clock neurons in Drosophila entrain differentially to light and temperature. *Journal of biological rhythms*, 25(6), pp.387-398.
- Yoshii, T., Todo, T., Wülfbeck, C., Stanewsky, R. and Helfrich-Förster, C., 2008. Cryptochrome is present in the compound eyes and a subset of Drosophila's clock neurons. *Journal of Comparative Neurology*, 508(6), pp.952-966.

- Yoshii, T., Vanin, S., Costa, R. and Helfrich-Förster, C., 2009. Synergic entrainment of Drosophila's circadian clock by light and temperature. *Journal of Biological Rhythms*, 24(6), pp.452-464.
- Yu, W., Houl, J.H. and Hardin, P.E., 2011. NEMO kinase contributes to core period determination by slowing the pace of the Drosophila circadian oscillator. *Current Biology*, 21(9), pp.756-761.
- Zanini, D., Giraldo, D., Warren, B., Katana, R., Andrés, M., Reddy, S., Pauls, S., Schwedhelm-Domeyer, N., Geurten, B.R. and Göpfert, M.C., 2018. Proprioceptive opsin functions in Drosophila larval locomotion. *Neuron*, 98(1), pp.67-74.
- Zehring, W.A., Wheeler, D.A., Reddy, P., Konopka, R.J., Kyriacou, C.P., Rosbash, M. and Hall, J.C., 1984. P-element transformation with period locus DNA restores rhythmicity to mutant, arrhythmic Drosophila melanogaster. *Cell*, 39(2), pp.369-376.
- Zhang, R., Du, J., Zhao, X., Wei, L. and Zhao, Z., 2020. Regulation of circadian behavioural output via clock-responsive miR-276b. *Insect Molecular Biology*.
- Zhang, R., Du, J., Zhao, X., Wei, L. and Zhao, Z., 2021. Regulation of circadian behavioural output via clock-responsive miR-276b. *Insect Molecular Biology*, 30(1), pp.81-89.
- Zhang, X., Zabinsky, R., Teng, Y., Cui, M. and Han, M., 2011. microRNAs play critical roles in the survival and recovery of *Caenorhabditis elegans* from starvation-induced L1 diapause. *Proceedings of the National Academy of Sciences*, 108(44), pp.17997-18002.
- Zhang, Y. and Emery, P., 2013. GW182 controls Drosophila circadian behavior and PDF-receptor signalling. *Neuron*, 78(1), pp.152-165.
- Zhang, Y., Lamba, P., Guo, P. and Emery, P., 2016. miR-124 regulates the phase of Drosophila circadian locomotor behavior. *Journal of Neuroscience*, 36(6), pp.2007-2013.
- Zhang, L., Chung, B.Y., Lear, B.C., Kilman, V.L., Liu, Y., Mahesh, G., Meissner, R.A., Hardin, P.E. and Allada, R., 2010a. DN1p circadian neurons coordinate acute light and PDF inputs to produce robust daily behavior in Drosophila. *Current Biology*, 20(7), pp.591-599.
- Zhang, Y., Liu, Y., Bilodeau-Wentworth, D., Hardin, P.E. and Emery, P., 2010b. Light and temperature control the contribution of specific DN1 neurons to Drosophila circadian behavior. *Current Biology*, 20(7), pp.600-605.
- Zhang, Z., Cao, W. and Edery, I., 2018. The SR protein B52/SRp55 regulates splicing of the period thermosensitive intron and mid-day siesta in Drosophila. *Scientific reports*, 8(1), pp.1-13.
- Zhao, X., Bergland, A.O., Behrman, E.L., Gregory, B.D., Petrov, D.A. and Schmidt, P.S., 2016. Global transcriptional profiling of diapause and climatic adaptation in Drosophila melanogaster. *Molecular biology and evolution*, 33(3), pp.707-720.

Zheng, X., Koh, K., Sowcik, M., Smith, C.J., Chen, D., Wu, M.N. and Sehgal, A., 2009. An isoform-specific mutant reveals a role of PDP1 $\epsilon$  in the circadian oscillator. *Journal of Neuroscience*, 29(35), pp.10920-10927.

Zhong, L., Bellemer, A., Yan, H., Honjo, K., Robertson, J., Hwang, R.Y., Pitt, G.S. and Tracey, W.D., 2012. Thermosensory and nonthermosensory isoforms of *Drosophila melanogaster* TRPA1 reveal heat-sensor domains of a thermoTRP Channel. *Cell reports*, 1(1), pp.43-55.

Zhou, J., Yu, W. and Hardin, P.E., 2016. CLOCKWORK ORANGE enhances PERIOD mediated rhythms in transcriptional repression by antagonizing E-box binding by CLOCK-CYCLE. *PLoS genetics*, 12(11), p.e1006430.

Zhu, J.Y., Heidersbach, A., Kathiriya, I.S., Garay, B.I., Ivey, K.N., Srivastava, D., Han, Z. and King, I.N., 2017. The E3 ubiquitin ligase Nedd4/Nedd4L is directly regulated by microRNA 1. *Development*, 144(5), pp.866-875.

Zonato, V., Collins, L., Pegoraro, M., Tauber, E. and Kyriacou, C.P., 2017. Is diapause an ancient adaptation in *Drosophila*??. *Journal of insect physiology*, 98, pp.267-274.

Zonato, V., Vanin, S., Costa, R., Tauber, E. and Kyriacou, C.P., 2018. Inverse European latitudinal cline at the timeless Locus of *Drosophila melanogaster* reveals selection on a clock gene: Population genetics of ls-tim. *Journal of biological rhythms*, 33(1), pp.15-23.